GEOLOGICA ULTRAIECTINA

Mededelingen van de
Faculteit Aardwetenschappen der
Rijksuniversiteit te Utrecht

No. 74

The evolution of the Piemonte-Ligurian ocean

A structural study of ophiolite complexes in Liguria (NW Italy)

EILARD H. HOOGERDUIJN STRATING

Voor Prof Schuiling

GEOLOGICA ULTRAIECTINA

Mededelingen van de
Faculteit Aardwetenschappen der
Rijksuniversiteit te Utrecht

No. 74

The evolution of the Piemonte-Ligurian ocean

A structural study of ophiolite complexes in Liguria (NW Italy)

The evolution of the Piemonte-Ligurian ocean

A structural study of ophiolite complexes in Liguria (NW Italy)

De evolutie van de Piemonte-Ligurische oceaan - Een structurele studie van ofioliet complexen in Ligurië (NW Italië)

(met een samenvatting in het Nederlands)

PROEFSCHRIFT

TER VERKRIJGING VAN DE GRAAD VAN DOCTOR AAN DE RIJKSUNIVERSITEIT TE UTRECHT, OP GEZAG VAN DE RECTOR MAGNIFICUS PROF. DR. J.A. VAN GINKEL, INGEVOLGE HET BESLUIT VAN HET COLLEGE VAN DEKANEN IN HET OPENBAAR TE VERDEDIGEN OP MAANDAG 7 JANUARI 1991 DES NAMIDDAGS TE 16.15 UUR

DOOR

EILARD HINDERICUS HOOGERDUIJN STRATING

GEBOREN OP 23 AUGUSTUS 1962 TE WINSCHOTEN

PROMOTOR: PROF. DR. H.J. ZWART
CO-PROMOTOR: DR. R.L.M. VISSERS

CIP-GEGEVENS KONINKLIJKE BIBLIOTHEEK, DEN HAAG

Hoogerduijn Strating, Eilard Hindericus

The evolution of the Piemonte-Ligurian ocean : a structural study of ophiolite complexes in Liguria (NW Italy) / Eilard Hindericus Hoogerduijn Strating. - [Utrecht: Instituut voor Aardwetenschappen der Rijksuniversiteit Utrecht]. - (Geologica Ultratraiectina, ISSN 0072-1026 ; no. 74)
Proefschrift Utrecht. - Met lit. opg. - Met samenvatting in het Nederlands.
ISBN 90-71577-27-9
SISO ital 565 UDC 55 (262.11) (234.41) (043.3)
Trefw.: Ligurië : geologie.

CONTENTS

DANKBETUIGING (Acknowledgement) 1

SAMENVATTING (Summary in Dutch) 2

RIASSUNTO (Summary in Italian) 4

CHAPTER 1

Introduction and summary 7

CHAPTER 2

The change from Alpine to Apennine polarity in the Ligurian Apennines: A case for gravitational collapse of an intraoceanic accretionary wedge 13
2.1 Introduction 13
2.2 Stratigraphy 15
2.3 Deformational structures in the Bracco area 17
2.4 Reconstruction of the pre-F3 structure in the Mélange Nappe 20
2.5 Correlation of the deformation in the Bracco area with other areas in the Ligurian Apennines 22
2.6 Metamorphism 23
2.7 Tectonic implications 24

CHAPTER 3

The Alpine structure of the Voltri Massif and Sestri-Voltaggio Zone 27
3.1 Introduction 27
3.2 The Voltri Massif 27
3.3 The structure of the Sestri-Voltaggio Zone 44
3.4 The structure of the Lavagna Nappe 53
3.5 Contact relations between the Voltri Massif, the Sestri-Voltaggio Zone and the western Lavagna Nappe 54
3.6 The large-scale structure of the Voltri Massif, the Sestri-Voltaggio Zone and the western Lavagna Nappe 55

CHAPTER 4

Alpine olivine- and titanian clinohumite-bearing assemblages and its implications for the mechanical behaviour of subducting oceanic mantle 61
4.1 Introduction 61
4.2 Alpine structures and metamorphism in the Erro-Tobbio ultramafics and gabbroic dykes 62

4.3 Tectono-metamorphic evolution of the Erro-Tobbio Unit 68
4.4 The mechanical behaviour of the Piemonte-Ligurian oceanic crust during subduction 74
4.5 Implications for shear stresses in the upper part of a subduction zone 79
4.6 Conclusions 80

CHAPTER 5

Non-adiabatic uplift of peridotites and shear localization in the upper mantle during incipient oceanic rifting 83
5.1 Introduction 83
5.2 Extension-related structures in the Erro Tobbio lherzolite 84
5.3 Pressure-temperature evolution and conditions during deformation 95
5.4 Implications for tectonic models of incipient oceanic rifting 99
5.5 Rheological implications for models of continental breakup 101
5.6 Conclusions 102

CHAPTER 6

The evolution of the Piemonte-Ligurian ocean: a synthesis 107
6.1 Introduction 107
6.2 Main geological events in the Ligurian Alps and Apennines from the Middle Triassic till the Eo-Oligiocene 107
6.3 Previous tectonic interpretations: further constraints 111
6.4 Large-scale kinematic framework 114
6.5 The Piemonte-Ligurian ocean: a synthesis 117
6.6 Conclusions 126

REFERENCES I

APPENDIX

Mineral Chemistry XIV

CURRICULUM VITAE XVIII

ENCLOSURE 1: Structural sections through the Bracco ophiolite complex (Ligurian Apennines, Italy)

ENCLOSURE 2: Tectonic map of the Northeastern Voltri Massif (Liguria, Italy)

ENCLOSURE 3: Tectonic map of the Erro-Tobbio Unit, Northeastern Voltri Massif (Liguria, Italy)

Dankbetuiging (Acknowledgements)

Hierbij wil ik de gelegenheid nemen iedereen te bedanken die heeft bijgedragen aan het onderzoek en het tot stand komen van dit proefschrift.

In de eerste plaats dank ik mijn promotor Professor H.J. Zwart. Hij heeft mij de gelegenheid gegeven om volledig zelfstandig dit onderzoek uit te voeren. Veel dank ben ik verschuldigd aan mijn co-promotor Reinoud Vissers. Zijn begeleiding en kritische vragen zijn zeer stimulerend geweest en hebben een grote invloed gehad op mijn wetenschappelijk denken. De steun van Pim van Wamel is vooral in de eerste fase van het onderzoek van doorslaggevend belang geweest. Daarnaast stond hij altijd klaar om opheldering te verschaffen als ik dreigde vast te lopen in regionale geologische problemen.

I would like to thank Professor Dr. John Dewey and Dr. John Platt, for allowing me to visit the Geological Department in Oxford (England). Their open-minded and dynamic approach towards structural geology and tectonics have been very stimulating, and have helped me clarify several aspects of my research.

De gesprekken met en colleges van professor Sierd Cloetingh en professor Rinus Wortel hebben in grote mate bijgedragen tot het ontwikkelen van mijn kennis van de tectonofysica.

Veel dank ben ik verschuldigd aan mijn kamergenoten Dirk van der Wal en Jurriaan Gerretsen, die steeds het geduld hebben opgebracht om naar de meest ruwe versies van nieuwe ideeën te luisteren. Chris Spiers, Collin Peach, Martin Drury, Hans de Bresser, Raymond Franssen, Rob van der Hilst en Rob Govers hebben eveneens als klankbord en produkt-bewakers gediend.

The cooperation with Giovanni Piccardo, Betta Rampone and Marco Scambelluri (Genova) has been very inspiring, especially since they never stopped trying to transform me into a petrologist. Giovanni also providing the Italian translation of the abstract.

Karin, jij hebt mij op moeilijke momenten altijd weten te motiveren om door te gaan met mijn onderzoek.

Tot slot wil ik alle andere personen bedanken die direct of indirect een bijdrage hebben geleverd aan mijn onderzoek en de voltooiing van het proefschrift.

Samenvatting

In dit proefschrift wordt met behulp van gecombineerde stukturele en petrologische methoden de geodynamische evolutie van de Piemonte-Ligurische oceaan bestudeerd. De data voor deze studie zijn afkomstig uit een aantal ofioliet complexen die ontsloten zijn in de Ligurische Alpen en Apennijnen (NW Italië).

Het doel is het vaststellen van de belangrijkste processen die een rol hebben gespeeld bij initiële oceanische rifting en de opening van het Piemonte-Ligurische bekken en tevens bij de subductie van oceanische lithosfeer. De conclusies voortkomende uit deze studie zijn in eerste instantie van toepassing op de situatie in de Piemonte-Ligurische oceaan en de dynamiek van gebergtevorming in de Alpen en Apennijnen. De processen zijn waarschijnlijk tevens van toepassing op de geodynamische evolutie van hedendaagse oceanische rifts (Rode Zee), passieve marges van langzaam-spreidende oceanen (Atlantische Oceaan), en marginale bekkens (Japanse Zee, Tyrrheense Zee, Cayman Trog).

Een veel voorkomend fenomeen in Phanerozoische gebergte ketens zijn ofioliet zones nauw geassocieerd aan domeinen met een regionale hoge-druk lage-temperatuur (HD) metamorfose.

Het is algemeen aanvaard dat deze ofioliet zones relicten representeren van oude, meestal kleine, oceanische bekkens die geflankeerd werden door passieve continentale marges. Het sluiten van zulke bekkens gebeurde vaak al zeer kort na het beeindigen van oceanische spreiding en resulteerde in het verplaatsen van fragmenten van de oceanische lithosfeer op de continentale marges. De synkinematische groei van HD index mineralen geeft aan dat de verplaatsing van ofioliet complexen voornamelijk plaats vond in subductie zones.

Een goed voorbeeld van een kort-levend oceanisch bekken is de Piemonte-Ligurische oceaan. Dit bekken maakt deel uit van de Tethys, een complexe, ongeveer oost-west georienteerde Mesozoische zeestraat, die aan de noordkant geflankeerd werd door N. Amerika en Eurazië en aan de zuidkant door Z. Amerika, Afrika en Arabië. De Piemonte-Ligurische oceaan werd volledig gesloten tijdens het Vroeg Tertiair waarbij fragmenten van de lithosfeer geincorporeerd werden in de Alpen en Apennijnen.

In Hoofdstuk 2 en 3 van het proefschrift worden de relaties besproken tussen subductie-gerelateerde deformatie en metamorfose zoals die aangetroffen zijn in de Ligurische ofiolieten. In de laag-gradig metamorfe ofioliet complexen in de Ligurische Apennijnen (Hoofdstuk 2) wordt aangetoond dat km-schaal, west- (Alpien) vergente, isoclinale plooien eerder gevormd zijn dan oost- (Apennijns) vergente plooiing en overschuiving. De eerste Apennijns-vergente structuren blijken vlak-liggende afschuivingen te zijn.

De ofioliet complexen van de Ligurische Alpen hebben een cyclus doorlopen van HD metamorfose (glaucofaanschist- tot eclogiet facies). De piek metamorfose is gekoppeld aan (N)NW- (Alpien) gerichte opschuivingen. Daaropvolgende laaggradige metamorfose duidt op bijna isothermale opheffing in samenhang met NW- en SE gerichte, vlak-liggende afschuivingen.

In dit proefschrift wordt gesuggereerd dat de Alpien-vergente strukturen gevormd zijn gedurende het Laat Krijt tot Paleoceen in een deformatie complex dat geassocieerd was aan een oostelijk hellende, intraoceanische, subductie zone. De afschuivingen en de omslag van Alpiene- naar Apennijnse transport richtingen zijn geinitiëerd gedurende het Paleoceen als gevolg van gravitatief ineenzakken van het deformatie complex. Het ineenzakken was waarschijnlijk het gevolg van een sterke afname van de subductie snelheid in de Piemonte-Ligurische oceaan.

In Hoofdstuk 4 wordt het mechanische gedrag van oceanische mantel gesteenten (peridotiet) tijdens subductie besproken. De subductie-gerelateerde deformatie in peri-dotiet is sterk gelokaliseerd in serpentiniet mylonieten.

Als gevolg van synkinematische dehydratie van antigoriet ontstonden zeer fijnkorrelige olivijn-houdende assemblages langs "shear bands" in deze serpentiniet mylonieten. Dit blijkt onder piek-eclogitische condities (450-550°C, 1400-1600 MPa) te zijn gebeurd. De microstructuur van de "shear bands" suggereert dat diffusie-kruip en het glijden langs korrelcontacten een belangrijke rol hebben gespeeld tijdens de deformatie. Het vrijkomen van vloeistoffen tijdens de dehydratie van antigoriet in de serpentiniet mylonieten leidde tot het opbouwen van zeer hoge vloeistof drukken en resulteerde in het breken van het peridotitische nevengesteente. De breuk systemen in de peridotiet zijn gedeeltelijk opgevuld met olivijn-houdende assemblage die vrijwel identiek zijn aan de assemblages in de serpentiniet mylonieten. Om onder eclogiet-facies condities breuk systemen in peridotiet te kunnen genereren blijkt de vloeistof druk gelijk te moeten zijn geweest aan ongeveer 0.9 maal de lithostatische druk.

Vroege rift-gerelateerde structuren, die in mantel peridotieten zijn ontwikkeld, worden besproken in Hoofdstuk 5. Het kan worden aangetoond dat bulk extensie van de Piemonte-Ligurische lithosfeer werd geaccommodeerd door gelokaliseerde deformatie in 100 m- to km-schaal shear zones. De ontwikkeling van deze shear zones is gelieerd aan tektonische denudatie van de peridotieten van diepe naar ondiepe lithosferische niveaus in een initiële oceanische rift. De microstructuren in de shear zones geven aan dat de rheologie van de diepere delen van de Piemonte-Ligurische lithosfeer het beste beschreven worden met een vloeiwet voor dislocatie kruip van natte olivijn. Echter, de ontwikkeling van fijnkorrelige amfibool-houdende peridotiet mylonieten, suggereert dat de deformatie in de bovenste 10 tot 20 km van de lithosfeer gecontroleerd kan zijn geweest door diffusie kruip en het glijden langs korrelcontacten.

Als conclusie van hetgeen in voorgaande hoofdstukken is besproken, wordt in Hoofdstuk 6 een synthese van de geodynamische evolutie van de Piemonte-Ligurische oceaan gepresenteerd. Deze synthese omvat een periode die begint in het Midden Trias met de aanzet tot rifting, en eindigt in het Eo-Oligoceen met de overgang van subductie naar continent-continent collisie.

Riassunto

In questa tesi viene investigata l'evoluzione geodinamica dell'oceano Ligure-Piemontese mediante metodi strutturali e petrologici combinati. I dati che supportano questo lavoro sono derivati dallo studio di vari complessi ofiolitici affioranti nelle Alpi Liguri e nell'Appennino (Italia Nord-occidentale). La tesi intende investigare i processi più importanti coinvolti in [1] l'impostazione del rift oceanico e l'apertura del bacino, e [2] la subduzione della litosfera oceanica. Le conclusioni raggiunte da questo studio si applicano principalmente alla situazione del bacino oceanico Ligure-Piemontese e alla dinamica dei processi orogenici nelle Alpi e nell'Appennino. I processi dedotti per l'oceano Ligure-Piemontese possono, tuttavia, anche giocare un ruolo rilevante nell'evoluzione geodinamica di rift oceanici attuali (es. Mar Rosso), di margini di oceani di "tipo Atlantico" a bassa velocità di spreading, e di bacini marginali (es. Mar del Giappone, Mar Tirreno, Bacino di Cayman).

Una caratteristica comune delle cinture orogeniche fanerozoiche è rappresentata dalle zone ofiolitiche associate a domini con metamorfismo regionale di alta pressione e bassa temperatura (HP). E'generalmente riconosciuto attualmente che queste zone ofiolitiche rappresentano relitti di preesistenti bacini oceanici, generalmente piccoli, limitati da margini continentali passivi. La chiusura di questi bacini oceanici durante i movimenti convergenti delle placche comunemente si verificò in un intervallo di tempo relativamente breve, dopo la fine della fase di spreading oceanico, e portò all'appilamento e alla messa in posto di frammenti di questa litosfera oceanica (le ofioliti s.s.) al di sopra dei margini adiacenti. La crescita sincinematica di minerali ed associazioni indice di HP dimostra che le ofioliti evolvettero generalmente in zone di subduzione.

Un esempio ben noto di bacino oceanico di vita breve è rappresentato dall'oceano Ligure-Piemontese. Questo bacino rappresenta un poccolo segmento della Tetide, un complesso mare mesozoico, approssimamente sviluppato in senso Est-Ovest, che separava Nord America e Eurasia, verso Nord, da Sud America, Africa e Arabia, verso Sud. L'oceano Ligure-Piemontese venne completamente chiuso durante il Terziario precoce, e frammenti di questa litosfera furono messi in posto come unità tettoniche di sovrascorrimento nelle Alpi e nell'Appennino.

Nei Capitoli 2 e 3 di questa tesi vengono discussi i rapporti fra deformazione e metamorfismo, collegati alle subduzione, nelle ofioliti liguri. Nei complessi ofiolitici a metamorfismo di basso grado dell'Appennino ligure (Cap. 2) viene dimostrato che pieghe isoclinali a scala chilometrica e vergenti a Ovest (cioè Alpine) si svilupparono prima dei piegamenti e degli scorrimenti diretti verso Est (cioè Appenninici), e che le più antiche strutture a vergenza appenninica sono rappresentate da faglie estensionali a basso angolo. Le ofioliti con più elevato grado metamorfico delle Alpi Liguri (Cap. 3) furono sottoposte ad un ciclo di metamorfismo di HP (da facies a Scisti Blu ad eclogiti), associato a scorrimenti con direzione (Nord-) Nord-Ovest, e ad una successiva risalita connessa a faglie estensionali di basso angolo con direzione Nord-Ovest e Sud-Est. Viene sostenuta l'interpretazione che le strutture a vergenza alpina si sono formate durante il tardo Cretacico-Paleocene in un cuneo di accrezione associato ad una zona

di subduzione intraoceanica, immergentesi ad Est. Viene discusso come il processo di fagliatura estensionale ed il cambio di polarità, da direzioni di trasporto alpine ad appenniniche, iniziò durante il Paleocene in risposta a collasso gravitativo di questo prisma di accrezione. Viene suggerito che il collasso fu indotto da un decremento nella velocità di subduzione nell'oceano Ligure-Piemontese.

Il Capitolo 4 riguarda il comportamento meccanico delle rocce del mantello oceanico (cioè le peridotiti) durante la subduzione. La deformazione connessa alla subduzione nelle peridotiti è localizzata nelle miloniti serpentinitiche. La crescita di associazioni mineralogiche ad olivina, a grana ultrafine, lungo le bande di shear in queste miloniti serpentinitiche si sviluppò durante le decomposizione sincinematica dell'antigorite sotto le condizioni del picco eclogitico (450-550°C, 1400-1600 MPa). L'assetto microstrutturale delle bande di shear indica che la deformazione coinvolse una componente importante di scorrimento dei limiti dei granuli dell'olivina, governata dalle diffusione. I fluidi liberati durante la decomposizione dell'antigorite nelle miloniti serpentinitiche produssero fratturazione idraulica nelle peridotiti incassanti. Le fratture idrauliche sono riempite con associazioni mineralogiche ad olivina simili a quelle sviluppate lungo le bande di shear. E' stato stimato che le pressioni dei fluidi furono circa 0.9 volte la pressione litostatica, in modo a permettere la fratturazione della peridotite in condizioni di facies eclogitica.

Nel Capitolo 5 vengono discusse le strutture precoci di rift sviluppate nelle peridotiti di mantello. Viene dimostrato che la estensione globale della litosfera ligure-piemontese fu resa possibile da deformazioni localizzate in zone di shear nel mantello superiore, di dimensioni variabili fra 0.1 e 5 Km. Lo sviluppo di queste zone di shear è legato al denudamento tettonico delle peridotiti, che risalirono da livelli litosferici profondi a livelli superficiali in un rift oceanico incipiente. Le microstrutture nelle zone di shear mostrano che la reologia delle parti più profonde del mantello litosferico ligure-piemontese è meglio descritta da una legge di flusso per scorrimento delle dislocazioni per l'olivina in presenza di fluidi. Lo sviluppo di miloniti peridotitiche ad anfibolo a grana fine, tuttavia, suggerisce che a profondità dell' ordine di 10-20 Km nel mantello litosferico la deformazione può essere controllata da scorrimento dei limiti dei granuli dell'olivina, governata dalle diffusione in presenza di fluidi.

Il Capitolo 6 presenta una sintesi dell'evoluzione geodynamica dell'oceano Ligure-Piemontese. L'intervallo di tempo considerato comprende l'inizio medio-Triassico del rifting fino alla transizione da subduzione a collisione continentale nell'Eo-Oligocene.

CHAPTER 1

Introduction and summary

A common feature in Phanerozoic orogenic belts are ophiolite zones closely associated with domains of high-pressure, low-temperature regional metamorphism. It is widely recognized nowadays that these ophiolite zones represent remnants of former oceanic basins, in general boarded by passive continental margins comparable to those of the present-day Atlantic ocean (Moores 1982; Knipper et al. 1986; Nicolas 1989). Closure of such an oceanic basin during convergent plate movements leads to stacking and emplacement of fragments of its lithosphere (the ophiolites ss.) onto the adjacent margins. The synkinematic growth of high-pressure, low-temperature index minerals such as glaucophane, lawsonite and omphacite indicates that ophiolite emplacement commonly occurs in regions characterized by low thermal gradients, i.e. subduction zones (Ernst 1975; Dewey 1976).

Plate tectonic (e.g. Dewey et al. 1973; Dercourt et al. 1986) and palinspastic (e.g. Trümpy 1982; Gasanov 1986) reconstructions of these former oceanic basins suggest that most of them were limited in size and that they never reached the dimensions of present-day oceans. In addition radiometric evidence in many cases indicates a narrow time span between cessation of oceanic spreading and the onset of convergence and subduction (e.g. Abbate et al. 1985).

The geodynamic evolution of these small oceanic basins, now preserved as ophiolites in mountain belts, has hitherto mainly been studied on the basis of the tectono-sedimentary evolution of the continental margins, the sediments deposited on the ocean floor, and the petrological and chemical characteristics of the oceanic crustal and upper mantle rocks. A powerful tool in ophiolite geology involves an integrated structural and petrological study of these oceanic rocks (Nicolas 1989 and references therein), but ophiolite studies principally based on structural techniques are still scarce.

A well studied example of a short-lived oceanic basin is the Piemonte-Ligurian ocean. This basin represents a small segment of the Tethys, a complex, approximately east-west trending Mesozoic sea separating N America and Eurasia to the north from S America, Africa and Arabia to the south (Dewey et al. 1973). After a period of continental rifting, accretion of oceanic crust in the Piemonte-Ligurian ocean during

the Late Jurassic continued for approximately 25 Ma (cf. Winterer & Bosellini 1981). Plate convergence leading to subduction of oceanic crust started during the Early Cretaceous, i.e. within 25 Ma after cessation of oceanic spreading (Hunziker 1974). The Piemonte-Ligurian ocean became completely closed in the Early Tertiary, when fragments of its lithosphere were emplaced as thrust units in the Alps and Apennines (Fig. 1.1).

In this thesis, the geodynamic evolution of the Piemonte-Ligurian ocean is investigated by means of combined structural and petrological methods. It aims to assess the most important processes involved in [1] incipient oceanic rifting and opening of the basin, and [2] subduction of oceanic lithosphere. The conclusions drawn from this study primarily apply to the situation in the Piemonte-Ligurian ocean, and the dynamics of orogeny in the Alps and Apennines. However, strong analogies exist

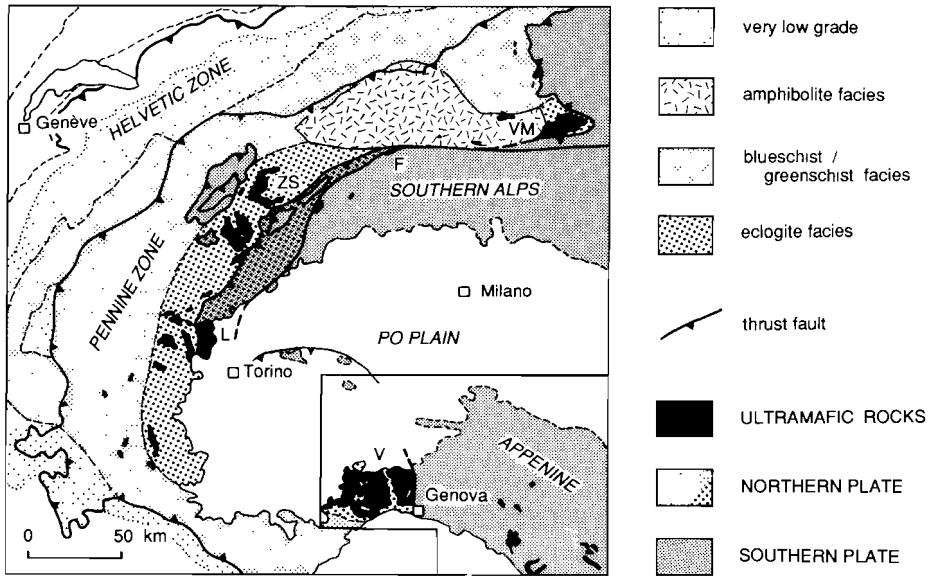

Fig. 1.1 Tectonic setting of the western and Ligurian Alps, and the northern Apennines. The southern Alps and northern Apennines belong to the southern (i.e. Adriatic) lithospheric plate which was thrust over the northern (i.e. European) plate during subduction and continental collision. The south-dipping suture zone between these plates is marked by a zone of Late Cretaceous, high-pressure low-temperature eclogite facies metamorphism. Most fragments of the Piemonte-Ligurian oceanic lithosphere (ophiolites and ultramafic massifs) occur within this eclogite facies domain. Note that the north-western part of the southern plate (i.e. Sesia-Lanzo Zone, including the Lanzo peridotite body) is also affected by eclogite facies metamorphism. Abbreviations: V= Voltri Massif, L= Lanzo peridotite, ZS= Zermatt-Saas ophiolites, F= Finero peridotite, VM= Val Malenco ophiolites. The area outlined is shown in Figure 1.2.

between the Piemonte-Ligurian ophiolites and oceanic lithosphere exposed in present-day oceanic rifts (i.e Red Sea), along margins of slow-spreading "Atlantic-type" oceans, and in marginal basins (Sea of Japan, Tyrrhenian Sea, Cayman basin). Since the development of these basins is a topic of debate (e.g. Moores 1982; Bonatti 1988; Jolivet et al. 1989; Tatsumi et al. 1989), it is suggested that the processes, inferred here for the case of the Piemonte Ligurian ocean, may also play a role in the geodynamic evolution of these modern basins.

The data underlying this thesis are derived from a number of ophiolite complexes exposed in the Ligurian Alps and Apennines (Fig. 1.1, 1.2). In this region, a sequence of low-grade (prehnite-pumpellyite facies) to high-pressure low-temperature (eclogite facies) metamorphic ophiolites and related sediments allows a study of the structural and metamorphic evolution of oceanic lithosphere in a subduction zone which evolved into a zone of continental collision. In addition, a structural study of the low-grade ophiolites in the Apennines (Bracco Massif) and of a large body of mantle peridotites in the Ligurian Alps (Erro-Tobbio peridotites in the Voltri Massif) enables the identification of the main processes during incipient oceanic rifting and opening of the Piemonte-Ligurian ocean.

Chapter 2 of this thesis discusses the deformation of the low-grade Bracco ophiolite complex in the Ligurian Apennines (Fig. 1.2). It is demonstrated in these ophiolites that km-scale, west- (i.e. Alpine) vergent, isoclinal folds developed prior to east- (i.e. Apennine) directed folding and thrusting, and that the earliest Apennine-vergent structures are low-angle extensional faults. The syn-metamorphic, Alpine-vergent isoclinal folds are interpreted to have formed at shallow levels (less than about 15 km), during the Late Cretaceous to Paleocene, in an accretionary wedge associated with an easterly dipping, intraoceanic subduction zone. It is argued that the polarity change, from Alpine to Apennine transport directions, initiated in response to gravity collapse of this accretionary wedge. In view of the coincidence of this polarity change with a drastic decrease of the convergence velocity between Africa and Europe during the Paleocene, it is suggested that collapse of the accretionary wedge leading to the onset of Apennine-vergent tectonics may have been induced by a decreasing rate of subduction in the Piemonte-Ligurian ocean.

Chapter 3 presents a detailed analysis of the relationships between deformation and metamorphism in the thrust units of the Voltri Group, the Sestri-Voltaggio Zone and the western Lavagne Nappe (Fig. 1.2). The PT trajectories are unraveled for five thrust units which went through a cycle of subduction and subsequent uplift. Shear sense criteria indicate that all structures developed during progressive (N)NW directed thrusting, which implies that the kinematic framework did not significantly change during this evolution. The peak high-pressure metamorphic assemblages in each of the units indicate equilibration at maximum depths ranging from about 50 km (1400 to 1600 MPa*) for the units in the Voltri Group to about 20 km (600 to 800 MPa) for the

* 100 MPa = 1 kbar

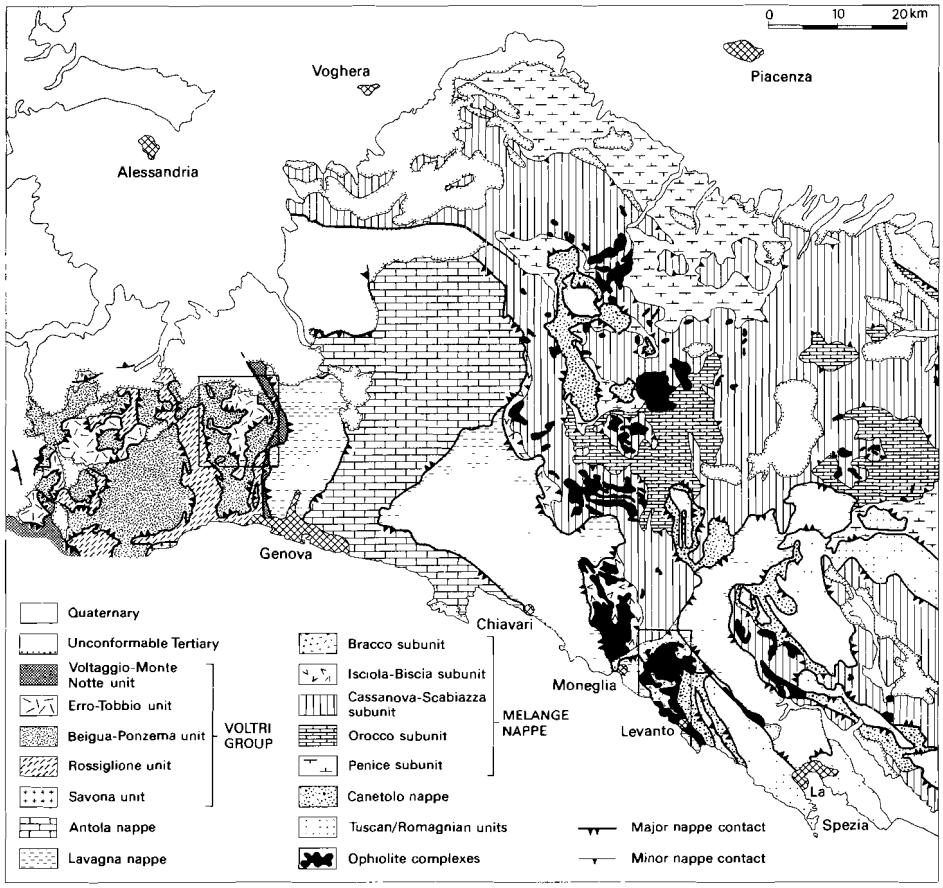

Fig. 1.2. Tectonic map of the Ligurian Alps and Apennines showing the regional setting of the ophiolite complexes studied in this thesis. The area outlined north of Genova indicates the area of detailed structural analysis in the northeastern Voltri Massif, shown in Appendix 2. The geology of the Bracco ophiolite complex, located in the area indicated near Levanto, is shown in Figure 2.1.

Sestri Voltaggio Zone and western Lavagna Nappe. The contact relationships of these thrust units point to juxtaposition in a very late stage of the tectono-metamorphic evolution, involving NW and SE directed, low-angle extensional faulting under greenschist to zeolite facies conditions.

Chapter 4 focusses in more detail on the tectono-metamorphic evolution of the Erro-Tobbio peridotite, the uppermost tectonic unit of the Voltri Group (Fig. 1.2), and addresses the mechanical behaviour of oceanic mantle rocks during subduction. The subduction-related deformation in the peridotite is strongly localized in serpentinite mylonites. This suggests that shear stresses along shallow parts of the subducting plate

contact may have been controlled by the rheology of serpentinite, rather than by the much stronger rheology of basaltic or gabbroic rocks. The deformation in these mylonites under peak eclogitic conditions (450-550 °C, 1400-1600 MPa) is closely related to the breakdown, towards higher temperatures, of antigorite into olivine + titanian clinohumite-bearing assemblages. These olivine-bearing assemblages notably developed as very fine-grained aggregates along shear bands. The microstructure of the shear bands suggests that the deformation involved an important component of diffusion-accommodated grainboundary sliding of wet, fine-grained olivine. This implies that the imposed deformation in the serpentinite mylonites may have been accommodated at flow stresses below 5 MPa, thereby drastically reducing the shear stresses along the plate contact at depths below about 40 km.

In addition to this reaction-enhanced softening, fluids released during prograde, synkinematic breakdown of antigorite in the serpentinite mylonites induced hydraulic fracturing of the peridotite wall rock. The hydraulic fractures in the peridotite are filled with olivine-bearing assemblages similar to those developed along the shear bands. Fluid pressures are estimated to have been about 0.9 times the lithostatic pressure (fluid pressure ratio $\lambda = 0.9$) such as to allow fracturing of peridotite under eclogite facies conditions.

In chapter 5, the early rift-related structures developed in the Erro-Tobbio peridotites are discussed. It is demonstrated that bulk extension of the Piemonte-Ligurian lithosphere was accommodated by localized deformation in 100 m to km-scale upper mantle shear zones. The development of these shear zones is allied to the progressive uplift of the peridotites from deep to shallow lithospheric levels in an incipient oceanic rift. Thermobarometry of the different shear zone structures suggests, that the peridotite followed a subsolidus and non-adiabatic PT trajectory during uplift. This uplift history seems more consistent with tectonic denudation of the mantle rocks along low-angle normal shear zones than with uplift in a mantle diapir system.

The localization of deformation in shear zones implies that the bulk strength of the extending Piemonte-Ligurian upper mantle became controlled by the rheology of the shear zone rocks. The microstructures in the Erro-Tobbio shear zones indicate, that the rheology of the deeper parts of the Piemonte-Ligurian lithospheric mantle are best described by a dislocation creep flow law for wet olivine. The development of fine-grained, amphibole-bearing peridotite mylonites, however, suggests that in the upper 10 to 20 km of the lithospheric mantle the deformation may have been controlled by diffusion-accommodated grainboundary sliding of wet olivine. The structures in the Erro-Tobbio peridotite indicate, that thermo-mechanical models of lithosphere extension, which involve a mechanically strong and homogeneously deforming upper mantle in an advancing stage of rifting, are inappropriate to describe oceanic rifting in the Piemonte-Ligurian domain.

Chapter 6 presents a synthesis of the evolution of the Piemonte-Ligurian ocean. The timespan considered comprises the Middle Triassic onset of rifting till the transition from subduction to continental collision in the Eo-Oligocene. Jurassic opening of the Piemonte-Ligurian ocean involved slightly to strongly asymmetric extension, ac-

commodated by a network of low-angle, normal shear zones in the lower crust and upper mantle. Cretaceous-Tertiary convergence in the Piemonte-Ligurian basin was partially accommodated by underplating along an east-dipping, intraoceanic subduction zone. Deformation of the rocks of the Sestri-Voltaggio Zone and the Ligurian units occurred in the subduction hanging wall. The high-pressure metamorphic Voltri-Group represents a stack of underplated oceanic units. The uplift of the Voltri-Group rocks, as well as the incipient stages of easterly directed tectonic transport resulting in the development of the Apennine orogene, are inferred to have been induced by gravitational collapse and extension of the intraoceanic accretionary wedge in response to a Paleocene decrease of the rate of subduction.

CHAPTER 2

The change from Alpine to Apennine polarity in the Ligurian Apennines: A case for gravitational collapse of an intraoceanic accretionary wedge

2.1 INTRODUCTION

In discussions on the relationships between the deformation in the Alps and the northern Apennines, a central problem has always been the relative timing of the westerly (i.e. Alpine) directed with respect to the easterly (i.e. Apennine) directed folding and thrusting. Since the early seventies Alpine directed structures have been reported from the Lavagna Nappe in the Ligurian Apennines (e.g. Elter & Pertusati 1973; Grandjaquet & Haccard 1977; Cortesogno et al. 1979b), and it is now well established that the Alpine directed structures predate the extensive Apennine directed folding and thrusting (Grandjaquet & Haccard 1977; Van Wamel et al. 1985; Van Zutphen et al. 1985; Marroni et al. 1988). The strongly deformed rocks of the Lavanga Nappe constitute the sedimentary cover of an ophiolitic basement. The studies on the deformation in the Lavagna Nappe, however, did not include the mafic and ultramafic basement rocks, hence uncertainty existed on the effect of Alpine directed deformation on the ophiolitic basement. In addition, no consensus exists as to the mechanisms driving the change from Alpine to Apennine directed structures. Models proposed range from a subduction polarity change (e.g. Boccaletti et al. 1980) to buoyancy and uplift of an Alpine accretionary wedge (Van Wamel 1987).

In this chapter a detailed structural analysis is presented of the deformation in the Lavagna Nappe, the ophiolitic Mélange Nappe and the Canetolo Nappe in the Bracco area. In this area it is possible to demonstrate that Alpine directed folding also affected the ophiolitic basement. In addition it is argued that the change from Alpine to Apennine polarity may have been induced by a decreasing subduction-rate, which is inferred to have led to gravitational instability and collapse of an Alpine, intraoceanic accretionary wedge.

Parts of this is chapter have been published as:
Hoogerduijn Strating E.H. & Van Wamel W.A. 1989. The structure of the Bracco ophiolite complex (Ligurian Apennines, Italy): a change from Alpine to Apennine polarity. J. Geol. Soc. Lond., 146, 933-944.

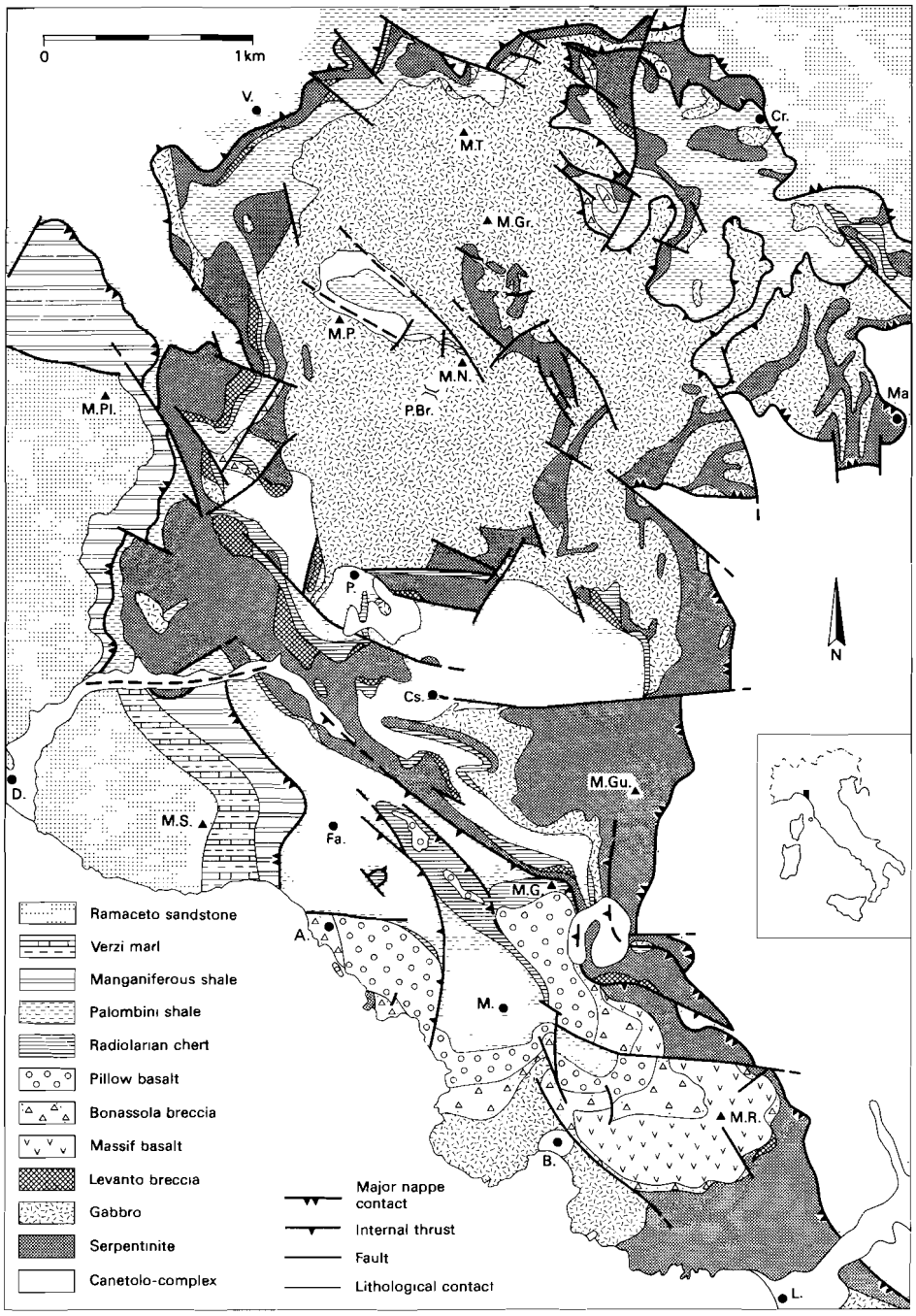

Fig. 2.1. Geological map of the Bracco ophiolite complex A= Anzo, B= Bonassola, Cr= Canu, Cs=Castagnola, D= Deiva Marina, Fa=Framura, L= Lèvanto, M= Montaretto, Ma= Mattarana, M.Gr= Mt. Groppi, M.Gu= Mt. Guaitarola, M.N.=Mt. S. Nicolao, M.P= Mt. Pietra di Vasca, M.Pl= Mt. Pian del Lupo, M.R= Mt. Rossola, M.S= Mt. Serra. M.T= Mt. Taversa, P= Piazza, P.Br= Passo del Bracco, V=

2.2 STRATIGRAPHY

Using tectonic superposition, recognition of basal thrust contacts and internal stratigraphy, three nappes are distinguished in the Bracco area (Fig. 2.1, 2.2). The uppermost Lavagna Nappe consists of a turbidite sequence which evolved from a distal to a proximal facies through time. In the underlying Mélange Nappe an ophiolite complex with its pelagic sedimentary cover is exposed. The lowermost Canetolo Nappe is characterised by numerous olistostromes, containing olistoliths from the overlying nappes. The stratigraphic nomenclature of Van Wamel et al. (1985) is used and the detailed stratigraphy of each nappe is as follows (see Fig. 2.2):

The Lavagna Nappe

The oldest sediments observed in the Lavagna Nappe of the Bracco area are manganiferous shales with intercalations of siltstones and fine grained terrigenous sandstones (Manganiferous shale), grading upward into a sequence of marls with

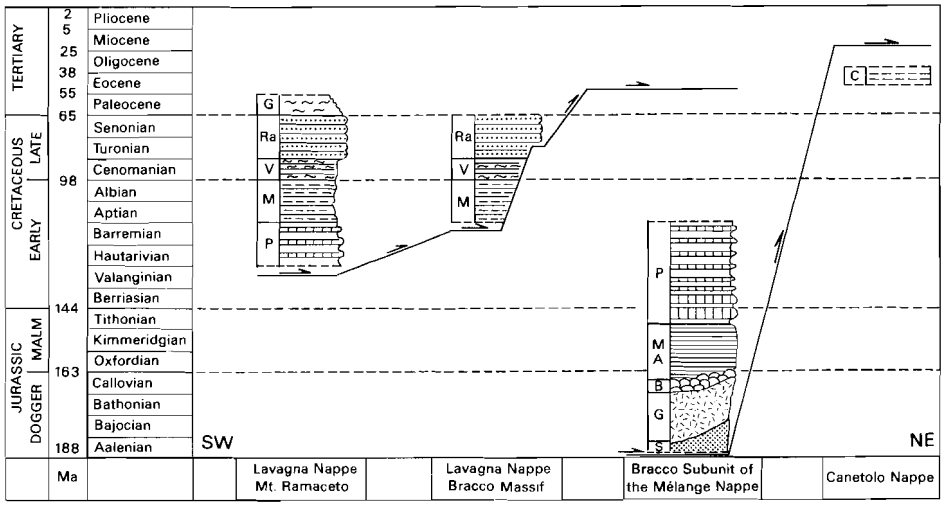

Fig. 2.2. Stratigraphy of the thrust units in the Bracco area and of the Lavagna Nappe in the Ramaceto area. Timescale adopted from Harland et al. (1982). P = Palombini shale, M = Manganiferous shale, V = Verzi marl, Ra = Ramaceto sandstone, G = Giariette shale, S = Serpentinite, Ga = Gabbro, B = Basalt and ophiolitic breccias, MA = Mt. Alpe chert, C = Canetolo complex.

interbeds of shales and calcarenites (Verzi marl). These formations are interpreted as an Aptian to Turonian (Meccheri et al. 1986) sequence of distal terrigenous clastic turbidites, intercalated in hemipelagic shale (Casnedi 1982). The uppermost formation in the Lavagna Nappe is the Ramaceto sandstone, a Turonian to Maastrichtian (Monechi & Treves 1984, Meccheri et al. 1986) turbidite sequence. Towards the NW progressively older stratigraphic units occur in the Lavagna Nappe. In the area of Mt. Ramaceto (Fig. 1.2, north of Chiavari), Van Zutphen et al. (1985) and Meccheri et al.

(1986) described a stratigraphic transition from the Manganiferous shales to underlying Palombini shales, similar to the Palombini shales described from the Mélange Nappe (see below). North of Genova the Palombini shales in the Lavagna Nappe are underlain by an ophiolitic basement (Chapter 3.4), comparable to that described from the Mélange Nappe (see below) and consisting of chert, pillow basalt and serpentinite of supposedly Late Jurassic age (e.g. Cortesogno & Haccard 1984). Moreover, in the area of Mt. Ramaceto, a stratigraphic contact exists between the Ramaceto sandstone and the overlying Giariette shale Formation (Fig. 2.2) of multicoloured shales and intercalated olistostromes of Paleocene age (Monechi & Treves 1984). The olistostromes point to extensive synsedimentary deformation during the Paleocene (Van Zutphen et al. 1985; Meccheri et al. 1986).

The Mélange Nappe

The Mélange Nappe consists of a laterally varying sequence of ultramafic, mafic and sedimentary rocks. The basal lithologies of this ophiolite complex are serpentinite and gabbro. At the contact between serpentinite and overlying lithologies, carbonate- and hematite rich serpentinite breccias occur (Levanto breccia, ophicalcite; Cortesogno et al. 1978). In the Mt. Rossola-Framura area (Fig. 2.1) the serpentinite-gabbro-ophicalcite basement is stratigraphically overlain by a volcano-sedimentary complex consisting of massive basalt, monomict and polymict ophiolite breccias (Bonassola breccia; Cortesogno et al. 1978) and pillow basalt. Zircon fission track dating yields Middle Jurassic ages of 161 to 185 Ma for the gabbro and Middle Callovian ages of 164 to 166 Ma for the basalt (Bigazzi et al. 1973). The sedimentary cover consists of radiolarian chert with siliceous shale (Mt. Alpe chert) of Middle/Late Callovian to Tithonian age (Baumgartner 1987) overlain by pelagic black shales alternating with siliceous limestone beds of Tithonian (?) to Aptian age (Palombini shale; Cortesogno et al. 1987). The limestone beds are interpreted as distal turbidites of resedimented hemipelagic calcilutite (Decandia & Elter 1972; Andri & Fanucci 1975).

The Canetolo Nappe

The Canetolo Nappe in the Bracco area consists of black shales with interbeds of turbiditic siltstones, fine grained sandstones and calcisiltites. Sedimentation was interrupted by intra-formational slumps and by numerous olistostromes, containing olistoliths from both the Mélange Nappe and the Lavagna Nappe. The constituent rock sequence is a disrupted equivalent of the "Argille e Calcare", a series of distal terrigenous clastic turbidites, intercalated in hemipelagic shales, deposited on and at the base of a continental slope (Montanari & Rossi 1982). Towards the east this rock sequence becomes increasingly disrupted and intercalated with progressively younger shales (Montanari & Rossi 1982). An Eocene to Middle (?) Oligocene age has been inferred for the Canetolo Nappe in the Bracco area, although this dating is not very accurate due to scarcity and reworking of microfossils (Abbate 1969).

2.3 DEFORMATIONAL STRUCTURES IN THE BRACCO AREA

In the following section a detailed description of the deformational structures in the Lavagna, Mélange and Canetolo Nappe is presented. In each nappe the folding phases are labelled in their sequence of development, as inferred from overprinting relationships. It should be noted, however, that each nappe may have gone through a similar deformation sequence, resulting in a similar set of geometrically related structures, although not necessarily at the same moment in geological time.

The Lavagna Nappe

The oldest structures observed in the Lavagna Nappe are dm-scale SW (Alpine) facing asymmetric isoclinal folds (F1) and a well developed axial-plane slaty cleavage (S1). The S1 cleavage is overprinted by a 500 m-scale, NE (Apennine) facing, tight recumbent fold (F2) with an axial plane crenulation cleavage (S2; see Enclosure 1: section 6). This fold is associated with thrusts which sole into the basal nappe contact. This suggests that the development of this latter fold and the thrusts is closely related to the emplacement of the Lavagna Nappe over the Mélange Nappe. Riedel shears developed in the fault rocks of the nappe contact and internal thrusts indicate transport towards the NE. The basal nappe contact of the Lavagna Nappe climbes up-section in the direction of transport from the Manganiferous shale in the SW to the Ramaceto sandstone in the NE.

The S2 cleavage is refolded by dm-scale conjugate folds (F3), indicating shortening in a NE-SW direction. Development of these structures was presumably related to the final stages of nappe emplacement. All older structures, including the basal thrust contact, dip 40° SW near Deiva Marina and 25° NE near Carro (Enclosure 1; section 6). These orientations result from the development of a regional scale antiformal culmination (F4) which post-dates the NE directed emplacement of the Lavagna Nappe over the Mélange Nappe. In addition, all older structures show a 15 to 20° WNW inclination.

The Mélange Nappe

The oldest structure observed in the area is a penetrative slaty cleavage (S1) which is parallel to the axial plane of local isoclinal folds (F1; Fig. 2.3). When the effect of later folding is removed, the F1 folds face SW. Mesoscopic structures related to this Alpine directed deformation phase are preferably developed in the Palombini shale. In many localities there is an obvious shear strain component associated with this cleavage (Fig. 2.3A, B). A considerable part of this shear strain component is thought to have accumulated during F1 folding. In the area around Montaretto (Fig. 2.1) the younging direction in the Palombini shale and the asymmetry of mesoscopic SW facing F1 folds are consistent with a normal limb of a major F1 fold. F1 folds around Framura, Castagnola, Piazza and in the zone curving around the western side of the gabbroic Bracco Massif (Fig. 2.1) also face SW. Fold asymmetry and overturning of the bedding in these areas indicates the presence of major F1 hinges. Both normal and overturned Palombini shale sequences are underlain by an upright ophiolite sequence and overlain by an overturned

ophiolite sequence. The upright and overturned sequences are separated by a low-angle fault. Riedel shears developed along this fault contact indicate a NE directed transport of the hanging wall, i.e. opposite to the SW facing direction of the F1 folds. NE of the Bracco Massif F1 folds are very common. They are dominantly symmetrical and are NE facing (Fig. 2.3C). Boudinage, and transposition of the bedding to the plane of S1 suggest an important component of extension parallel to the foliation. The change of the facing from SW to NE clearly results from refolding (F3, see below).

Locally, NE vergent asymmetric folds (F2) overprint F1 structures in both the normal and overturned Palombini shale sequences. There is no foliation developed in relation to these folds. No relationships have been found between the F2 folds and the low-angle fault separating the upright from the overturned F1 folded Palombini shale sequences.

The F1 and F2 structures and the low-angle fault are refolded by 500 m-scale NE-vergent recumbent F3 folds (Enclosure 1). These folds represent the typical Apennine directed structures recognized by earlier workers (e.g. Abbate 1969; Decandia & Elter 1972; Pertusati & Horrenberger 1976; Galbiati 1978). The F3 folds show an axial plane crenulation cleavage (S3, see Fig. 2.4), and they are closely associated with thrusts related to emplacement of the nappe. In the area around Castagnola and Piazza no clear S3 cleavage is developed and no F3 folds are observed. NE of the Bracco Massif, however, F3 structures are again predominant. As already suggested by Decandia and Elter (1972) and Galbiati (1978), the NE margin of the Bracco Massif appears to be a NE-vergent antiform. However, the structure must be more complex than previously thought (Enclosure 1; sections 6, 8 to 11). Rather than a clear F3 antiformal closure, the structure consists of a slightly asymmetric F3 folded hanging wall, thrust over a strongly shortened footwall. The S3 cleavage in both the hanging- and footwall is subhorizontal or dips slightly NE. In the footwall a SW dipping duplex is recognized, with horses of serpentinite-ophicalcite-chert and Palombini shale sequences (Enclo-

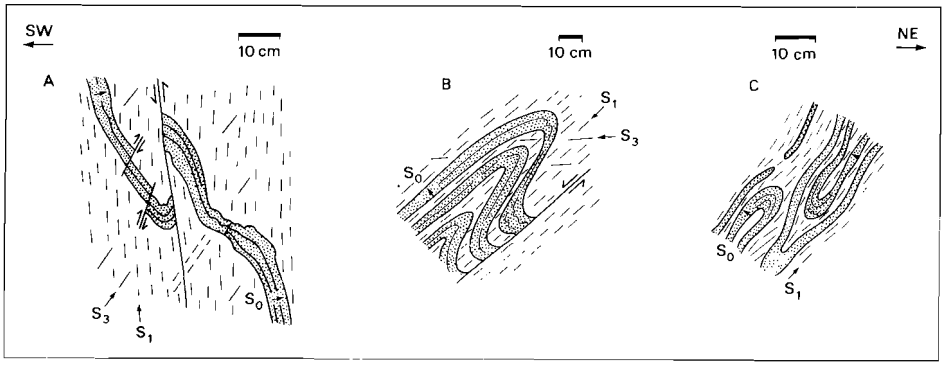

Fig. 2.3. Examples of mesoscopic F1 folds in Palombini shale of the Mélange Nappe. Folds shown in [A] (1 km NW of Montaretto; Enclosure 1, section 3) and [B] (1 km S of Carro; Enclosure 1, section 6) are typical examples of asymmetric folds with a distinct shear strain component associated with the S1 cleavage. [C] Symmetric isoclinal folds and boudinage in the plane of the S1 foliation (1 km SW of Carro; Enclosure 1, section 8). Arrows indicate observed younging directions. Note that all three examples are located in steep to overturned limbs of F3 folds.

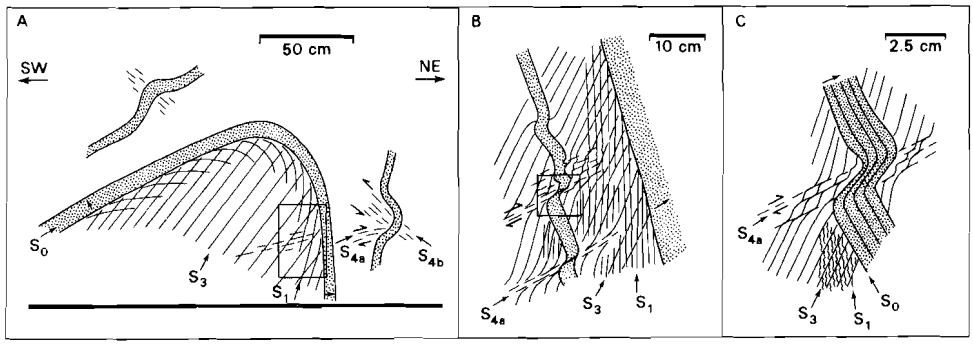

Fig. 2.4. Schematic representation, based on field sketches and photographs, of a road-cut near Montaretto (Mélange Nappe; Enclosure 1, section 2), showing bedding and S_1 cleavage in Palombini shale refolded by F_3. The S_3 crenulation cleavage is refolded by conjugate F_4 folds and associated crenulation cleavages (S_{4a}, b). Small arrows indicate younging directions. Insets in [A] and [B] indicate locations of [B] and [C].

sure 1; sections 8 to 11). The basal contact of the Mélange Nappe represents the floor thrust, whereas the basal contact of the overlying Lavagna Nappe constitutes the roof thrust. Riedel shears and striations developed along the basal nappe contact and the internal thrusts of the Mélange Nappe consistently indicate tectonic transport towards the NE.

F4 kinkbands and conjugate folds (Fig. 2.4), locally accompanied by a conjugate set of crenulation cleavages (S4a and S4b), are common in the Palombini shales. These structures overprint F3 folds and internal thrusts and their orientations are consistent with ongoing SW-NE directed shortening. The conjugate folds probably developed during the waning stages of nappe transport. After thrusting of the Lavagna over the Mélange Nappe, the two units have been refolded, leading to the development of a regional-scale NW-SE trending antiformal culmination (F5; see Enclosure 1, section 6), followed by a 20 to 30° NE tilting and the development of (N)NE-(S)SW trending monoclines (F6).

The Canetolo Nappe

Within the Canetolo Nappe, only local open to tight NE (Apennine) facing folds (F1) are encountered (not included in Enclosure 1). Occasionally, a weak cleavage is developed in the hinge-zones. The development of a NW-SE trending antiformal culmination and the NW tilting, described above, are also observed in the Canetolo Nappe.

2.4 RECONSTRUCTION OF THE PRE-F3 STRUCTURE IN THE MELANGE NAPPE

The deformational structures described above imply that the change from SW to NE directed structures is associated not only with the development of NE facing F2 and F3 folds superimposed on earlier SW vergent F1 folds, but also with the development, at least in the Mélange nappe, of a major low-angle fault. This fault shows a NE directed movement sense, transects a large-scale SW directed F1 structure, and is folded by F3. The development of this fault is therefore crucial to the general change in polarity from Alpine to Apennine transport directions, which renders a reconstruction of the pre-F3 geometry extremely interesting. Such a reconstruction is shown in Figure 2.5A. For the purpose of this reconstruction it has been assumed that the approximately coaxial F3, F4 and F5 folds are all cylindrical and can thus be restored by simple unfolding in a plane perpendicular to the mean fold axis of these folds. Movements along internal thrusts and vertical faults have been restored as accurately as possible.

The reconstruction shows a normal and an overturned ophiolite sequence, separated by a zone of either normal or overturned Palombini shale. The normal and overturned sequences are separated by a low-angle fault which cuts down-section from SW to NE (Fig. 2.5A). After unfolding, the Palombini shale sequence shows internal deformation characterized by SW-facing recumbent F1 folds. Towards the NE the z-asymmetric isoclinal folds (looking NW) in the overturned Palombini shale sequence pass into a zone with symmetric isoclinal folds, which marks the transition from the overturned limb to the hinge zone of an F1 fold. This hinge zone is characterized by a very

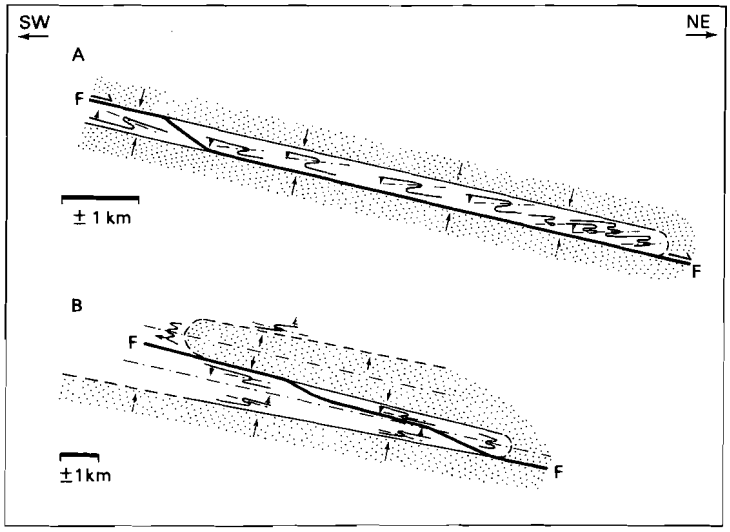

Fig. 2.5. [A] Reconstruction of the pre F3 structure in the Bracco Subunit, obtained after unfolding of F3, F4 and F5 and restoration of movements along internal thrusts and vertical faults. Shaded area: ophiolite complex; blank area: Palombini shale sequence. Observed younging directions (arrows), mesoscopic F1 folds and low-angle fault (F) are indicated. [B] Reconstructed F1 structure before movement along low-angle NE-dipping extensional fault (F).

pronounced NE-SW directed extension and transposition of the bedding into the S1 foliation plane (Fig. 2.3C). Both in the overturned and in the normal sequences the shear strain component associated with the S1 foliation indicates a SW directed displacement of the hanging wall (Fig. 2.3A, B).

The mesoscopic structures described above thus point to the former existence of a large Alpine vergent recumbent F1 fold with an overturned limb-length of at least 7 kilometres (Fig. 2.5B). Due to moderate outcrop conditions, only one outcrop allowed to assess a NE directed movement sense on the low-angle fault between the normal and overturned sequences. This indicates that the structure is an extensional fault, consistent with the omission of an F1 hinge zone in most of the southwestern part of the area (Fig. 2.5A, 2.6).

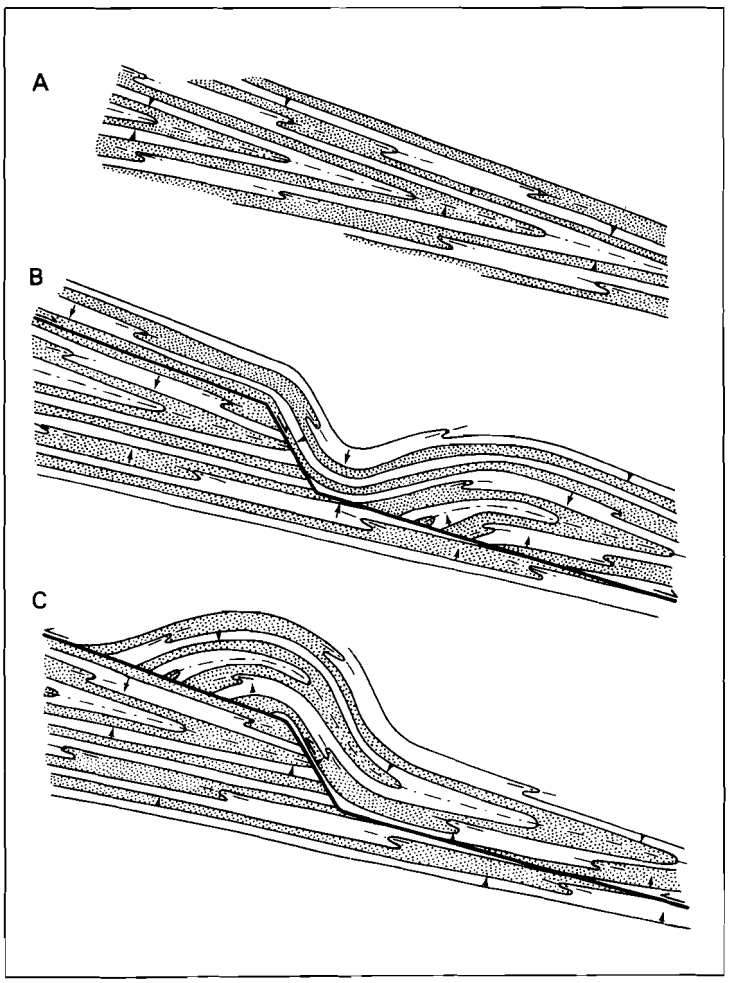

Fig. 2.6. Schematic representation of structures expected when an isoclinal recumbent fold [A] is dissected by an extensional fault [B] or thrust [C]. The structure resulting from extension [B] is consistent with the omission of a hinge zone, and juxtaposition of an overturned limb and a normal limb.

The above interpretation of the pre-F3 structure in the Mélange Nappe of the Bracco area is strongly analogous to that of the pre-F3 structure inferred for the Lavagna Nappe in the area of Mt. Ramaceto (Van Zutphen et al. 1985). These workers reconstructed a major SW-facing isoclinal F1 fold with an overturned limb-length of at least 10 km. This latter structure is also dissected by a low-angle NE dipping extensional fault (the Mt. Rondanara fault) which cuts down-section towards the NE.

From these reconstructions it emerges that km-scale Alpine vergent isoclinal folds were dissected by low-angle Apennine directed extensional faults, most probably related to the development of Apennine vergent asymmetric F2 folds. The development of these structures predated extensive Apennine directed recumbent folding (F3) and nappe emplacement. The observation that the earliest Apennine-directed structures were low-angle normal faults, suggests that the change of polarity involved extension, hence thinning, of the early developed Alpine structures.

2.5 CORRELATION OF THE DEFORMATION IN THE BRACCO AREA WITH OTHER AREAS IN THE LIGURIAN APENNINES

The structures described here from the Lavagna, Mélange and Canetolo Nappes in the Bracco area can be correlated with similar deformation histories of these units documented by Van Wamel et al. (1985), Van Zutphen et al. (1985) and Meccheri et al. (1986) in regions to the NW. This correlation is schematically shown in Fig. 2.7. The deformation in the Lavagna Nappe of the Bracco area can largely be correlated with the deformation history of the Lavagna Nappe in the Mt. Ramaceto area (Fig. 2.7; Van Wamel et al., 1985; Van Zutphen et al., 1985), except for the F2 open folding which has not been observed at Bracco, presumably because of the small dimensions of the present study area.

The earliest structures described by Van Wamel et al. (1985) and Meccheri et al. (1986) from the Mélange Nappe in areas to the NW (Fig. 2.7), are NE directed tight to isoclinal recumbent folds. Earlier SW facing isoclinal folds such as described here have not been recognized in those areas. The Mélange Nappe occurs in a similar tectonic position underneath the Lavagna Nappe, and large parts of the stratigraphy of the Mélange Nappe in the Bracco area can be correlated with the Iscioli-Biscia Subunit of the Mélange Nappe to the NW (Van Wamel et al. 1985). It should be noted, however, that the stratigraphy of the Mélange Nappe in the Bracco area is equally reminiscent of the ophiolitic basement of the Lavagna Nappe near Genova. In addition, the deformation history appears to be almost identical to the deformation history of the Lavagna Nappe (Fig. 2.7). Therefore, it is not clear whether the ophiolites in the Bracco area represent a basal part of the Lavagne Nappe or, alternatively, a subunit of the Mélange Nappe. For present purposes, the ophiolites of the Bracco area are arbitrarily ascribed to the Mélange Nappe, and are mapped as the Bracco Subunit (Fig. 1.2, 2.8). These considerations have led to the following subdivision of the Mélange Nappe shown in Fig. 1.2: the Bracco Subunit, the Iscioli-Biscia Subunit, the Cassanova-Scabiazza Subunit, the Orocco Subunit and the Penice Subunit. Palinspastic recon-

LAVAGNA NAPPE (VAN ZUTPHEN et al. 1985)	LAVAGNA NAPPE (THIS STUDY)	BRACCO SUBUNIT OF THE MÉLANGE NAPPE (THIS STUDY)	OTHER SUBUNITS OF THE MÉLANGE NAPPE (VAN WAMEL et al. 1985)	CANETOLO NAPPE (THIS STUDY)	CANETOLO NAPPE (VAN WAMEL et al. 1985)
F1: SW FACING ISOCLINAL FOLDING WITH AXIAL PLANAR FOLIATION (S1)	F1: SW FACING ISOCLINICAL FOLDING WITH AXIAL PLANAR FOLIATION (S1)	F1: SW FACING ISOCLINICAL FOLDING AXIAL PLANAR FOLIATION (S1)			
F2: OPEN FOLDS WITHOUT AXIAL PLANAR FOLIATION EXTENSIONAL FAULTING	NOT OBSERVED	F2: NE RECUMBENT FACING FOLDS NO AXIAL PLANE FOLIATION EXTENSIONAL FAULTING			
F3: NE FACING OPEN-TIGHT FOLDING WITH AXIAL PLANAR FOLIATION (F3)	F2: NE FACING TIGHT FOLDING WITH AXIAL PLANAR FOLIATION (S2)	F3: NE FACING TIGHT FOLDING WITH AXIAL PLANAR FOLIATION (S3)	F1: NE FACING TIGHT FOLDING WITH AXIAL PLANAR FOLIATION IN HINGES (S1)		
F4: OPEN-VERY OPEN FOLDING LOCALLY WITH AXIAL PLANAR FOLIATION (S4)	F3: CONJUGATE FOLDING WITH SET OF CLEAVAGES (S3A, S3B)	F4: CONJUGATE FOLDING WITH SET OF CLEAVAGES (S4A, S4B)	F2: NE FACING OPEN TIGHT FOLDING WITH AXIAL PLANAR FOLIATION IN HINGES (S2)	F1: NE FACING TIGHT FOLDING WITH LOCALLY AXIAL PLANAR FOLIATION (S1)	F1: NE FACING OPEN TIGHT FOLDING
F3 AND F4 RELATED TO NAPPE EMPLACEMENT	F2 AND F3 RELATED TO NAPPE EMPLACEMENT	F3 AND F4 RELATED TO NAPPE EMPLACEMENT	NAPPE EMPLACEMENT	F1: RELATED TO NAPPE EMPLACEMENT	NAPPE EMPLACEMENT
F5: NW-SE TRENDING UNDULATION	F4: NW-SE TRENDING UNDULATION	F5: NW-SE TRENDING UNDULATION	F3: NW-SE TRENDING UNDULATION	F2: NW-SE TRENDING UNDULATION	F2: NW-SE TRENDING UNDULATION
F6: ENE-WSW TRENDING UNDULATION	F5: NW TILTING	F6: NW TILTING	F4: ENE-WSW TRENDING UNDULATION	F3: NW TILTING	F3: ENE-WSW TRENDING UNDULATION

Fig. 2.7. Schematic correlation between the deformation histories in the Lavagna, Mélange and Canetolo Nappes. See text for discussion.

struction (Van Wamel et al. 1985) suggest that the Bracco Subunit originally occupied the most internal, and the Penice Subunit the most external position.

The deformation history of the Canetolo Nappe described by Van Wamel et al. (1985) from regions to the NW, is identical to that of the Canetolo Nappe in the Bracco area (Fig. 2.7).

In this context it needs to be emphasized that nappe emplacement was diachronous (Van Wamel et al. 1985). The Lavagna Nappe was thrust over the Mélange Nappe during Paleocene-Eocene times, whereas thrusting of the mutually stacked nappes over the Canetolo Nappe occurred not before the Early Miocene. Only the post-nappe deformation in the various units occurred simultaneously.

2.6 METAMORPHISM

The rocks of the Lavagna Nappe have been subjected to a low-grade metamorphism ranging from zeolite facies in the Bracco area (200-300°C, 200-300 MPa; Cortesogno

& Venturelli 1978; Bonazzi et al.,1987), up to low-pressure blueschist facies north of Genova (300-350°C, 600-700 MPa; see Chapter 3.4). Cortesogno et al. (1979b) infer that the highest metamorphic grade was attained during the development of the slaty cleavage (S1), whereas subsequent folding (F3, F4) and nappe emplacement occurred under decreasing metamorphic conditions.

This is consistent with illite crystallinity studies in the Mt. Ramaceto area (Van Wamel et al. 1985) indicating that the highest metamorphic grade (high-grade zeolite facies) was attained before thrusting of the Lavagna Nappe over the Mélange Nappe (i.e. pre-F3). On the basis of illite crystallinity data (Cerrina Ferroni et al. 1985; Bonazzi et al. 1987) and mineral paragenesis in the ophiolitic rocks (Cortesogno & Venturelli 1978), a zeolite facies metamorphism has been inferred for the Bracco Subunit. Based on coal-rank data in the Canetolo Nappe, a high-diagenetic grade has been determined by Cerrina Ferroni et al. (1985).

2.7 TECTONIC IMPLICATIONS

According to Van Wamel (1987) the km-scale Alpine vergent isoclinal folds in the Lavagna Nappe developed during the Late Cretaceous to Paleocene in an accretionary wedge associated with an easterly dipping, intraoceanic subduction zone (Fig. 2.8A). Whole rock K/Ar dating of the zeolite to low-pressure blueschist metamorphism in the northern Apennines (Schamel 1974; Beccaluva et al. 1981) yields Late Cretaceous to earliest Paleocene ages between 59 and 83 Ma. The ophiolites from the Voltri Massif, affected by intense ductile deformation synchronous with peak high-pressure metamorphism during the Late Cretaceous, are considered to represent remnants of the subducted oceanic lithosphere (Piccardo et al. 1977; Hoogerduijn Strating et al. 1990; see also Chapters 3 and 4).

The Paleocene marks the onset of a reorganisation of plate movements in the Tethys (Dercourt et al. 1986; Dewey et al. 1989) leading to a drastic decrease of the convergence-rate between Africa and Europe, from about 10 km/Ma during the Late Cretaceous to less than 2 km/Ma during the Paleocene (cf. Dewey et al. 1989; Platt et al. 1989). Subduction in the Piemonte-Ligurian ocean ceased due to partial underplating of the European continental margin in the Late Eocene (Vanossi et al. 1984; see also Chapter 6), resulting in a change to a tectonic regime dominated by continental collision. Paleocene-Eocene deformation in the Ligurian Apennines was characterized by low-angle extensional faulting with an Apennine sense of movement and dissecting the early Alpine structures (Fig. 2.8B). Subsequently, Apennine directed recumbent folding, thrusting and nappe emplacement led to the development of a pile of nappes consisting of the Lavagna Nappe and the various subunits of the Mélange Nappe.

The above observations are consistent with a tectonicx scenario in which the polarity change from Alpine to Apennine transport directions took place in response to gravity collapse of the accretionary wedge built up during subduction. At the onset of the Paleocene, convergence in the Piemonte-Ligurian ocean had lasted for approximately 35 Ma. This timespan will have been long enough for the Alpine accretionary wedge

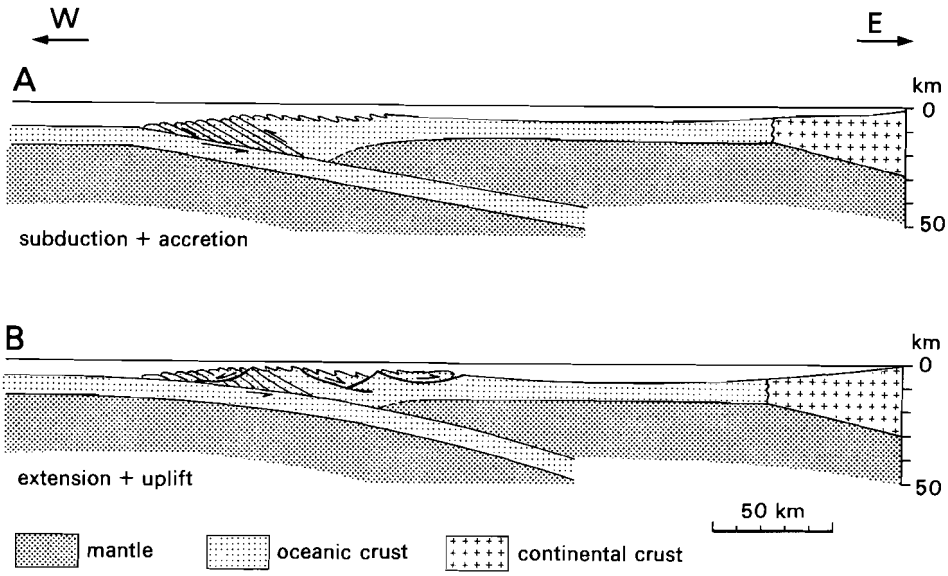

Fig. 2.8. Diagram illustrating a tectonic scenario for the Late Cretaceous and Paleocene in the Ligurian part of the Piemonte Ligurian ocean. [A] Intraoceanic subduction and development of an accretionary wedge during the Late Cretaceous to Paleocene. The Lavagna Nappe and Bracco Subunit were derived from the eastern side of the wedge (see Chapter 6). The high-pressure rocks of the Voltri Massif suffered peak metamorphic conditions in the subducting slab (see Chapters 3, 4, and 6). The other subunits of the Mélange Nappe (lacking the Alpine directed folding) were derived from the area in between the eastern edge of the accretionary wedge and the base of the continental slope (see also Chapter 6). The sediments of the Canetolo Nappe have been deposited on and at the base of the continental slope.[B] Slowing of subduction during the Paleocene resulted in gravitational collapse and presumably slight uplift of the accretionary wedge. The Lavagna Nappe and Bracco Subunit were emplaced in an easterly direction.

to attain mechanical (Platt 1986) and thermal equilibrium (Ernst 1988; Van den Beukel & Wortel 1988). It is generally accepted that a subduction-accretion complex can be treated as a wedge shaped continuum which behaves as a single, mechanically continuous, dynamic unit (e.g. Price 1973; Chapple 1978; Platt 1986). This implies that the wedge will deform internally in order to accomodate for changing boundary conditions such as subduction-rate and the ratio of frontal accretion versus underplating. An increase of subduction-rate may thus lead to shortening and thickening of the wedge; a decrease of subduction-rate may cause extension (Dahlen 1984; Platt 1986). In addition, the age and the descent velocity of the subducting oceanic lithosphere may have affected the stability of the wedge (cf. England & Wortel 1980; Vlaar & Cloetingh 1984). Note that the age of the lithosphere in the Piemonte-Ligurian ocean at the onset of subduction is suggested to have been less than about 55 Ma (Hoogerduijn Strating 1990; Chapter 6). Generally, in case of subduction of young, buoyant oceanic lithosphere, an increase of convergence rate may lead to relative subsidence of the overlying accretionary wedge. In contrast, a decrease may cause relative uplift of the wedge (cf.. England & Wortel 1980; Mitrovica et al. 1989). However, compared to the short-term vertical movements resulting from the internal deformation of the wedge,

these thermally-induced buoyancy effects are expected to be less pronounced (Wortel pers. comm. 1989). Although these effects have as yet not been quantified, it seems that a decreasing rate (Paleocene) and, eventually, cessation (Late Eocene) of subduction in the Piemonte-Ligurian ocean may well have led to uplift, gravitational instabilit and extension of the Alpine accretionary wedge. It is suggested here that the gravity collapse of the Alpine structures, the change to Apennine polarity in the Lavagna Nappe and Bracco Subunit, and the subsequent gravitational nappe emplacement in the Ligurian Apennines occurred in response to this decrease of subduction-rate.

In this tectonic scenario of a collapsing accretionary complex, it is expected that associated high-pressure metamorphic terrains have been exhumed rapidly. Such an event may be reflcted in a tectono-metamorphic evolution showing decompression under nearly isothermal to slightly decreasing temperature conditions (Thompson & England 1984; Platt 1986; Ernst 1988). Moreover, substantial movement on low-angle normal faults can result in juxtaposition of nappes showing an abrupt increase in metamorphic grade downward across these faults. In Chapter 3 it will be demonstrated that all of these phenomena are found in the Voltri Massif, the Sestri-Voltaggio Zone and the adjacent Lavagna Nappe (see Fig. 1.2).

ACKNOWLEDGEMENT

Andy Barnicoat (Leeds) is thanked for his comments and suggestions on the original manuscript published in the J. Geol. Soc. London.

CHAPTER 3

The Alpine structure of the Voltri Massif, Sestri-Voltaggio Zone and western Lavagna Nappe.

3.1 INTRODUCTION

Since many decades the Sestri-Voltaggio (SV) Zone (Fig. 1.2, 3.1) has played an important role in discussions on the boundary between the Alps and Apennines (e.g. Schneider 1935; Görler & Ibbeken 1963; Elter & Pertusati 1973; Schamel 1974; Cortesogno et al. 1979b). With the introduction of plate tectonics to the geology of the Alpine-Apennine arc (e.g., Boccaletti et al. 1971; Laubscher 1971) the N-S trending SV zone has been interpreted by most authors as a pre-Oligocene, sinistral transcurrent zone, while major E-W trending, sinistral transpressional faults of Neogene age have been inferred along the southern and northern margins of the Voltri Massif. These transcurrent faults are thought to have accommodated for Cenozoic rotational and lateral movements between the Eurasian and Adriatic plates (e.g. Dercourt et al. 1986; Laubscher 1988). In view of the crucial role of this area in any geodynamic interpretation, an astonishing contrast exists between on the one hand the abundance of kinematic analysis from the central and western Alps, and on the other hand the general lack of such data from the Ligurian Alps and Apennines (see Coward & Dietrich 1989; Platt et al.1989).

Detailed structural analyses of the Voltri Massif were not available to date, whilst recent studies in the Sestri-Voltaggio Zone and western Lavagna Nappe (e.g. Cortesogno & Haccard 1984; Marini 1984) yield conflicting interpretations. The aim of this chapter is to present an integrated structural analysis of the north-eastern Voltri Massif, the Sestri-Voltaggio Zone, and the western Lavagna Nappe. The implications of these structural data for the large-scale kinematics of the Alps-Apennine system are discussed in Chapter 6.

3.2 THE VOLTRI MASSIF

The large-scale structure of the Voltri Massif is dominated by a number of subhorizontal thrust sheets (Fig. 3.2; e.g. Chiesa et al. 1975; Piccardo et al. 1977). These thrust sheets compose the "Voltri Group", and include from the bottom upward the Voltri-Rossiglione (VR) Unit of Mesozoic high-pressure (HP) calcschists and metavolcanics,

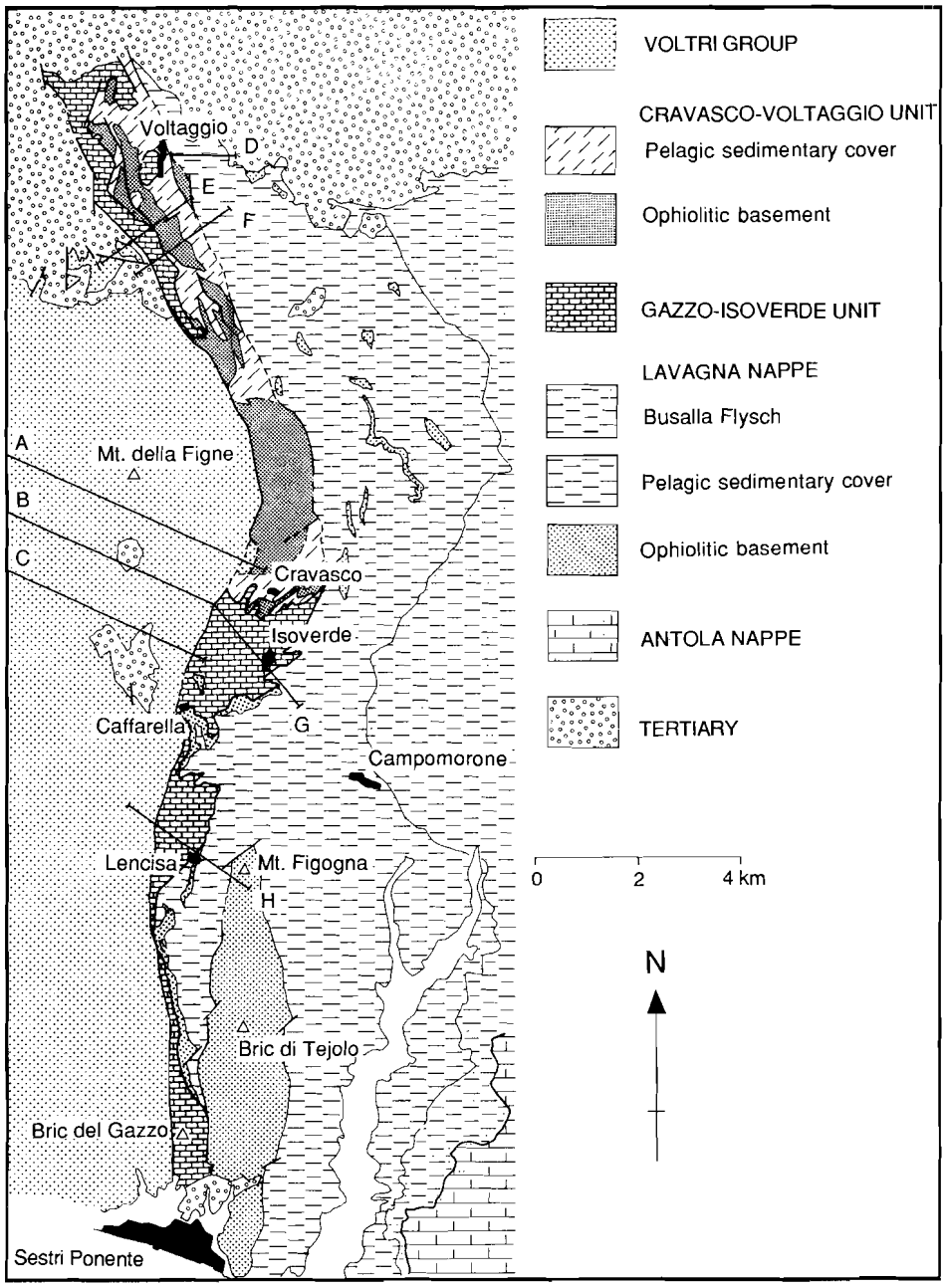

Figure. 3.1. Tectonic map of the Sestri-Voltaggio Zone, showing location of cross sections across the north-eastern Voltri Massif (sections A, B and C: Fig. 3.24) and Sestri- Voltaggio Zone (sections E, F, G, and H: Fig. 3.17).

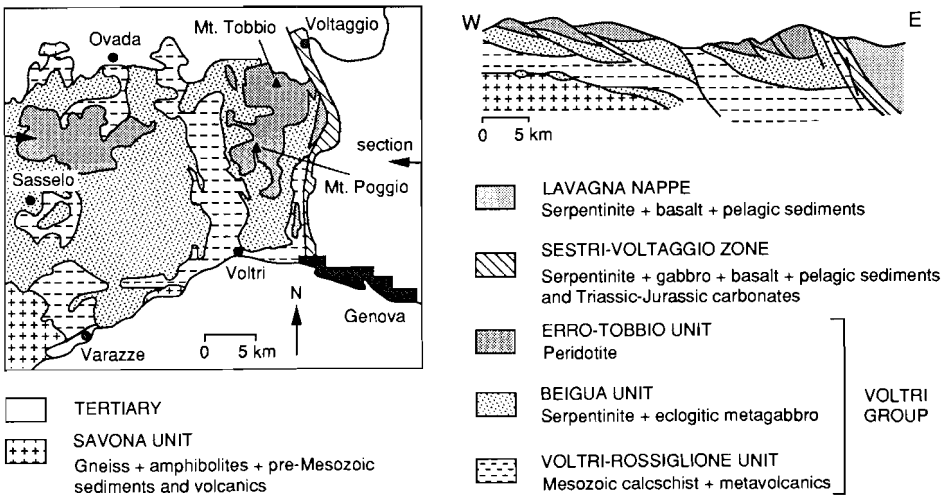

Figure. 3.2. Tectonic sketch-map and cross section showing the large-scale structure of the Voltri Massif, Sestri-Voltaggio Zone and western Lavagna Nappe. Approximate location of section shown on map.

the Beigua Unit of dominantly antigorite serpentinites with eclogitic metagabbros, and the Erro-Tobbio (ET) peridotites. A major thrust zone separates the Voltri Group from the underlying Savona Unit of Hercynian gneiss and amphibolites showing HP-greenschist to blueschist facies metamorphism related to the Alpine collision (e.g. Messiga 1987). The Voltri Group is tectonically overlain by blueschist facies ophiolitic and sedimentary rocks of the Sestri-Voltaggio Zone, in turn overlain by prehnite-pumpellyite to low-pressure blueschist facies ophiolites and sediments of the Lavagna Nappe.

The lithologies and geochemical characteristics of the VR and Beigua Units sugget that they represent fragments of an "oceanic" type lithosphere. They closely resemble the ophiolite sequences of the Internal Ligurian ophiolites in the Northern Apennines (i.e. Lavagna Nappe and the Bracco and Iscioli-Biscia Subunits of the Mélange Nappe; Piccardo et al. 1990). In contrast, the lithological and chemical characteristics of the ET peridotites strongly indicate an initially subcontinental origin, similar to the peridotites of Lanzo (Western Alps) and the External Ligurids (Cassanova-Scabiazza Subunit of the Mélange Nappe; Piccardo et al. 1990; Chapter 5).

On the basis of mesoscopic and microscopic overprinting relationships a sequence of deformational structures is recognized in each thrust unit. The timing between the development of these structures and the growth of metamorphic minerals is assessed primarily from microtextural relationships. The P-T conditions inferred here for the stability of the metamorphic assemblages are based on experimental phase equilibria and thermobarometers derived from hydrostatic experiments. This may pose some problems, as deviant conditions may be expected in natural rocks in case of equilibration under non-hydrostatic conditions. Any reduction of the partial pressure of water

will tend to reduce the temperatures for (de)hydration reactions. Thermodynamic calculations and experiments suggest that this effect is limited to several tens of degrees (e.g. Fyfe et al. 1978). Furthermore, dislocations induced in mineral lattices during deformation lead to an increase of the Gibbs free energy, which may affect reaction kinetics and favour the persistence of metastable phases in deforming rocks (Helgeson et al. 1978). Lack of experiental data, however, inhibits to quantify this effect. With these shortcomings in mind, the estimated P-T conditions for each deformation-metamorphism episode have primarily been based on experimental phase equilibria, while additional thermobarometers are used. Thermometry in mafic lithologies is based on the partitioning of Mg and Fe (Kd) between coexisting clinopyroxene and garnet (Ellis & Green 1979). This thermometer accounts for the influence of the grossular contents of garnet (X_{Ca}) on this equilibrium. Pressure constraints have been inferred from the jadeite contents of omphacite produced by the reaction albite = omphacite + quartz (Holland 1980), the pressure sensitive variation of the Si^{4+} content in phengitic mica (Massone & Schreyer 1987), and the crossite content of Ca-amphibole in the presence of albite, Fe-oxides and chlorite (Brown 1977).

All thrust units in the Voltri Group show an eclogite, a blueschist-eclogite, and a greenschist facies stage of mylonitic deformation. On the basis of correlation via the metagabbros of the Beigua Unit, these three tectono-metamorphic episodes are labelled D2-M2, D3-M3 and D4-M5 in each unit. A pre-eclogitic stage is labelled D1-M1, and a static barroisitic stage M4. In addition two stages of brittle deformation associated with the growth of zeolite facies minerals (M6) are labelled D5 and D6. Where any of these stages has not been recognized (e.g. pre-eclogitic D1-M1), episodes have been grouped (e.g. D1/2-M1/2). In the rocks of the Sestri-Voltaggio zone the same correlation applies, albeit that D2 and D3 occurred under blueschist- and D4 and D5 under prehnite-pumpellyite facies conditions. In the western Lavagna Nappe peak metamorphic D1/2 deformation involved low-pressure blueschist facies conditions, followed by prehnite-pumpellyite facies D3/4 deformation. All other deformational stages occurred under lower grade conditions. It should be noted that these episodes only refer to a relative timing on the basis of geometrical criteria.

The Voltri Rossiglione (VR) Unit

In view of recent structural work (D'Antonio et al. 1984; Amendolia & Capponi 1985; Capponi et al. 1986, 1987) and the generally poor outcrop conditions, this study of the VR Unit has been confined to areas close to the contact with the overlying Beigua Unit.

The dominant lithologies are calcschists and micaschists with local interbeds of quartzite and marble. Lenticular bodies of metabasite, largely replaced by an albite-actinolite-epidote (i.e. prasinite) assemblage, and serpentinite are commonly emplaced into the metasediments along shear zones or faults. Locally preserved primary contacts between the metabasites and the metasediments show a stratigraphy which strongly resembles that of the ophiolitic sequences in the Internal Ligurids. From the bottom upward the sequence consists of prasinite, quartzite sometimes associated with marble, calcschist and micaschist (Amendolia & Capponi 1985).

Calcschists

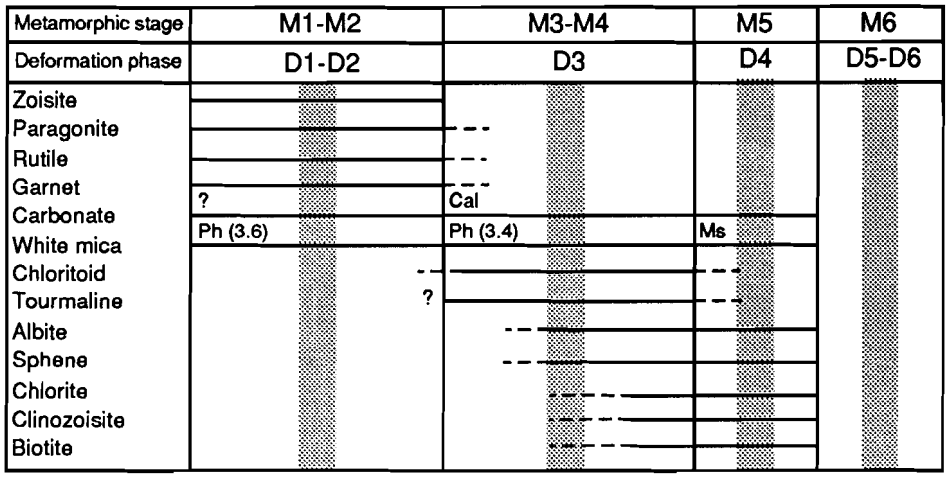

Metabasites

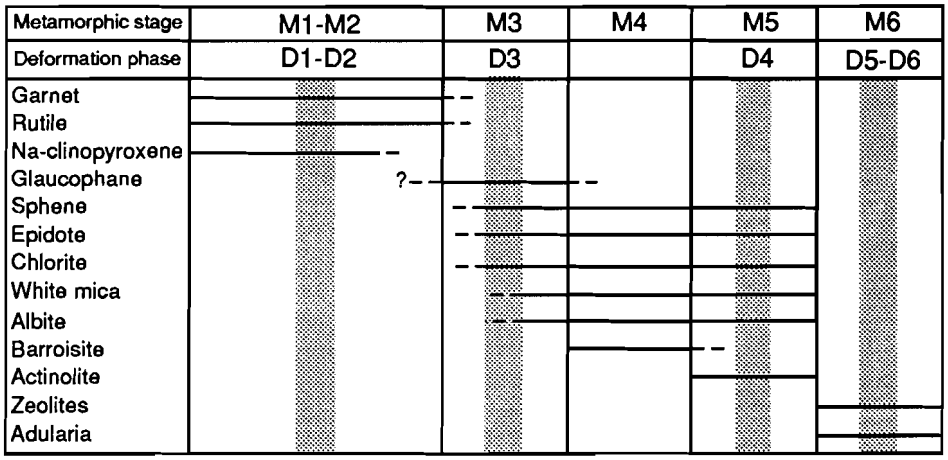

Figure 3.3. Relationships between deformation and metamorphism in the calcschists (modified after Cimmino & Messiga 1979) and metabasites (modified after Piccardo et al. 1979) of the Voltri-Rossiglion Unit

The deformation in the metasediments resulted in a generally 40 to 60° E dipping penetrative schistosity locally associated with isoclinal folds (D1/2). Some of these folds are isoclinally refolded and evolved progressively into sheath folds (D3). The metasediments are intensely recrystallized. E-W to SE-NW trending mineral lineations are developed on the foliation planes, and extensional crenulation cleavages (ecc's; Platt & Vissers 1980) or shear bands overprinting the schistosity are common. Although recognition of these early structures is hampered by later compositional banding and extensive transposition of the bedding and folds, the kinematic indicators and microstructures suggest that the D1/2 and D3 deformation in the VR Unit involved

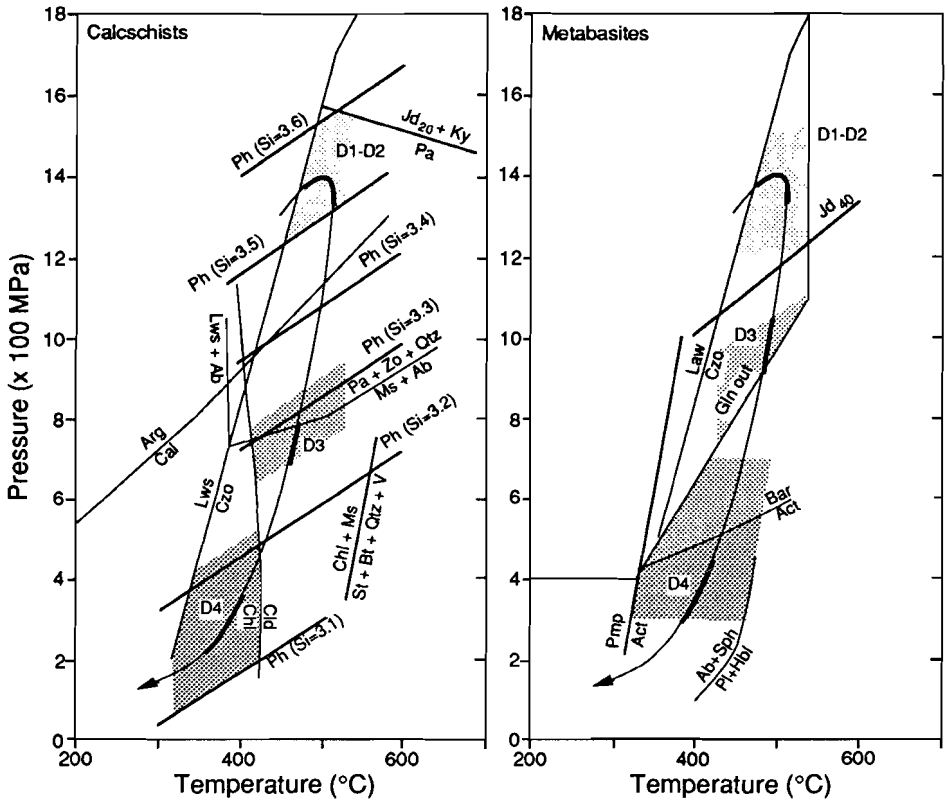

Figure 3.4. PT path inferred for the calcschists and metabasites from the Voltri-Rossiglione Unit. Aragonite (Arg)-calcite (Cal) transition after Johannes & Puhan (1971). Reaction paragonite (Pa) + zoisite (Zo) + quartz (Qtz) = muscovite (Ms) + albite (Ab) or lawsonite (Lws) + Ab after Franz & Althaus 1977. Reaction Pa + Gnt + Zo + Qtz = Omph + kyanite (Ky): Koons 1986. Lower stability of phengite (Ph) for various silicium contents after Massone & Schreyer 1987. Lws-clinozoisite (Czo) transition after Barnicoat & Fry 1986. Lower stability limit of staurolite (ST) + biotite (BT) + Qtz, and the cloritoid (Cld)-chlorite (Chl) transition after Hoscheck 1969. Glaucophane (Gln) out after Maresch 1977. Reaction Ab = Qtz + omphacite with variable jadite contents (Jd40) after Holland 1980. Reaction pumpellyite (Pmp) + Chl = Actinolite (Act) + epidote after Liou et al. 1983. Lower stability limit of barroisite (Bar) after Ernst 1979. Reaction Ab + sphene (Sph) = plagioclase (Pl) + hornblende (Hbl) after Moody et al. 1983.

W to NW directed thrusting in a ductile shear regime. Mineral assemblages associated with the earliest folds are rare due to intense greenschist facies recrystallization (D4-M5; see Fig. 3.3). Locally, however, garnet, rutile, silica-rich phengite ($Si_{3.6}$, range 3.5-3.7; Cimmino & Messiga 1979), paragonite, and zoisite occur, while paragonite breaks down during progressive deformation (D3), and chloritoid becomes stable with albite, sphene, phengite with lower silica contents ($Si_{3.4}$, range 3.3-3.5; Cimmino & Messiga 1979) and locally chlorite (Fig 3.3). The stability of garnet, paragonite, zoisite and phengite (Si>3.5) suggests eclogite facies metamorphic conditions of 450 to 550°C, at pressures between 1200 and 1500 MPa (Fig. 3.4, M1/2). The syn-D3

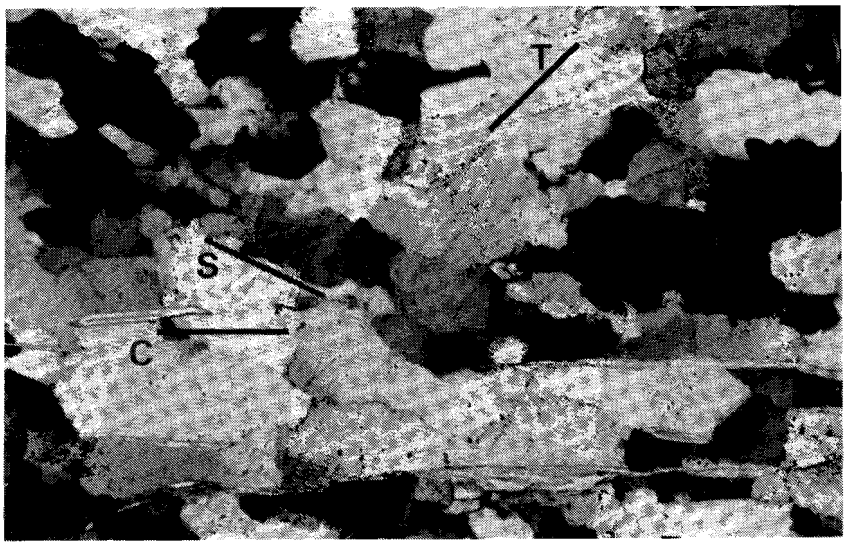

Figure 3.5. Photomicrograph (crossed nicols) showing oblique grainshape fabric developed in quartzite from the Voltri-Rossiglione unit. The obliquity of this fabric (S) with respect to the foliation plane defined aligned micas (C) indicates a sinistral sense of shear. Healed microcracks are visible as trails of fluid inclusions (T). Width of micrograph 0.64 mm.

assemblage of phengite, chloritoid and albite points to an evolution towards blueschist facies conditions of 700-900 MPa at temperatures exceeding 400°C (Fig. 3.3; M3/4), whilst the average Si content of phengite ($Si_{3.4}$) suggests that recrystallization may have started at pressures of about 1000 MPa.

The composite fabric described above is refolded in m-scale, open to tight, asymmetric W to NW facing folds, associated with a fanning crenulation foliation. Generally, these folds are non-coaxial and have 40-60° E to SE dipping axial planes. Oblique grainshape fabrics (i.e. type II S-C fabric; Lister & Snoke 1984) developed in the quartzites during this stage (Fig. 3.5). Such fabrics, as well as ecc's in the schists, indicate that folding occurred during W to NW directed ductile thrusting. A synkinematic greenschist facies assemblage developed of chlorite, muscovite ($Si_{3.1}$, range 3.0-3.25; Cimmino & Messiga 1979) and quartz (growing at the expense of chloritoid), with albite, biotite, clinozoisite and tourmaline (Fig. 3.3). The inferred P-T conditions are 200 to 400 MPa, at temperatures between 350 and 425°C (Fig. 3.4).

The mineral chemistry of the metabasites intercalated in the calcschists has not been studied to date, hence considerable uncertainty extists as to the equilibration conditions of the various assemblages observed (Fig. 3.3, 3.4). An early eclogitic stage (M1/2-D1/2) is indicated by the probably synkinematic growth of Na-clinopyroxene, garnet and rutile (Piccardo et al. 1979). Most metabasites have preserved a banded fabric, consisting of preferentially oriented glaucophane, chlorite, epidote, white mica, albite and sphene (M3-D3). This mylonitic fabric is tentatively correlated with the D3 (sheath) folds in the metasediments. Barroisite, in the presence of sphene, epidote,

chlorite, white mica and alblite (M4), grows statically at the expense of glaucophane, garnet and Na-clinopyroxene. Simultaneous with open D4 folding in the calcschists, a synkinematic greenschist facies (M5) assemblage of actinolite, sphene, epidote, white mica and albite developed in the metabasites.

All structures described above in the schists and metabasites are overprinted by open, NW verging folds associated with brittle thrusts (D5/6). Widely spaced kink-like crenulation cleavages are developed in the hinges of these folds. Kinematic indicators in the fault gouge (i.e. Riedel shears) point to thrusting towards the W-NW, while zeolite facies assemblages reported from brittle fractures and faults (Cortesogno et al. 1979b) suggest deformation at low-grade metamorphic conditions.

The Beigua Unit

The lithology of the Beigua Unit is dominated by antigorite serpentinites with occasional rhodingitic dykes, and 1m to 100 m-scale lenticular bodies of metagabbro and locally meta-basalt.

The earliest fabric (D1) observed in the serpentinites is a penetrative shear-induced foliation associated with isoclinal folds and possibly sheath folds (Fig. 3.6). In many localities this D1 fabric involves a composite structure made-up of a foliation overprinted by narrowly spaced ecc's. Gradual transitions from massive and essen-

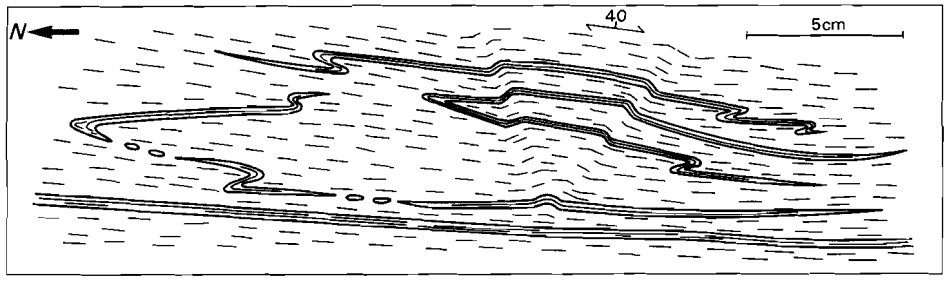

Figure 3.6. Map-view of a folded rodingite layer (garnet + vesuvianite) in foliated antigorite serpentinite. The penetrative axial-plane foliation is the oldest fabric observed in the Beigua serpentinite. Both foliation and magnetite lineation dip 40° ESE, such that the plane of drawing is at a high angle to the shear direction. The opposite vergences in the uppermost rhodingite band are consistent with a sheath fold geometry. The structure is deformed by a conjugate set of kinkbands.

tially undeformed, to strongly foliated serpentinite are common. This suggests that D1 strain was highly heterogeneous on a length scale between 1 dm and at least 100 m. Ecc's, asymmetric porphyroclast systems (Passchier & Simpson 1986) and the orientation of mineral lineations (Fig. 3.7) all indicate that these structures developed during WNW directed ductile thrusting of the hanging wall. On the micro-scale, the D1 foliation is defined by preferentially oriented antigorite, chlorite and magnetite (M1), while in the ecc's this assemblage is replaced by fine grained olivine + antigorite + chlorite + diopside + titanian clinohumite (D2/3-M2/3, Fig. 3.8; cf. Cimmino et al. 1979). The growth of these olivine-bearing assemblages is interpreted to result from progressive synkinematic dehydration of antigorite in the shear bands at temperatures

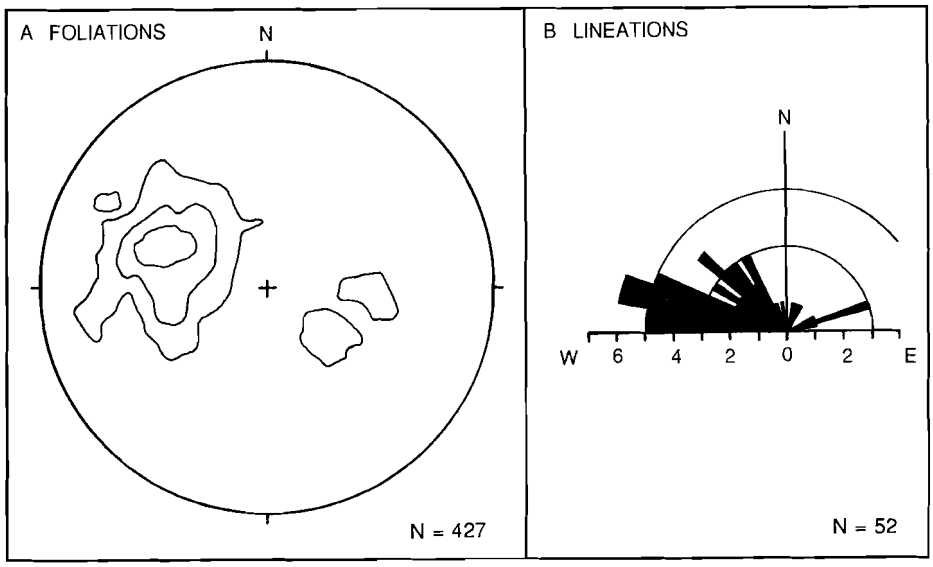

Fig. 3.7. A: Poles to shear-induced foliation planes in the Beigua serpentinites. Equal-area lower hemisphere projection, contours at 2, 4 and 6% per 1% area. Maximum value counted: 7.7%. B: Rose diagram showing the bearing of magnetite and antigorite lineations on the shear-induced foliation planes.

of about 500°C (Fig. 3.9; see Chapter 4.3 for a detailed discussion on the stability of this assemblage). Olivine-bearing assemblages also occur in small veins dissecting the foliation.

The composite D1-D3 fabric and the olivine-bearing veins are locally refolded by small-scale WNW vergent folds accompanied by a crenulation cleavage (D4). Towards the contact with the underlying VR Unit and the overlying ET Unit these crenulations are very intense, and complete transposition of the D1-D3 fabric in these areas is common. The D4 crenulations are associated with growth of antigorite and magnetite at the expense of olivine, while very close to the contact with the VR unit, extensive replacement occurs of antigorite by tremolite + talc + chlorite + calcite + dolomite (Fig. 3.8). The stability of these assemblages suggests lower temperature conditions, probably in the greenschist facies (Fig. 3.9; see below), during emplacement of the Beigua- onto the VR Unit.

The synmetamorphic D1-D3 and D4 structures are overprinted by multi-stage brittle deformation (D5/6), characterized by the development of faults and kink-like folds. Structures associated to faults on the outcrop-scale include cataclastic fault breccias and fault gouges in which synthetic Riedel shears developed. X-ray diffraction analyses show that antigorite in the gouge is replaced by lizardite and chrysotile, suggesting temperatures below 300°C during cataclasis. The orientation of striations on brittle faults (Fig. 3.10) and kinematic indicators in the gouges (i.e. Riedel shears), point to WNW to NNW directed thrusting.

The tectono-metamorphic evolution of the eclogitic Mg and Fe-Ti (i.e. ilmenite/

Serpentinites

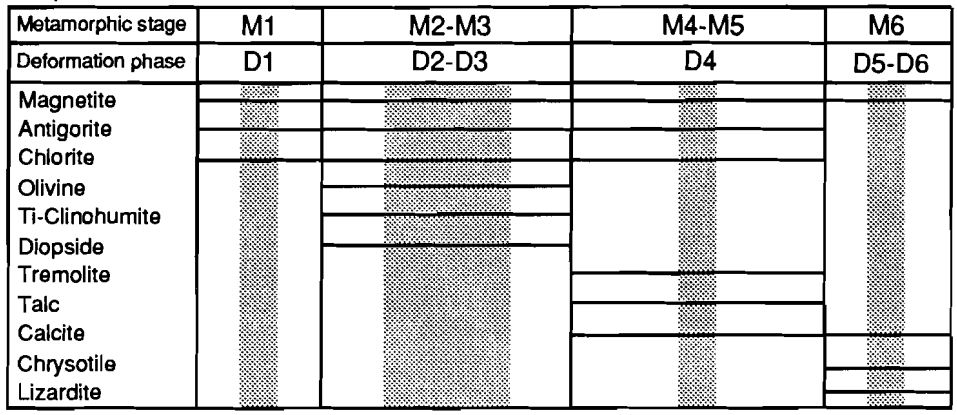

Metagabbros

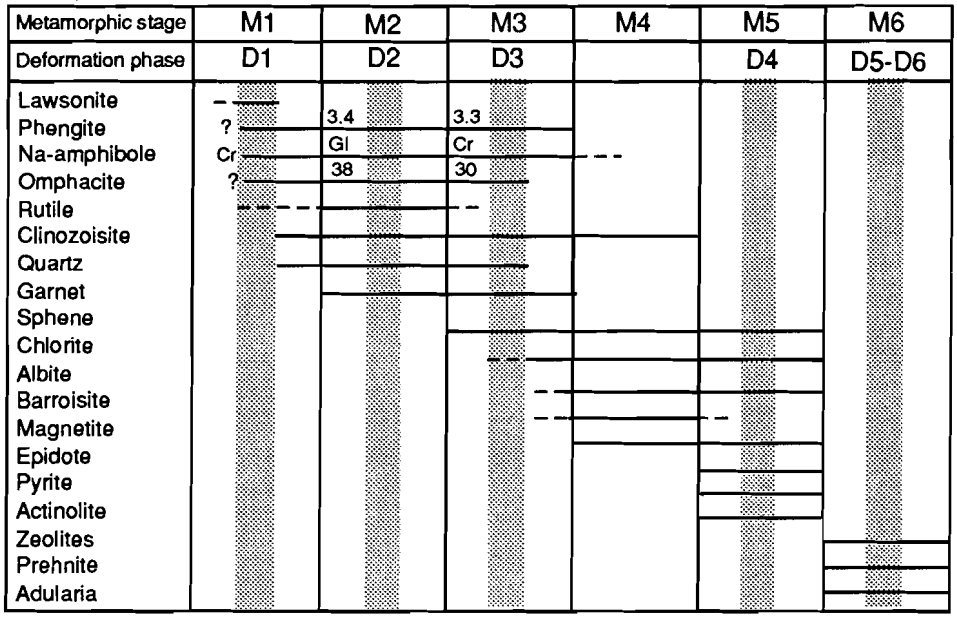

Figure 3.8. Relationships between deformation and metamorphism in the serpentinites and metagabbros of the Beigua Unit.

rutile/sphene-bearing) metagabbros in the Beigua Unit has already been studied in detail (e.g. Messiga & Piccardo 1974; Chiesa et al. 1975; Ernst 1976; Messiga et al. 1983; Scambelluri 1988). The oldest structure observed in the metagabbros is a shear-induced foliation defined by aligned clinopyroxene crystals. This foliation is cut by metabasaltic dykes. No relics are preserved of the stable mineral assemblage developed during this deformation event. However, these structures are remarkably similar to "oceanic" amphibolite facies mylonites developed in gabbros prior to basaltic dyke

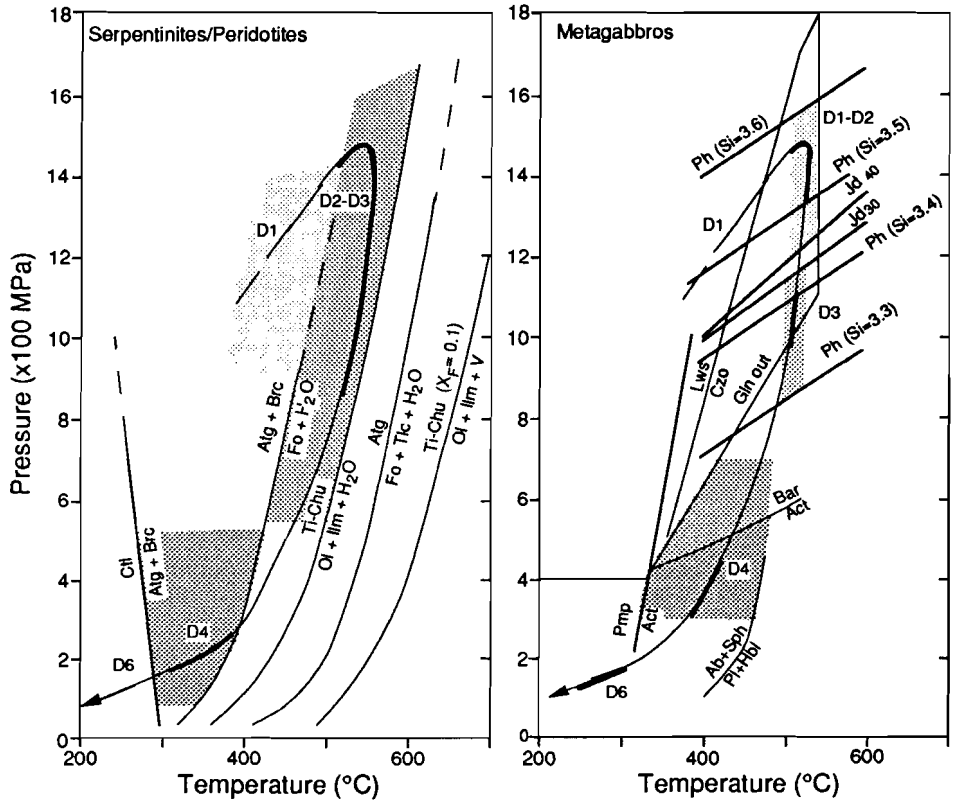

Figure 3.9. PT path inferred for the serpentinites and metagabbros of the Beigua Unit. Reactions similar to Fig. 3.4 except for reactions chrysotile (Ctl)= antigorite (Atg) + brucite (Brc), Atg + Brc = forsteritic olivine (Fo) and Atg + Fo + talc (Tlc) taken from Evans et al. 1976. Breakdown of Ti-clinohumite (Ti-Chu) to olivine (Ol) + ilmenite (Il) for different fluorine contents (X_F) after Engi & Lindsley 1980.

intrusion (e.g. Hoogerduijn Strating 1988; see also Chapter 3.4.2). Given this textural analogy, it is inferred here that these structures may also have been developed as "oceanic" high-temperature mylonites.

The dykes and metagabbros are deformed in metre to hundred metre-scale shear zones, characterized by a penetrative foliation of omphacite (Jd_{38}), glaucophane, garnet, rutile, quartz, clinozoisite, phengite ($Si_{3.4}$) and apatite (D2-M2; Fig. 3.8). This assemblage also developed in strain shadows of omphacite pseudomorphs (Jd_{28}) after pyroxenes of magmatic origin (Fig. 3.11A). The foliation bends around these porphyroclasts which are locally rimmed by coronas of more jadeitic omphacite (Fig. 3.11B). Olivine, only present in Mg metagabbros, is transformed into talc, Na-clinopyroxene, clinozoisite, chlorite and Ca-clinoamphibole. In a sample of a virtually undeformed Mg-gabbro with well developed coronitic textures, olivine pseudomorphs also contain chloritoid. Chloritoid is partially overgrown by talc and commonly occurs close to the contact with domains of originally plagioclase (cf. Kienast & Pognante

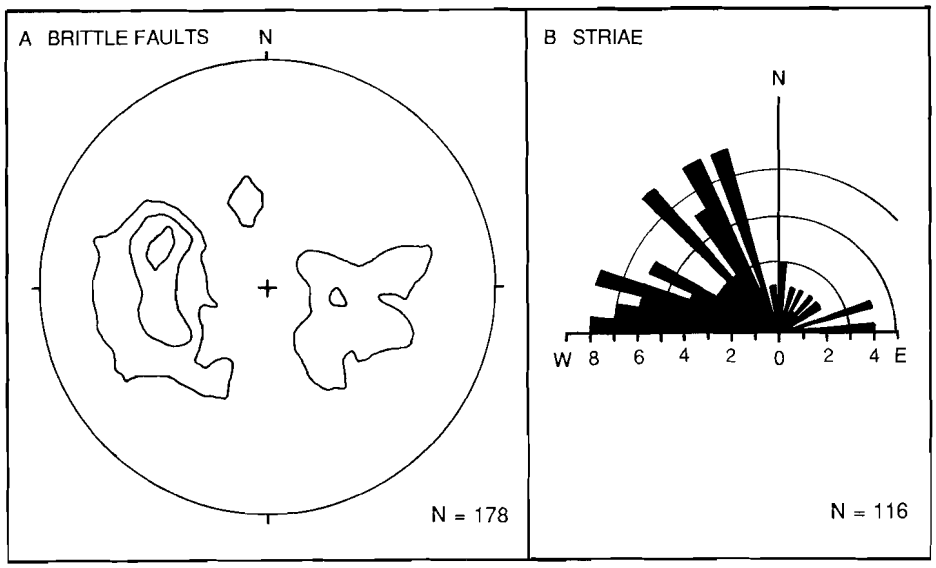

Figure 3.10. [A] Poles to brittle fault planes with a dip less than 65° in the Beigua and Erro-Tobbio Units. Equal area lower hemisphere projection, contours at 2, 4 and 6% per 1% area. Maximum value counted: 7.3%. [B] Rose diagram showing bearing of striae on brittle faults with dip less than 65°.Figure 3.10. [A] Poles to brittle fault planes with a dip less than 65° in the Beigua and Erro-Tobbio Units. Equal area lower hemisphere projection, contours at 2, 4 and 6% per 1% area. Maximum value counted: 7.3%. [B] Rose diagram showing bearing of striae on brittle faults with dip less than 65°.

1988). Thermobarometry of Mg (Messiga et al. 1983) and Fe-Ti metagabbros (Messiga et al. 1983; this study) suggests synkinematic eclogitic conditions of 500-530°C (Kd = 23-30, X_{Ca} = 0.29) and 1200-1500 MPa (Fig. 3.9). Slightly higher P-T estimates of 520 to 570°C (Kd= 10-14, X_{Ca}= 0.17) and 1200-1600 MPa are obtained from a metabasalt with a stable assemblage of omphacite (Jd_{38}), garnet, glaucophane, phengite ($Si_{3.6}$), rutile and quartz (see Appendix A2 for mineral chemistry). Glaucophane and omphacite mineral lineations show a general W-E to NW-SE orientation. Shear sense criteria such as asymmetric porphyroclast systems or ecc's are rare, however, when present they indicate a westerly directed displacement of the hanging wall.

Some of the largest M2 garnets in the metagabbros enclose a foliation consisting of crossite, paragonite, clinozoisite, Na clinopyroxene and sometimes rutile suggesting that earlier deformation has occurred, possibly under blueschist facies conditions (D1-M1; Fig. 3.7). In addition rectangular shaped pseudomorphs of clinozoisite + paragonite + quartz may indicate that lawsonite was also stable during this stage (Messiga et al. 1989).

The eclogitic foliation is locally overprinted by metre-scale shear zones with a foliation of crossite, clinozoisite, sphene, garnet, and sometimes omphacite (Jd_{30}), while crossite and phengite ($Si_{3.3}$) grew at the expense of omphacite porphyroclasts in the wall rock (D3-M3). Apatite porphyroclasts may be abundant in these shear zones and locally constitute up to 30% volume of the rock. These shear zones are inferred to have developed under blueschist to eclogite facies conditions of 500 to 525°C (Kd= 26-33,

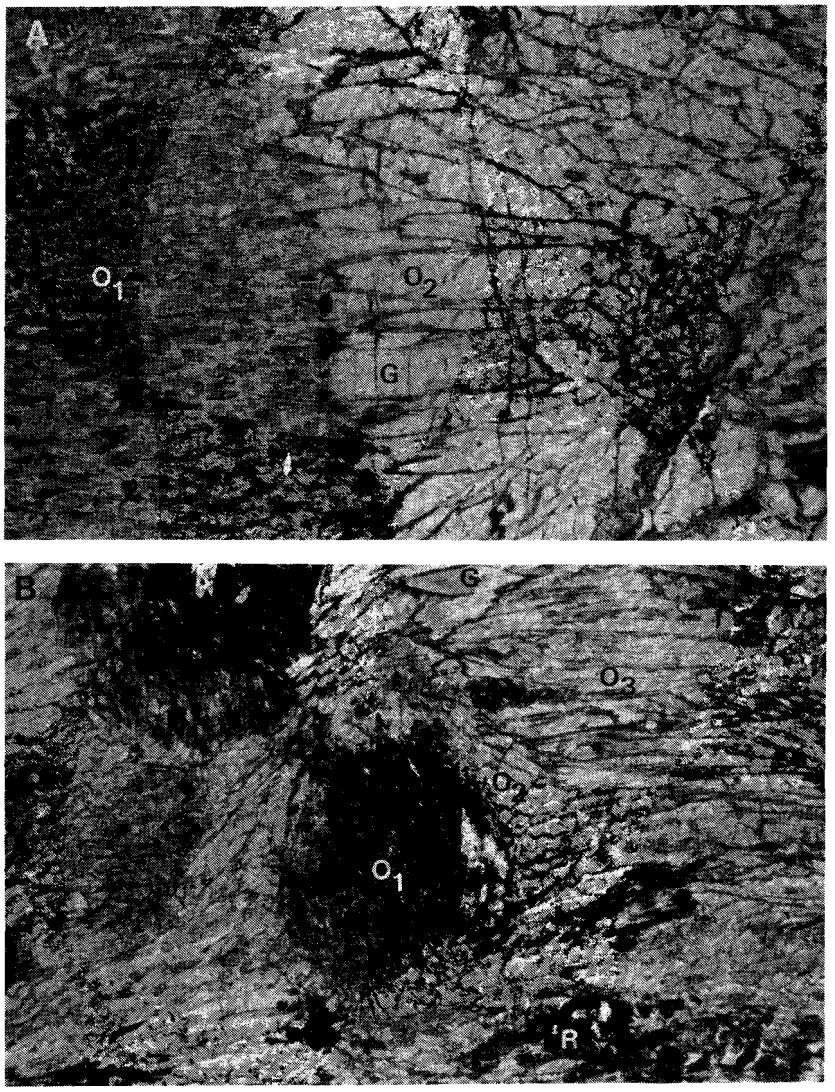

Figure 3.11. Photomicrographs (plane polarized light) of sheared eclogitic metagabbros from the Beigua Unit. A: Strain shadow with omphacite (O2) and glaucophane (G) adjacent to magmatic pyroxene completely pseudomorphosed to omphacite (O1). Note the strong growth zonation in the glaucophane. B: Magmatic pyroxene pseudomorphosed to omphacite (O1) and surrounded by a coronitic rim of omphacite (O2). The rimmed porphyroclast is embedded in a strongly foliated matrix consisting of omphacite (O3), glaucophane (G) and rutile (R). Width of both micrographs 1.4 mm.

X_{Ca}= 0.32) and 800 to 1100 MPa (see Appendix A2 for mineral chemistry).

Static replacement of omphacite, glaucophane and crossite by barroisite in the presence of albite, clinozoisite, chlorite, sphene and magnetite is very common (M4). The stability of this assemblage and the crossite contents of the barroisite suggest that recrystallization occurred at 400 to 500°C and 500 to 700 MPa. Scambelluri (1987) and

Messiga et al. (1989) describe symplectites of barroisite and Ca plagioclase (An_{47}) replacing garnet and Na-clinopyroxene from coronitic Fe-Ti metagabbros and cummingtonite + garnet + NaCa-amphibole (winchite) from mylonitized Fe-Ti metagabbros. According to experimental phase equilibria the Ca-rich composition of these assemblages is consistent with higher (i.e. amphibolite facies) equilibration temperatures during this stage. An alternative explanation involves selective Na-leaching by fluids migrating through the gabbros, thereby enhancing the stability of Ca-rich assemblages (cf. Messiga et al. 1989). There are no data available at present to discriminate between these two hypotheses.

Synkinematic transformation of barroisite to actinolite in the presence of albite, chlorite, epidote, sphene, magnetite and pyrite is common. This greenschist facies transformation at 350 to 450°C and 200 to 500 MPa is associated with the development of metre-scale shear zones and recumbent folds with axial plane crenulation foliations (D4-M5; Fig. 3.9). Kinematic indicators point to progressive NW directed ductile thrusting of the hanging wall during this stage. Brittle deformation in the metagabbros (D5/6) is restricted to the development of local shear fractures with zeolitic assemblages (M6; Cortesogno et al. 1979b).

Correlation between the early deformational structures in the serpentinites and metagabbros is difficult. However, the mutual evolution towards temperatures of over 500°C under eclogitic conditions strongly suggests, that the antigorite foliation in the serpentinites developed simultaneous with the blueschist to eclogite facies foliation preserved in M2 garnets in the metagabbros. The progressive deformation of the serpentinites leading to the development of olivine-bearing ecc's and veins most probably correlates with the peak eclogite (D2-M2) and eclogite-blueschist facies (D3-M3) shear deformation in the gabbros. Small eclogitic lenses are folded during D4, and the greenschist facies crenulations in these deformed metagabbros correlate with the antigorite-bearing (i.e. olivine-free) D4 crenulations in the surrounding serpentinite.

The Erro-Tobbio Unit

The dominant lithologies in the Erro-Tobbio unit are lherzolite, strongly foliated serpentinite, and metagabbroic and basaltic dykes. The petrology of these lithologies is described in detail in Chapter 4. Only for the purpose of correlation with the other units, deformation-metamorphism relationships are discussed briefly in this section. The earliest Alpine imprints recorded in these rocks are numerous serpentinite mylonites, characterized by a synkinematic assemblage of antigorite, chlorite and magnetite (D1-M1; Fig. 3.12, 3.13). In ecc's, developed progressively in these shear zones, this assemblage breaks down to fine grained olivine, Ti-clinohumite, diopside, magnetite, antigorite and chlorite (D2-M2). The shear-induced foliations are deformed in olivine bearing crenulations (D3-M3). In addition, olivine + Ti-clinohumite-bearing veins are very common, both in the serpentinite mylonites and the peridotite wall rock. Crenulations (D4) of the foliations and veins are associated with the break-down of olivine to antigorite (M4/5). Kinematic indicators and the orientation of magnetite and chlorite lineations (Fig. 3.14) show that all these structures developed

Serpentinites/Peridotites

Metamorphic stage	M1	M2-M3	M4-M5	M6
Deformation phase	D1	D2-D3	D4	D5-D6
Magnetite				
Antigorite				
Chlorite				
Olivine				
Ti-Clinohumite				
Diopside				
Pyrite			?	
Brucite				
Tremolite				
Chrysotile				
Lizardite				

Metagabbros

Metamorphic stage	M1-M2	M3-M4	M5	M6
Deformation phase	D1-D2	?	?	?
Chloritoid		not developed in samples studied		
Talc				
Omphacite	? 90			
Chlorite				
Garnet				
Zoisite				
Clinozoisite				
Quartz				
Albite				
Ca-amphibole				

Fig. 3.12. Relationships between deformation and metamorphism in the peridotites, serpentinite mylonites and metagabbos of the Erro-Tobbio Unit.

during progressive NNW directed ductile thrusting of the hanging wall. It should be noted that apart from the continuous reactivation of already existing shear zones, new shear zones were generated during each deformational stage. Younger sets of antigorite-bearing crenulations and ecc's deforming preexisting shear-induced foliations are common and suggest an inversion of the movement sense to easterly directed transport (D5). Brittle faults and folds (D6) are common and are associated with lizardite-chrysotile-magnetite gouges. Riedel shears and striations (Fig. 3.14) developed in the gouges point to dominantly WNW to NNW and, to a lesser extent, to SE directed thrusting of the hanging wall (D6).

Due to the almost complete insensitivety of the (de)hydration reactions in the ultramafic system to pressure (Fig. 3.13; Evans 1977), no pressure constraints are available. This implies, that only on the basis of a correlation with the deformation in the metagabbroic dykes (see below and Chapter 4.3) it is possible to assign the above assemblages to a prograde metamorphic history culminating at eclogite facies condi-

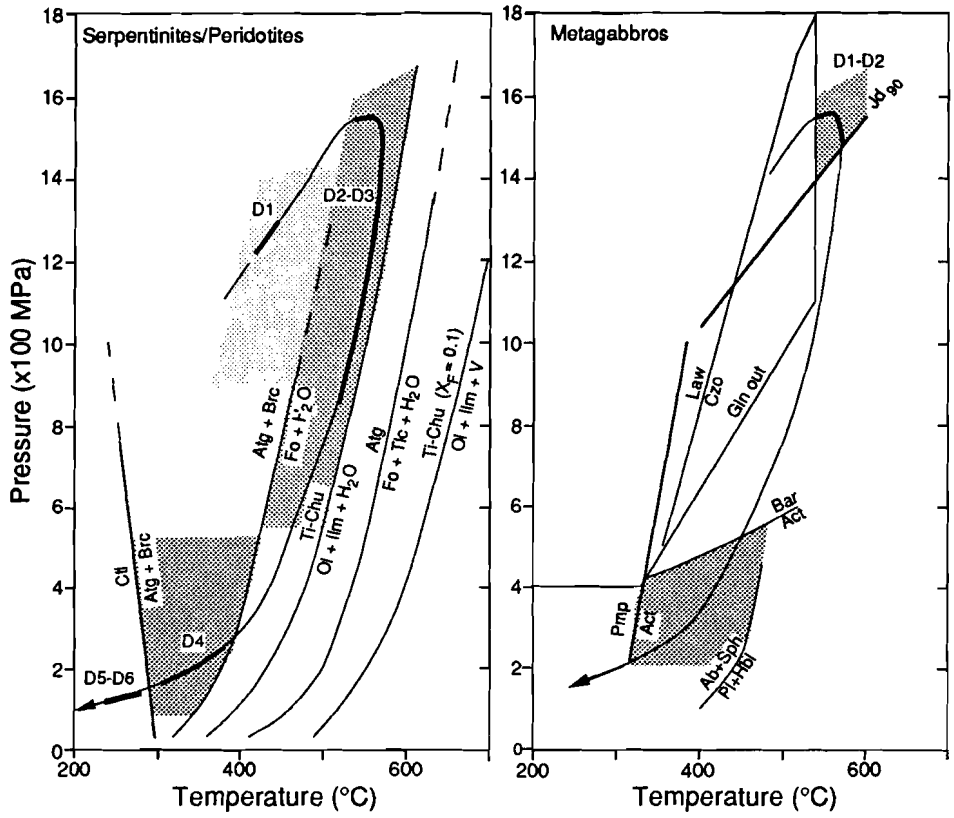

Fig. 3.13. P-T paths inferred for the peridotites, serpentinite mylonites and gabbroic dykes in the Erro-Tobbio Unit. Reactions similar to Fig 3.9.

tions. In any case the antigorite-bearing D1 fabric has developed at temperatures between 300°C and 450 to 500°C, while the presence of olivine and fluorine-free Ti-clinohumite (Chapter 4.3) suggets peak temperatures between 500 and 600°C during D2/3. Break-down of olivine points to temperatures between 300 to 450°C during D4 and D5. Lizardite + chrysotile bearing assemblages are restricted to brittle fault gouges, suggesting temperatures below 300°C during brittle deformation (D6).

The Mg-gabbroic dykes in the peridotites are transformed into eclogitic flaser gabbros (D1/2-M1/2). On the micro-scale, these flaser gabbros are characterized by large omphacite pseudomorphs (Jd_{29-42}) developed after magmatic pyroxene, surrounded by a foliated matrix of jadeite (Jd_{85-91}), garnet, clinozoisite and quartz replacing magmatic plagioclase (Scambelluri et al. 1990). Magmatic olivines in these metagabbros are transformed into aggregates of preferentially oriented chlorite, omphacite (Jd_{39-49}), clinozoisite and talc (Scambelluri et al. 1990; Chapter 4.2). The synkinematic transformations are preceded by static growth of garnet, omphacite, talc, chlorite and chloritoid, producing coronitic rims between original mineral domains. Garnet-pyroxene thermometry has not yet been carried out, but the mineral assemblage

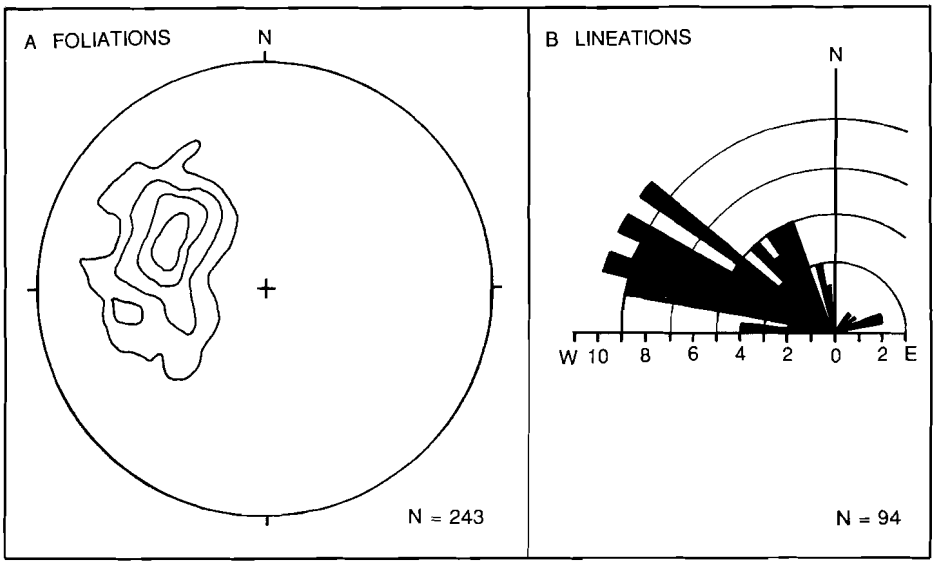

Figure 3.14. A: Poles to shear-induced foliation planes in serpentinite mylonites in the Erro-Tobbio Unit. Equal area lower hemisphere projection, contours at 2, 4, 6 and 8 % per 1% area. Maximum value counted: 10.3%. B: Rose diagram showing bearing of magnetite and antigorite lineations on shear-induced foliation planes in serpentinite mylonites.

suggests temperatures in excess of 500°C at pressures above 1600 MPa (Fig. 3.13). In the samples studied a greenschist facies retrogressive assemblage of Ca amphibole and albite is found in original plagioclase domains (Fig. 3.12, 3.13).

Correlation between the structures in the gabbroic dykes and the peridotites strongly suggests the simultaneous development of some of the olivine-bearing fractures in the peridotites, the dehydration of serpentine along ecc's in the serpentinite mylonites, and mylonitization of the metagabbros under peak eclogitic conditions (Chapter 4.3).

Contact relations between the thrust units of the Voltri Group

The contact of the Beigua serpentinites with underlying calcschists of the Voltri-Rossiglione Unit is commonly marked by extensive transformation to talc-, chlorite- and carbonate-bearing assemblages (Messiga pers. comm. 1988). Locally, this transformation resulted in the development of a tectonic melange consisting of blocks of serpentinite, eclogitic metagabbro and calcschists embedded in a talc-chlorite-tremolite-calcite-dolomite schist. In the overlying Beigua serpentinites close to these melanges, the matrix assemblage is developed synkinematically along D4 foliations. Towards the contact the amount of matrix material increases progressively such that D4 crenulated serpentinite blocks become embedded in a foliated talc schist. Eclogitic metagabbros and metabasalt are surrounded by a foliated reaction rim in which the original mineral phases are transformed into a greenschist assemblage of albite, actinolite, magnetite, sphene, pyrite and chlorite. Within lenticular bodies of calcschist a chloritoid-bearing

D3 foliation is preserved. This foliation is deformed along the margins of the bodies and chloritoid is replaced by chlorite, quartz and muscovite. These observations show that juxtaposition of the Beigua Unit on the VR Unit occurred under greenschist facies conditions (M5) and was associated with D4 folding both in the calcschists and in the serpentinites.

The contact between the Beigua and ET unit, though intensely deformed during ongoing ductile and brittle thrusting (Fig. 3.23), is essentially marked by serpentinite mylonites. These mylonites have an antigorite-chlorite-magnetite (i.e. olivine-free) foliation. D1-D3 composite fabrics in the Beigua serpentinites bend into these serpentinite mylonites and olivine associated with this D1-D3 composite fabric becomes unstable. In addition, D4 crenulations are particularly common close to the contact. These textural and petrographic observations suggest that juxtaposition of the two units occurred under greenschist facies conditions (M5) simultaneous with the generation of D4 (olivine-free) serpentinite mylonites in the ET Unit and D4 crenulations in the Beigua Unit.

3.3. THE STRUCTURE OF THE SESTRI-VOLTAGGIO ZONE

Stratigraphy

Two tectonic units have been distinguished in the SV Zone: the ophiolitic Cravasco-Voltaggio (CV) Unit and the calcareous Gazzo-Isoverde (GI) Unit (Cortesogno et al. 1979b; Fig. 3.1). The stratigraphy of the CV Unit is virtually identical to the ophiolite sequence of the Bracco Massif, and consists of serpentinite, gabbro and minor ophicalcite, overlain by basalts (usually pillow lavas) with intercalations of ophiolitic breccias. The sedimentary cover is represented by cherts and recrystallized siliceous limestones (equivalent to the Calpionella limestone), which are overlain by black shales with interbeds of recrystallized siliceous limestone (equivalent to the Palombini shale). The GI Unit is characterized by a Mesozoic shelf sequence (Marini 1982; Cortesogno & Haccard 1984) of Late Triassic neritic dolomites (Carnian-Norian) overlain by the Lencisa Formation, an alternation of thick, partially recrystallized, fossiliferous limestone beds with thin shale layers (Rhaetian-Hettangian) grading upward into massive, partially recrystallized limestone beds with chert nodules (Sinemurian-Pliensbachian; Marini 1982). This turbiditic sequence consisting of redeposited neritic carbonates is covered by (hemi)pelagic black shales with thin recrystallized calcareous interbeds (Torbi Formation: Middle/Late Liassic-Malm?; Marini 1982). The Triassic-Jurassic shelf sequence was deposited on a granitic basement (quartzdiorites and granodiorites) of Carboniferous (?) age with a thin cover of schists and metaconglomerates tentatively correlated with the Permo-Triassic "Verrucano" (Ibbeken et al. 1984). Strong lateral facies variations in the Lencisa Formation presumably reflect syndepositional tectonic activity during rifting (Norian-Rhaetian) and subsidence (Hetangian-Sinemurian and Pliensbachian-Toarcian) of the shelf (cf. Marini 1982).

Relationships between deformation and metamorphism in the Cravasco-Voltaggio Unit

The oldest structures preserved in the CV Unit are amphibolite facies shear zones in the gabbros. Distinct deformation gradients are reflected by fabrics ranging from a very faint alignment of slightly flattened and rotated pyroxene crystals to strongly foliated amphibole-bearing mylonites, with a synkinematic mineral assemblage of brown hornblende, clinopyroxene, albite and epidote. The shear zones are cut by locally undeformed basaltic dykes in which magmatic pyroxenes are partially trans-

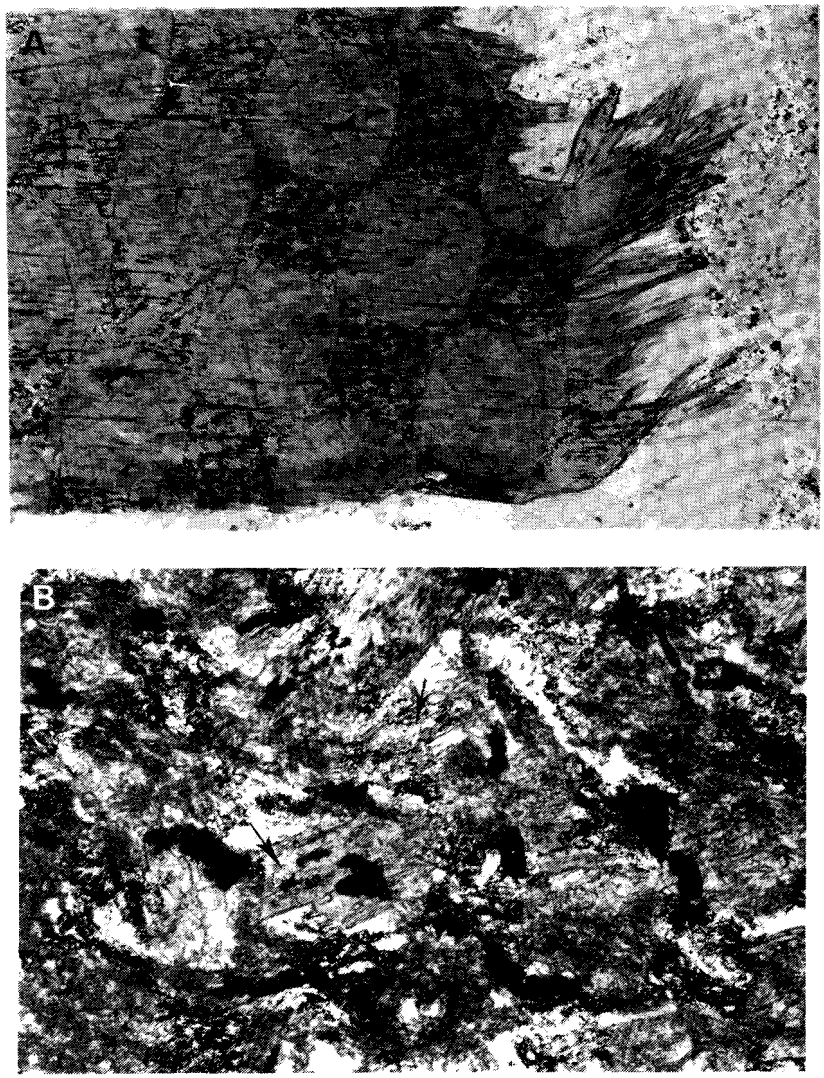

Figure 3.15. Photomicrographs showing Alpine high pressure overprint on high temperature ocean floor metamorphic assemblage. [A] Pseudomorph of brown hornblende after magmatic pyroxene in gabbro statically overgrown by crossite fibers. [B] Magmatic pyroxenes (arrows) in basaltic dyke, transformed to brown hornblende and rimmed by crossite.

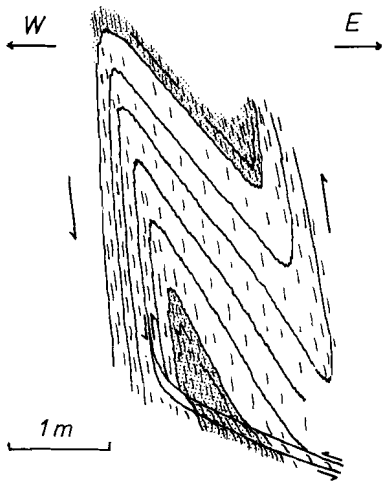

Figure 3.16. Field sketch of isoclinal fold in Calpionella limestone in a quarry south of Voltaggio. The westernmost limb is strongly sheared. The axial-plane foliation is a spaced pressure solution cleavage. The sense of shear is inferred from oblique fabrics in quartz lenses and from extensional crenulation cleavages. Note that the hinge of the antiform is dissected by a ductile shear zone (near bottom), which also had a top to the west sense of movement.

formed into brown hornblende. Static growth of brown green and green (actinolitic) hornblendes + chlorite + albite marks a retrograde history from peak amphibolite- towards greenschist facies conditions. Both the gabbroic and basaltic lithologies show an Alpine high-pressure metamorphic overprint reflected by the growth of crossite (Fig. 3.15; see below). This tectono-metamorphic evolution indicates that the amphibolite facies shear zones developed during an early (Jurassic?) stage of ocean floor metamorphism. Similar textural relationships are observed in the metagabbros of the Beigua Unit (Chapter 3.2.2), while identical structural and petrological features are common in gabbroic massifs in the Ligurian Apennines and Tuscany (e.g. Cortesogno et al. 1975; Hoogerduijn Strating 1988). Therefore, it is tentatively concluded that all three units experienced a similar stage of ocean floor metamorphism associated with localized deformation in shear zones, prior to basalt intrusion.

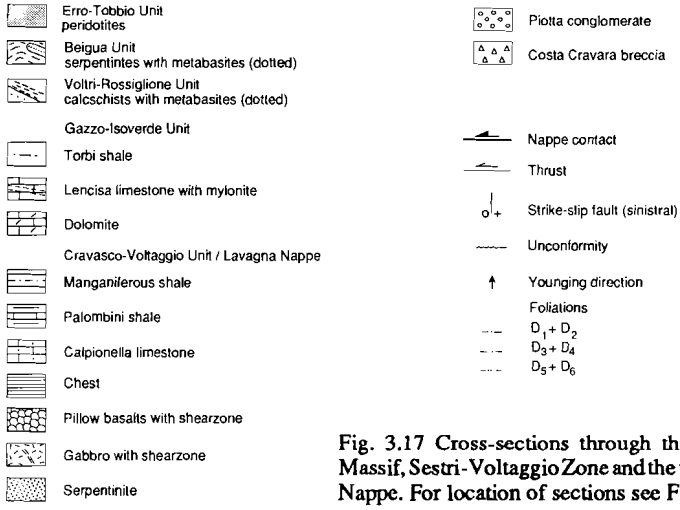

Fig. 3.17 Cross-sections through the eastern Voltri Massif, Sestri-Voltaggio Zone and the western Lavagna Nappe. For location of sections see Fig. 3.1.

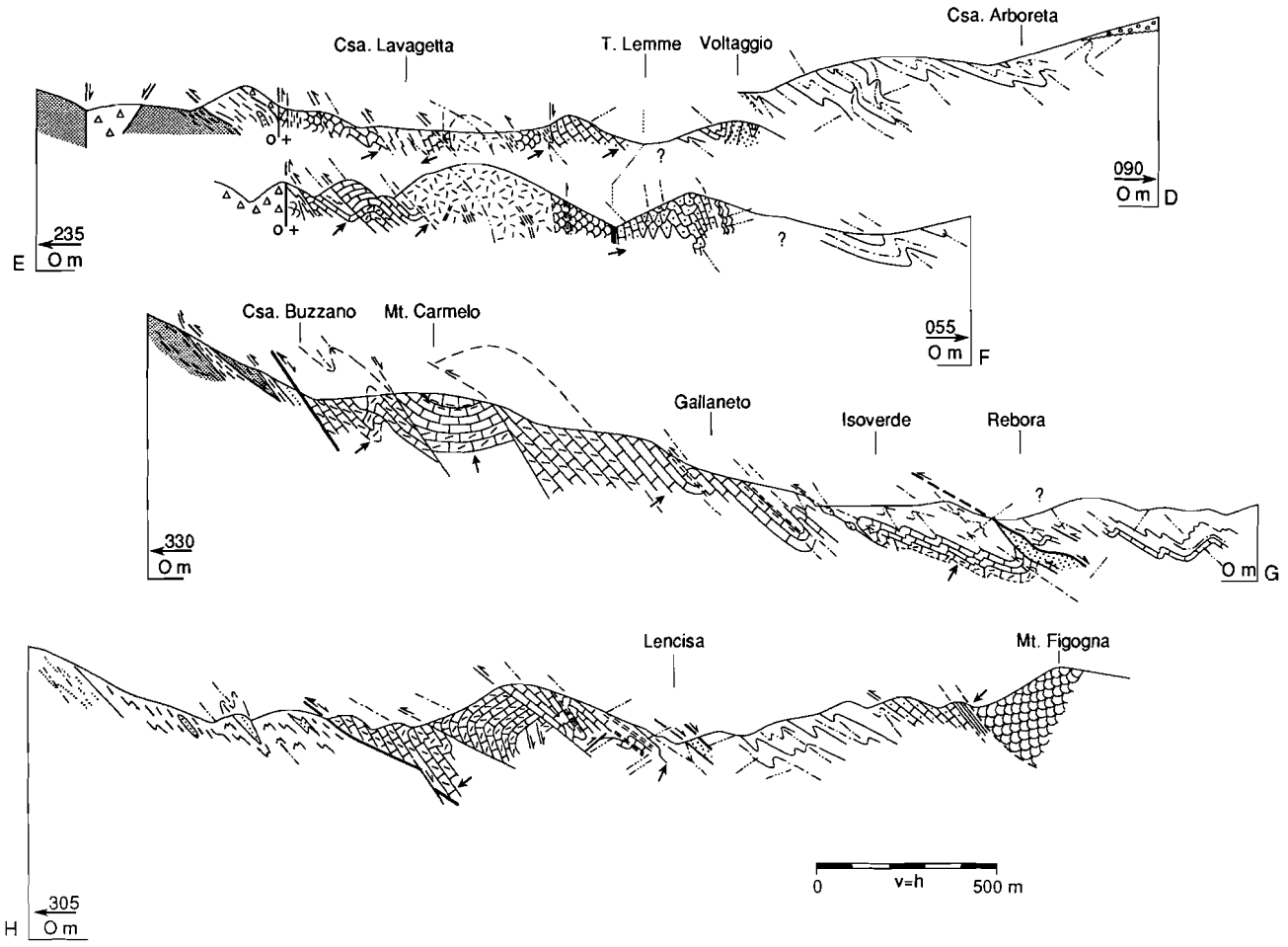
Csa. Lavagetta
T. Lemme
Voltaggio
Csa. Arboreta
090
0 m
D
235
0 m
E
055
0 m
F
Csa. Buzzano
Mt. Carmelo
Gallaneto
Isoverde
Rebora
330
0 m
0 m
G
Lencisa
Mt. Figogna
305
0 m
H
0
v=h
500 m

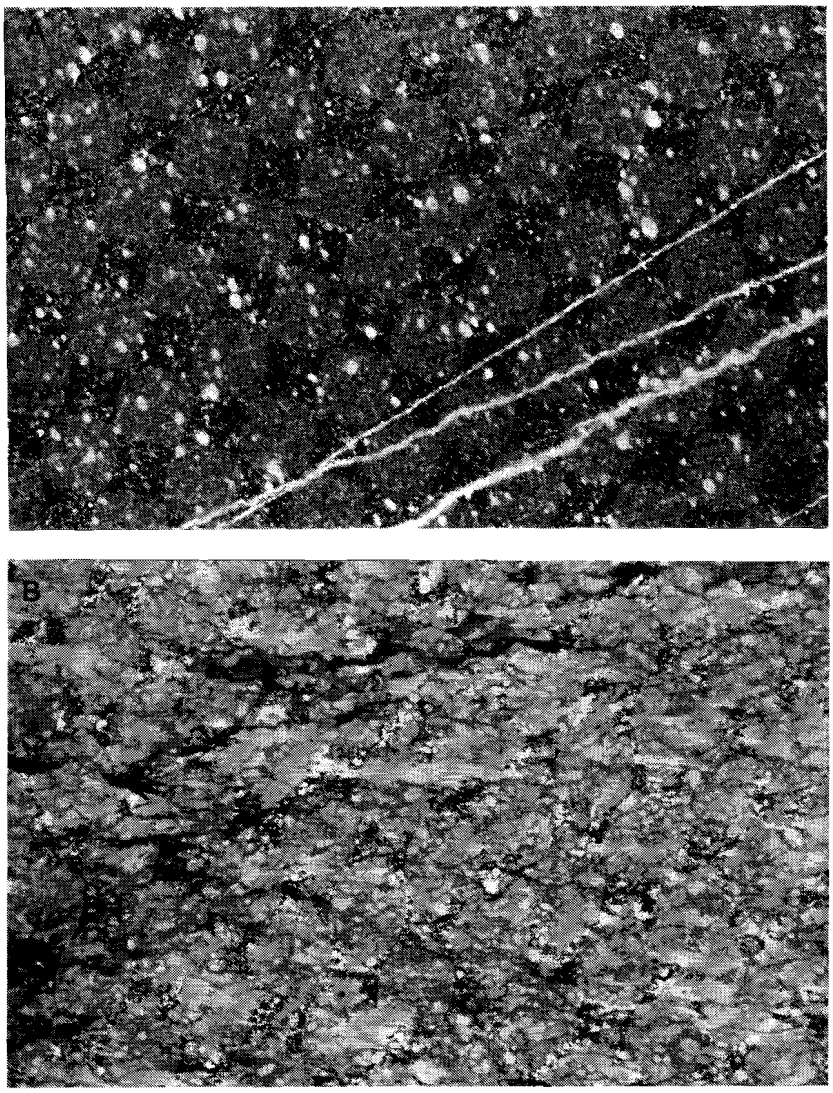

Figure 3.18. Photomicrographs of [A] undeformed Calpionella limestone from the Iscioli Biscia Subunit of the Melange Nappe (plane polarized light), and [B] strongly deformed and recrystallized Calpionella limestone from the Cravasco Voltaggio Unit (crossed nicols). Width of both micrographs 1.5 mm. Note extensive grain growth and development of calcite ribbons accentuating the shear-induced foliation in [B].

All lithologies of the CV Unit are affected by Alpine deformation which led to the development of a pervasive foliation in the sediments and shear zones in the ophiolitic basement. The deformation in the sedimentary sequences is represented by dm- to 100 m-scale isoclinal folds with extremely stretched and thinned western or overturned limbs (Fig. 3.16; Fig. 3.17 section F, T. Lemme). The folds are associated with the

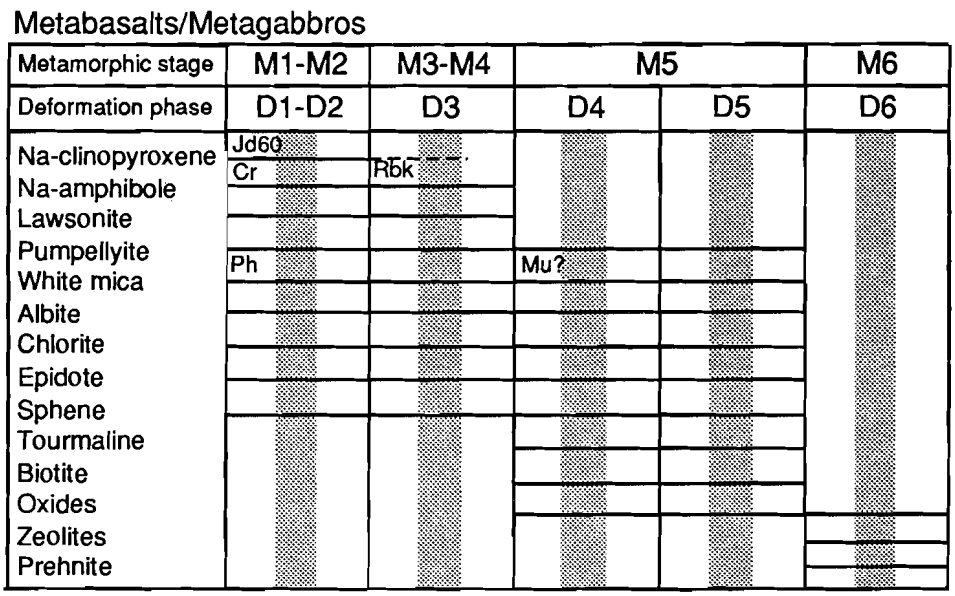

Fig. 3.19. Relationships between deformation and metamorphism in the metabasites of the Cravasco-Voltaggio Unit

development of a pressure solution cleavage in the calcareous lithologies, and a slaty cleavage in the pelites (D1/2). The calcareous lithologies show intense grain growth, crystal-plastic deformation and concomitant recrystallization (compare Figs. 3.18A and B). In the sheared siliceous limestones, quartz concentrated in small lenses parallel to the foliation and locally shows a weak oblique grain shape fabric. With ongoing deformation (D3/4) the mylonitic fabric in the sheared limestones deformed in cm-spaced ecc's, while small shear zones dissect the isoclinal folds (Fig. 3.16). In pelitic sequences this stage is reflected by NW vergent folds and easterly dipping crenulation foliations. The oblique grain shape fabrics, the ecc's, and the fold asymmetry suggest that the D1-D3/4 structures developed in a progressive (simple) shear regime. All previous structures are overprinted by asymmetric folds with predominantly E and minor W dipping axial planes (D5), and chevron folds with subhorizontal to slightly W dipping axial planes and associated to east dipping normal faults (D6). D5 structures are predominantly W vergent, while all D5 structures are E vergent (see Fig. 2.23, sections E and F). All structures are dissected by steep N-S to NNW-SSE trending, sinistral strike slip faults (D7)

In the ophiolitic basement, ductile shear zones developed with a foliation defined by preferentially oriented crossite, epidote, chlorite, lawsonite (notably in rims of pillow basalts), sphene, Na clinopyroxene, phengite and minor pumpellyite (D1/2-M1/2; Fig. 3.19). Relic magmatic pyroxenes transformed into omphacitic to aegirine-augitic pyroxenes (Jd_{5-30}) and crossite, while the original plagioclase recrystallized into fine grained equiaxed albite agregates associated with phengite, chlorite, pumpellyite, crossite and omphacitic to jadeitic pyroxene (Jd_{50-70}) (mineral compositions from

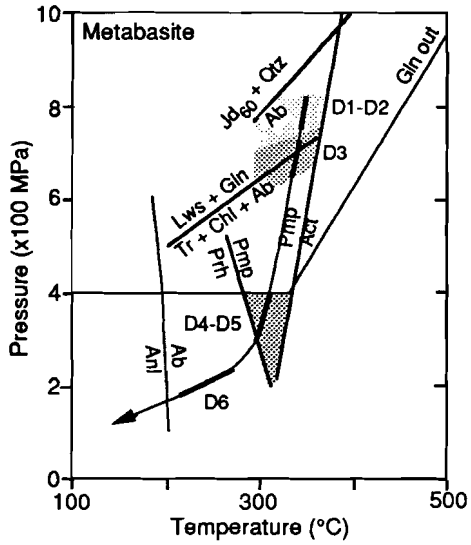

Fig. 3.20. P-T path inferred for the metabasites in the Cravasco-Voltaggio Unit, Sestri-Voltaggio Zone. Reaction similar to Fig 3.8. In addition lower stability limit of Lws + Gln after Perchuk & Aranovich 1980, Prehnite (Phr)-Pmp transition after Nitsch 1971, Alb-analcite (Anl) transition after Liou 1971.

Cortesogno et al. 1979a). The stability of these assemblages suggests synkinematic blueschist facies conditions of 300 to 350°C at 700 to 800 MPa. Asymmetric porphyroclasts systems and the orientation of mineral lineations indicate that these structures developed during WNW to NW directed thrusting of the hanging wall. The foliation is cut by albite + crossite crack-seal (Ramsay 1980) veins, and both structures are deformed in cm-scale isoclinal folds (D3) with an associated crenulation cleavage defined by oriented lawsonite, Na-amphibole (probably Mg-Riebeckite, cf. Cortesogno et al. 1979b), phengite, chlorite, epidote and pumpellyite (M3/4). This mineral assemblage suggests slightly lower pressures of 600 to 700 MPa for D3 (Fig. 3.20).

Many new shear zones developed under prehnite-pumpellyite facies conditions (D4, M5). These shear zones are locally asssociated with 100 m-scale folds, deforming both the ophiolitic basement and the pelagic sedimentary cover (see Fig. 3.17 sections E and F, Csa. Lavagetta). Kinematic indicators in these shear zones point to predominant westerly and minor easterly directed ductile thrusting of the hanging wall during this stage. The shear-induced foliations are locally dissected by albite-epidote crack-seal veins. Crenulation of the shear-induced foliations (Fig. 3.21) and the veins in these ductile thrust zones is common and suggests inversion of the movement sense to easterly directed transport (D5). Both D4 and D5 are characterized by the synkinematic growth of albite, chlorite, epidote, pumpellyite, white mica (muscovite?), biotite, tourmaline (close to the contact with siliceous limestones) and sphene (M5). Inferred PT conditions during D4 and D5 are 200-300°C at pressures between 200 and 400 MPa (Fig. 3.20). The presence of prehnite-zeolite facies assemblages (M6) along easterly dipping normal faults and N-S to NNW-SSE trending, sinistral strike-slip faults (cf. Argenti et al. 1986) points to ongoing deformation (D6/7) at progressively decreasing temperatures (around 200°C).

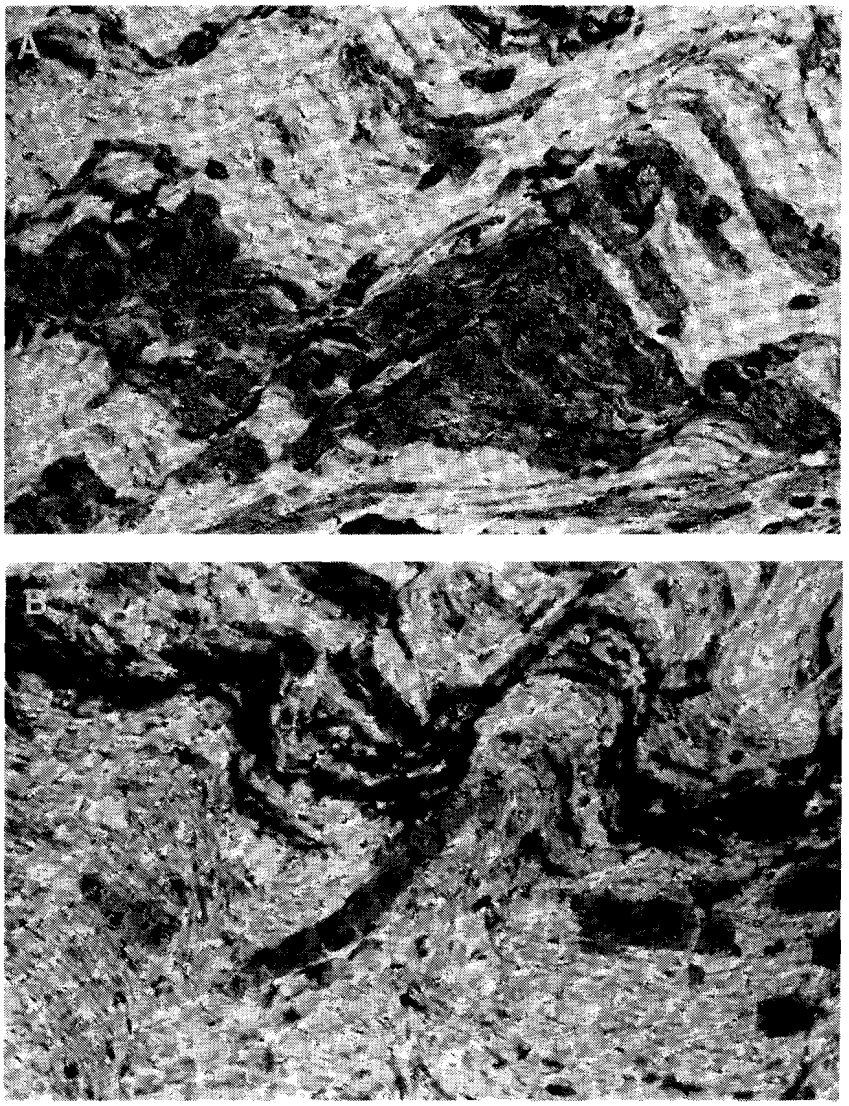

Figure 3.21. Photomicrographs (plane polarized light) of D5 crenulation in a D4 shearzone developed in pillow basalts of the Cravasco-Voltaggio Unit, Sestri-Voltaggio Zone. [A] Spaced crenulation cleavage deforming D4 shear- induced foliation consisting of alternating albite + white mica (muscovite?) and pumpellyite + sphene + albite + white mica + tourmaline + oxide bands (dark bands). Width of micrograph 0.61 mm. [B] D4 tourmaline deformed by D5 micro fold. Width of micrograph 0.15 mm.

Relationships between deformation and metamorphism in the Gazzo-Isoverde Unit

The earliest structures (D1/2; D1.0 of Marini 1984) observed in the Gazzo-Isoverde Unit are metre- to hundred metre-scale isoclinal folds and metre-scale mylonite zones in the bedded limestones, and open to tight, 10 to 100 m-scale folds and brittle faults

in the dolomites (Fig. 3.17 sections G and H). The pelitic interbeds show a penetrative axial-planar slaty cleavage, whereas the limestone beds display a widely spaced pressure solution cleavage. The mylonites generally occur in the overturned and/or western limbs of the isoclinal folds (Fig. 3.17, sections G and H). In these mylonites, the micritic limestone is completely transformed into extensively twinned calcite ribbons in a matrix of fine grained calcite showing oblique grain shape fabrics. In addition, fibrous calcite occurs in pressure fringes adjacent to opaques and virtually unstrained quartz grains. The calcite ribbons and the pressure fringes define an E-W to SE-NW trending stretching lineation. In the pelitic Torbi Formation structures on the outcrop-scale attributed to D1/2 include isoclinal folds and sheath folds. Recrystallized calcite fibers and pyrite crystals with pressure fringes define a stretching lineation in these rocks. Kinematic indicators point to (N)W directed ductile thrusting. Unfortunately the bulk chemical composition of the calcareous lithologies in the GI Unit preclude the growth of diagnostic metamorphic minerals, which hampers the assessment of the PT conditions during deformation. However, scarce porphyroblasts of lawsonite, phengite, chlorite and Na-amphibole (Chiesa et al. 1975; Cortesogno et al. 1979b) seem consistent with peak blueschist facies conditions during D1/2 (cf. Cortesogno et al. 1979b).

Refolding of the D1/2 folds by strongly non-coaxial D3/4 folds (D1.1 from Marini 1984) resulted in type II (mushroom) to type III interference patterns (Ramsay 1967). Asymmetric, NW vergent D3/4 folds are very common in the Torbi shales near Isoverde (Fig. 3.17 section G), and in the calcareous sequences near Csa. Lavagetta (Fig. 3.17 sections E and F). On a micro-scale, the development of a D3/4 axial-plane crenulation foliation is associated with the break-down of lawsonite and Na-amphibole, and the synkinematic growth of white mica and chlorite, which suggest lower metamorphic conditions (possibly prehnite-pumpellyite facies) during this stage (cf. Cortesogno et al. 1979b). The latest stages of folding (D5 and D6; D2.0 and D2.1 from Marini 1984) all occurred under low grade (prehnite-zeolite facies?) to non-metamorphic conditions and resulted in the development of brittle faults and open kink-like folds (Fig. 3.17 sections G and H). In the pelitic sequences a spaced fracture cleavage developed, while pressure solution cleavages are found in the calcareous lithologies. D5 structures may be both east and west vergent, while easterly directed thrusting and east-vergent folding characterizes D6. All structures are dissected by steep N-S to NNW-SSE trending sinistral strike-slip faults (D7)

The contact between the Cravasco-Voltaggio and Gazzo-Isoverde Unit

Well exposed contacts between the CV and GI units are rare. These contacts are folded by D3/4 and younger folds (cf. Marini 1984), while metamorphic assemblages in mylonitized metabasalts at the contact (D4) indicate synkinematic prehnite-pumpellyite facies conditions (M5). This suggests that the contact was established at the onset of D4. Asymmetric porphyroclast systems developed in D4 mylonite zones and ecc's in the pelitic sequences show that the CV Unit became emplaced essentially in a north westerly direction on the GI Unit (cf. Cortesogno & Haccard 1984).

3.4 THE STRUCTURE OF THE WESTERN LAVAGNA NAPPE

Stratigraphy

The stratigraphy of the western Lavagna Nappe is largely comparable to that of the ophiolitic and sedimentary sequences of the eastern Lavagna Nappe and the Mélange Nappe (e.g. Cortesogno & Haccard 1984; Marini 1989; see Chapter 2, Fig 2.2), however, stratigraphic correlation is hampered due to recrystallization and intense deformation of the sedimentary sequences. From the bottom upward the ophiolitic basement consists of serpentinite, ophicalcite and pillow basalts with subordinate ophiolitic breccias and sands. Siliceous shales and radiolarian chert locally overlain by siliceous limestones (equivalent to the Calpionella limestone) constitute a pelagic sedimentary sequence overlain by black shales with interbeds of siliceous limestone (Palombini shales). This sequence passes upward into the "Busalla Flysch" (Cortesogno & Haccard 1984) consisting of manganiferous shales ("Argilliti di Montànesi", equivalent to the Manganiferous shale Formation) overlain by shales and marls with intercalations of calcareous and arenaceous turbidites (Ronco Formation; equivalent to the Verzi marls). Based on ammonites a Middle to Late Albian age is attributed to the base of the Ronco Formation (see Cortesogno & Haccard 1984).

Deformation in the western Lavagna Nappe

The deformation in the western Lavagna Nappe is characterized by a penetrative slaty cleavage (D1/2) in the pelitic sediments associated with strongly non-coaxial isoclinal folds, while local shear zones developed in the ophiolitic basement. Synkinematic

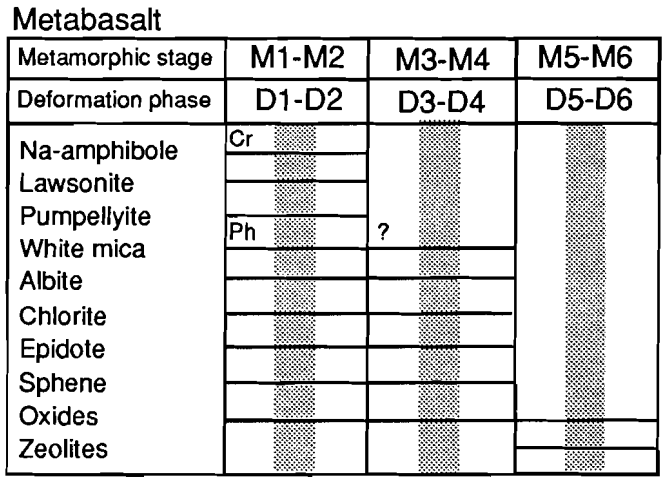

Fig. 3.22. Relationships between deformation and metamorphism in the metabasites of the western Lavagna Nappe.

growth of pumpellyite, albite, phengite, chlorite and epidote is common in foliated basalts (Fig. 3.22). In addition to previously reported lawsonite (e.g. Cortesogno et al. 1979a), the basalts of Mt. Figogna (Fig. 3.1) also contain blue amphibole (crossite to Mg-arvedsonite, Fig. 3.22). The stability of this assemblage and the chemical composition of the blue amphiboles (Na_2O: 6.20-7.56 wt%) suggest maximum pressures between 600 and 700 MPa at temperatures between 300 and 350°C (Fig. 3.23). Later crenulation of the shear-induced foliations and development of non-coaxial folds (D3/4) is associated with the stability of albite, white mica, chlorite, epidote and pumpellyite in the metabasalts. Kinematic indicators suggest that D1/2 and D3/4 resulted from progressive NW directed ductile thrusting. All structures are overprinted by brittle faults associated with asymmetric east-vergent folds (D5/6). In the metabasalts zeolite facies assemblages developed in D5/6 fractures suggesting temperatures of about 200°C during this stage (cf Argenti et al. 1986; Fig. 3.23).

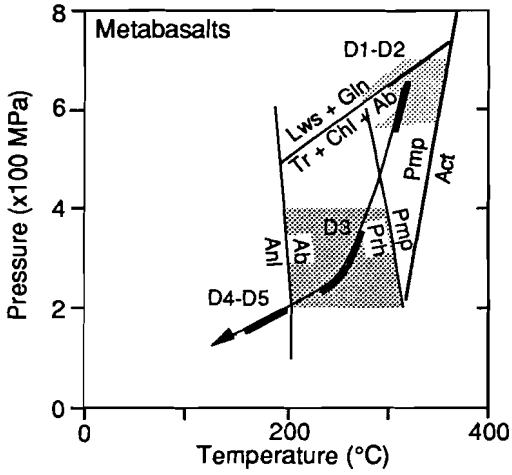

Fig. 3.23. P-T path inferred for the metabasalts of the western Lavagna Nappe. Similar to Fig. 3.20.

3.5 CONTACT RELATIONS BETWEEN THE VOLTRI MASSIF, THE SESTRI-VOLTAGGIO ZONE AND THE WESTERN LAVAGNA NAPPE.

All studied contacts between the SV Zone and the Voltri Massif (the Sestri Voltaggio Line s.s.) are brittle faults. In the central part of the SV Zone the contact strikes approximately NNE-SSW (Fig. 3.1) and dips 40 to 50° ESE (Fig. 3.17 sections G and H). Kinematic indicators and the orientation of striations point to early north-west directed thrusting (D5?) followed by eastward reactivation (D6?). High-angle normal faults dissecting the contact are common. In the northern part of the SV Zone the NNW-SSE striking contact (Fig. 3.1) is vertical or dips to the east, and clearly truncates NNE-SSW trending imbrications and back thrusts in the eastern part of the Voltri Massif (see geological map Enclosure 2). Subhorizontal to slightly SSE plunging striations and a sinistral sense of shear suggest a transcurrent to oblique thrust character of the contact (cf. Schamel 1974). The differences in orientation and character of the contact suggests a transition from a frontal ramp in the south to an oblique ramp further north.

From a cartographic point of view, determination of the boundary between the pelitic sequences of the CV, GI and western Lavagna Nappe is very difficult, if not impossible. In the southern part of the SV zone this has led to strongly contrasting interpretations (e.g. compare Cortesogno & Haccard 1984 and Marini 1984, 1989). Cortesogno and Haccard (1984) defined the "Complesso Indeterminato" comprising pelitic sequences with calcareous and arenitic interbeds and lenticular bodies of serpentinite and metabasalt. The presence of Na-amphibole and pumpellyite in the metabasalt led them to interpret this unit as part of the SV zone. However, the presence of Na-amphibole in the metabasalts of the Mt. Figogna (defined as part of the Lavagna Nappe by Cortesogno & Haccard 1984) renders the discrimination of a separate unit redundant. In addition, there is no distinct stratigraphic or structural discontinuity across the alleged contact between the "Complesso Indeterminato" and the western Lavagna Nappe. Therefore, the pelitic sequences in the southern part of the SV zone are mapped as part of the western Lavagna Nappe (cf. Marini 1984, 1989). Only one outcrop near Cravasco (Fig. 3.1) has been found which allows to determine a sinistral strike-slip movement across this part of the contact between the SV zone and the western Lavagna Nappe. In the southern part of the SV Zone the contact dips 30 to 50° ESE. Further north the contact has not been found exposed. Easterly dipping, brittle normal faults and steep N-S trending sinistral strike-slip faults are common close to the contact.

3.6 THE LARGE-SCALE STRUCTURE OF THE VOLTRI MASSIF, SESTRI-VOLTAGGIO ZONE AND WESTERN LAVAGNA NAPPE

Figures 3.17 and 3.24 show a series of sections across the Sestri-Voltaggio Zone and the north-eastern Voltri Massif (see Fig. 3.1 and Enclosure 2 for location). The post-D4 (i.e. nappe emplacement) structure of the Voltri Massif (Fig. 3.24) is dominated by folds, NW directed imbricate faults and hinterland dipping duplexes. The roof-thrusts of these duplexes is generally the reactivated basal contact of the ET Unit. The character of the floor thrust is not clear, however, the rare incorporation of slices of calcschists in the duplexes (Fig. 3.24, section CC') suggests that the floor thrust is located at or slightly below the basal contact of the Beigua Unit. Out-of-sequence thrusts dissecting the roof thrust are common. Backthrusts in the the Erro-Tobbio Unit occur at the trailing edge of duplexes and near the contact with the Sestri-Voltaggio Zone (Fig. 3.23 section AA'). Steep N-S (sinistral) and ENE-WSW (dextral) trending strike-slip faults (Fig. 3.25) dissect both the nappe contacts and the duplex systems, and can be correlated with the D7 strike-slip faults observed in the Sestri-Voltaggio Zone.

The large scale structure of the SV Zone (Fig. 3.17) is dominated by west-vergent D3/4 folds and thrusts, overprinted by west-directed and, to a lesser extent, east-directed D5 imbrications and folds, and east-vergent D6 folds and thrusts. At the outcrop-scale, many of these brittle D5 and D6 structures are associated with low-angle extensional faults, while at a larger scale some of the faults cut down-section in the direction of transport, suggesting that these structures may be interpreted as low angle extensional

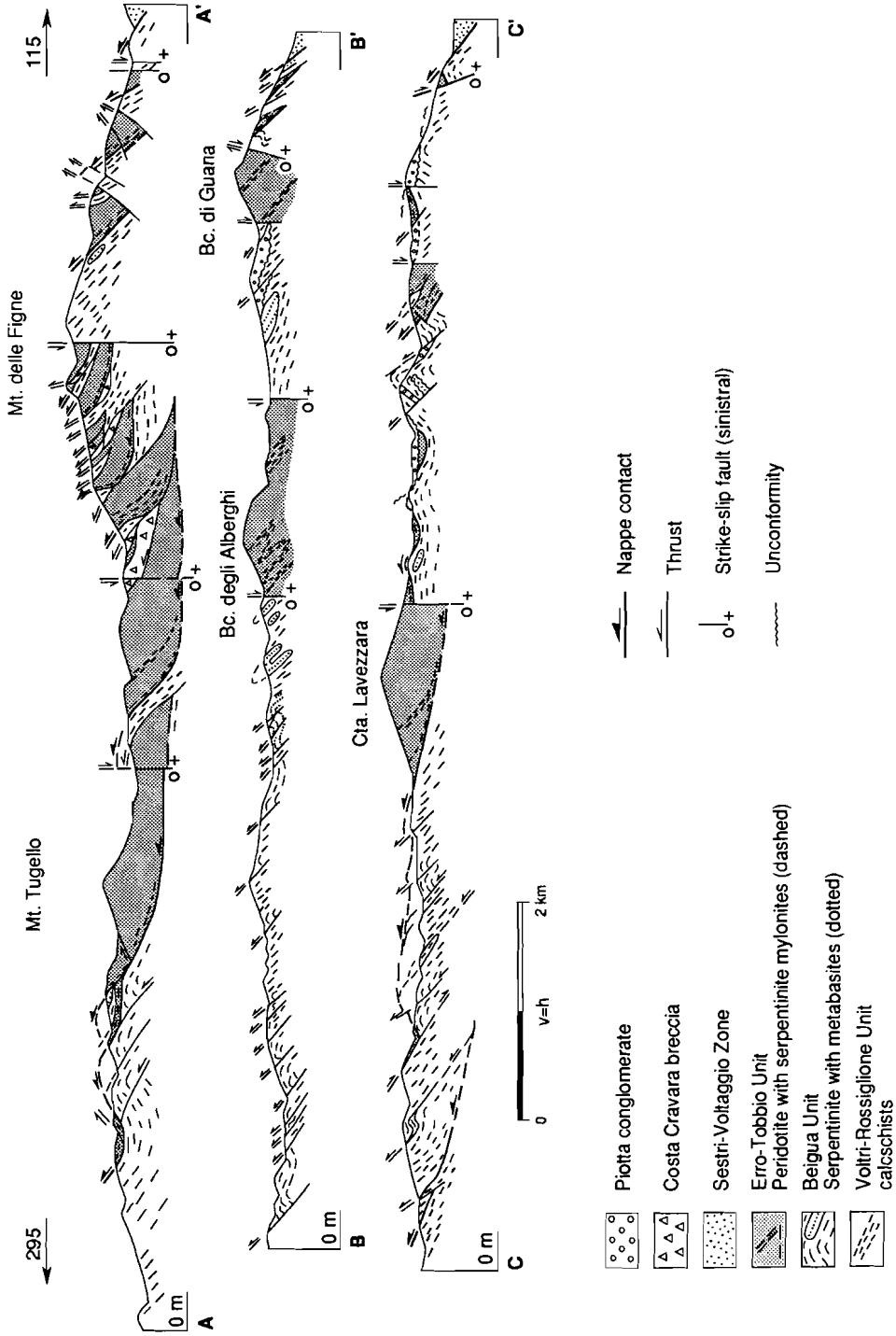

Figure 3.24. Cross-sections through the north-eastern part of the Voltri Massif. For location of sections see Fig. 3.1 and Enclosure 2.

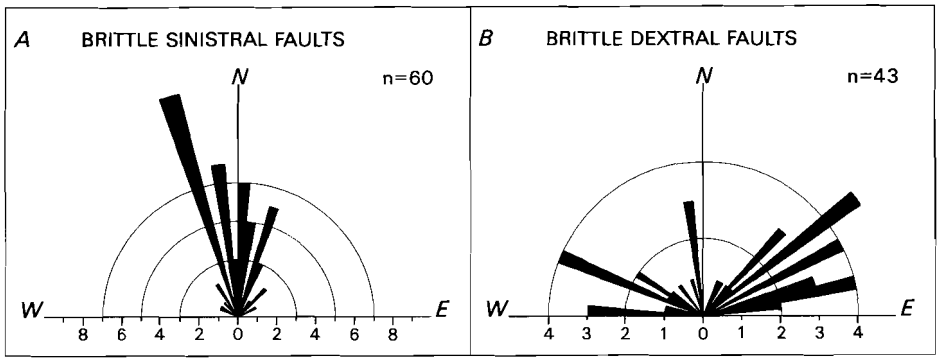

Figure 3.25. Rose diagrams showing strikes of steep (dip more than 65°) sinistral [A] and dextral [B] brittle strike-slip faults in the Erro Tobbio and Beigua Unit.

faults. Extensional D6 structures are particularily common close to the eastern and western contacts of the SV Zone.

The kinematic analysis in the Voltri Massif, the Sestri-Voltaggio Zone and the western Lavagna Nappe shows that nearly all ductile and brittle structures developed during progressive (N)NW directed thrusting. This implies that, during the tectono-metamorphic evolution, the kinematic framework in which the stack of high-pressure metamorphic units was developed did not change significantly.

A compilation of PT trajectories from the thrust units in the Voltri Group (Fig. 3.26) shows a zonation with the highest pressure rocks at the top of the structural pile. This juxtaposition is consistent with the general metamorphic zonation found in the Alps and other high-pressure metamorphic belts (Ernst 1975). In contrast, the contacts between the Voltri Group and the SV Zone, and between the SV Zone and the western Lavagna Nappe represent zones of juxtaposition of low-pressure units onto high-pressure units. This is reflected by the "pressure gaps" of 800 and 100 MPa, respectively, across these contacts (Fig. 3.26). A discontinuity of 100 MPa obviously falls within the uncertainty limits of available thermobarometric methods, however, the 800 MPa gap can only be explained by tectonic denudation of the Voltri Group rocks along post-eclogitic (low-angle) normal faults such as to omit about 26 kilometres of structural overburden (cf. Platt 1986). This observation is consistent with the extensional character of D5 and D6 structures in the SV Zone and Lavagna Nappe. Moreover, the PT-trajectories (Fig. 3.26) show that decompression occurred under decreasing temperature conditions. This type of retrograde PT evolution suggests fairly rapid exhumation, presumably in an extending subduction complex (Thompson & England 1984; Platt 1986; Ernst 1988).

Dating of the deformation events is difficult due to a lack of radiometric data. On the basis of a comparison with radiometric data from the western Alps (K-Ar, Ar-Ar, Rb-Sr: Hunziker 1974; Hunziker & Martinotti 1984) and Corsica (Ar-Ar, Rb-Sr: Maluski 1977; Cohen et al. 1981), Late Cretaceous ages between 100 and 80 Ma are inferred

here for the peak HP metamorphism in the Voltri Group. Phengite separated from a eclogitic metabasite in the Beigua Unit yields a Middle Eocene 45.2±1.8 My cooling age (Ar-Ar dating by D. Rex, Leeds), which is consistent with Eo-Oligocene whole rock K-Ar ages of 36 and 41 Ma obtained from calcschists of the Voltri Group exposed adjacent to the southern part of the SV Zone (Schamel 1974; see geological map Enclosure 2). Black shales in the western Lavagna Nappe yielded Late Paleocene cooling ages of 59 and 60 Ma close contact with the SV Zone, and a Senonian 81 Ma cooling age away from this contact (Schamel 1974). In view of the inferred peak metamorphic conditions of the western Lavagna Nappe and the K-Ar blocking temperatures in micas (Fig. 3.26), the 81 Ma probably represents the age of blueschist

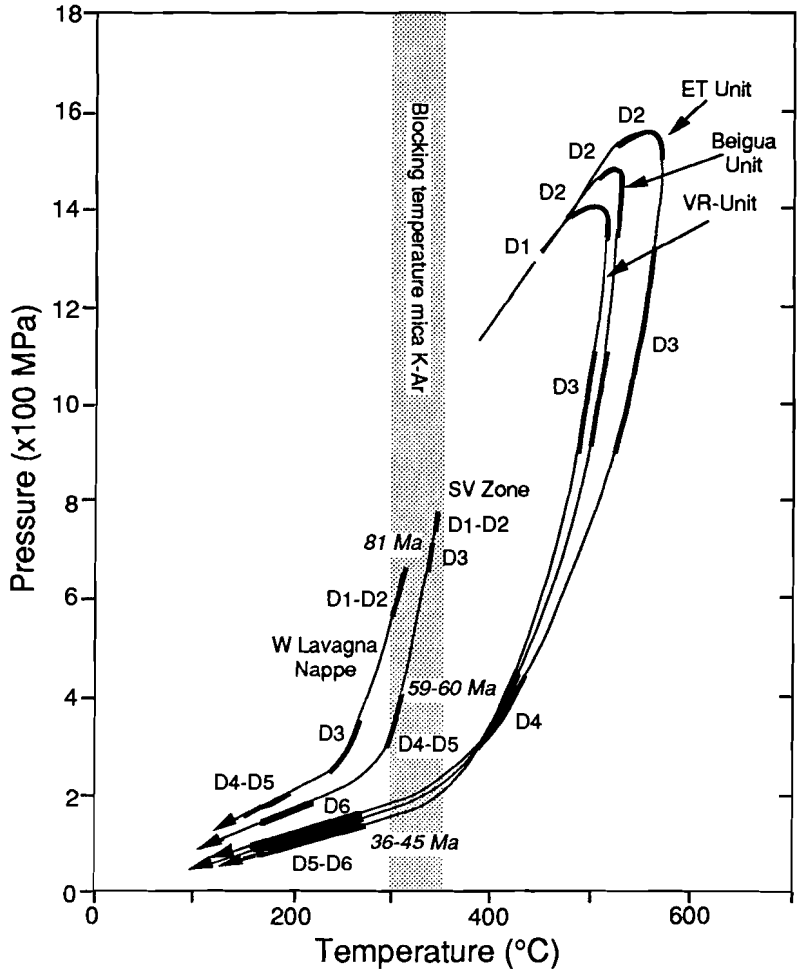

Fig. 3.26. Compilation of PT trajectories inferred for the thrust units of the Voltri Group (taken from Figs. 3.4, 3.9 and 3.13), the Cravasco-Voltaggio Unit of the Sestri-Voltaggio Zone (Fig. 3. 19) and the metabasites of the western Lavagna Nappe (from Fig. 3.22). K-Ar cooling ages from Schamel (1974; whole rock) and Rex (1991 unpublished, phengite separate). For further explanation see text.

metamorphism in this unit, which corresponds well with the inferred Late Cretaceous age for peak HP metamorphism. The younger cooling ages from the Voltri Group consistently suggest progressive uplift and cooling of the deeper structural (i.e. higher grade) units.

The basal sequences of the Tertiary Piemonte basin (Fig. 1.2, 3.1) are represented by Late(?) Eocene to Early Oligocene peridotite scarp breccias (Costa Cravara breccia) and Early to Middle Oligocene conglomerates and sands (Piotta conglomerate; see Lorenz 1969; Haccard & Lorenz 1979). The Piotta conglomerates are deposited in continental to shallow marine alluvial fan systems and contain fragments of all (ultra)mafic and metasedimentary lithologies in the Voltri Group. This indicates that by Oligocene times the HP units were emerged and subject to erosion. In view of the Middle Eocene to Earliest Oligocene cooling ages in the Voltri Group, this implies that the units were uplifted from about 6 to 9 km depth within 10 Ma, i.e minimum uplift rates of about 0.5 to 1.0 mm/y. Locally, the breccias and conglomerates are tectonically intercalated with units of the Voltri Group. Folded unconformities which truncate brittle folds and thrusts (Fig. 3.23, section CC') suggest pronounced synsedimentary brittle deformation (D5, D6) in the Voltri Group during the Eo-Oligocene. The alluvial fan deposits of the Tertiary Piemonte basin are covered by marls of Late Oligocene-Early Miocene age deposited in a open marine environment. Compressional tectonics and angular unconformities (up to 40°) in these marls indicate continuing deformation during Oligo-Miocene times and show that the SV Zone remained active, hence that the generally accepted pre-Oligocene age of this transcurrent zone (e.g. Laubscher 1988) is incorrect.

CHAPTER 4

Alpine olivine- and titanian clinohumite-bearing assemblages in the Erro-Tobbio peridotite: some implications for the mechanical behaviour of subducting oceanic mantle

4.1 INTRODUCTION

The Erro-Tobbio (ET) Unit is dominantly made up of peridotite, intruded by relatively few metagabbroic and basaltic dykes of oceanic (MORB) affinity. Many structures and metamorphic assemblages in the peridotite developed prior to the intrusion of the mafic dykes, and it is inferred that this deformation and volcanism was related to rifting and opening of the Piemonte-Ligurian ocean (see Chapter 5).

In addition to this early, extension-related evolution, numerous structures in the ET unit are clearly related to the Alpine history of subduction and subsequent collision (see Chapter 3). These include [1] serpentinite mylonites, developed in a NNW directed ductile thrust system (Fig. 3.23), and forming a 10 to 100 m-scale network of anastomosing and cross-cutting shear zones which separate relatively coherent peridotite bodies, [2] brittle vein systems within these peridotite bodies which are filled with mineral assemblages younger than those developed during lithosphere extension and mantle uplift, [3] shear-induced deformation structures in the gabbroic and basaltic dykes clearly associated with synkinematic high-pressure assemblages, and [4] late stage brittle folds and faults deforming all previous structures and related to NW directed imbrication of the ET peridotites with Tertiary sediments (See Chapter 3.6).This implies that, apart from the Tertiary brittle imbrications [4], the Alpine evolution of the ET unit involved ductile deformation as well as brittle fracturing under essentially metamorphic conditions in a subduction environment.

Previous studies in the ET Unit (Cimmino et al. 1979; Piccardo et al. 1988) have shown that the Alpine evolution of the peridotite is closely related to the development

Parts of this chapter are to be published as:
Scambelluri M., Hoogerduijn Strating E.H., Piccardo G.B., Vissers R.L.M. & Rampone E. 1990. Alpine olivine- and titanian clinohumite-bearing assemblages in the Erro-Tobbio peridotite (Voltri Massif, N.W. Italy). J. Metam. Geol., 8, in press.
Hoogerduijn Strating E.H. & Vissers R.L.M. 1991. Dehydration-induced fracturing of eclogite-facies peridotites: implications for the mechanical behaviour of subducting oceanic mantle. Tectonophysics, submitted.

of antigorite (Ant) + olivine (Ol) + titanian clinohumite (Ti-Chu)-bearing assemblages. Until recently, however, little was known about the relative timing between the development of these Ol-bearing assemblages and the subduction-related deformation in the peridotites and metagabbroic dykes (Hoogerduijn Strating et al. 1990). In addition, the studies in the ET peridotite (Hoogerduijn Strating et al. 1990) and other high-pressure metamorphic terrains in the Alps (e.g. Rubie 1983; Pognante 1985; Barnicoat & Fry 1986; Philippot 1987) have provided valuable information on the character and geometry of the deformation to be expected in a subduction environment. Hardly any attention, however, has been paid to the information these structures may provide on the mechanical behaviour of rocks under high-pressure metamorphic conditions, and the physical conditions pertaining in subduction zones.

In Chapter 3 the relationships between the deformation and metamorphism in the ET Unit and the other units in the Voltri Group are briefly discussed. The purpose of this chapter is [1] to describe in detail the relationships between the subduction and collision-related structures in the ET Unit and the equilibration of Ol-bearing and eclogitic assemblages, [2] to assess the Alpine tectono-metamorphic evolution of the ET Unit, [3] to estimate the fluid pressures leading to fracturing of the peridotite, and [4] to discuss the implications of shear localization and transient high fluid presssures on the rheology of subducting slabs.

4.2 ALPINE STRUCTURES AND METAMORPHISM IN THE ERRO-TOBBIO ULTRAMAFICS AND GABBROIC DYKES

The following section describes the dominant meso- and microscopic structures developed in both the serpentinite mylonites, the sheared gabbroic dykes, and in the peridotite wall rock, and their relationships with the Ol-bearing and eclogitic assemblages. A schematic compilation of these relationships is shown in Figure 4.1. It should be noted, however, that none of the studied outcrops or thin-sections do simultaneously show all the described relationships. This implies that the relative timing between the structures developed in different lithologies remains somewhat uncertain. The abbreviations used are listed in Table 4.1.

Table 4.1. List of abbreviations

Atg	=antigorite	Mag	=magnetite
Brc	=brucite	Ol	=olivine
Chl	=chlorite	Omp	=omphacite
Cld	=chloritoid	Ox	=oxides
Ctl	=chrysotile	Py	=pyrite
Czo	=clinozoisite	Qtz	=quartz
Di	=diopside end member	Ti-Chu	=titanian clinohumite
Grt	=garnet	Tlc	=talc
Ilm	=ilmenite	Tr	=tremolite
Jd	=jadeite end member	Zo	=zoisite

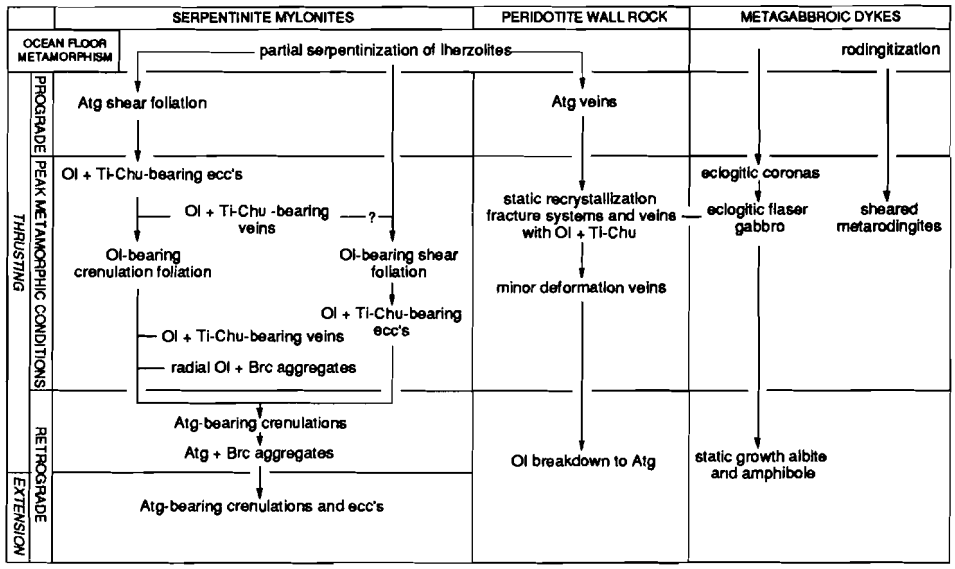

Fig. 4.1. Diagram showing the observed relationships between deformation and metamorphism in the serpentinite mylonites, peridotite wall rock and metagabbroic dykes in the ET Unit.

Serpentinite mylonites

Serpentinite mylonites in the ET Unit are developed in a ductile thrust system (Chapter 3.2), and occur as cm to m-scale serpentine-rich, and strongly foliated bands within the peridotite. Most serpentinite mylonites show a distinctly gradual transition from partially serpentinized and weakly foliated peridotites in the margins of these zones to strongly foliated serpentinite mylonites in the centres. Along with the passage from the low strained peridotite to the highly strained serpenitine mylonite, the shear-induced foliations rotate into parallelism with the margins of the mylonite zones (Fig. 4.2 A). Relatively simple shear zone geometries such as shown in Figure 4.2 A are rare, however. In general, the serpentinite mylonites show very complex relationships

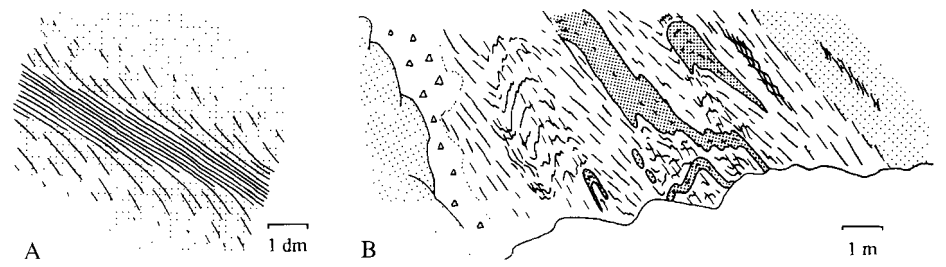

Fig. 4.2. Schematic representation, based on field sketches and photographs, of serpentinite mylonite thrust zones developed in serpentinized peridotite wall rock (light shading). [A] cm-scale shear zone with shear-induced foliation bending into the serpentinite mylonite. [B] Complex serpentinite mylonite with both extensional- and compressional crenulation cleavages, and deformed dunite lenses (dark shading).

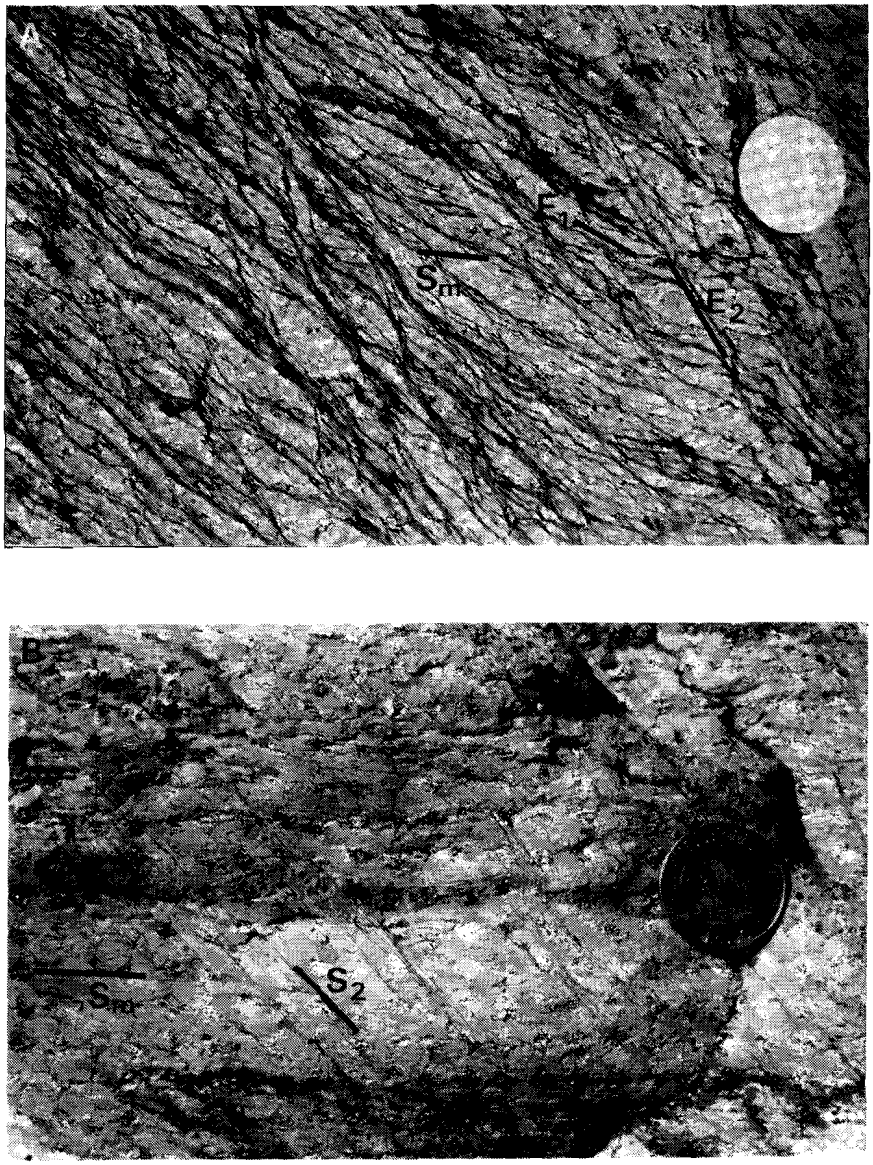

Fig. 4.3. Macroscopic Ol-bearing structures developed in serpentinite mylonites. [A] Multiple set of Ol-bearing ecc's (E_1 and E_2) deforming an Ol-free shear foliation (S_m), and indicating a dextral sense of shear. Diameter coin 2.5 cm. [B] Ol-bearing crenulations (S_2) deforming an Ol + Ti-Chu-bearing vein and an Ol-free shear foliation (S_m). Diameter coin 2.5 cm. [C] Folded Ol + Ti-Chu-bearing vein in

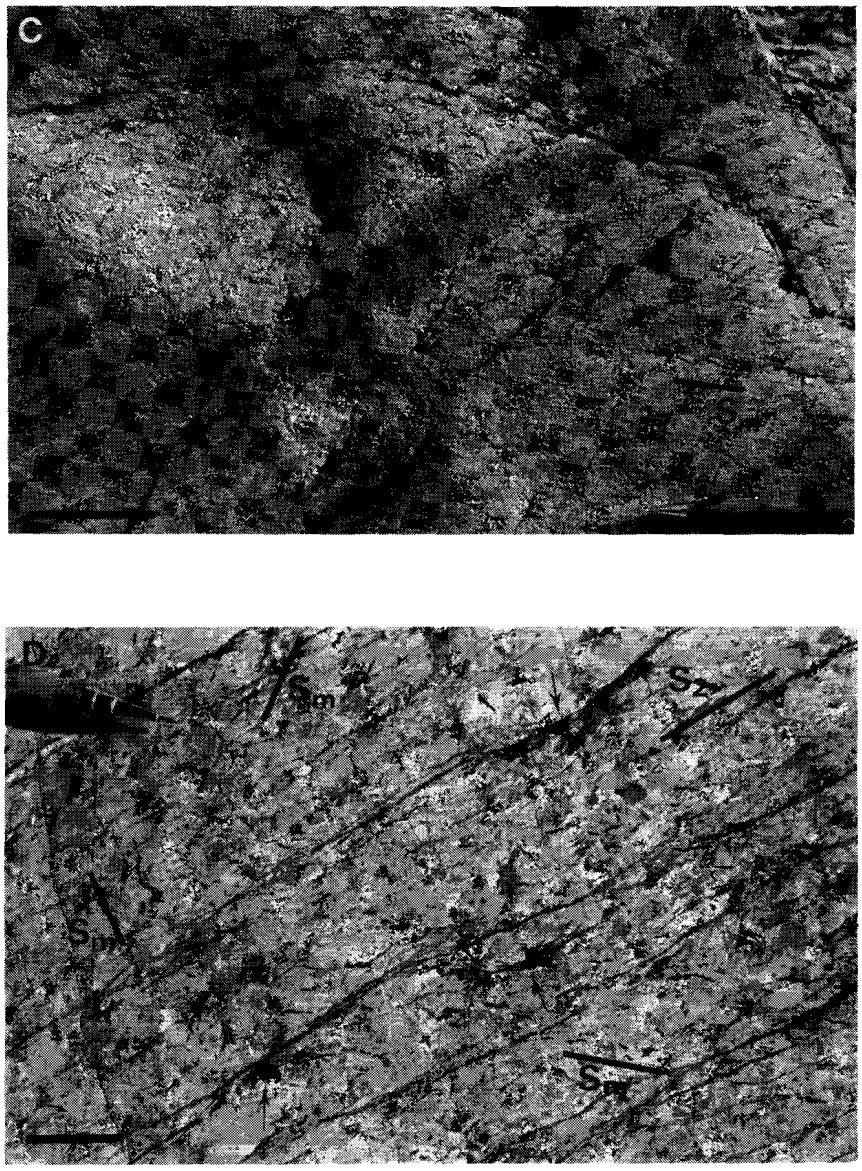

serpentinite mylonite with Ol-bearing shear foliation (S_m). Scale bar 5 cm. [D] Ol-bearing crenulation foliation (S_2) with overgrowth of radial Ol + Brc aggregates (arrows). Trace of shear foliation indicated by S_m. Scale bar 2 cm.

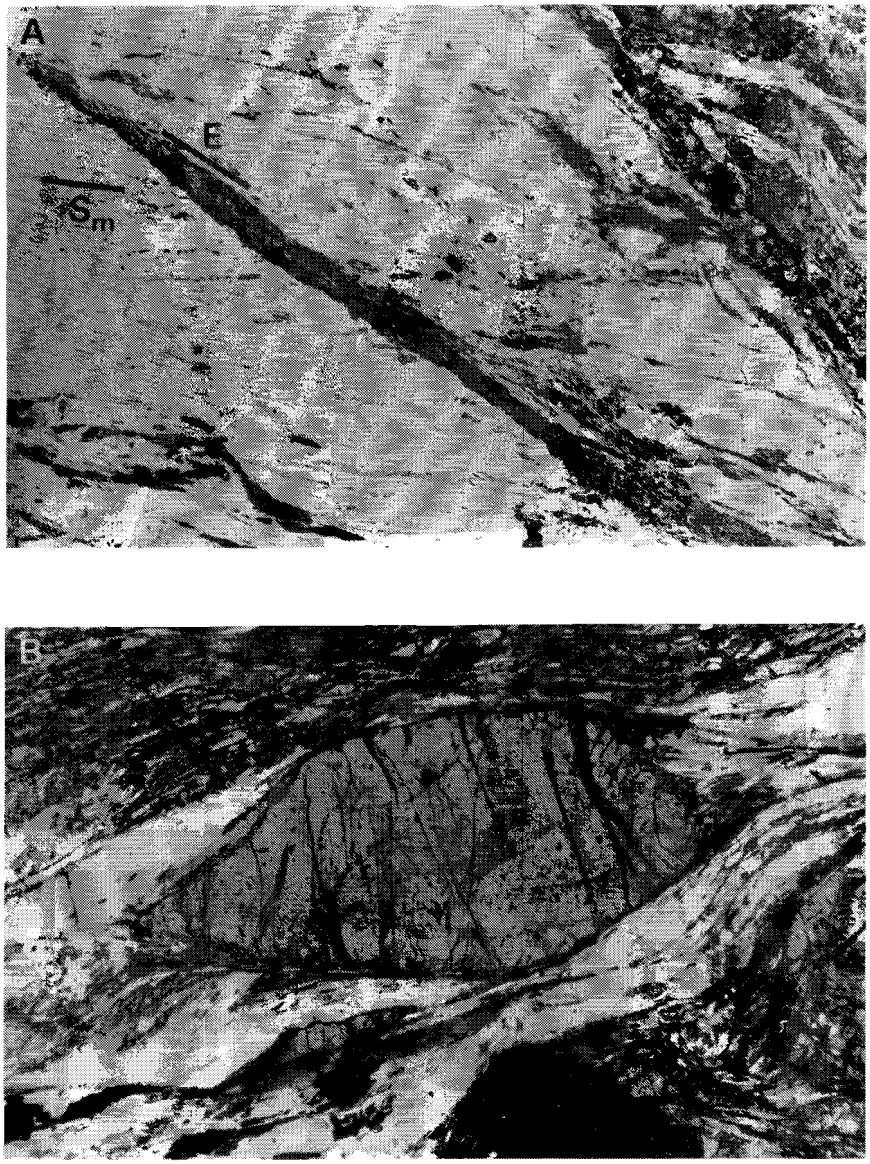

Fig. 4.4. Microscopic Ol-bearing structures developed in serpentinite mylonites (plane polarized light). [A] Ol-free shear foliation (S_m) overprinted by fine-grained Ol + Ti-Chu + Mag-bearing ecc (E) and indicating a dextral sense of shear. Width of micrograph 1.40 mm. [B] Asymmetric titanian clinohumite porphyroclast in serpentinite mylonite with Ol + Di + Atg + Mag foliation. Sense of shear is dextral. Note

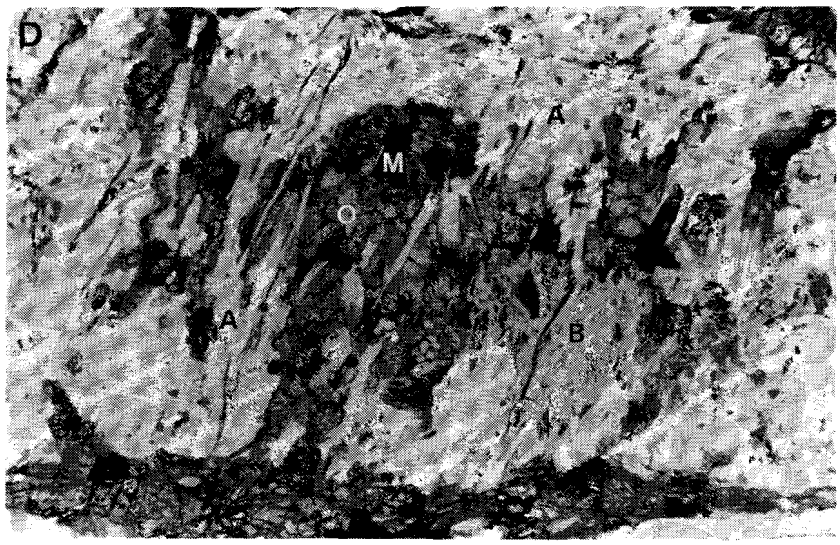

the growth of fibrous Ti-Chu + Atg + Mag in the strain shadows. Width of micrograph 1.4 mm. [C] Crenulation of Ol + Ti-Chu + Mag + Atg-bearing ecc. In sheared limbs the assemblage breaks down to antigorite. Width of micrograph 0.54 mm. [D] Olivine (O) + brucite (B) + magnetite (M) aggregate overgrown by antigorite (A). Width of micrograph 0.64 mm.

between shear-induced foliations, extensional and compressional crenulation cleavages, and veins (Fig. 4.2 B). These complex structures, however, are confined to the strongly foliated serpentinite in the mylonites and have not been developed in the peridotite wall rock.

The gradual transition from partially serpentinized peridotite in the margins to pure serpentinite in the centres of the mylonites, reflects progressive synkinematic hydration of the wall rock within these shear zones. The development of single and locally multiple sets of extensional crenulation cleavages (ecc's, Fig. 4.3A) as well as folding and crenulation of the shear induced foliations (Fig. 4.3B) point to a progressive WNW directed thrust-sense displacement across these mylonite zones. In some mylonites younger sets of crenulation foliations and ecc's indicates late-stage extensional reactivation of some of these complex thrust zones (Fig. 4.1, see also Chapter 3.2).

At the microscale, the shear induced foliation is defined either by oriented Atg+ chlorite (Chl) + magnetite (Mag) (i.e. Ol-free) or by Atg + Ol + Ti-Chu + diopside (Di) (hence Ol-bearing) assemblages. However, the most conspicuous Ol +Ti-Chu-bearing assemblages are developed along the single and multiple sets of ecc's which deform these foliations (Fig. 4.3A). This suggests that the serpentinite mylonites progressively developed under changing metamorphic conditions (Fig. 4.1). Ol-bearing ecc's (Fig. 4.4A) consist of fine-grained Ol + Ti-Chu + Atg + Mag + pyrite (Py) ± Chl ± brucite (Brc). The equidimensional to elongated olivine grains and the other phases show a moderate to strong shape preferred orientation. This assemblage is interpreted as having developed syntectonically during partial dehydration of the serpentinite in the ecc's. Similar ultrafine-grained olivine in microscopic shear zones has been produced experimentally during syntectonic dehydration of intact serpentinite and serpentinite gouges (Rutter & Brodie 1988a).

Discordant cm-scale veins filled with a coarse-grained Ol + Ti-Chu + Mag + Atg + Py ± Di assemblage are very common in the serpentinite mylonites, and developed at various stages during the deformation history (Fig. 4.1). In serpentinite mylonites with an Ol-free shear foliation the veins dissect the foliation and the Ol-bearing ecc's, but are overprinted by the Ol-bearing crenulation foliations (Fig. 4.3B). The crenulations in turn are locally cut by a second generation of Ol-bearing veins. In contrast, the development of serpentinite mylonites with an Ol-bearing shear foliation clearly postdate the development of Ol + Ti-Chu-bearing veins. In these mylonites the veins are folded (Fig. 4.3C) or boudinaged and a fine-grained, fibrous assemblage of Atg + Ol + Ti-Chu or Atg + Ti-Chu + Mgt developed in the strain shadows of large crystals of olivine and Ti-clinohumite respectively (Fig. 4.4B). In many cases the Ol-bearing ecc's and crenulations are overgrown by radial aggregates of coarse-grained olivine and brucite (Fig. 4.3D). Subsequent deformation led to crenulation of the shear foliations, Ol-bearing ecc's, veins, and deformation of the Ol + Brc aggregates. In the hinge zones of the crenulations the Ol-bearing assemblages break down to Atg ± oxides (Ox) (Fig. 4.4C) which marks the onset of retrogression. Other distinctly retrogressive features are aggregates of Atg + Brc growing at the expense of Alpine olivine associated with minor titanian clinohumite (Fig. 4.4D).

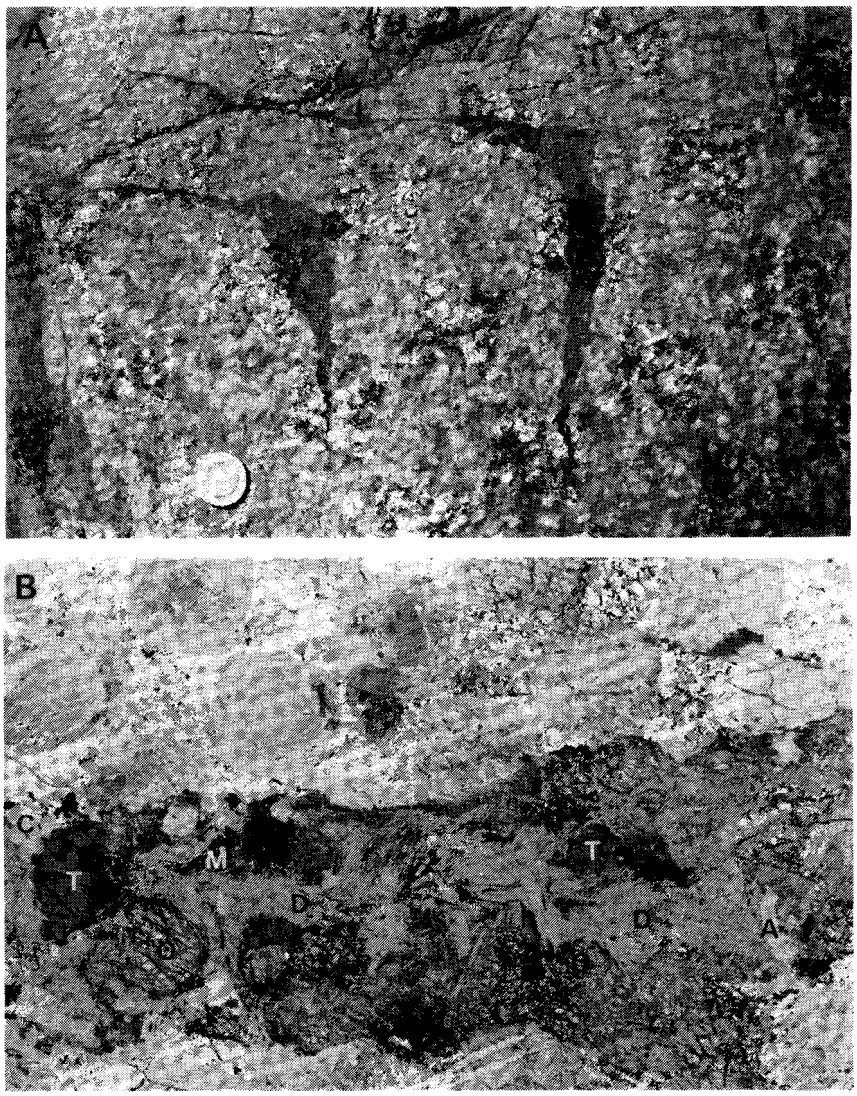

Fig. 4.5. [A] Olivine-bearing tapering veins oriented perpendicular to fracture termination in the peridotite. Diameter coin 2.5 cm. [B] Micrograph of olivine-bearing vein in strongly serpentinized peridotite wall. Fracture filling consists of coarse olivine (O) and Ti clinohumite (T) grains in a finer grained matrix of diopside (D), magnetite (M), chlorite (C) and antigorite (A). Width of micrograph 35 mm.

Peridotite wall rock

In the peridotite wall rock adjacent to the serpentinite mylonites, the original mantle assemblages are partially transformed to mesh-textured chrysotile (Ctl) after olivine, tremolitic amphiboles (Tr) after pyroxenes, and by Chl + Mag after spinel. These static transformations, which are very common in Alpine peridotites (e.g. Bearth 1967; Pognante 1981), are thought to reflect a stage of ocean floor metamorphism. The

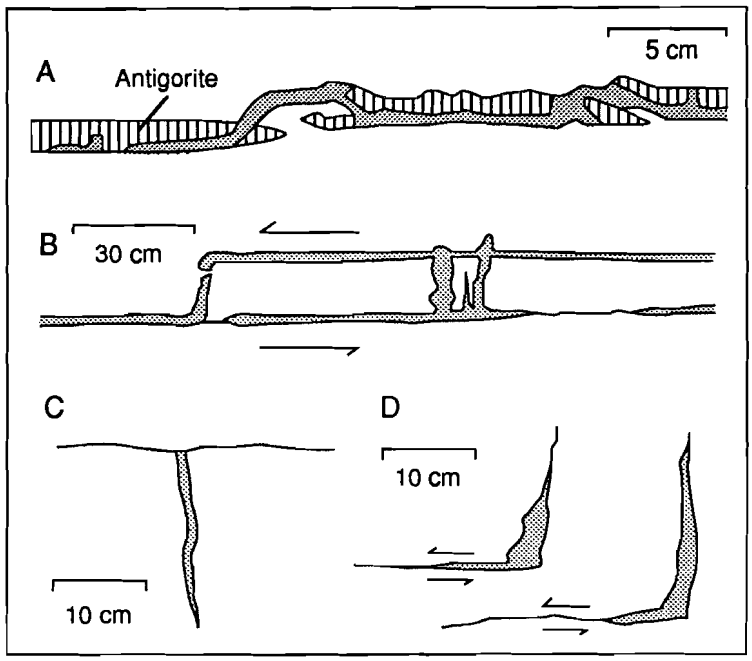

Fig 4.6. Geometry of fracture systems with olivine-bearing assemblages (stippled) in the Erro-Tobbio peridotite. [A] Antigorite crack-seal vein "intruded" by olivine and titanian clinohumite. [B] Paired olivine-bearing fracture system with tensile bridges. [C] Tensile fracture perpendicular to olivine-bearing fracture. [D] Tensile fractures developed at olivine-bearing fracture terminations

prograde onset of the Alpine metamorphic evolution in the peridotites is marked by the development of Atg + Mag ± Brc crack-seal veins, which dissect the earlier mantle and oceanic assemblages (Fig. 4.1). In turn, all the above microtextures are statically overgrown by neoblastic Ol + Atg + Ti-Chu, which preferentially developed at the expense of mantle olivine. In addition, this Alpine assemblage commonly includes diopside replacing earlier mantle pyroxenes. However, the most conspicuous structures related to the Alpine evolution of the peridotites are veins and cracks filled with an assemblage of Ti-Chu + Ol + Di + Mag ± Atg ± Chl (Fig 4.5, 4.6; Cimmino et al. 1979; Piccardo et al. 1988; Hoogerduijn Strating et al. 1990). The coarse-grained vein minerals may be zoned, and contain numerous fluid inclusions, which indicates that fluids, presumably hydrous, were present during mineral growth. Locally, these veins developed along the early Atg-bearing veins (Fig. 4.6A). In general, however, the veins are associated with single or paired sub-planar shear-fracture systems, developed in macroscopically intact peridotite, and oriented more or less parallel to the serpentinite mylonites. Offsets of pre-existing markers (i.e. early antigorite veins) across these fracture systems indicate WNW directed, thrust-sense displacements along these brittle faults, i.e. identical to the inferred movement sense of the serpentinite mylonites. The Ol-bearing assemblage occurs in tapering veins, oriented at a high angle to the fractures, but also along the fractures and in tensile bridges linking paired fractures (Fig. 4.6B, C, D). Fracturing of the peridotite was accompanied by minor

plastic deformation leading to the development of microscale olivine-bearing shear zones and deformation of serpentine minerals in the wall rock adjacent to the fractures and veins. Frequently, the vein minerals are slightly deformed and partially recrystallized to preferably oriented, fibrous Ol + Ti-Chu + Atg + Ox, indicating minor deformation of the veins at peak metamorphic conditions.

The above peak assemblages are statically overgrown by retrogressive Atg ± Ox ± Brc associations, while the latest stages of retrogression are characterized by coronitic Tr + Ctl rims in between mantle diopside relics and granular Ol + Atg ± Ti-Chu aggregates (Fig. 4.2).

Metagabbroic dykes

The metagabbroic dykes in the peridotite commonly show intense rodingitization, which is generally explained by metasomatic processes related to ocean floor metamorphism (e.g. Piccardo et al. 1980). Based on mineralogical and textural relics, a primary magmatic assemblage has been inferred of Cr-rich clinopyroxene, plagioclase and olivine. During the Alpine evolution, most of the dykes are sheared and transformed into metarodingites (Fig. 4.1) characterized by fractured and rotated clinopyroxene porphyroclasts in a foliated matrix of Di + Chl + zoisite (Zo) + Mag ± garnet (Grt) (Hoogerduijn Strating et al. 1990).

Although most gabbroic dykes in the ET unit are metarodingites, few dykes which escaped early rodingitization are marked by chloritoid-bearing, eclogitic assemblages. Similar high-pressure metamorphosed, chloritoid-bearing metagabbroic dykes have been documented from the Lanzo peridotite of the Western Alps by Kienast and Pognante (1988). The metagabbros in the ET unit commonly have a flaser-type foliated structure marked by strongly deformed omphacite crystals, suggesting plastic deformation of these dykes during HP metamorphism. Offsets of pre-existing markers (i.e. pyroxenite bands in the peridotite wall rock) across the deformed dykes, obliquity of the foliations with respect to the margins of the dykes, and the occurrence of asymmetric porphyroclast systems indicates that the plastic deformation involved an important component of non-coaxial flow.

At the microscale, primary Cr-rich clinopyroxene in the eclogitic metagabbros is fractured and pseudomorphosed to either single grains of omphacite (Omp) or to coarse-grained granoblastic omphacite (Jd_{29-42}) aggregates. These porphyroclasts and aggregates are recrystallized along fractures and margins into finer-grained more jadeitic omphacite (Jd_{44-47}). The primary plagioclase is completely transformed into fine-grained aggregates of impure jadeite (Jd_{85-91}) + Zo ± Grt ± rare quartz (Qtz) with a moderate to strong shape preferred orientation (see Appendix A1 for composition impure jadeite). The domains of previous primary olivine are transformed into aggregates of preferably oriented Chl + clinozoisite (Czo) + Omp (Jd_{39-49}) ± talc (Tlc). These microstructures are consistent with semi-brittle to ductile behaviour of the dykes under eclogitic conditions (cf. Carter & Kirby 1978). The boundaries between the olivine and plagioclase domains are marked by thin, disrupted coronitic rims of fine-grained garnet. Chloritoid (Cld) coexisting with Omp + Chl ± Tlc is concentrated near this contact. Relics of a granoblastic rim of Omp + Cld ± Tlc occur at the contact

between domains of previous olivine and clinopyroxene, whereas fine-grained garnet is preserved in between the pyroxene and plagioclase domains. The presence of these disrupted coronitic rims in between primary mineral domains suggests, that the synkinematic transformation to eclogitic assemblages was preceded by a partial static recrystallization (cf. Rubie 1983; Pognante 1985). The retrograde evolution of the metagabbros is reflected by the blastesis of albite and amphibole aggregates in the plagioclase domains (Fig. 4.1).

Locally, thin tapering veins filled with an Ol + Ti-Chu-bearing assemblage occur within the peridotite adjacent to sheared gabbroic dykes. The veins, generally with a length up to 0.5 m, are oriented at a high angle to the dykes and run from within the deformed margins into the surrounding peridotite. In addition, some of the paired fracture systems with associated Ol-bearing tensile bridges bend into the margins of the gabbroic dykes without displacement of the gabbro-peridotite contact. These field relationships strongly suggest that the high pressure ductile deformation in the metagabbroic dykes occurred simultaneous with crack propagation, shear fracturing and subsequent filling in the peridotite wall rock.

4.3 TECTONO-METAMORPHIC EVOLUTION OF THE ERRO-TOBBIO UNIT

The structural and petrological data indicate that the ET peridotites were affected by a complex tectono-metamorphic evolution related to Alpine subduction and collision. The pertinent mineral reactions involved in the Alpine metamorphic cycle are shown in Figure 4.7. The prograde chrysotile-antigorite transition could be related to reaction 3, in response to a temperature increase. There are no data available to constrain the pressures during this early stage. The stability field of the Atg + Ol + Ti-Chu peak metamorphic assemblage lies within the antigorite stability field (Trommsdorff & Evans 1980), and is limited towards lower temperatures by the reaction Atg + Brc = Ol + H_2O (Fig. 4.7, reaction 4), and to higher temperatures by the reaction Atg = Ol + Tlc + H_2O (Fig. 4.7, reaction 6). The breakdown of Ti-Chu, towards higher temperatures, to produce Ol + ilmenite (Ilm) has not been observed in the samples studied. The conditions for this reaction strongly depend on the fluorine content of the Ti-Chu, since small amounts of fluorine will rapidly expand the Ti-Chu stability field to higher temperatures (compare reactions 5 and 7 in Fig. 4.7; Engi & Lindsley 1980; Evans & Trommsdorff 1983). Microprobe analysis (Appendix A1) show that the titanian clinohumite is essentially fluorine-free ($\leq$ 0.05 wt% F), hence reaction 5 can be regarded as an upper limit for the peak metamorphic assemblage.

The field relationships show that at least some of the Ol + Ti-Chu-bearing veins in the peridotite developed during ductile deformation of the gabbroic dykes. The synkinematic growth of jadeite (see Appendix 2 for mineral chemistry) and quartz at the expense of plagioclase in some of these dykes suggests that the ET Unit may have reached pressures in excess of 1300-1600 MPa at temperatures between 450 and 550°C (Fig. 4.7; cf. Holland 1983). The local evidence for static growth of Omp + Cld ± Chl prior to deformation of the gabbroic dykes equally suggests high pressure eclogite

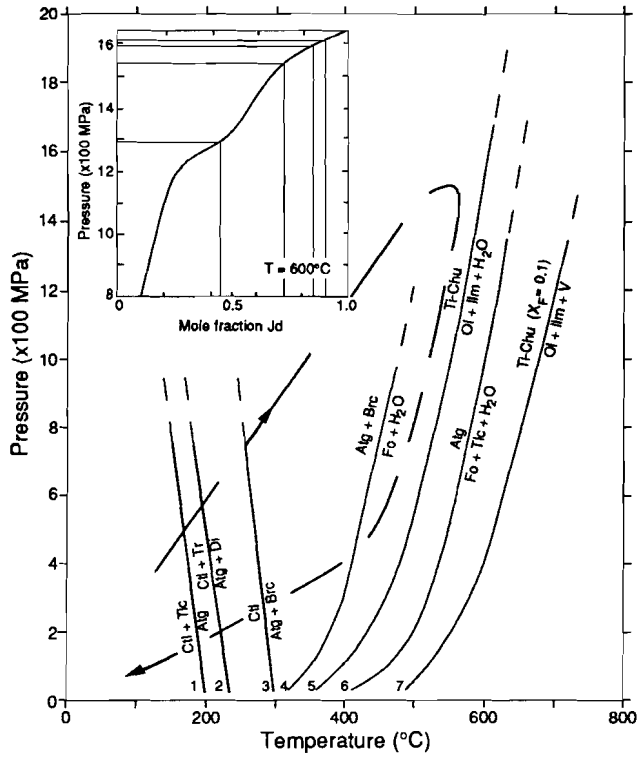

Fig. 4.7. P-T diagram showing inferred metamorphic history of the ET peridotite with reference to mineral equilibria in the serpentine multisystem (reactions 1, 3, 4, 6 after Evans et al. 1976) and the tremolite-diopside-bearing serpentine system (reaction 2 after Oterdoom 1978). Breakdown reactions for fluorine-free Ti-Chu (5) and fluorine-bearing (X_F=0.1) Ti-Chu (7) after Engi & Lindsley (1980). Inset: Minimum pressure estimate at 600°C according to the jadeite mol fraction in sodic pyroxenes coexisting with quartz in primary plagioclase domains (Holland 1983).

facies conditions (cf. Guiraud et al. 1990). It should be noted, that no such pressure control is available for the majority of the Ol-bearing microstructures. It is, therefore, unknown whether most of the peak metamorphic assemblages developed at the same high pressure conditions or, alternatively, during nearly isothermal decompression (Fig. 4.7, see also Chapter 3.2).

In the peridotites as well as in the serpentinite mylonites, the onset of cooling is marked by the breakdown of olivine and titanian clinohumite to Atg + Fe-Ti Ox ± Brc which is roughly represented by reaction 4 (Fig. 4.7). The latest stage of retrogression resulted in the development of coronitic Ctl + Tr assemblages in between mantle diopside and the Ol + Atg ± Ti-Chu aggregates (Fig. 4.7, reaction 2).

The Alpine PT evolution inferred here for the ET peridotite and crosscutting gabbroic dykes (Fig. 4.7) is consistent with those inferred for the other thrust units in the Voltri Group (Chapter 3), which are also characterized by decompression under nearly isothermal conditions.

4.4 THE MECHANICAL BEHAVIOUR OF THE PIEMONTE-LIGURIAN OCEANIC CRUST DURING SUBDUCTION

The structural and petrological data summarized above suggest a close relationship, at peak pressure conditions, between ductile thrusting, dehydration reactions, the presence of fluids, (semi-)brittle shear-fractures, (transiently) open cracks, and the growth of eclogite facies mineral assemblages. It seems likely, therefore, that the shear-fractures and olivine-bearing veins in the peridotite developed in response to syn-kinematic fluid release in the serpentinite mylonites, which implies that fluid-assisted brittle failure may occur in subducting slabs, at depths down to at least 40 km. The hypothesis of hydraulic fracturing in the ET peridotite is now tested by considering a number of mechanical constraints.

Laboratory constraints

Extrapolation of laboratory data to geological conditions is hampered by many uncertainties (e.g. Carter & Tsenn 1987). The brittle fracture strength of rocks increases markedly with pressure and may be described by a modified Coulomb shear-failure criterion (e.g. Ohnaka 1973). However, this criterion does not account for thermally activated processes such as stress-aided chemical corrosion and plastic deformation at tips of microcracks (Anderson & Grew 1977). These processes generally have a weakening effect, hence a modified Coulomb criterion can be expected to represent an upper bound on the brittle fracture strength. The brittle domain is limited by a temperature-dependent transition to the ductile regime in which deformation is dominated by creep processes. The transition from entirely brittle to entirely ductile deformation is gradual, and rocks in this transtionion zone are inferred to show semi-brittle behaviour (Carter & Tsenn 1987). Figure 4.8 shows the shear-fracture strength of Capri serpentinized peridotite (Murrell & Ismail 1976) for various fluid pressure ratios, and the creep strength for dry Frederick diabase (Shelton & Tullis 1981) and wet Åheim dunite (Chopra & Paterson 1981). There are no experimentally derived laws which describe the semi-brittle behaviour of rocks. For want of better data, gabbro is treated as a coarse-grained diabase. This first order approximation seems justified in view of the grain-size insensitivity of dislocation creep mechanisms. However, the gabbroic dykes at Voltri show clear evidence of semi-brittle deformation and synkinematic transformations to fine-grained eclogitic assemblages which may have resulted in drastic weakening (Rubie 1983). Therefore, a dislocation creep flow law will probably lead to serious overestimates of the flow stress, hence the calculated values for diabase can at best be considered to provide an upper limit to the creep strength of the gabbroic rocks.

It follows from Figure 4.8 that a wide range of conditions exists in which dunite may deform by brittle mechanisms whilst diabase deforms by ductile flow. In order to explain the brittle structures observed in the ET peridotite, we consider the mechanical behaviour at depths between 40 and 60 km. Van den Beukel and Wortel (1988) calculated the temperature distribution in subduction systems, and constructed geotherms

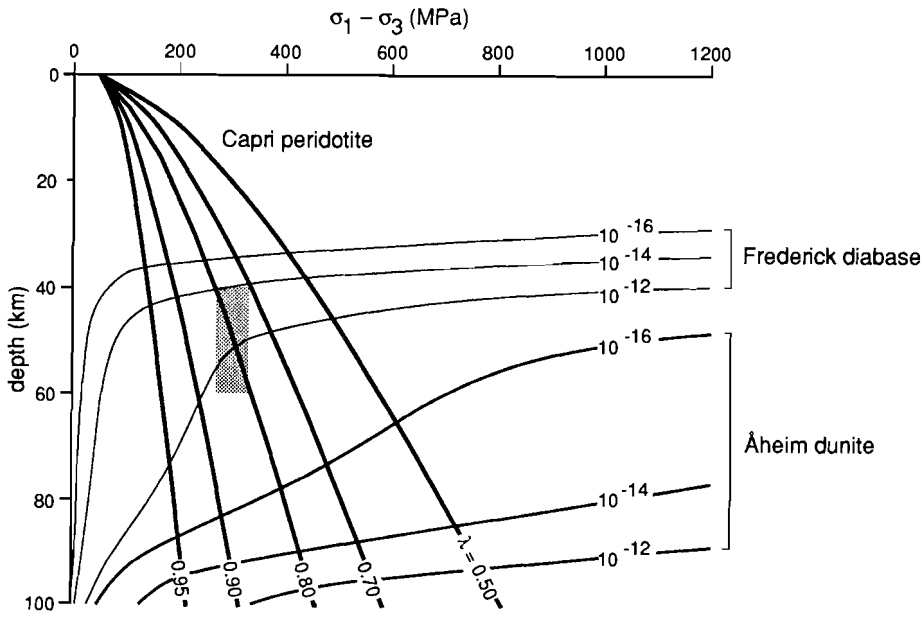

Fig. 4.8. Creep strength (σ_1-σ_3) using extrapolated flow laws for dry Frederick diabase (experimental conditions: creep and constant strain rate tests 10^{-4}-$4x10^{-8}$ s^{-1}; T= 650-1125°C; P_{conf}= 1500 MPa (solid medium), $\Delta\sigma$= 100-1300 MPa; Shelton & Tullis 1981) and wet Åheim dunite (experimental conditions: constant strain rate tests 10^{-3} - 10^{-6} s^{-1}; T= 1000-1210°C; P_{conf}= 300 MPa (gas); $\Delta\sigma$= 112-740 MPa; Chopra & Paterson 1981) for strain rates of 10^{-12}, 10^{-14} and 10^{-16} s^{-1}. Assumed rock density is 3000 kg/m^3. Increasing depth or lithostatic pressure (P_l) has been taken equivalent to increasing temperature according to the subduction geotherm TDIO3 calculated by Van den Beukel and Wortel (1988). The brittle shear strength is calculated for various fluid pressure ratios (λ) using the expression $(\sigma_1\text{-}\sigma_3)_{eff} / C = 1 + K [\sigma_3(1\text{-}\lambda)/C]^n$ (after Ohnaka 1973). $\lambda = P_f/P_l$, where P_f is the pore fluid pressure. The values for n, K (exponent and coefficient of pressure dependence), and C (compressive failure strength at 0.1 MPa) are derived from a best fit to the data of Capri serpentinized peridotite (experimental conditions: constant strain rate 10^{-5} s^{-1}; undrained; T= 420°C; P_{conf}= 103-552 MPa (gas); Murrell & Ismail 1976). At depths between 40 and 60 km diabase deforms in a ductile manner. Even at relatively high differential stresses, however, brittle shear failure of peridotites will only occur at high fluid presssure ratios. At 300 MPa, inferred fluid pressure ratios at fracturing are about 0.8 (shaded area).

along the upper part of the subducting plate. These geotherms are distinctly non-linear and the gradients strongly depend on shear heating at the plate contact and thus on the adopted oceanic crustal rheology. The peak eclogitic conditions inferred for the ET peridotite correspond well to those calculated for a subducting slab with a wet diorite crustal rheology (their model TDIO3). Using this geotherm, the P-T conditions at depth between 40 and 60 km correspond to about 1200-1800 MPa and 450-550°C. The gabbro dykes in the ET peridotite show plastic deformation under these conditions, which corresponds well with the inferred rheological behaviour of diabase (Fig. 4.8).

The peridotite shows brittle fractures, however, expected only in the presence of high fluid pressures. This is demonstrated in Figure 4.8, which shows that even under relatively high differential stress conditions (about 300 MPa), pore fluid pressures (P_f) close to the lithostatic pressure (P_l) are needed to fracture the peridotite ($\lambda = P_f/P_l \approx 0.8$).

Fluid release and fluid pressure during serpentinization

In order to explore the feasibility of high fluid pressures in the ET peridotite during subduction metamorphism, the dehydration of a 0.1 m wide serpentinite mylonite zone is considered in a volume of 1 m^3 of peridotite (Fig. 4.9). The mylonite contains 1 mm thick shear bands, spaced 1 cm from one another, and oriented at a angle of 20° to the margins of the mylonite zone. These values roughly correspond to the dimensions observed in the field. Dehydration is assumed to occur in the shear bands only (volume about 9100 cm^3) and follows the reaction 1 Atg + 1 Brc = 2 Fo + 3 H_2O. At increasing fluid pressure this reaction will shift to higher temperatures, however, this shift is limited to about 100°C. The reaction reduces the volume of the solids to about 5200 cm^3, equivalent with a volume reduction of the entire mylonite zone of about 4%. Following Halbach and Chatterjee (1982), the resulting vapour pressure would be about 100 MPa if no volume loss is allowed. However, the microstructures indicate that the dehydration occurs synkinematically, and it may be expected that the plastic deformation will allow a pore space reduction until the fluid pressure approaches lithostatic values (e.g. Kerrich et al. 1984). A volume reduction may be achieved by thinning of the mylonite zone due to movement along the shear bands. This can be described by s = D.sin (20°), where s is the shortening across the mylonite, and D the sum of the displacements along each individual shear band in the metre-long segment (cf. Norrell et al. 1989). The fluid pressure will equal the lithostatic pressure (± 1400 MPa) after a width reduction of 2%, attained at 1.9 mm displacement along each shear

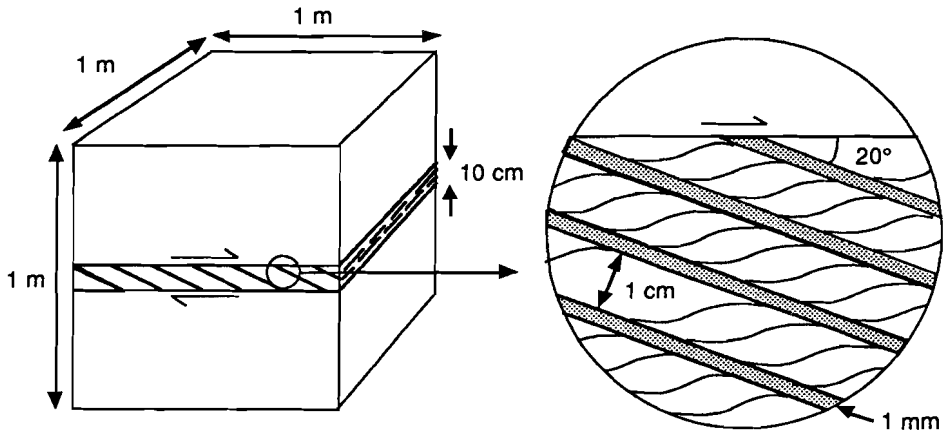

Fig. 4.9. Geometrical relationships in an hypothetical serpentinite mylonite (see text for details).

band. These values correspond to a shear strain of approximately 0.52.

From the above analysis it follows that synkinematic dehydration reactions in the serpentinite mylonites can easily produce fluid pressures close to lithostatic values in serpentinite mylonite zones, which, presumably, leads to a hydraulic gradient between the mylonite zone and the peridotite wall rock. In response, fluids will tend to migrate into the wall rock, and as long as the rate of fluid production in the serpentinite mylonites exceeds the bulk fluid migration rate in the system, fluid pressures in the peridotite will rise. Whether this results in hydraulic failure along discrete fractures depends on the maximum fluid pressures attained, the magnitude of the deviatoric stresses, and the mechanical properties of the rocks involved (e.g. Yardley 1983).

Fluid pressures during hydraulic fracturing

The different rock types involved and their contrasting rheological behaviour constrain the fluid pressures during fracturing of the peridotite. An upper bound follows from the fact that fluid overpressurization (i.e. $\lambda \geq 1.0$) is limited by the tensional strength (T) of the rocks since hydraulic tensile fracturing will occur when $P_f = \sigma_3 + T$, hence $\lambda \leq 1 + T/\sigma_3$. For present purposes σ_3 is considered to be equal to the lithostatic pressure. This assumption seems reasonable, in view of the observation that earthquake focal mechanism solutions (e.g. Yosshi 1979; Page et al. 1989) suggest a nearly vertical orientation of the least compressive stress along the subduction plate boundary. The tensile strength strongly depends on fracture mechanics parameters and prevailing environmental conditions. However, available laboratory measurements (e.g. Atkinson & Meredith 1987) do not allow a valid estimation of the tensile strength of rocks under eclogitic conditions. For want of better data, the tensile strength under atmospheric conditions will be used, and is calculated for all lithologies assuming that initial flaws are penny-shaped grain-boundary microcracks (Lawn & Wilshaw 1975, p. 59). Fluid overpressurization is thus limited by the lithology with the lowest tensile strength, i.e. serpentinite. A further constraint on λ follows from the observation that the serpentinite mylonites and the gabbroic dykes were ductile while the peridotite deformed by brittle mechanisms. This implies that the brittle shear failure strength of gabbro and serpentinite must have exceeded the ductile flow strength of these materials. The critical values of P, T, λ and strain rate at which this transition from brittle to ductile behaviour occurs are calculated on the basis of a dislocation creep flow law and a modified Coulomb criterion. Since experiments suggest that the flow stresses of gabbro exceed those of serpentinite, the mafic rocks provide the upper limit. A lower bound to λ follows from the occurrence of purely tensile fractures in the peridotite, which implies that the maximum effective differential stress at failure should obey $(\sigma_1 - \sigma_3)_{eff} \leq 4T$ (Secor 1969). The calculated tensile strength of peridotite is 46.9 MPa, suggesting that the effective differential stress at failure did not exceed 200 MPa. Taking this value, a modified Coulomb failure criterion (e.g. Ohnaka 1973) provides the corresponding P-λ conditions at which the shear-fractures in the peridotite may have developed.

The calculated upper and lower limits discussed above are shown in Figure 4.10. Maximum fluid pressure ratios are strongly strain-rate dependent, and it is inferred that the transient fluid pressures must have reached about 0.9 times the lithostatic pressure

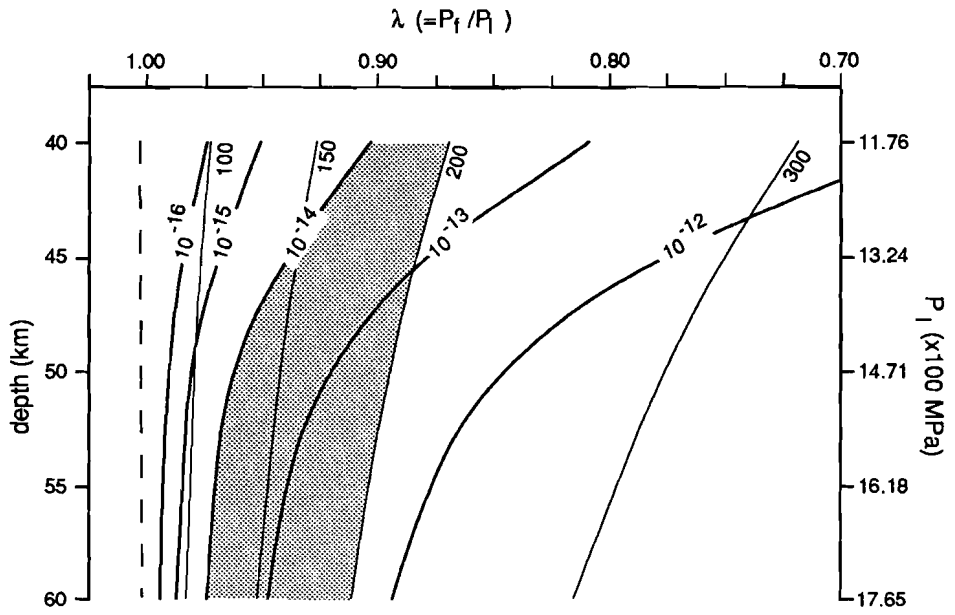

Fig. 4.10. Dependence of λ on depth (or P_l). Dashed line indicates maximum possible λ at hydraulic tensile fracturing calculated for serpentinite (T=12.3 MPa). Thick lines indicate maximum λ values (strain rate dependent) calculated using the extrapolated flow law for dry diabase and the shear strength for Nahant gabbro (experimental conditions: constant strain rate test 2.4×10^{-4} s^{-1}; room temperature; P_{conf}= 42-517 MPa (oil); Byerlee, 1968). The thin lines indicate minimum λ values (differential stress dependent) for Capri peridotite (Murrell and Ismail, 1976). The shaded area represents feasible λ values for a strain rate of 10^{-14} s^{-1} and a maximum differential stress of 200 MPa. For further details see text.

in order to produce the structures observed in the ET peridotite. Reduction of the gabbro flow stress in view of the inferred semi-brittle behaviour (cf. Carter & Kirby 1978) and the reaction-enhanced softening would shift the strain-rate dependent maximum λ curves to the left. A decrease of the tensile strength of peridotite due to thermally activated processes will lead to fracturing at lower differential stresses, hence also shift the lower bound on λ towards higher values. The behaviour of peridotite is inferred to be semi-brittle instead of brittle, hence shear failure at given conditions of P, T and Δσ would probably have occurred at lower fluid pressures, thus shifting the lower boundary to λ to lower values. With the presently available rheological data it is not possible to quantify these effects, but the analysis presented above probably provides a good first order approximation of the transiently high fluid pressures to be expected in subducting slabs.

4.5 IMPLICATIONS FOR SHEAR STRESSSES IN THE UPPER PART OF A SUBDUCTION ZONE

The structures in the ET peridotite show, that deformation in the upper 60 km of the subduction zone was strongly localized in serpentinite mylonites. The petrological data suggest that these mylonite zones became olivine-bearing at a depth below about 35 km.

Experimental studies on serpentinite show that, irrespective of the dependence of shear strength on mineralogy and initial texture (Raleigh & Paterson 1965; Murrell & Ismail 1976; Rutter & Brodie 1988a), the material generally starts to show macroscopic ductile behaviour at conditions which approximately correspond to those prevailing at a depth of about 30 km in a subduction zone. The flow strength of serpentinite at geological strain rates is not well constrained. Extrapolation of Rutter and Brodie's experimental data to geological strain rates yields maximum shear stresses around 100 MPa at 300°C. At temperatures around 450°C the experimentally deformed serpentinite becomes olivine-bearing and shear stresses drop dramatically. Rutter & Brodie (1988a) suggest that the deformation of the serpentinite at these elevated temperatures was controlled by diffusion-accommodated grain boundary sliding of ultrafine-grained olivine developed along microscopic shear zones in the serpentinite. These experimentally produced bands with fine-grained olivine are very similar to the fine-grained olivine-bearing shear bands observed in the ET serpentinite mylonites. There are as yet no fabric or TEM studies on these fine-grained bands, but the general equidimensional grain shape fabric may indicate that similar diffusion-controlled deformation mechanisms have been operative. The average olivine grainsize in the ecc's in the ET serpentinite mylonites is 10 μm (ranging from 5 to 30 μm). According to "wet" diffusion creep flow laws (Karato et al. 1986; Rutter & Brodie 1988a,b) at a strain rate of 10^{-13} s^{-1}, the flow stresses in the Ol-bearing serpentinite mylonites would not have exceeded 75 MPa at 450°C and 5 MPa above 500°C (Fig. 4.11).

The above discussion shows that the shear stresses in peridotite-dominated subduction zones would probably not exceed 60 MPa in the upper 30 km, and decrease to less than 5 MPa below 40 km (Fig. 4.11). These values correspond fairly well with those calculated by Van den Beukel and Wortel (1988) for subduction zones with an oceanic crustal rheology dominated by wet diorite. However, shear stresses in their models decrease gradually from about 100 to 10 MPa in the depth range between 40 and 90 km, whereas the shear stresses inferred here for a peridotite dominated subduction zone decrease very rapidly in the depth range between 30 and 40 km. This will lead to a substantial decrease of shear heating at the plate contact below 30 km depth, which may have a strong effect on the thermal structure of the overlying accretionary wedge. In addition, the fluids released during dehydration reactions may result in a transient but significant strength reduction of all lithologies in the upper part of the subducting slab. The structures in the ET peridotite demonstrate such transient weakening of peridotites at temperatures around 500°C, in response to the breakdown of antigorite.

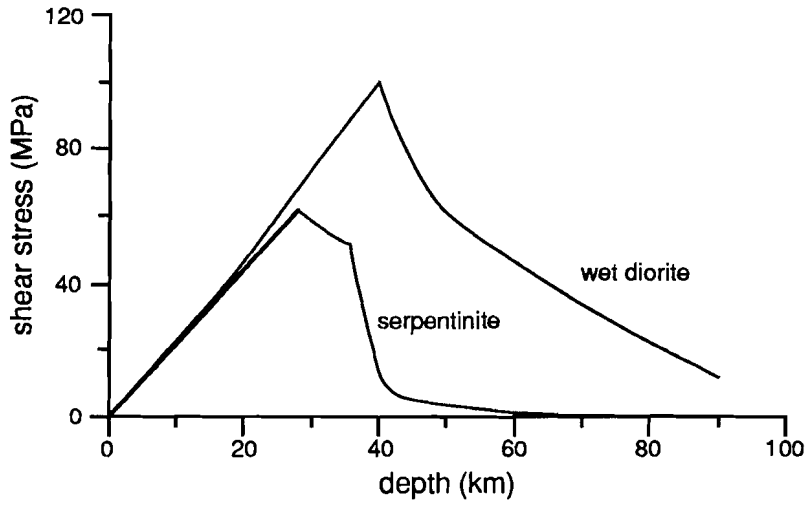

Fig. 4.11. Shear stress versus depth profiles for wet diorite (from Van den Beukel & Wortel 1988) and serpentinite. Adopted geotherm: TDIO3 (Van den Beukel &Wortel 1988). The upper 27 km of the serpentinite profile are characterized by brittle frictional sliding following Byerlee's (1978) relationship. A gouge is assumed to be present along the plate contact, which implies (cf. Engelder et al. 1975), that the coefficient of internal friction will be close to that for sliding between clean surfaces of serpentinite (i.e 0.25 on the basis of experiments of Ohnaka 1973). Following Davis et al. (1983) an average fluid pressure ratio of 0.7 is assumed in the shallow parts of the decollement. According to experimental data of Rutter and Brodie (1988a; stress relaxation tests $7x10^{-3}$-$2x10^{-8}$ s^{-1}, T=300-400°C, P_{conf}= 180MPa (fluid), P_f= 30 MPa, $\Delta\sigma$= 83-182 MPa) extrapolated to 10^{-13} s^{-1}, Byerlee's relation breaks down at 27 kilometres depth and crushed serpentinite gouge would deform by cataclasis and frictional sliding in combination with blastesis of serpentine. Below 36 kilometres depth (T>450°C) neoblastic olivine is assumed to develop along shear bands in the gouge and the deformation is accomplished by diffusion-accommodated grain boundary sliding (flow law derived by Rutter & Brodie 1988a; same experiments as above, T= 450-600°C; see also Rutter & Brodie 1988b).

It is envisaged that the break-down of other hydrous minerals in mafic and ultramafic rocks (i.e. amphibole, chlorite, mica) may similarly lead to transient weakening of the subducting slab.

4.6 CONCLUSIONS

The mineral assemblages and microstructures observed in the ET ultramafics reflect an Alpine tectono-metamorphic evolution presumably related to Late Cretaceous intraoceanic subduction and subsequent collision. It is characterized by: [1] a prograde evolution from low-grade (oceanic) to intermediate temperature conditions, associated with the development of Atg-bearing serpentinite mylonites, [2] an Ol + Ti-Chu-bearing climax assemblage which developed under eclogitic conditions (>1300-1600 MPa, 450-550°C) and possibly during subsequent nearly isothermal decompression. This Alpine metamorphic evolution was closely associated with progressive ductile

deformation along the Atg-bearing serpentinite mylonites, initiation of new Ol-bearing serpentinite mylonites, shearing of the gabbroic dykes, and fracturing of the peridotite, and [3] a cooling history marked by the onset of olivine breakdown in combination with progressive deformation along the serpentinite mylonites.

The observed structures allow to place some constraints on the mechanical behaviour of the ET peridotites during subduction. These constraints may be applicable to peridotite dominated subduction zones in general.

- Antigorite break-down under eclogitic conditions results in hydraulic fracturing. This implies that despite the dominance of localized ductile deformation, transient brittle failure may occur at depth of 50 to 70 km in subducting slabs. Inferred fluid pressure ratios needed to fracture the peridotite are about 0.9.
- Shear stresses along the subducting plate contact in the Piemonte-Ligurian ocean are controlled by the rheology of serpentinite mylonites. Experimental studies on serpentinite (Rutter & Brodie 1988) and olivine (Karato 1986; Rutter & Brodie 1988a) suggest that maximum shear stresses of about 60 MPa may have been reached at 30 km depth, while below 40 km depth they have decreased to less than 5 MPa.
- Dehydration reactions in the ET serpentinite mylonites may have resulted in transient but significant strength reductions of the subducting slab.

ACKNOWLEDGEMENTS

In april 1989 Giovanni Piccardo, Marco Scambelluri and Betta Rampone (Genova) have drawn Reinoud Vissers' and my attention to the Alpine olivine-bearing assemblages in the ET peridotites. Our joint work on these structures has been a great pleasure. I would like to thank Kate Brodie (Manchester), Volkmar Tromsdorff and Reto Gieré (Zürich) for their valuable comments on the manuscript for the J. Metam. Geol. Discussions with Colin Peach and Chris Spiers (Utrecht) and written communications with Neville Carter (Texas A&M) and Terry Engelder (Pennsylvania State) have been very helpful.

CHAPTER 5

Shear localization in the Piemonte-Ligurian upper mantle during incipient oceanic rifting, and non-adiabatic uplift of peridotites

5.1 INTRODUCTION

Many aspects of tectonics in the lithosphere are controlled by the rheological behaviour of the peridotitic upper mantle (e.g. Goetze & Evans 1979; Kirby 1985). This observation has motivated research on the rheology of olivine involving both experimental deformation studies (e.g. Avé Lallemant & Carter 1970; Karato et al. 1980, 1986; Chopra & Paterson 1981, 1984) and studies of naturally deformed peridotites (e.g. Den Tex 1969; Nicolas et al. 1971; Green & Radcliffe 1972; Gueguen 1977; Avé Lallemant 1985; Nicolas 1986a). These studies confirm that similar types of mechanisms operate in naturally and experimentally deformed olivine rocks, i.e. grainsize independent dislocation creep, grainsize dependent diffusion creep and dynamic recrystallization (Kirby 1985; Carter & Tsenn 1987).

Most geophysical models assume bulk homogeneous deformation of the upper mantle controlled by dislocation creep of olivine. There is, however, strong geological (Brodie 1980; Brodie & Rutter 1987; Handy 1989; Downes 1990) and geophysical evidence (Warner & McGeary 1987; Klemperer 1988; Reston 1990) for shear localization and concomitant grainsize reduction in the upper mantle. In the Erro-Tobbio (ET) lherzolites of the Voltri Massif, structures are preserved which are related to incipient rifting and opening of the Piemonte-Ligurian ocean (e.g. Bezzi & Piccardo 1971; Hoogerduijn Strating et al. 1989). These structures record the progressive uplift of the lherzolites from asthenospheric to shallow lithospheric levels, and show the importance, at least in the Piemonte-Ligurian lithosphere, of shear localization and grainsize reduction during lithospheric rifting.

Parts of this chapter have been published as:
Drury M.R., Hoogerduijn Strating E.H. & Vissers R.L.M. 1990. Shear zone structures and microstructures in mantle peridotites from the Voltri Massif, Ligurian Alps, N.W. Italy. Geol. Mijnbouw, 69, 3-17.
Hoogerduijn Strating E.H., Piccardo, G.B. Rampone, E., Scambelluri M., Vissers R.L.M., Drury M.R. & Van der Wal D. 1990. The structure and petrology of the Erro-Tobbio peridotite (Voltri Massif, NW Italy): A two-day excursion with emphasis on processes in the upper mantle. Ofioliti, 15, 119-184.

The purpose of this chapter is: [1] to use field and microstructural information to unravel the Triassic-Jurassic extension-related deformation history of the ET lherzolites, [2] to interpret the uplift history of the lherzolites in terms of a tectonic model for oceanic rifting, and [3] to address the implications of shear localization, grainsize reduction, and hydration on the upper mantle rheology during incipient oceanic rifting.

5.2 EXTENSION-RELATED STRUCTURES IN THE ERRO-TOBBIO LHERZOLITE

Form-surface mapping in ET lherzolites clearly shows that, within relatively coherent bodies bounded by Alpine serpentinite mylonites and brittle faults, a variety of structures exist which developed prior to the Alpine thrust zones (Enclosure 3). These older structures include fragments of a granular spinel-lherzolite wall rock, transected by four different shear zone structures: spinel-bearing peridotite tectonites, spinel/

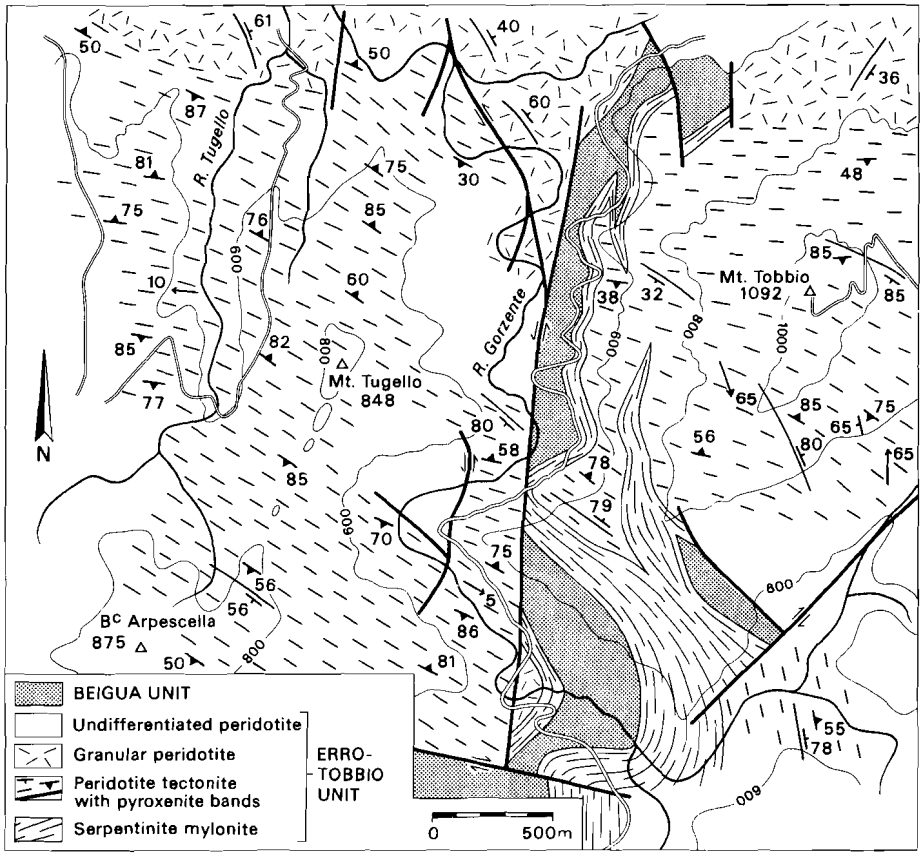

Fig. 5.1. Structural map of the Mt. Tobbio area.

plagioclase-bearing peridotite mylonites, chlorite-bearing peridotite mylonites, and serpentinite mylonites (Hoogerduijn Strating et al. 1989). This section describes the structures and microstructures features observed in the granular spinel lherzolite wall rock and in the different shear zone structures.

Granular spinel lherzolite

Within the northern part of the map area (Fig. 5.1, Enclosure 3) an E-W trending region occurs in which no shear-induced foliations have been developed. The lherzolites in this part of the area have a homogeneous and coarse-grained (0.5-1 cm) granular texture, and all mineral phases have a similar grainsize. In such virtually undeformed granular lherzolites, orthopyroxene, spinel and clinopyroxene often occur in clusters (Fig. 5.2). These clusters are thought to originate from precursor garnets decomposed during depressurization and recrystallization in the spinel lherzolite stability field (Smith 1977; Green & Brunley 1988). The microstructure of the granular lherzolite is illustrated in Fig. 5.3A. The olivine and pyroxene grains show minor internal deformation, characterized by incidental kink-like subgrain boundaries, and most grains show a weak undulatory extinction.

The granular lherzolites locally contain a cm to m-scale compositional banding of dunite and pyroxenite, which delineates a uniform to smoothly curved pattern on the km-scale (Fig. 5.1). Dunites generally occur as pyroxene-free rims on either side of pyroxenite bands, and are interpreted as depleted walls adjacent to intrusive pyroxenite dykes (e.g. Nicolas 1986b). It is assumed that these intrusive pyroxenites developed in response to high-pressure partial melting of garnet lherzolites during asthenospheric upwelling (cf. Loubet & Allègre 1982). However, the fertile composition of the ET

Fig. 5.2. Field aspect of granular peridotite showing clusters of orthopyroxene, clinopyroxene and spinel. Diametre coin is 2.5 cm.

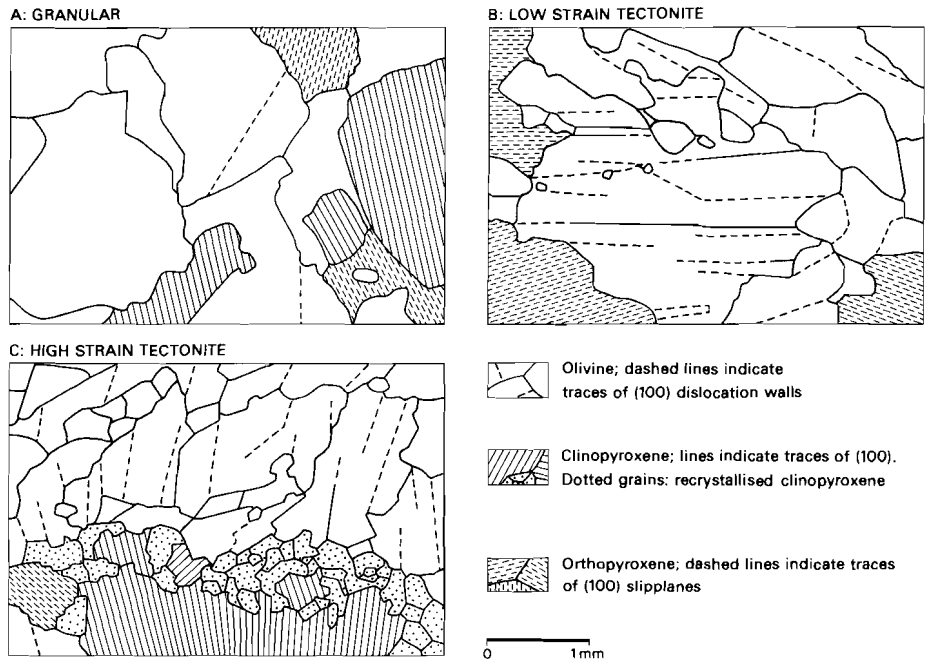

Fig. 5.3. Line drawings from thin-sections showing the microstructure from [A] granular, [B] low-strain peridotite tectonite and [C] high-strain peridotite tectonite.

lherzolites (Ernst & Piccardo 1979; Ottonello et al. 1979) indicates that this high-pressure, and also subsequent low-pressure partial melting described below, must have been limited. Isotope studies (Polvé & Allègre 1980; Hamelin & Allègre 1988) suggest that many western Mediterranean lherzolites underwent high-pressure partial melting sometime during the Proterozoic. It is therefore unclear whether this early magmatic stage occurred during the onset of Triassic-Jurassic rifting, or, alternatively, if it represents an older event unrelated to the Mesozoic tectonics in the area.

Although the pyroxenites and their depleted dunitic walls may be folded, no axial planar foliation has been developed. The lherzolite and pyroxenite in the hinges of these folds show coarse-grained spinel-bearing equilibrium textures, suggesting that folding occurred prior to complete annealing recrystallization in the spinel lherzolite stability field.

In few locations pyroxenite bands are cut by dunite veins. Continuity of the spinel pyroxenites through the dunite veins is suggested by aligned trails of spinel grains in the dunite, which may indicate a replacement rather than an intrusive origin. However, some dunites show cumulate textures of subhedral olivine and pyroxene with intercumulus clinopyroxene and plagioclase. The development of these discordant dunite veins and the selective leaching of pyroxenes from the lherzolite/pyroxenite walls are ascribed to a combination of low-pressure fractional crystallization of an ascending basaltic melt, and reaction of this melt with the wall-rock (e.g. Quick 1981).

Peridotite tectonites

The bulk of the ET lherzolites studied have a well-developed foliation defined by the shape preferred orientation of deformed pyroxene, spinel and olivine grains. This tectonite foliation has a relatively constant orientation on a km-scale (Fig. 5.1, Enclosure 3). Stretching lineations in the plane of the tectonite foliation are common, but their orientation may vary.

In the Mt. Tobbio area (Fig. 5.1) a transition has been mapped between granular- and foliated lherzolites. This transition is remarkably gradual, from virtually undeformed granular lherzolites in the north, through low- and intermediate-strain tectonites to distinctly high-strain tectonites to the south. Apart from a clearly increasing intensity of the foliation across this transition, an increasing strain is strongly suggested by increasing aspect ratios of deformed pyroxene grains and decreasing angles between primary pyroxenite layers and the foliation. In low-strain tectonites the primary layering is oblique to the foliation (Fig. 5.4), whereas in high-strain tectonites this primary layering is virtually parallel to the foliation.

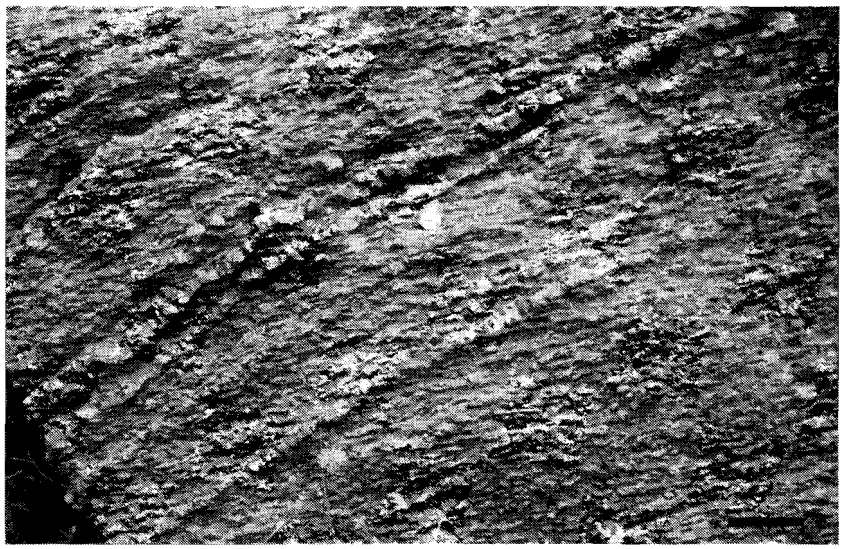

Fig. 5.4 . Field aspect of tectonite foliation (horizontal) at a distinct angle to pyroxenite bands. Scale bar is 10 cm.

Locally, within the tectonites, metre-scale folds of pyroxenite layers occur, and the tectonite foliation is axial planar to these folds. In addition, folded pyroxenites such as those observed in the granular lherzolites are refolded in the tectonite deformation zone (Fig. 5.5), resulting in type III fold interferences (Ramsay 1967).

The microstructure of moderately foliated, presumably low-strain tectonites is dominated by large olivine grains showing sharply defined, high angle kink-like subgrains with undulatory extinction (Fig. 5.3B, 5.6A). Large olivine grains are not preserved in tectonites with a more intensely developed foliation. Instead, the micro-

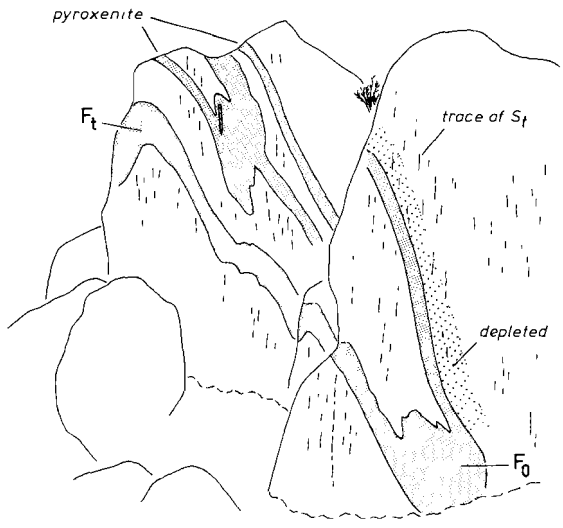

Fig. 5.5. Sketch after field photograph showing type III fold interference of pyroxenite bands with depleted harzburgitic margins in peridotite tectonites. The oldest fold hinge (F_0) has no associated axial planar foliation (S_t). The tectonite foliation is axial planar to the youngest generation of folds (F_t). Height outcrop is about 1.5 meter.

structure is characterized by smaller (0.5-1.5 mm) elongate to tabular shaped grains (Fig. 5.3C, 5.6B) with weakly curved to straight boundaries and moderate development of sub-boundaries and undulatory extinction. The elongate new olivine grains in the highly strained tectonites have similar sizes as the kink-like subgrains developed at lower strains. The presence of fluid inclusions in the recrystallized olivine suggests that small amounts of fluid may have been present during deformation. In some high-strain tectonites, the shape preferred orientation of the elongate new olivine grains defines a second foliation oblique to the tectonite foliation defined by stretched pyroxenes and spinels. This microstructure is geometrically similar to that developed in type II S-C quartz and calcite mylonites (Lister & Snoke 1984), and strongly suggest a component of non-coaxial deformation during the development of the tectonite (Van der Wal et al. 1991). This is also suggested by the distinctly oblique orientation, with respect to the tectonite foliation, of lattice fabrics of olivine (Fig. 5.7). The fabrics are consistent with dominant slip, during deformation, on the olivine high temperature [a] {0kl} system.

The orthopyroxene grains in the low-strain tectonites have similar sizes as those in the granular peridotites. Undulatory extinction is common and kinkbands are well developed but there is no evidence of recrystallization. In the high-strain tectonites the orthopyroxene grains are flattened due to slip on the (100) planes and are slightly recrystallized. In contrast, clinopyroxene occurs as highly deformed clasts of original grains, extensively recrystallized to an equiaxed smaller grainsize (0.1-0.5 mm, Fig. 5.3C). In places in the high-strain tectonites, such recrystallized clinopyroxene aggregates define distinctly asymmetric σ-type porphyroclast systems (Passchier & Simpson 1986).

In both low- and high-strain tectonites, the spinel is deformed into irregularly shaped, elongate aggregates accentuating the tectonite foliation. In fresh samples, the contacts between brown Al-spinel and olivine or pyroxenes are sharp without any reaction

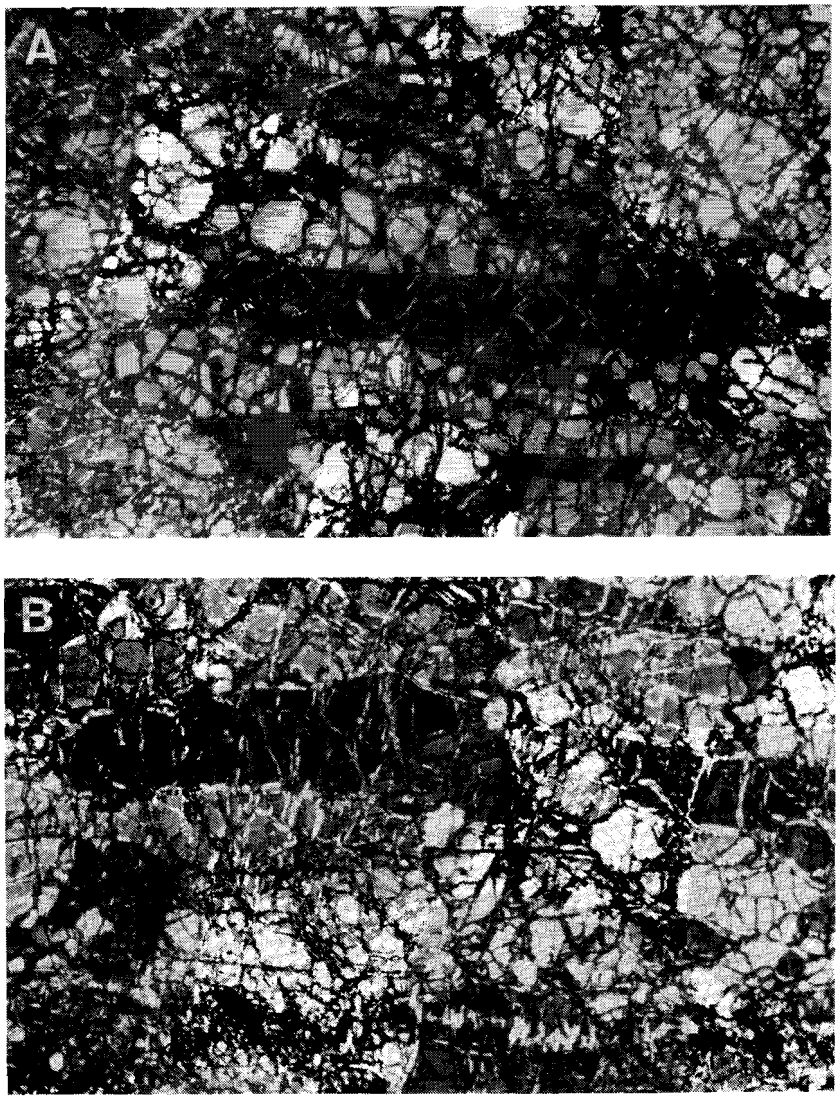

Fig. 5.6. Photomicrographs of tectonite microstructures. [A] Large olivine grain with sharply defined kink-like subgrains in low-strain peridotite tectonite. [B] Tabular shaped recrystallized olivine grains in intermediate-strain peridotite tectonite. Width of both micrographs is 1.6 mm.

products, suggesting that the tectonites developed in the spinel lherzolite stability field.

In summary, several features of the tectonites suggest a component of simple shear during deformation. These include the oblique orientation of lattice and grain shape fabrics, and the asymmetric porphyroclast systems, but also the map-scale progressive rotation of pyroxenite bands into parallelism with the tectonite foliation (Fig. 5.1, 5.2) which reflects a strain gradient, from virtually undeformed granular rocks to highly strained tectonites. The spinel-bearing tectonites are therefore interpreted as part of a

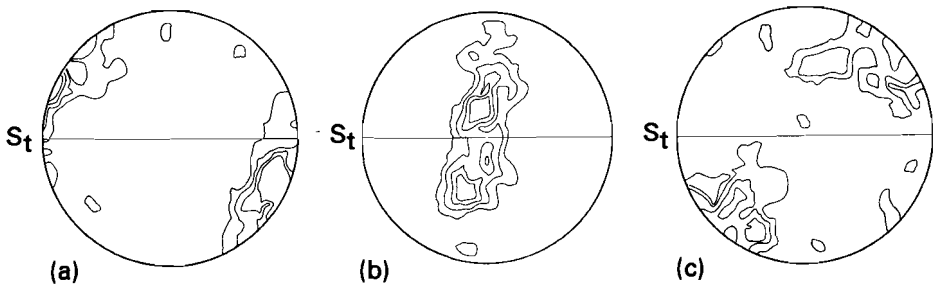

Fig. 5.7. Lattice preferred orientation patterns of recrystallized olivine in peridotite tectonites. Note the distinct point maximum of [a] axes and the (partial) girdle distribution of the [b] and [c] axes. The fabric asymmetry points to dextral non-coaxial flow. Tectonite foliation indicated by St. Number of measurements: 100, contours drawn at 2, 4, 6 and 8%.

km-scale shear zone, initiated in a granular spinel lherzolite wall rock.

Discordant dunite veins, similar to those described from the granular lherzolite, also occur in the gneissic lherzolite where they dissect the tectonite foliation. Locally, thin gabbroic veins occur with very irregular shaped contacts with the foliated lherzolite. Nicolas (1986b) has ascribed the development of such gabbroic veins to "in situ", low-pressure partial melting of the lherzolite. Both the dunite- and the gabbroic veins suggest that the peridotite underwent low-pressure partial melting and reacted with ascending basaltic melts after the development of the tectonite foliation.

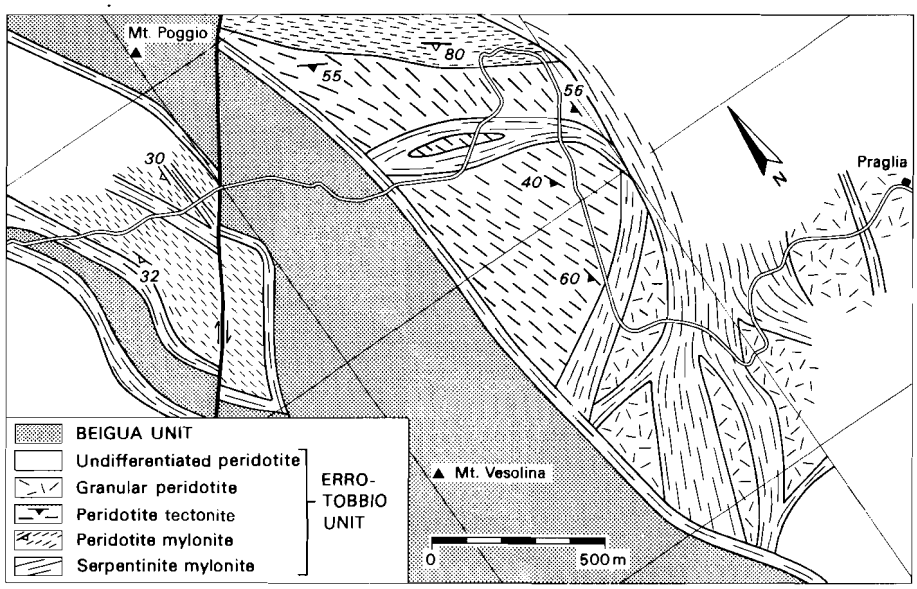

Fig. 5.8. Structural map of the area around Mt. Poggio and Mt. Vesolina.

Peridotite mylonites

In the southern part of the area studied (Fig. 5.8, Enclosure 3) the tectonite foliation is overprinted by a mylonitic fabric developed in dm to 100 m-scale peridotite mylonite zones (Fig. 5.9). In thier present orientation, brought about by Alpine ductile and brittle thrusting, the peridotite mylonite zones generally dip SW. Asymmetric porphyroclast systems of intensely deformed pyroxenes in combination with a distinct stretching lineation defined by these pyroxenes indicate a S to SE sense of movement across these mylonite zones. Both tectonite and mylonite structures in the lherzolites are cut by mostly steep Mid Ocean Ridge (MOR)-type basaltic and gabbroic dykes. Most of these dykes have been transformed into metarodingites during Alpine deformation and metamorphism (See Chapter 4.2).

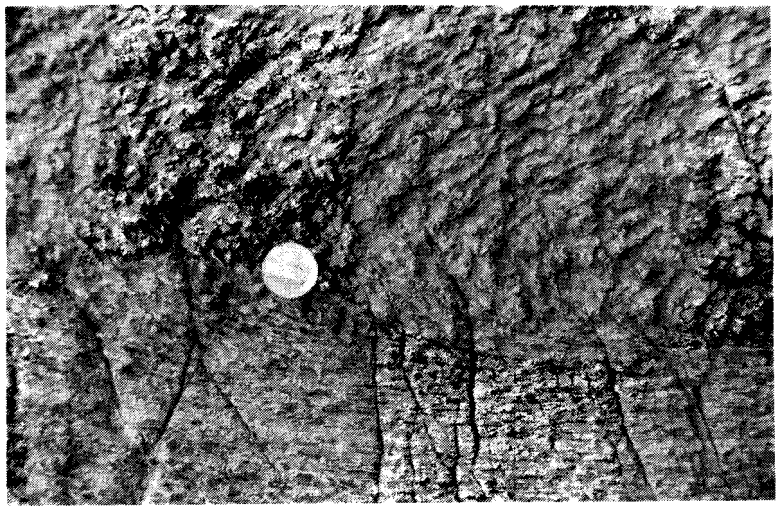

Fig. 5.9. Detail of a peridotite mylonite shear zone in the Praglia area. Note progressive bending of the tectonite foliation into the mylonite zone, and the pervasive shear foliation in the mylonite. Shear zone boundary is oriented horizontal. Sense of shear is sinistral. Diametre coin is 2.5 cm.

The mylonitic microstructures are characterized by thin bands and lenticular domains, less than 2 mm thick, made up of a fine-grained (10-150 μm) recrystalllized olivine mosaic (Fig. 5.10) enclosing porphyroclasts of olivine and pyroxene of 1-3 mm diameter. The olivine porphyroclasts show undulatory extinction and contain poorly defined sub-boundaries. Fabric studies of the recrystallized olivine grains (Fig. 5.11) suggest slip on the olivine [c](010) and [c]{hk0} systems. The asymmetry of the lattice fabric with respect to the mylonitic foliation points to deformation in a non-coaxial flow regime. The bands and lenticular domains are bound by anastomosing thin layers of ultrafine-grained (2-30 μm) material described below, giving the microstructure a fluidal aspect (Fig. 5.10), similar to that described from some kimberlite xenoliths (Boullier & Gueguen 1975).

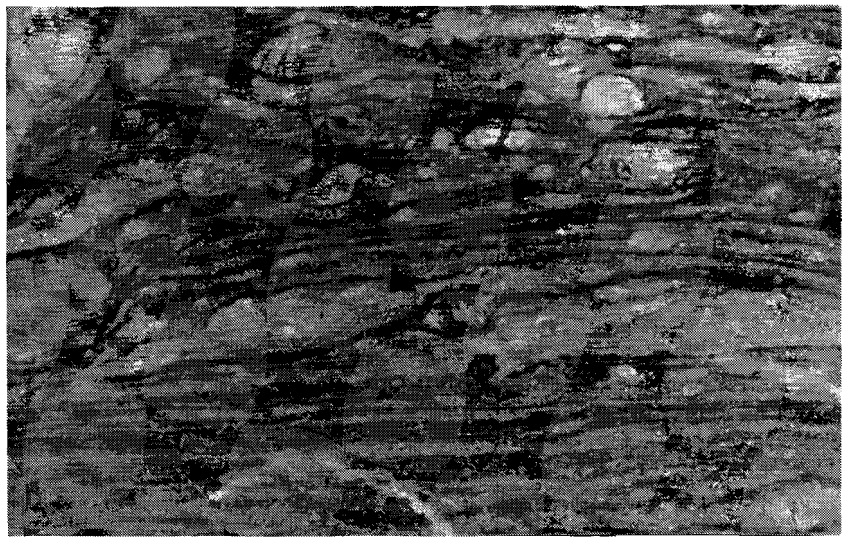

Fig. 5.10. Fluidal microstructure in peridotite mylonite defined by very fine-grained (2-30 mm) bands of recrystallized olivine + pyroxene + amphibole adjacent to rounded pyroxene porphyroclasts (dark bands on micrograph) in a fine-grained (10-150 mm) olivine matrix (lighter coloured bands on micrograph). Sigma-type asymmetry of porphyroclast systems indicates a dextral sense of shear. Width of micrograph is 7.2 mm.

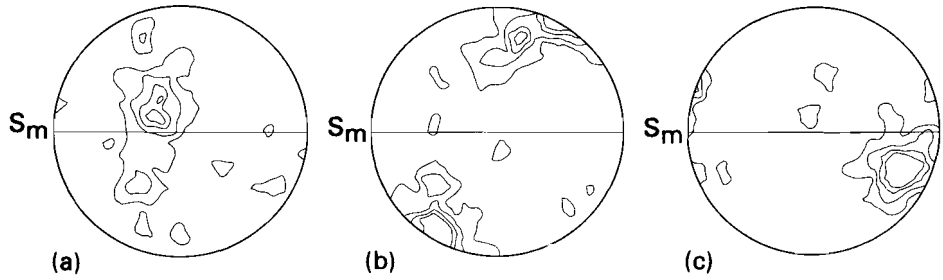

Fig. 5.11. Lattice preferred orientation of recrystallized olivine in peridotite mylonite. Note distinct point maximum of the [c] axes and the partial girdle distribution of the [a] and [b] axes. The fabric asymmety indicates a dextral non-coaxial flow regime. The mylonitic foliation is indicated by Sm. Number of measurements: 100, contours drawn at 2, 4, 6 and 8%.

The small size of the clinopyroxene porphyroclasts suggests that originally large grains have been fractured and micro-boudinaged during mylonitic deformation (cf. Boullier 1980), while the orthopyroxenes became extremely flattened due to slip on (100) planes. These deformed orthopyroxenes frequently show recrystallization along their margins into an equigranular aggregate of finer grained ortho- and clino-pyroxene.

Apart from the macroscopic shear zones developed at a distinct angle to earlier tectonite foliations, mylonitic fabrics also occur in some high-strain tectonites, where

Fig. 5.12. Photomicrograph showing high-strain tectonite with a clinopyroxene porphyroclast and an oblique olivine grainshape fabric (Sb) indicating dextral non-coaxial flow. This fabric is dissected by mylonitic bands (Sm), characterized by a distictly smaller recrystallized olivine grainsize. Width of micrograph is 3.4 mm.

they are developed as thin bands of very fine-grained olivine parallel to the tectonite foliation (Fig. 5.12). These structures suggest that some of the spinel-bearing tectonites evolved, with progressive deformation, into spinel/plagioclase-bearing peridotite mylonites. In such mylonitized high strain tectonites, "in-situ" gabbroic veins are folded which suggests that low-pressure partial melting pre-dates the mylonitic deformation.

Two types of peridotite mylonite can be distinguished on the basis of the stable mineral assemblage during deformation, i.e. spinel/plagioclase peridotite mylonites and chlorite peridotite mylonites. In the spinel/plagioclase-bearing mylonites, pyroxenes break down to form fine-grained syntectonic edenitic to pargasitic amphibole, both as fibre growths on disrupted, pulled-apart pyroxene clasts (Fig. 5.13) and in the anastomosing, very fine-grained bands adjacent to lenticular coarser grained (10-150 μm) olivine domains. These bands are made up of an intimately mixed aggregate of [1] equiaxed to slightly elongate olivine grains with relatively low dislocation densities (i.e. much lower than in the coarser grained olivines; Drury et al. in prep.), [2] ortho- and clinopyroxene grains showing little or no preferred orientation and virtually free of dislocations (Drury et al. in prep.), and [3] up to 30% of fine-grained amphibole. The development of these amphibole-rich bands strongly suggests extensive infiltration of hydrous fluids into the mylonite zones. The microstructure and chemistry of the mineral phases in the fine-grained bands (Appendix A3) suggest, that the breakdown of pyroxene involved a reaction of the form orthopyroxene + clinopyroxene + spinel + H_2O + Na_2O + CaO = olivine + hornblende. The extreme grainsize reduction in these bands is therefore inferred to have occurred by nucleation of new phases, albeit that a contribution by rotation recrystallization or cataclastic processes cannot be excluded.

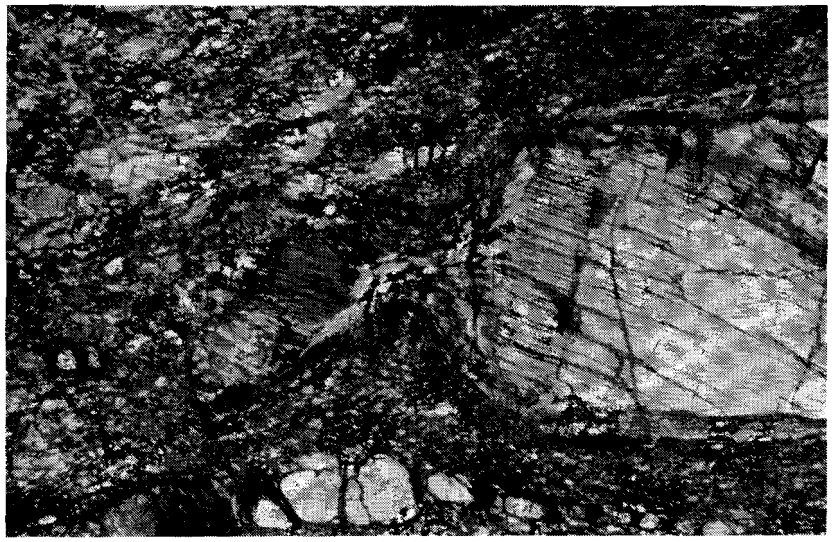

Fig. 5.13. Photomicrograph showing coarse-grained hornblende fibers in the pressure shadows of an extended orthopyroxene porphyroclast. The fine-grained material mantling the pyroxene also consists of hornblende, while the matrix of the mylonite is made up of fine-grained recrystallized olivine. Width of micrograph is 1.5 mm.

In some plagioclase-free mylonites, brown Al-spinel porphyroclasts are broken and show very fine-grained tails of irregularily shaped spinel mixed with equally fine-grained amphibole and olivine. In plagioclase-bearing mylonites, and in most mylonitized high-strain tectonites the Al-spinel porphyroclasts are transformed into intensely flattened aggregates of dark brown to opaque CrAl-spinel (see Appendix A3 for chemical composition) rimmed by plagioclase, suggesting that the spinel-plagioclase transition involved reaction-enhanced softening (cf. White & Knipe 1978).

In the chlorite-bearing peridotite mylonites, the presence of trains of magnetite grains with dark brown Cr-spinel cores, surrounded by chlorite rims with a strong shape preferred orientation, points to synkinematic break-down of Al-spinel. Olivine in these mylonites is recrystallized to a very small (e.g. 10-30 μm) grainsize. Both ortho- and clinopyroxenes are fractured and extended parallel to the foliation. The neck zones of the boudinaged pyroxenes are filled with chlorite and, occasionally, with tremolitic amphibole. However, the elongated shape of the porphyroclasts and the presence of disrupted rims of small equant pyroxene grains point to ductile deformation and concomitant recrystallization prior to fracturing. This suggests that the chlorite-bearing mylonites started to deform at elevated temperatures, possibly close to those prevailing during the development of the spinel/plagioclase-bearing mylonites.

Serpentinite mylonites

Some chlorite-bearing peridotite mylonites contain mm-scale shear bands of preferably oriented antigorite. Antigorite also developed synkinematically at the expense of

olivine and orthopyroxene in strain shadows of porphyroclasts, suggesting that these peridotite mylonites evolved retrogressively into serpentinite mylonites. In the area SW of Mt. Dra (Enclosure 3) high strain tectonites are overprinted by an anastomosing network of serpentinite mylonites. The serpentinite mylonites are characterized by a foliated microstructure of antigorite, antigorite-chlorite and chlorite-magnetite bands. Porphyroclasts systems of olivine and pyroxene with tails of antigorite and chlorite are very common. These mylonite zones are cut by Alpine serpentinite mylonites (see Chapter 4), and show no evidence for growth of olivine, titanian clinohumite and antigorite, characteristic for the Alpine tectono-metamorphic evolution. The serpentinite mylonites of the Mt. Dra are therefore interpreted as the lowest-grade, most hydrated shear zone structures developed in the ET lherzolites during oceanic rifting.

5.3 PRESSURE-TEMPERATURE EVOLUTION AND CONDITIONS DURING DEFORMATION

A variety of methods has been proposed to determine equilibration conditions for lherzolites. Most commonly, closure (i.e. minimum) temperatures are estimated from the diopside-enstatite miscibility gap (Wood & Banno 1973; Wells 1977) and the partitioning of iron and magnesium between ferromagnesian phases (garnet, pyroxene, olivine and spinel; e.g. Gasparik 1984). Other thermometers incorporate the solubility of Ca and Al in ortho- (e.g. Sachtleben & Seck 1981; Gasparik 1984) and clinopyroxenes (Gasparik 1984), which can also be used as a barometer in the presence of anorthite or garnet (e.g. Gasparik 1984). Mercier et al. (1984) proposed an empirical barometer which is based upon the partitioning of diopside in coexisting ortho- and clinopyroxenes, corrected for Na dilution effects in natural systems. Calibration of these thermobarometers occurred under a wide range of conditions (0.1-4000 MPa, 800-1700°C), and is based on experiments with simple chemical systems such as CaO-MgO-SiO_2 (CMS) or CaO-MgO-Al_2O_3-SiO_2 (CMAS). However, experimental difficulties are reflected in many inconsistencies among such studies (Gasparik 1984). Moreover, the results acquiredfrom these thermobarometers when applied to natural rocks depend on [1] deviations of the ideal cation ordering on sites of coexisting mineral phases (e.g. Cundari et al. 1986), [2] diffusion kinetics of the cations involved, [3] grainsize and [4] cooling-rate. These variables will influence the closure temperature at which a given cation exchange reaction ceases, and may explain the commonly observed temperature differences of up to 150°C when applying different thermobarometers. At present, however, these effects have not been quantified.

With the above shortcommings in mind, three thermometers (Wood & Banno 1973; Wells 1977; Sachtleben & Seck 1981), a thermobarometer (Gasparik 1984) and a barometer (Mercier et al. 1984) have been used to estimate the approximate equilibration conditions of the ET granular lherzolites and the different shear zone structures (Table 5.1). Recrystallized pyroxenes in each sample generally show a scatter of Ca contents and Ca/Al ratios, which according to Mercier et al. (1984) may reflect variable degrees of exsolution and/or serpentinization, rather than differences in

		I	II	III	IV	V
A	GRANULAR SPINEL PERIDOTITE	1104±71°C	1030±68°C	1090±78°C	1080±60°C	2070±600 MPa
B	SPINEL PERIDOTITE TECTONITE	1030±11°C	924±12°C	1016±7°C	1035±50°C	1370±250 MPa
C	PLAGIOCLASE PERIDOTITE MYLONITE	1010±2°C	940±34°C	986±25°C	990±50°C 500-700 MPa	810±460 MPa
D	MYLONITIZED PLAGIOCLASE-BEARING HIGH STRAIN TECTONITES	980±17°C	895±39°C	971±45°C	935±15°C 500-600 MPa	800±420 MPa
E	SPINEL PERIDOTITE MYLONITE	901±13°C	783±9°C	898±25°C	635±100°C	750±320 MPa
	Gradient granular peridotite to peridotite tectonite	3.3 °C/km	4.7 °C/km	3.3 °C/km	2.0 °C/km	
	Gradient granular peridotite to plagioclase peridotite mylonite	2.3 °C/km	2.2 °C/km	2.6 °C/km	2.2 °C/km	
I: Wood & Banno 1973 II: Wells 1977 III: Sachtleben & Seck 1981 IV: Gasparik 1984 V Mercier et al. 1984						

Table 5.1. Estimations of equilibration conditions for the different microstructures in the Erro-Tobbio lherzolites. Estimations are based on the orthopyroxene-clinopyroxene thermometers of Wood and Banno (1973; I) and Wells (1977; II), the Ca-solubility in orthopyroxene coexisting with clinopyroxene (Sachtleben & Seck 1981; III), clino- and orthopyroxene thermobarometry of Gasparik (1984; IV), and the empirical barometer of Mercier et al. (1984; V). The cooling gradient are calculated using the pressure estimates of Mercier et al. (1984).

equilibration conditions. Therefore, pyroxenes with relatively high or low Ca/Al ratios (due to exsolution) and Ca concentrations (due to exsolution and/or serpentinization) were discarded from the analyses. Representative microprobe analyses from coexisting olivine, spinel, ortho- and clinopyroxene from the different microstructures are shown in Appendix A3. The above methods yield fairly consistent equilibration temperatures, with a notable exception for the results obtained with the Wells (1977) thermometer which yields significantly lower temperature values. The Mercier et al. (1984) barometer results in a distinct trend, from equilibration at high pressures for the granular lherzolite, to low pressures for the peridotite mylonites. Consistent pressure estimates were obtained from the plagioclase-bearing lherzolites using both the thermobarometer of Gasparik (1984) and the barometer of Mercier et al. (1984). Figure 5.14 shows the uplift path for the ET lherzolites based upon a best fit to the data of Sachtleben & Seck (1981) and Mercier et al. (1984). It should be noted, that the inferred uplift path may shift to lower temperatures depending on the thermometer applied, but that the cooling gradient involved does not change significantly (Table 5.1).

The occurrence of clusters of clinopyroxene, orthopyroxene and spinel in the granular lherzolites suggests that they originate from depressurized garnet lherzolites (Smith 1977; Green & Burnley 1988; see Fig. 5.15), affected by complete static recrystallization in the spinel lherzolite stability field. The bulk-rock and mineral composition of the granular lherzolite approaches that of undepleted spinel lherzolite xenoliths, suggesting a sub-continental origin for the ET lherzolite (Fig. 5.15). Thermobarometry of pyroxene cores yields average temperatures ranging between 1030 and 1100°C at 2100 MPa confining pressure for this recrystallization event, i.e. significantly lower than the dry solidus for fertile upper mantle compositions (Fig. 5.14 A).

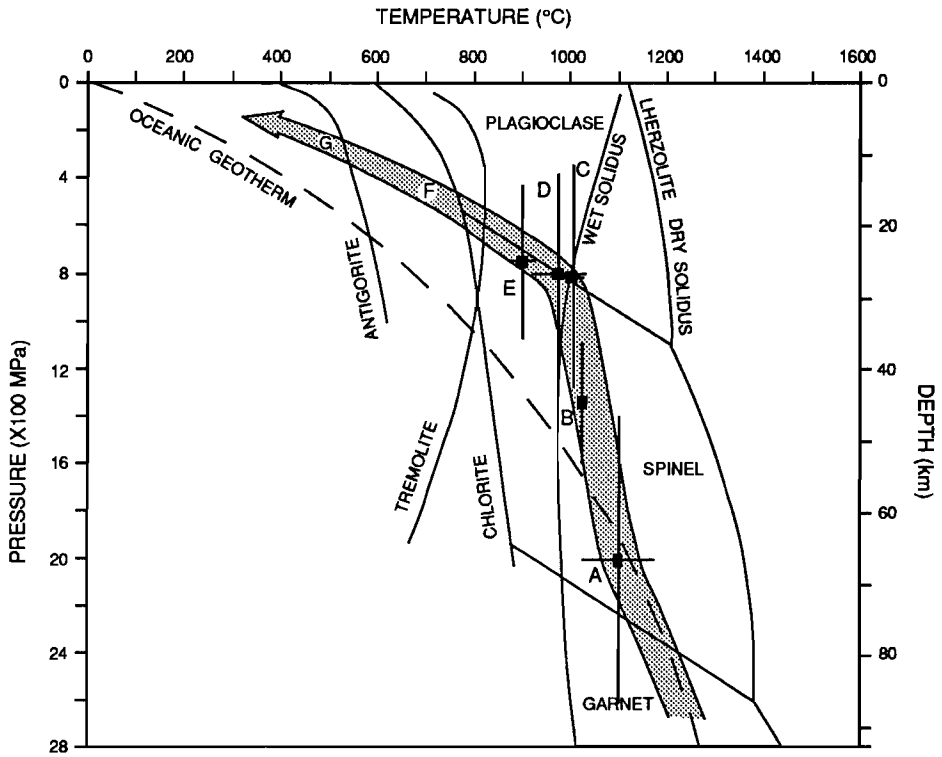

Fig. 5.14. P-T path inferred for the ET lherzolites, based upon a best fit to data obtained from the thermometer of Sachtleben and Seck (1981) and barometer of Mercier et al. (1984; see Table 5.1) in a phase diagram for the reactions in the system CaO-MgO-Al_2O_3-SiO_2-H_2O below 700°C (after Evans et al. 1976) and in the system CaO-MgO-Al_2O_3-SiO_2-Na_2O-H_2O above 700°C (after Jenkins 1983). Lherzolite wet solidus after Wyllie (1979) and lherzolite dry solidus after Takahashi and Kushiro (1983). The geotherms are from Mercier (1980). Inferred conditions are marked as follows: [A] static recrystallization granular lherzolites, [B] spinel peridotite tectonites, [C] plagioclase-bearing peridotite mylonites, [D] plagioclase-bearing mylonitized tectonites, [E] spinel-bearing peridotite mylonites, [F] chlorite-bearing peridotite mylonites and [G] serpentinite mylonites.

The mineral assemblage in the tectonites is the same as that in the granular lherzolites i.e. olivine + orthopyroxene + clinopyroxene + Al-spinel, indicating that the development of the kilometer-scale tectonite shear zone occurred in the spinel lherzolite field. Estimated conditions for the development of the tectonites, as obtained from recrystallized pyroxene grains, are between 920 and 1040°C at pressures of about 1400 MPa (Fig. 5.14 B).

The mineral chemistry of recrystallized pyroxene pairs in a plagioclase-bearing peridotite mylonite and in a plagioclase-bearing mylonitized high-strain tectonite yield average temperatures between 890 and 1010°C at pressures between 500 and 800 MPa (Fig. 5.14 C,D). Lower temperatures between about 800 and 900°C at 750 MPa confining pressure are obtained from recrystallized pyroxene pairs in the spinel-bearing peridotite mylonites (Fig. 5.14 E). These temperature estimate are consistent

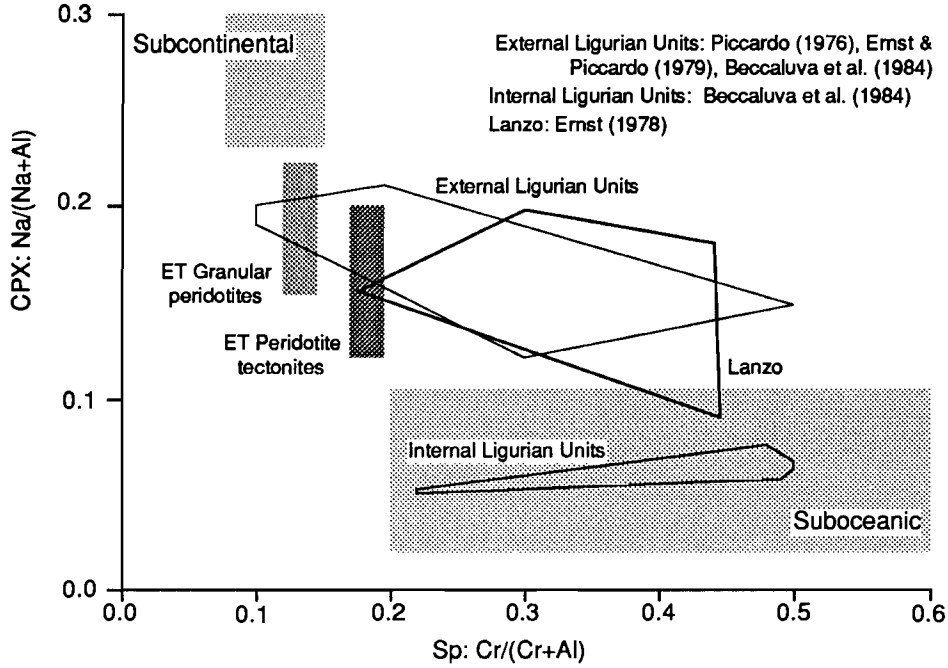

Fig. 5.15. Discriminative diagram showing compositional variations of Na/(Na + Al) in clinopyroxene (CPX) versus Cr/(Cr + Al) in associated spinel (SP) from ET granular lherzolites and perditotite tectonites (recrystallized clinopyroxenes; see Appendix A3 for representative mineral chemistry). Shaded fields indicate compositions of coexisting spinel and clinopyroxene in subcontinental and suboceanic lherzolites as defined by Ishiwatari (1985) and Bonatti and Michael (1989).

with the synkinematic growth of edenitic to pargasitic amphibole which would suggest maximum temperatures of about 950°C (cf. Oba 1980; Jenkins 1983). The estimated PT conditions for the peridotite mylonites plot very close to the transition between the spinel and plagioclase lherzolite fields, which is consistent with the observation that both Al-spinel and CrAl-spinel + plagioclase occur in these mylonite zones (cf. Obata 1980).

The stability of olivine, chlorite and tremolitic amphibole in the chlorite-bearing peridotite mylonites suggests temperatures between 500 and 800°C, while the breakdown of olivine producing antigorite indicates temperatures between 300 and 500°C for the serpentinite mylonites (Fig. 5.14 F, G). No pressure constraints are available for these two structures.

The development of mesh-textured chrysotile at the expense of olivine, and the rhodingitization of the basaltic and gabbroic dykes (see also Chapter 4.2) suggest, that the peridotite was affected by low-temperature ocean floor metamorphism ($T \leq 300°C$).

The PT path inferred for the ET lherzolites (Fig. 5.14) suggests uplift from deep levels in the sub-continental lithosphere towards the ocean floor at temperatures distinctly

below the lherzolite dry solidus. However, the generation of gabbroic "in situ" melt veins, subsequent to the development of the spinel-bearing tectonites but prior to mylonitization, points to minor low-pressure partial melting during uplift. Such relatively low temperature melting can only have occurred in the presence of volatiles (Wyllie, 1979). Hydration of the peridotite prior to the mylonitic deformation is consistent with the presence of fluid inclusions in recrystallized olivines in the peridotite tectonites, with the presence of amphibole porphyroclasts in some peridotite mylonites, and with rare interstitial pargasitic hornblendes in the tectonites (Piccardo, pers. comm. 1989). Unfortunately, no conclusive microstructural evidence has been found as yet to ascertain the stability of hydrous minerals during development of the peridotite tectonites or the "in situ" melt veins. It should be noted, however, that a completely hydrated lherzolite following the same PT uplift path as the ET lherzolites would already have started to melt at relatively high pressures in the spinel or garnet lherzolite field (Fig. 5.14). The exclusive presence of low-pressure, plagioclase-bearing melt veins suggests, that significant fluid infiltration into the ascending lherzolite only occurred at shallow lithospheric levels, close to the spinel-plagioclase lherzolite transition.

5.4 IMPLICATIONS FOR TECTONIC MODELS OF INCIPIENT OCEANIC RIFTING

Pure-shear versus simple-shear extension

Conflicting views on symmetric, pure shear (e.g. McKenzie 1978) versus asymmetric, simple shear (e.g. Wernicke 1985) extension of the continental lithosphere has triggered many studies on the geometry and processes involved in extension of continental lithosphere and incipient oceanic rifting. The discrimination of symmetric versus asymmetric extension has largely concentrated on 1) structures and geometries observed on deep seismic sections (e.g. Allmendinger et al. 1987; Warner & McGeary 1987; Klemperer 1988; Reston 1990), and 2) comparison of model calculations with measured surface responses in terms of vertical movements, heat-flow, gravity anomalies and magmatism (e.g. Rowley & Sahagian 1986; Buck et al. 1988; Garfunkel 1988; Voggenreiter et al. 1988; Issler et al. 1989; Latin & White 1990).

Relatively little attention has been paid to the possible response of the upper mantle to different modes of extension. Uplift of peridotites in both continental and oceanic rifts is generally thought to occur in mantle diapirs (e.g. Nicolas 1986b). Heat transport in diapirs is assumed to be controlled by convective flow only, which means that the system is adiabatic. This implies that ascending and cooling mantle diapirs follow an adiabatic gradient of about 0.6 °C/km (McKenzie, 1984). Such adiabatic gradients are typical for oceanic basins with well developed (symmetric) spreading ridges (e.g. Forsyth 1977). In contrast, the P-T estimates for the ET lherzolite, as obtained from pyroxene thermobarometers, suggest uplift involving a distincly non-adiabatic gradient between about 2 and 5 °C/km (Table 5.1). On the basis of these data, the uplift of the ET lherzolites seems inconsistent with mantle diapirism.

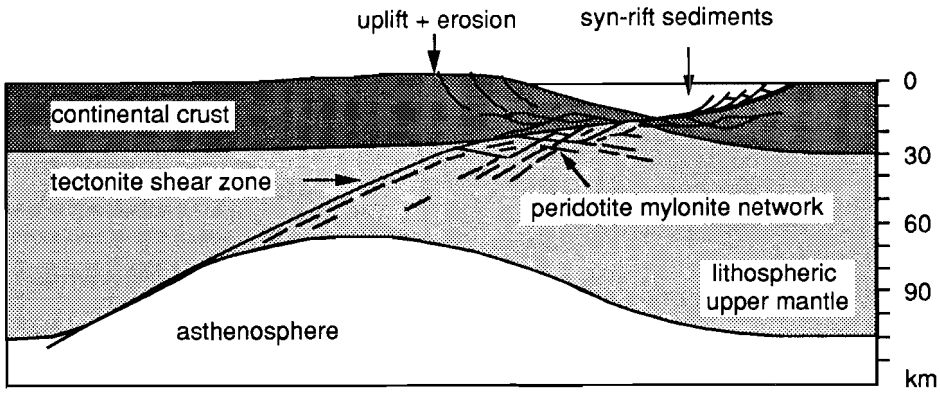

Fig. 5.16. Asymmetric extensional model for tectonic exhumation of upper mantle peridotites as inferred for the Piemonte-Ligurian ocean. Note the development of a network of mylonitic shear zones near the base of the crust, accomodating progressive uplift of the ET lherzolites towards shallower levels.

An explanation for the inferred non-adiabatic cooling gradients may be provided by a model study of Ruppel et al. (1988). These authors calculated the thermal response of continental lithosphere on pure and simple shear extension, assuming that heat transport was controlled by conduction only. Lower crustal rocks uplifted from 30 to 10 km depth show slightly different P-T-t evolutions depending on the selected extensional geometry. In a rift dominated by pure shear extension, the rocks cool relatively slowly. In contrast, lower crustal rocks in the foot wall of an inclined crustal detachment cool more rapidly due to continuous contact with relatively cool hanging wall rocks. Variations in extension/uplift rate or dip of the extensional detachment appear to have little effect on these general results. From similar model studies applying conductive (Buck et al. 1988) or convective (Latin & White 1990) heat transport, it follows that extensive partial melting of the asthenospheric mantle may only occur during pure shear extension, while partial melting during simple shear extension will be very limited or will not occur at all. In view of these results, the relatively fertile composition of the ET lherzolites due to very limited partial melting (less than 10%; Ottonello et al., 1979) and the distinctly non-adiabatic cooling history seem more consistent with tectonic denudation in a slightly to strongly asymmetric, simple shear-dominated oceanic rift (Fig. 5.16).

A similar conclusion as to the mode of incipient oceanic rifting in the Piemonte-Ligurian ocean has been drawn on the basis of [1] inferred syn-rift vertical movements on the Jurassic, European continental margin now exposed in the western Alps (Rudkiewicz 1988), and [2] the tectono-metamorphic evolution of the ophiolite complexes in the western Alps and northern Apennines (Lemoine et al. 1987; Hoogerduijn Strating 1988; see also Chapter 6).

Comparison with other ophiolite massifs and modern oceanic basins

Piccardo et al. (1990) have compared the lherzolites of the ET unit with ultramafics pertaining to different paleogeographic settings of the Piemonte-Ligurian ocean. The Alpine-Apennine lherzolites show variable compositions (Fig. 5.15), ranging from relatively undepleted lherzolites in the External Ligurids (Cassanova Scabbiaza subunit in the Ligurian Apennines; Fig. 1.2) through the ET and Lanzo (Western Alps) lherzolites, to strongly depleted lherzolites in the internal Ligurids (Bracco and Isciola Biscia subunits of the Ligurian Apennines; Fig. 1.2). These compositional variations are markedly analogous with compositional variations existing between marginal (Galicia- and Gorringe Banks, eastern Atlantic; Zabargad Island, northern Red Sea) and mid-oceanic peridotites from modern oceans and oceanic rifts (Piccardo et al. 1990). Based on these petrological and chemical characteristics, the lherzolites of the External Ligurids are thought to represent fragments of a subcontinental lithospheric mantle which underwent non-adiabatic decompression and limited "wet" partial melting during the early stages of rifting. In contrast, the peridotites from the internal Ligurids are thought to represent refractory residua after significant "dry" low-pressure partial melting, generating MORB-type magmas from an adiabatically upwelling asthenospheric upper mantle

Similar to the ET lherzolites of the Mesozoic Piemonte-Ligurian ocean, marginal lherzolites exposed in modern, asymmetric oceanic rifts (i.e. Zabargad Island; Piccardo et al. 1988) seem to follow a non-adiabatic subsolidus uplift path. In addition, the early evolution of many continental margins of slow-spreading oceans and marginal or back-arc basins seems to be dominated by low angle detachments (Kastens et al. 1988; LePichon & Barbier 1988; Mutter et al. 1989) and uncovering of sheared peridotites on the ocean floor (Bonatti et al. 1981; Boillot et al. 1987; Kastens et al. 1988; Nicolas 1989, p. 260).

Following Sengör and Burke (1978) and Voggenreiter et al. (1988), the above observations may suggest that, similar to many modern oceanic rifts and slow-spreading oceans, the development of the Piemonte-Ligurian ocean has been characterized by an incipient rifting stage dominated by [1] slightly to strongly asymmetric extension, [2] "passive" upwelling of the subcontinental mantle due to tectonic denudation, [3] limited "wet" partial melting, and [4] development of lherzolite-type ophiolites with discontinuous, relatively thin crustal sequences lacking a sheeted dyke complex.

5.5 RHEOLOGICAL IMPLICATIONS FOR MODELS OF CONTINENTAL BREAKUP AND OCEANIC RIFTING

In the previous section some inferences are made concerning the role of the upper mantle during continental breakup and incipient oceanic rifting leading to the development of the Piemonte-Ligurian ocean. In addition, a comparison with modern oceanic basins suggests that this geodynamic scenario may be applicable to other

oceanic rifts and slow-spreading oceans. It follows, that knowledge of the mechanical behaviour of the extending upper mantle is of prime importance in understanding the process involved in continental breakup. Therefore, this section wil focus on the influence of shear zones on the mantle rheology.

Irrespective of the exact macro-scale geometry, the tectonite shear zone and crosscutting mylonites in the ET lherzolites indicate that deformation of the Piemonte-Ligurian upper mantle, during lithosphere extension and breakup, became progressively localized in a network of relatively narrow, fine-grained and hydrated mylonite zones. It follows that the bulk strength of the lithospheric mantle must have become controlled by the rheology of the shear zone rocks. This may have caused a drastic reduction in bulk strength, since experimental evidence (Karato et al. 1986; Rutter & Brodie 1988b) indicates that wet olivine rocks weaken considerably with decreasing grainsize, due to a change in dominant deformation mechanism from grainsize insensitive dislocation creep to diffusion-controlled grainsize sensitive mechanisms. In addition, progressive transformation to hydrated weaker phases such as edenitic amphibole and chlorite may have weakened the shear zone rocks (White & Knipe 1978; Kirby 1985).

Several difficulties surround any attempt to estimate the effect of progressive shear localization on bulk lithosphere rheology. Apart from the many uncertainties with regard to the precise extensional geometry, progressive extension and breakup must lead to strength profiles which will evolve not only with the changing geotherm but also with the changing geometry of the developing shear zone system and with the deformation mechanisms operative within the shear zones. Of particular importance in the latter respect is the mechanism of grainsize reduction responsible for (or associated with) localization. In addition, there are uncertainties involved in extrapolating experimentally derived rheological data to natural rocks under natural conditions (e.g. Carter & Tsenn 1987). A rigorous analysis of shear localization mechanisms in upper mantle rocks is needed to quantitatively model the evolution of the bulk strength with time. However, a semi quantitative estimate of the rheological implications can be made for an average "steady state" case, by applying available rheological data and observed PT and grainsize data.

Interpretation of the microstructures: deformation mechanisms and rheology

The microstructures in the ET lherzolites suggest that flow in the large-scale tectonite shear zone was controlled by dislocation creep and concomitant dynamic recrystallization (i.e. rotation recrystallization) in the presence of minor quantities of water. Chopra and Paterson (1984) have shown that the presence of as little as 0.01 wt% H_2O added to pre-dried samples of dunite lowers the strength to stress levels comparable with wet specimens (> 0.1 wt% H_2O). Therefore, it seems warranted to model the rheology of the bulk tectonite shear zone with a dislocation creep flow law for wet olivine. This may also apply to the lenticular domains of fine-grained olivine in the mylonites. However, the most conspicuous microstructural change associated with the peridotite mylonites is the intense grainsize reduction of recrystallized olivine and pyroxenes in amphibole-bearing, very fine-grained fluidal bands. It has been suggested (section 5.2) that the small grainsize in the fluidal bands primarily resulted

from nucleation of new phases in response to the synkinematic break-down of pyroxenes. The microstructure of the ET peridotite mylonites is very similar to that in fluidal kimberlite xenoliths (Bouiller & Gueguen 1975), inferred to have resulted from diffusion-accommodated grain boundary sliding (in orthopyroxene) leading to some sort of superplasticty, i.e. extreme ductility involving power law creep with a stress exponent close to 1.

In view of the lack of well documented experimental evidence for superplasticity in ultramafic rocks, it is extremely difficult, if not impossible, to conclusively assess in naturally deformed material whether superplastic and/or diffusion-controlled deformation mechanisms have been rate controlling. Commonly quoted microstructural criteria consistent with superplasticity include very fine grainsizes less than 10 μm, equiaxed recrystallized grains, the lack of a strong lattice preferred orientation, a low degree of intragranular plastic deformation and low dislocation densities, and in the case of polymineralic rocks, extensive mixing of phases (Schmidt 1982). All these features are seen in the very fine-grained fluidal bands in the ET peridotite mylonites. This suggests that the deformation in these fluidal bands may have involved an important component of diffusion-accommodated grain boundary sliding. As a result these bands may have been much weaker than the mylonitic matrix, thus controlling the rheology of the peridotite mylonite zones. On this basis a dislocation creep flow law for "wet" olivine can be expected to seriously overestimate the flow stresses in the peridotite mylonites. Instead, a diffusion creep flow law should be more appropriate. Available experimental data do not allow a quantitative description of the behaviour of polymineralic aggregates with multiple rheologies (e.g. Schmid 1982; Jordan 1987, 1988). However, for present purposes we assume that the fluidal bands consist of "wet" olivine, in which deformation occurs by grain boundary diffusion plus grain boundary sliding. Provided that the grain boundary diffusivity of additional phases is not drastically different from olivine, this assumption is reasonable.

Given the above assumptions, olivine flow laws (Karato et al. 1986; Rutter & Brodie 1988b) can be used to illustrate the effect of a shift from dislocation to diffusion-controlled creep. For a constant strain rate, taken here as 10^{-12} s^{-1}, and a temperature of 900°C, the imposed deformation in the very fine-grained bands can be accommodated at a flow stress of about 0.01 MPa, i.e three orders of magnitude below the stress levels around 60 MPa expected in case of dry dislocation creep under those conditions. Conversely, for a constant flow stress of around 60 MPa, the strain rate in the very fine-grained bands may have been 5 orders of magnitude faster than the strain rate expected for the case of dry dislocation creep. It follows that the fluidal bands have been much weaker than the 10 to 150 μm olivine matrix, hence that the bulk rheology of the peridotite mylonite zones is controlled by the mechanical behaviour of the olivine-pyroxene-amphibole fluidal bands. This in turn implies that at shallow depth the rheology of the extending lithospheric mantle becomes controlled by such very fine-grained, hydrated, polymineralic aggregates, in which the deformation involved diffusion-accommodated grain boundary sliding.

Note, that the above reasoning ignores further potential weakening effects due to the progressive transformation, in the ET mylonites, to the chlorite- and antigorite-bearing assemblages. These assemblages are inferred to have developed at progressively

decreasing temperatures during uplift, in an advanced stage of bulk extension, towards the incipient ocean floor . It is clear that such transformations may have led to an enhanced weakening of the Piemonte-Ligurian uppermost mantle.

Discussion

Most geophysical models for extending continental lithosphere and incipient oceanic rifting follow Brace and Kohlstedt (1980) and Sawyer (1985) in assuming that the rheology in the peridotitic upper mantle is controlled by either dislocation creep of olivine or by brittle frictional sliding (e.g. Lynch & Morgan 1987; Bassi & Bonnin 1988; Braun & Beaumont 1989; Dunbar & Sawyer 1989). In all these models, the highest flow stresses are attained in the upper 10 to 20 kilometres of the lithospheric mantle, and the calculations invariably indicate a strong control exerted on the dynamics of the system by the behaviour of this mechanically strong layer.

Various workers have emphasized potential weakening effects due to shear localization in the upper mantle (e.g. Kirby 1985; Rutter & Brodie 1986). The implication of the ET shear zone structures is that localization of deformation during the earlier stages of continental rifting may progressively "remove" a significant part of the mechanically strong layer, thereby facilitating trans-lithospheric failure and continental breakup at much lower stresses than those expected for strictly temperature dependent dislocation creep (at constant microstructure) throughout the lithospheric mantle column. It is inferred here, that failure of the Piemonte-Ligurian lithosphere in fact occurred when shear localization proceeded to a stage that a (?)throughgoing shear zone system or network of shear zones existed in which grainsize reduction and/or transformation enhanced ductility allowed appreciable geological strainrates at very low stresses. This implies that the upper mantle had weakened considerably before appreciable extension was achieved. In this case the bulk lithosphere strength would have vanished by the time geologically significant deformation of the lithosphere occurred.

5.6 CONCLUSIONS

- Bulk extension of the Piemonte-Ligurian lithosphere was accommodated by localized deformation in 100 m to km-scale upper mantle shear zones. Four generations of shear zones developed in initially granular spinel lherzolite, i.e. spinel peridotite tectonites, spinel/plagioclase-bearing peridotite mylonites, chlorite-bearing peridotite mylonites, and serpentinite mylonites. The development of these shear zones is allied to the progressive uplift of the peridotites from deep to shallow lithospheric levels.
- The ET lherzolites were uplifted along a non-adiabatic, subsolidus trajectory. This PT evolution seems inconsistent with mantle diapirism. Instead, it strongly suggets that uplift of the ET lherzolites involved a mechanism of tectonic unroofing in a slightly to strongly asymmetric, oceanic rift.
- The deformation in the peridotite tectonites was dominated by dislocation creep and

dynamic recrystallization of wet olivine. In contrast, the microstructure of very fine-grained olivine-pyroxene-amphibole bands in the peridotite mylonites suggests an important contribution of diffusion-assisted grainboundary sliding. This switch of dominant deformation mechanism, during progressive localization of the deformation, may have had a significant effect on the bulk strength of the Piemonte-Ligurian upper mantle. This suggests, that thermo-mechanical models of lithosphere extension involving a mechanically strong homogeneously deforming upper mantle in an advanced stage of breakup are inappropriate for the case of inhomogeneous deformation of the upper mantle.

ACKNOWLEDGEMENTS

Martin Drury (Canberra) has made an enormous contribution to my work on the Erro-Tobbio Unit by recognizing the presence of different shear zone structures in the lherzolites. Based on his initial work, extensive form surface mapping has been carried out, supported by field work of Dirk van der Wal and other MSc students from the University of Utrecht. Discussions with Giovanni Piccardo (Genova), Adolphe Nicolas (Montpellier), Martin Drury (Canberra), Chris Spiers and Dirk van der Wal (Utrecht) have been of great help in understanding the petrological, structural and rheological problems encountered.

CHAPTER 6

The evolution of the Piemonte-Ligurian ocean: a synthesis

6.1 INTRODUCTION

The preceding Chapters have focussed on several aspects of the deformation of the Piemonte-Ligurian oceanic lithosphere. These include [1] the mechanical behaviour of the upper mantle during incipient oceanic rifting (Chapter 5) and subduction (Chapters 3 and 4), and [2] the deformation and tectono-metamorphic evolution of oceanic lithosphere in the intraoceanic subduction complex (Chapters 2 and 3). The purpose of this chapter is to present a synthesis which incorporates these aspects in a geodynamic scenario for the evolution of the Piemonte-Ligurian ocean.

There is a vast amount of literature concerning the Alpine orogenic cycle in the Piemonte-Ligurian realm, which includes stratigraphic, radiometric, structural and metamorphic data as well as plate tectonic reconstructions, concerned with the large-scale kinematics of the western Tethys. In order to constrain the tectonic history of those parts of the Piemonte-Ligurian realm now represented by the Ligurian ophiolite complexes, a review of the main geological events in the Alps-Apennine system is presented first. The timespan considered here comprises the onset of rifting in the Middle Triassic till the transition from subduction to continental collision in the Eo-Oligocene. In a next section, some of the existing tectonic interpretations are tested against the data presented in this thesis and in the current literature, followed by a short account of recent kinematic interpretations with regard to plate movements in the western Tethys. With these constraints, and on the basis of the geological data presented in the preceding Chapters, a synthesis is developed for the geological evolution of the Piemonte-Ligurian ocean and its role in the Alpine orogenic cycle.

6.2 MAIN GEOLOGICAL EVENTS IN THE LIGURIAN ALPS AND APENNINES FROM THE MIDDLE TRIASSIC TILL THE EO-OLIGOCENE.

Middle Triassic-Middle Jurassic

Rifting in the Piemonte-Ligurian part of the Mediterranean Tethys started during the Middle Triassic (Anisian-Ladinian, Martini et al. 1986), but did not lead to an appreciable extension before the Early Jurassic. The Jurassic extension comprised a

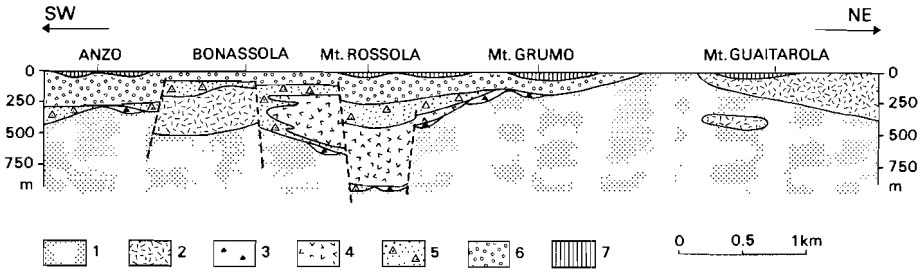

Fig. 6.1
Schematic reconstruction of a part of the Bracco ophiolite complex, showing an asymmetric graben, developed in a serpentinite-gabbro-ophicalcite oceanic crust, and filled with basalts and ophiolitic breccias (Hoogerduijn Strating 1988). Reference horizon is the base of the Early Cretaceous pelagic sequence of Calpionella limestone and Palombini shale. 1= serpentinite, 2= gabbro, 3= ophicalcite (Lèvanto breccia), 4= massive basalt, 5= polymict ophiolite breccia (Bonassola breccia), 6= pillow basalt, 7= radiolarian chert.

Lias and a Dogger cycle, the latter resulting in the actual opening of the oceanic basin (Lemoine et al. 1986; Lemoine & Trümpy 1987; Roux et al. 1988). For the present purposes it is emphasized, that there is no evidence, in the Piemonte-Ligurian domain, for a stage of regional-scale doming prior to rifting (Winterer & Bosellini 1981; Lemoine 1983; Lemoine et al. 1986).

Extension of the Jurassic carbonate shelf led to block faulting and was associated with deposition of submarine scarp-breccias and debris flows. The geological data available at present strongly suggest an asymmetric development of the European and Adriatic parts of the shelf during the Lias and Dogger. Firstly, the Adriatic/Southern Alpine margin is characterized by overall syn- and post-extensional subsidence during the Late Lias and Early Dogger (Winterer & Bosellini, 1981; Lemoine 1983; Fazzuoli & Scuazzoni 1988) while the European margin was characterized by uplift and erosion of the Briançonnais ridge. This ridge was emerged during the Early Dogger (Aalenian-Bajocian) and subsided rapidly during the Late Dogger and Malm (from the Bathonian-Callovian onward; Roux et al. 1988). Secondly, there is no well-defined "break-up" unconformity on the Adriatic margin (Winterer & Bosellini 1981), whereas on the European continental margin a marked "break-up" unconformity and transition to a pelagic facies is recognized. The age of this unconformity varies from Late Bajocian to Middle Oxfordian (most often Bathonian or Callovian; Lemoine & Trümpy 1987) which corresponds to the age of the oldest sediments deposited on the oceanic lithosphere (Late Bathonian to Early Callovian radiolarian chert; Baumgartner 1987; see Fig 6.1 for ophiolite stratigraphy).

Whole rock (K-Ar) and mineral (K-Ar, fission track) data from the low-grade Alpine, Corsican and Apennine ophiolites suggest, that intrusion of gabbros (Lias-Dogger: 212-161 Ma) occurred prior to or simultaneous with extrusion of basalts (Dogger: 176-164 Ma; Bigazzi et al. 1973; Bertrand & Delaloye 1976; Bortolotti & Gianelli 1976; Fontignie et al. 1982; Carpena 1983; Carpena & Caby 1984). Radiometric and biostratigraphic age zonations in the Apennine ophiolites (e.g. Bigazzi 1973; Abbate

et al. 1986) suggest a progressive generation of oceanic lithosphere, from the most external parts of the oceanic basin (External Ligurian Units), through intermediate zones (Internal Ligurian Units, Tuscany and Elba), to the most internal parts (Balagna Unit on Corsica). This age zonation corresponds with a petrological zonation in the various mantle fragments uplifted during rifting, from relatively undepleted lherzolites associated with light REE enriched transitional MOR basalts and locally continental crustal rocks in the external parts (i.e. External Ligurian Units, External western Alps, Calabria), to depleted lherzolites with normal MOR basalts in the internal parts (i.e. Internal Ligurian Units, Tuscany, Balagna Unit on Corsica, Internal western Alps; Beccaluva et al. 1984; Ottonello et al. 1984). The chemical differences between these two ophiolitic sequences most probably reflect variations in physical conditions and degree of partial melting (Beccaluva et al. 1984). While the lherzolites in the External Ligurids were affected by minor "wet" partial melting, the Internal Ligurian lherzolites underwent more extensive "dry" low-pressure partial melting (see also Chapter 5.4). The petrological as well as the age zonation suggest some sort of oceanic spreading mechanism in the Piemonte-Ligurian ocean.

Late Jurassic-Barremian

The generation of oceanic lithosphere in the Piemonte-Ligurian basin probably ceased during the Tithonian (Winterer & Boselini 1981; Abbate et al. 1984; Dercourt et al. 1986). The newly formed oceanic lithosphere was covered by a thin sequence of pelagic and hemipelagic sediments made up by radiolarian chert (Malm), Calpionella limestone (Berriasian-Valanginian) and Palombini shale (Hauterivian-Barremian; see Chapters 2 and 3). In the Alpine realm (i.e. Corsica, Ligurian and western Alps), the metamorphosed equivalents of these sediments are represented by quartzites, marbles, calcareous schists and micaschists (e.g. Voltri-Rossiglione Unit and other Schistes Lustrés units; Chapter 3). Coeval sedimentation on the rapidly subsiding European and Adriatic margins was dominated by the deposition of pelagic limestones and, during the Late Jurassic, of intermittant radiolarian chert (Passeri 1984; Vanossi et al. 1984).

Convergence leading to crustal thickening along the north-western margin of the Adriatic plate (Austroalpine Sezia-Lanzo zone) started during the Early Cretaceous (Hauterivian: 129±15 Ma; Rb-Sr whole rock data from Hunziker 1974; Oberhänsli et al. 1985).

Aptian-Albian

The sudden appearance of arenaceous turbidites and olistostromes in the pelagic sedimentary sequences of the Piemonte-Ligurian ocean (e.g. Manganiferous shale: Elter 1972; Matter et al. 1980; Galbiati 1985) marks the overall change to a compressional regime (Van Wamel 1987). This coincides with the differentiation, in the Ligurian realm (defined for present purposes as the eastern part of the Piemonte-Ligurian ocean), into an Internal and an External Ligurian basin, both underlain by oceanic lithosphere and separated by a submarine high referred to as the "Bracco Ridge" (Elter & Raggi 1965). In the Alpine realm to the west, an intraoceanic

subduction zone developed, and subducted rocks now exposed as thrust units in the internal parts of central and western Alps attained peak pressure conditions (about 1000-2000 MPa, up to 2800 MPa in the "continental" Dora Maira Massif) during this period (115 to 100 Ma, Oberhänsli et al. 1985; Hunziker et al. 1989). Distal turbidites and black shales were deposited in domains between the subduction complex and the European continental margin (e.g. Vanossi et al. 1984; Marini 1988). On the margin proper, the outer shelf area including the continental slope emerged, while hard grounds on the inner shelf reflect condensed pelagic sedimentation (Vanossi et al. 1984).

On the Apulian margin, large parts of the outer shelf were uplifted and eroded prior to deposition of hemipelagic shales with terrigenous clastic turbidites (Scisti Policromi). Meanwhile, deposition of calcareous turbidites (Scaglia) prevailed on the inner shelf (Fazzuoli & Sguazzoni 1986).

Cenomanian-Early Palaeocene

This stage of the Alpine cycle is characterized by ongoing subduction of Piemonte-Ligurian oceanic crust. Thick sequences of calcareous flysch (Helmintoid Flysch) reflect sedimentation on the basin plain between the European continental margin and the subduction complex (Marini 1988). Hemipelagic shales and pelitic limestones were deposited on the Albian-Cenomanian (?) hard grounds of the innner shelf (Dauphiné basin). The outer shelf, represented by the Briançonnais ridge, remained emerged during this stage, shedding breccias and arenaceous turbidites onto the inner shelf and the basin plain (Vanossi et al. 1984). The Palaeocene record is dominated by erosion and non-deposition, and reflects a period of overall regression on the European shelf (Jean et al. 1985).

In the Ligurian realm, deposition occurred of calcareous and arenaceous turbidites, representing basin plain and submarine fan environments, respectively (Sagri & Marri 1980). In the Internal Ligurian basin both calcareous (Ronco formation, Antola flysch) and arenaceous turbidites (Ramaceto sandstone) were deposited (Galbiati 1985). Sedimentation in the External domain was characterized by exclusively calcareous turbidites (Caio and Cassio flysches; Van Wamel et al. 1985). The presence of olistostromes, slumps and debris flows containing ophiolitic components in both the Internal and Extrernal Ligurian basin suggests that the submarine Bracco ridge separating the two basins eroded during pronounced synsedimentary tectonic activity until the Early Palaeocene (e.g. Van Wamel et al. 1985; Bertotti et al. 1986; Casnedi 1987).

The Apulian margin shows ongoing deposition of Scisti Policromi and Scaglia, however, discontinuities in the record suggest intermittent tectonic activity (Fazzuoli & Sguazzoni 1986).

W-facing recumbent folds (F1) of Early Palaeocene age developed in both the Lavagna Nappe and the Bracco Subunit of the Mélange Nappe (Hoogerduijn Strating & Van Wamel 1989; Chapter 2). Synkinematic metamorphism increased from prehnite-pumpellyite facies in the southeastern part of the Lavagna Nappe and Bracco Subunit to low-pressure blueschist facies in the western part of the Lavagna Nappe.

Late Palaeocene-Middle Eocene

Stacking of the Internal Ligurian nappes (Lavagna-, Mélange- and Antola Nappe) and juxtaposition on more external units resulted in cessation of calcareous flysch sedimentation in the External Ligurian basin during the Middle Eocene (Principi & Treves 1984; Van Wamel et al., 1985). On the Apulian inner shelf, deposition prevailed of calcareous flysch (Scaglia) grading upward into Middle Eocene marls, while on the outer shelf calcarenitic turbidites covered the hemipelagic shales (Scisti Policromi).

Sedimentation on the ocean floor in the Alpine realm was dominated by calcareous and arenaceous turbidites. From the Late Palaeocene-Early Eocene onward, flysch sedimentation was interrupted by olistostromes derived from the subduction complex. Flysch sedimentation ceased progressively from the internal (Palaeocene-Early Eocene: Moglio-Tèstico Serie of Marini 1988) to the external domains (Middle-Late Eocene: Albenga Flysch of Marini 1988).

The European outer shelf remained elevated or emerged till the Middle Eocene, while condensed sedimentation of distal turbidites prevailed on the inner shelf. Both the inner and outer shelf are covered by a Middle Eocene transgressive sequence of limestones, olistostromes, submarine fans and scarp breccias (Vanossi et al. 1984; Jean et al. 1985).

Late Eocene-Middle Oligocene

This period marks the end of several important orogenic events in the Alps-Apennine system. Penninic thrusting in the Alps (Trümpy 1980) as well as continental collision in Corsica (Harris 1985) and the Ligurian Alps (Vanossi et al. 1984; Marini 1988) ended in the Late Eocene or earliest Oligocene. Subsequent to deposition of precursor olistostromes, the European continental margin was partially subducted and underwent high-pressure greenschist facies metamorphism (400-600 MPa, 300-350°C; Goffé 1984; Messiga 1987). The HP units of the Voltri Massif, Sestri-Voltaggio Zone and Lavagna Nappe must have emerged and become subject to erosion at that stage, in view of the deposition of latest (?) Eocene ophiolitic scarp breccias and Oligocene alluvial fan deposits ("Molasse").

In front of the east- to northeastward moving Ligurian nappes, a hemipelagic foreland basin developed in which turbiditic sedimentation (Canetolo complex) was continuously interrupted by the influx of precursor olistostromes (Hoogerduijn Strating & Van Wamel 1989). Sedimentation in this foreland basin continued at least till the Middle Oligocene. On the adjacent Apulian shelf, deposition prevailed of hemipelagic shales and marls.

6.3 PREVIOUS TECTONIC INTERPRETATIONS: FURTHER CONSTRAINTS

Several conflicting interpretations exist with regard to the rifting and opening of the Piemonte-Ligurian basin. Furthermore, a variety of tectonic interpretations concern the subduction- and collision-related structures, and the problem how to incorporate

and explain the opposite tectonic vergences in the Alps and Apennines. In this section an attempt is made to evaluate these various studies in the light of the data presented in this thesis and in the literature.

Rifting and oceanization

On the basis of comparison with present-day oceanic lithosphere, three groups of tectonic interpretations have been put forward to explain the ophiolite sequences of the Alps and Apennines. According to the first group, the ophiolites were generated in a normal ocean with spreading ridges, but represent oceanic lithosphere originating from transform faults (Gianelli & Principi 1977; Ohnenstetter 1979; Abbate et al. 1980, 1984, 1988; Weissert & Bernoulli 1985; Ishiwatari 1985). A second group of interpretations suggests that the ophiolites represent remnants of lithosphere generated along a slow-spreading ridge in an Atlantic-type ocean (Barrett & Spooner 1977; Lagabrielle & Cannat 1990). A third group of hypotheses suggests that the Piemonte-Ligurian ocean was an embryonic oceanic basin (e.g. Bortolotti et al. 1976; Lombardo & Pognante 1982; Pognante et al. 1986). Several of these latter authors recognize that the generation of oceanic crust occurred by mechanisms not comparable to those prevailing in present-day oceans, but the nature of these mechanisms and the geometry of crustal deformation during rifting are not specified.

Any interpretation with regard to the development of oceanic crust in the Piemonte-Ligurian realm has to account for the sequence of lithologies making up the Jurassic ophiolite complexes in the Alps and Apennines. This sequence of lithologies is anomalous, not only in comparison with present-day oceanic lithosphere but also with respect to other ophiolite complexes (Moores 1982). This anomalous character of the Piemonte-Ligurian ophiolites is reflected by the absence of a sheeted dyke complex and the lack of a continuous, thick basaltic and gabbroic layer. Instead, the Piemonte-Ligurian oceanic crust is marked by asymmetric grabens (Hoogerduijn Strating 1988), in which vast amounts of ophiolitic breccias were deposited simultaneously with the outflow of lavas (e.g. Barrett 1977, see Fig. 6.1). Moreover, it can be demonstrated in many localities that prior to the outflow of these lavas and deposition of sedimentary breccias, serpentinized lherzolite and gabbro cropped out at the ocean floor (Abbate et al. 1980, 1984). The basalts (Ferrara et al. 1976; Ottonello et al. 1984; Beccaluva et al. 1989) and gabbros (Serri 1981; Hébert et al. 1989) of the Internal Ligurids show a considerable variation of trace element composition, which probably reflect variable degrees of fractionation of a tholeitic melt. These petrological and chemical data seem most consistent with magmas derived from short-lived, probably small, magma chambers, which typically occur underneath slow-spreading ridges (cf. Serri 1981; Harper 1988; Hébert et al. 1989).

The above considerations argue against interpretations of the Piemonte-Ligurian ophiolites involving a normal ocean with spreading ridges. An origin from transform-faults, as suggested in the first group of interpretations, seems also unlikely in view of the results of a structural study (Hoogerduijn Strating 1988) showing that the sense of movement and orientation of high-temperature shear zones, developed in the gabbros of the northern Apennine ophiolites, are inconsistent with these models.

The second group of interpretations explains the development of the submarine scarp breccias and stratigraphic omissions in the ophiolite sequences by normal faulting along a slow-spreading ridge. The petrological and chemical characteristics of the gabbros and basalts are consistent with this setting. However, the lack of sheeted dyke complexes and the only sporadic occurrences of dyke swarms in the ophiolites seem inconsistent with generation of the Piemonte-Ligurian oceanic crust along a mature ridge segment.

Lemoine et al. 1987 have proposed opening of the Piemonte-Ligurian basin in response to asymmetric extension accommodated by a westward dipping, low-angle normal shear zone. Deformation along this shear zone would have resulted in tectonic denudation of upper mantle rocks, while it also accounts for the absence of a spreading ridge. A slightly to strongly asymmetric extension model for the incipient stages of oceanic rifting is considered most likely, not only in view of the stratigraphic data clearly showing an asymmetric evolution of the European and Adriatic margins during the Lias-Dogger (Lemoine et al. 1986), but also in view of the non-adiabatic uplift path recorded in the ET lherzolites of the Voltri massif (Chapter 5). Such an asymmetric rift geometry is also consistent with the development of asymmetric grabens, filled with breccias and intercalated basalts derived from small, short-living magma chambers.

Subduction and collision

A major problem in tectonic studies of the subduction- and collision-related structures in the Alps and Apennines has always been to explain the opposite directions of nappe transport in these orogenic belts (see Chapter 2). These opposite transport directions have been interpreted in a variety of ways. A number of studies assume one (Principi & Treves 1984; Treves 1984; Hill & Hayward 1988) or several (Abbate et al. 1980, 1984, 1986) W dipping subduction zones, active throughout the Cretaceous-Tertiary deformation history. The Alpine (westward) nappe movements observed in the Voltri Massif and on Corsica are interpreted in such scenarios as late (i.e. Late Eocene) back thrusts. Alternatively, Boccaletti et al. (1971, 1980) and Reutter et al. (1978) have suggested a subduction polarity reversal ("flip over"). According to these authors a Late Cretaceous-Paleogene E dipping subduction zone has been responsible for the Alpine nappe movements, while a Neogene W dipping subduction zone has resulted in the Apennine nappe movements. Finally, there are tectonic interpretations which involve subduction along a single (Van Wamel et al. 1985; Bonazzi et al. 1987; Van Wamel 1987; Hoogerduijn Strating & Van Wamel 1989) or several E dipping subduction zones (Vanossi et al. 1984).

Large-scale geometries involving one or several W-dipping subduction zones are difficult to reconcile with Cretaceous, west-directed thrusting under HP metamorphic conditions, observed in the Voltri Massif (Chapter 3) as well as on Corsica (e.g. Gibbons et al. 1986). Moreover, such scenarios cannot account for the overprinting of east vergent onto west vergent folds and thrusts, as documented in the Sestri-Voltaggio Zone, Lavagna Nappe and Bracco Subunit (Chapters 2, 3). Aside these structural arguments, interpretations involving W dipping subduction zones including the "flip over" hypothesis are inconsistent with the results of seismic and gravimetric studies

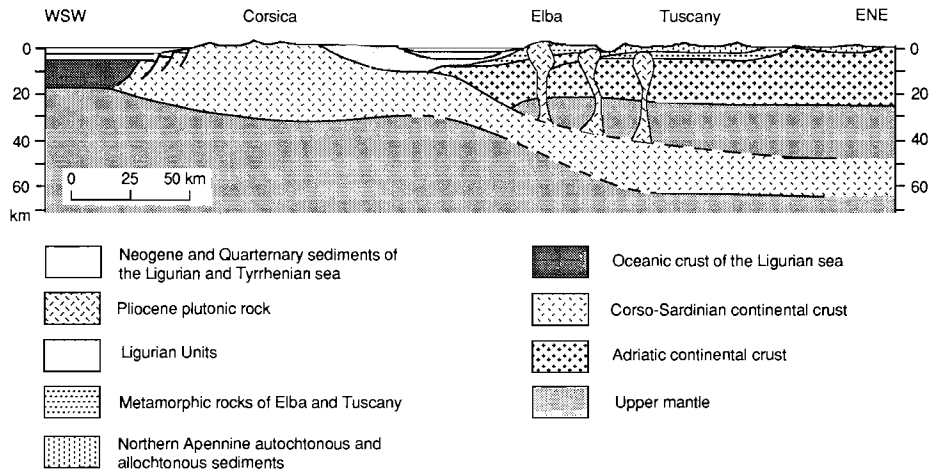

Fig. 6.2
Lithospheric doubling as inferred from seismic studies of Morelli er al. (1977) along the Corsica-Elba transect (after Reutter et al. 1978).

in northern Italy (Morelli et al. 1977; Giese et al. 1982). On the basis of these studies, a doubling has been inferred of the crust-mantle boundary (Moho) beneath the Apennines (Fig. 6.2). The Moho attached to Europe/Corsica dips below the Moho underneath the Apennines, suggesting underplating of the European/Corsican crust over a distance of at least 100 kilometres. Towards the western Alps this seismic structure becomes increasingly complex (Buness et al. 1991), however, its asymmetry does not change. It is currently believed that this lithospheric doubling (cf. Vlaar 1983) represents a relic of a Cretaceous east-dipping subduction zone, strongly modified during Tertiary continental collision. In case of the "flip over" mechanism or any of the other interpretations involving west-dipping subduction zones, one would expect the opposite asymmetry of such a doubled crustal structure.

Tectonic interpretations suggesting multiple, east-dipping subduction zone geometries such as proposed by Vanossi et al. (1984) seem unrealistic, in view of the presence of only one suture zone of high-pressure metamorphosed rocks of oceanic origin. In addition, multiple subduction geometries necessarily lead to the inference of subduction zones in domains such as the External Ligurids, which are characterized by east-vergent structures only. On the basis of these considerations, a tectonic interpretation involving one east-dipping subduction zone is favoured. Such a scenario is further developed below.

6.4 LARGE-SCALE KINEMATIC FRAMEWORK

During the last two decades, several plate tectonic models have been proposed for the Mesozoic-Cenozoic evolution of the Mediterranean and adjacent areas (e.g. Dewey et al. 1973; Biju-Duval et al. 1977; Smith 1982; Dercourt et al. 1986; Gealey 1988). All these models incorporate paleomagnetic (e.g. Pitman & Talwani 1972; Le Pichon et al. 1977; Savostin et al. 1986; Dewey et al. 1989) as well as geological data. Although the interpretations may vary in their details, a general consensus exists as to the role of the opening of the central and northern Atlantic ocean in controlling relative movements of the African and Iberian plates with respect to the European plate. The relative movement of the Adriatic microplate, "sandwiched" between Africa and Europe, is less well constrained.

Paleontological data suggest simultaneous development of the oldest oceanic crust (Callovian) in the Central Atlantic ocean (Sheridan 1988) and the Piemonte-Ligurian

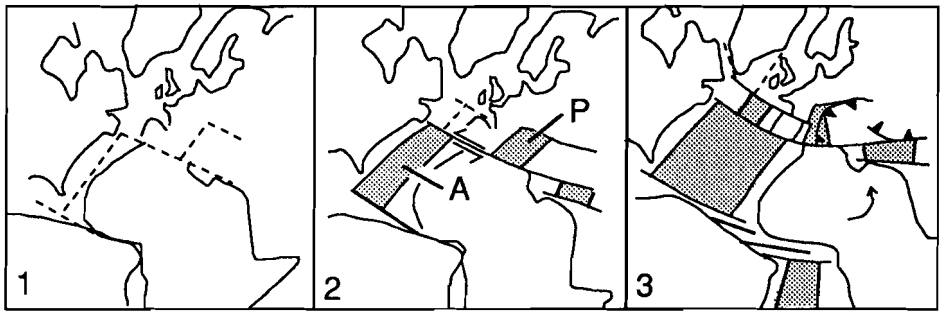

Fig. 6.3
Mesozoic evolution of the Tethys. [1] Triassic to Mid Jurassic continental rifting. [2] Mid Jurassic to Late Cretaceous oceanic rifting and oceanic spreading in the Piemonte-Ligurian (P) and central Atlantic (A) domain.. Oceanic spreading in the Piemonte-Ligurian domain ceased towards the end of the Late Jurassic. [3] Late Cretaceous opening of the northern and southern Atlantic and continued spreading in the central Atlantic. Rotation of Africa and Iberia with respect to Europe induce closure of the Piemonte-Ligurian ocean.

ocean (Baumgartner 1987). The two basins were linked by a system of transcurrent faults, and developed in response to a relative sinistral movement of Africa with respect to Europe/Iberia (Fig. 6.3). Iberia is generally believed to have been attached to Europe throughout the Jurassic and Early Cretaceous.

The Aptian-Albian marks an important change in the kinematics of the Mediterranean. Africa ceased its relative sinistral movement with respect to Europe. Instead, a counterclockwise rotation of Africa, induced by the opening of the southern Atlantic ocean (Fig. 6.3), led to northeasterly directed oblique convergence between the two continents (e.g. Dercourt et al. 1986; Dewey et al. 1989, and pers. comm. 1989). Rifting and tectonic denudation of mantle peridotites in the northern Atlantic domain started during the Early Cretaceous (Féraud et al. 1988), while the oldest oceanic crust off-

shore western Iberia and the onset of rifting in the Bay of Biscay are datad as Aptian (e.g. Srivastava et al. 1990). Continuation of magnetic anomaly 34 in the Bay of Biscay and along the British Isles (Srivastava et al. 1990) suggests northward propagation of the northern Atlantic and opening of the Bay of Biscay during the Santonian-Campanian. Based on these observations it is assumed that from the Aptian onward, Iberia started to separate from Europe and became attached to Africa.

In most plate tectonic reconstructions of the Mediterranean, Adria is interpreted to have been attached to the African plate throughout the Jurassic and Cretaceous, and many authors suggest that it did not become a separate microplate before the Tertiary (e.g. Laubscher & Bernoulli, 1977; Biju-Duval et al. 1977; Channel et al., 1979, Coward & Dietrich, 1989). These reconstructions seem to be supported by paleomagnetic data from the Italian peninsula (e.g. Lowrie 1986). However, the evaluation of these data is strongly hampered by the lack of a well-defined apparent polar wandering path for Africa (Lowrie 1986). In contrast to these paleomagnetic constraints, a growing body of geological data suggest that Adria may have acted as a semi-independent microplate throughout most of the Mesozoic and Cenozoic and has not been firmly attached to Africa. The most important of these geological data are:

- In the Eastern Mediterranean/Israel rifting, magmatism and crustal thinning started in the Middle Triassic and may possibly have resulted in ocean spreading by the end of the Lias (e.g. Garfunkel & Derin 1984). This extensional system was probably connected to the Piemonte-Ligurian and central Atlantic domains, and partially or completely disconnected Adria from Africa (see Fig. 6.3)
- Convergence between the Adriatic and European plate started in the Neocomian (crustal thickening in the Sezia-Lanzo zone: 129 Ma, Oberhänsli et al. 1985), whereas according to the plate motion of Africa with respect to Europe (Dewey et al., 1989 and pers. comm. 1989) this could not have occurred before the Aptian (119 Ma).
- The Late Cretaceous and Tertiary convergence direction between Adria and Europe as inferred from the kinematics of thrusts and strike-slip zones in the central, western and Ligurian Alps (WNW; Lacassin, 1989; Platt et al., 1989, see Chapter 3) is markedly different from the coeval relative movement of Africa with respect to Europe inferred from paleomagnetics (NNW; Dewey et al. 1989). Therefore, Adria could not have been attached to Africa.

For want of better constraints, it is assumed here that Adria has been attached to Africa till the Neocomian, which implies that it largely followed the Late Triassic-Jurassic sinistral movement of Africa with respect to Europe. This assumption implies that the Apulian plate was bounded to the north by an E-W trending, sinistral trans-tensional margin (e.g. Biju-Duval et al. 1977; Kelts, 1981; Weissert & Bernoulli 1985; Trümpy 1988), while a non-transform margin developed along the western boundary. For present purposes, Adria is assumed to have moved independent of Africa during the Cretaceous and Tertiary. Note, that a Late Cretaceous and a Late Eocene/Oligocene 15-25° counterclockwise rotation of Adria with respect to the present-day magnetic north is well established (Van den Berg 1983; Lowrie 1986).

6.5 THE PIEMONTE-LIGURIAN OCEAN: A SYNTHESIS

In section 6.3. it has been argued that Triassic/Jurassic rifting in the Piemonte Ligurian domain was most probably accommodated by a slightly to strongly asymmetric geometry of extensional faults and shear zones. Furthermore, the various geological and geophysical constraints strongly suggest that one east-dipping, intraoceanic subduction zone existed during the Late Cretaceous and Early Tertiary.

The tectonic interpretations of Lemoine et al. (1987) and Van Wamel (1987) provide a basis for respectively the Triassic/Jurassic and Cretaceous/Tertiary parts of the synthesis presented below. The scenario proposed by Vlaar and Cloetingh (1984) is used as a starting point for an interpretation in terms of geodynamics. The presently available data on the deformation in the Ligurian units (Chapters 2 and 3) and Voltri Group/Sestri-Voltaggio Zone (Chapter 3, 4 and 5), and geophysical model calculations presented in the literature, are incorporated here to arrive at a somewhat modified and further developed working hypothesis for the geological history of the Piemonte Ligurian oceanic crust (Fig. 6.4).

Middle Triassic-Jurassic: rifting and oceanization

From the Middle Triassic onward, the Alps/Apennine part of the Mesozoic Tethys underwent extension. The lack of evidence for regional-scale doming prior to rifting, and the non-adiabatic, subsolidus uplift history of the subcontinental Erro-Tobbio peridotites (Chapter 5.4) suggest, that the Piemonte-Ligurian ocean developed as a result of "passive" rifting (cf. Sengör & Burke 1978). Passive rifting implies that extension was mainly driven by externally applied tensile forces, rather than by body forces induced by a thermal anomaly in the upper mantle (i.e. a mantle plume or hot spot) underneath the rift basin. An explanation for such relative tensile forces to drive extension in the Piemonte-Ligurian domain may be provided by a consideration of the absolute plate movements in a hot spot reference frame. Such an analysis shows that, throughout the Triassic/Jurassic, Africa was lagging behind the other continents (e.g. Europe, North- and South America) in its progress over the mantle (Morgan 1981; Hynes 1990). The resulting velocity differences between the continental plates necessitate a sinistral transfer zone between the African/Adriatic- and European/ Iberian plate, consistent with the large-scale kinematic framework outlined above (Fig. 6.3). The imposed relative movements may thus have resulted in overall tensile forces in certain regions, leading to "passive" rifting in pull-apart domains such as the Piemonte-Ligurian ocean.

Extension in the Piemonte-Ligurian domain was rather slow (about 5 mm/y) from the Middle Triassic onward, but accelerated towards the end of the Middle Jurassic (about 20 mm/y; cf. Dercourt et al. 1986). This acceleration inevitably resulted in higher extensional strain rates. Kuznir and Park (1987) have shown that slow spreading may lead to strain hardening of the extending continental lithosphere. This may result in a continuous offset of the locus of rifting and lead to the creation of wide shelf areas with an overall low amount of extension, e.g. less than 20% Lias/Dogger stretching of the

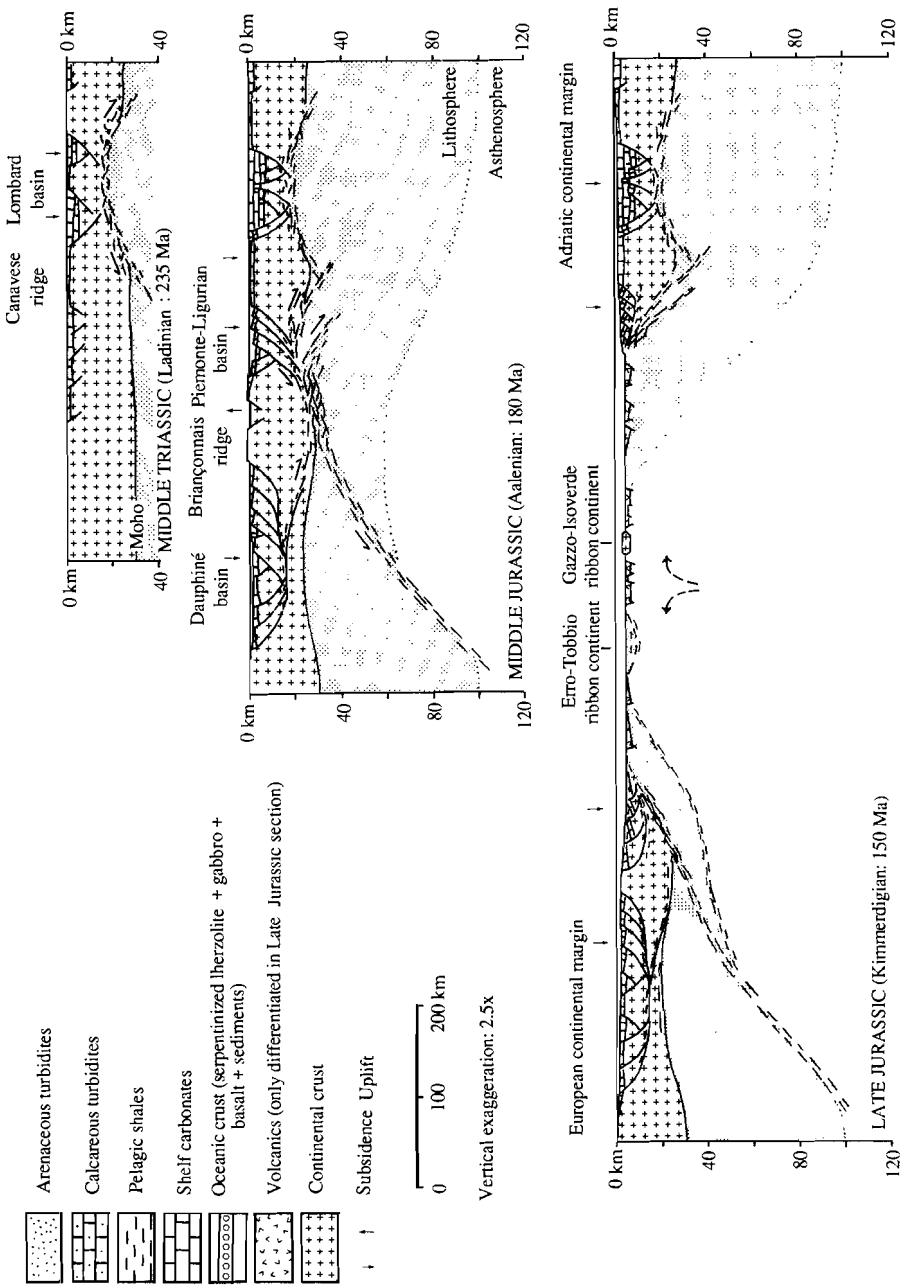

Fig. 6.4. Diagram illustrating the tectonic scenario proposed here for the evolution of the Piemonte-Ligurian ocean, starting with rifting in the Middle Triassic and ending shortly before the onset of continental collision. This scenario pertains to an approximatel E-W section through the oceanic lithosphere, now represented by the ophiolites of the Ligurian Alps and Apennines. The geometry of the

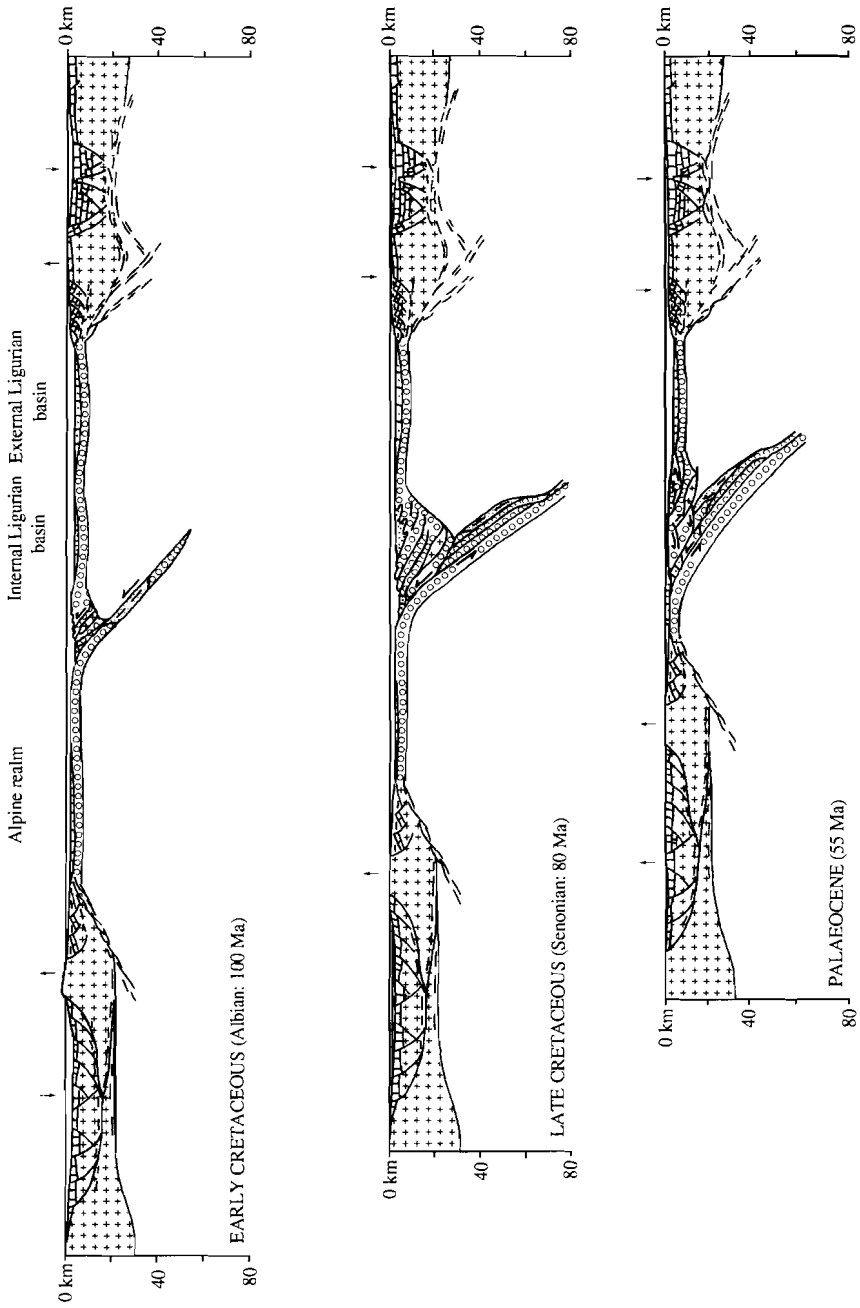

European and Adriatic continental margins during the Triassic-Jurassic are largely based on reconstructions of the western and southern Alps (Winterer & Bosellini, 1981; Lemoine et al. 1986; Lemoine & Trumpy 1987). Note that the detailed structure of the oceanic crust shown in the Late Jurassic section is replaced by a general signature for oceanic crust in the younger sections. See text for discussion.

European and Adriatic margins (Lemoine & Trümpy 1987; Fig. 6.4). In contrast, a strain-rate increase may enhance thermal softening of the continental lithosphere, thereby facilitating shear localization and incipient oceanic rifting, i.e. Bathonian-Callovian opening of the Piemonte-Ligurian ocean. Hydration, reaction-enhanced softening and a switch to diffusion-enhanced creep in mantle shear zones (Chapter 5) may have played a crucial role in allowing such lithosphere-scale shear localization.

Extension and block faulting of the continental upper crust was accommodated by movement on low angle extensional faults (e.g. Gillcrist et al. 1987; Lemoine et al. 1987; Rudkiewicz 1988; Fig. 6.4). The tectonic denudation of subcontinental, virtually undepleted mantle lherzolites (Erro-Tobbio unit, External Ligurian Units) indicates that one or several of these detachments must have rooted in the upper mantle (Hoogerduijn Strating et al. 1990; Chapter 5.4). It is unknown, however, how the upper-crustal extensional strains were transferred to the lower crust and upper mantle. In any case, the structures preserved in the Erro-Tobbio lherzolites indicate detachments in the upper mantle, characterized by a network of anastomosing (?), 100 m-scale fine-grained and hydrated mylonites directly below the Moho, grading downward into a kilometre scale "wet" tectonite shear zone surrounded by "dry" granular lherzolite.

The large-scale extensional geometry can possibly be assessed through comparison of the tectono-sedimentary evolution of the two continental shelfs, in order to identify characteristics expected for upper and lower plate margins (cf. Wernicke 1985; Lister et al. 1986). The contrast, emphasized above between synextensional (Lias-Dogger) subsidence of the Adriatic margin and uplift of the Briançonnais ridge on the European margin seems consistent with the isostatic vertical movements predicted for a lower and an upper plate margin, respectively (Lemoine et al. 1987). In addition, model calculations involving local isostatic compensation (Issler et al. 1989) suggest that the presence of a well-defined "break-up" unconformity (as observed on the European margin) is a typical upper plate feature. However, a strictly asymmetric, simple shear extensional geometry involving only one westerly dipping detachment as proposed by Lemoine et al. (1987; cf. Wernicke 1985) seems incompatible with the complex extensional geometry of the European shelf (Lemoine & Trümpy 1987), which is atypical for ideal upper plate margins (cf. Lister et al. 1986). Therefore, a less extreme, moderately asymmetrical geometry seems more likely. It is thus suggested here that extension may have been accommodated along a network of low angle detachments of which the westerly dipping ones were dominant (cf. Coward 1986: see Fig. 6.4).

Irrespective of the exact geometry, the overall subsidence of both margins during the Dogger/Malm and the transition to a pelagic facies is consistent with post-extensional thermal relaxation (e.g. Winterer & Bosellini, 1981; Lemoine et al. 1986).

Incipient oceanic rifting may have involved minor partial melting of a denudating and "wet" spinel-lherzolitic mantle of subcontinental origin, producing light-REE enriched basalts (T-MORB; External western Alps, Voltri, External Ligurids etc.; Beccaluva et al. 1984). With ongoing spreading (after about 10 My according to paleontological and radiometric data), more extensive low-pressure partial melting of adiabatically upwelling "dry" asthenospheric spinel/plagioclase lherzolites may have

become prominent, thereby generating magmas with a normal MOR affinity (Internal Ligurids, Internal western Alps etc.; Beccaluva et al. 1984). These N-MOR magmas probably fed small magma chambers in which progressive crystallization occurred of plagioclase/chromite-bearing dunites, olivine-bearing Mg-gabbros and Fe-Ti gabbros (Serri 1981; Hébert et al. 1989). It is envisaged that, simultaneous with crystallization, progressively more fractionated magmas were produced (cf. Harper 1988). Extrusion of these low-pressure fractionated, Ti-rich magmas was largely restricted to asymmetric grabens on the ocean floor (Fig. 6.4).

Discontinuities in the oceanic crustal sequences are common and are related to non-deposition and erosion, or pre-, syn- and post-extrusive normal faulting (e.g. Abbate et al. 1984; Hoogerduijn Strating 1988). In any case, all geological evidence suggests that ongoing spreading must have been "diffuse", rather than becoming localized in a spreading centre, which would have led to the development of a sheeted dyke complex. Actualistic counterparts of such "diffuse" spreading, albeit in a completely different tectonic setting, have been observed in marginal or back-arc basins (e.g. Watts et al. 1977; Moores 1982; Kastens et al. 1988).

During opening of the Piemonte-Ligurian oceanic basin, fragments of the outer shelf and associated continental lithosphere became separated from the continental margins, thereby creating ribbon continents partially or completely surrounded by oceanic-type crust (e.g. Lemoine & Trümpy 1987). In the Ligurian Alps and Apennines, the calcareous Gazzo-Isoverde Unit (Chapter 3) and the subcontinental peridotites of the Erro-Tobbio Unit (Chapter 5), now recognized as units of "continental" origin tectonically interleaved between units of "oceanic" origin, may represent fragments of such ribbon continents (Fig. 6.4; cf. Hoogerduijn Strating 1989, Bonatti 1990).

Early Cretaceous: onset of subduction

In the north Atlantic domain, rifting during the Neocomian and spreading during the Aptian induced a sinistral relative movement of the Iberian block with respect to Europe (e.g. Dercourt et al. 1986; Srivastava et al. 1990). Simultaneously, rifting and opening of the southern Atlantic led to a Late Cretaceous counterclockwise rotation of Africa, and Apulia (Van den Berg 1983; Lowrie 1986), with respect to Europe. In the Piemonte-Ligurian ocean this resulted in a change from an extensional to a compressional regime, and the onset of subduction along the northern and western margins of Adria (Dercourt et al. 1986).

Neocomian crustal thickening in the Sezia-Lanzo Zone (i.e. lower crust of the Adriatic plate) suggests that a southerly dipping subduction zone along the northern margin of Adria may have been located close to the continent-ocean boundary (e.g. Reutter et al. 1978; Platt 1986). In view of the inferred transform character of this margin, subduction may have been initiated along Jurassic transform faults, as such faults will have acted as preexisting mechanical discontinuities (cf. Casey & Dewey 1984). Along the western margin of Adria, convergence was accommodated in an intraoceanic subduction zone (e.g. Reutter et al. 1978; Van Wamel 1987; Hoogerduijn Strating & Van Wamel 1989; Chapter 2). Available structural data on extension-related, high-temperature shear zones in the gabbroic Bracco Massif (Hoogerduijn

Strating 1988) suggest, that transform faults in this section of the Piemonte-Ligurian ocean were oriented more or less perpendicular to the margins, i.e. parallel to the Jurassic spreading direction. It seems most unlikely, therefore, that initiation of a subduction zone in this part of the Piemonte Ligurian ocean would have occurred along a transform fault. Cloetingh et al. (1982, 1984) have shown, that for the initiation of subduction in such a case two competing cooling-effects have to be considered: the age-dependent density increase of the oceanic lithosphere which facilitates subduction of older lithosphere, and the age-dependent strengthening which hampers failure of older lithosphere. They have applied finite element techniques and an olivine depth-dependent lithospheric rheology to assess the feasibility of initiation of subduction zones along a passive (i.e non-transform) margin. The results of these calculations indicate, that in case of sufficiently high sediment loading or compressional forces, subduction may be initiated along a passive margin with an age of 20 to 30 Ma. At the onset of convergence in the Piemonte-Ligurian ocean, the passive margins were approximately 55 Ma old (Hoogerduijn Strating 1990) and therefore probably to old to fail. At the onset of convergence the youngest oceanic lithosphere in the Piemonte-Ligurian basin is inferred to have been about 25 Ma old (Hoogerduijn Strating 1990). Although the calculations of Cloetingh et al (1982, 1984) are not directly applicable to the initiation of an intraoceanic subduction zone, it seems likely that this young oceanic lithosphere has been dense enough to subduct and weak enough to fail (see also Van Wamel 1987). Therefore, the existing geological evidence for intraoceanic subduction in the Piemonte-Ligurian basin seems to be supported by these mechanical and thermal considerations (Fig. 6.4).

In view of the probably low density of the subducting young lithosphere, the subduction angle is inferred to have been small (less than 30° cf. England & Wortel 1980; Wortel 1980). This may have resulted in a geometric and geodynamic situation closely resembling that of lithospheric doubling as proposed by Vlaar (1983; see also Vlaar & Cloetingh 1984). A shallow subduction angle may also explain the absence of a volcanic island arc in the Piemonte-Ligurian ocean (Vlaar & Cloetingh 1984).

In view of the strong intraplate coupling generally inferred along shallow dipping subduction zones (e.g. Kanamori 1986) and the buoyancy of young oceanic lithosphere, compressional tectonics are expected to prevail in the subduction zone hanging wall (e.g. England & Wortel 1980). It has been suggested by Van Wamel (1987) and Hoogerduijn Strating (1990) that such compressional tectonics may account for the development of an Internal and External Ligurian basin in the Piemonte-Ligurian ocean. These basins, situated in the hanging wall of the eastward-dipping, intraoceanic subduction zone and filled with predominantly arenaceous and calcareous turbidites respectively (Fig. 6.4), may have developed by 100 km-scale buckling of the oceanic lithosphere (cf McAdoo & Sandwell 1985; Zuber 1987).

On both passive margins, the onset of convergence coincided with uplift of the outer shelfs (Fig. 6.4). In comparison with the pre-Aptian sedimentary sequences on the inner shelfs, the cover in both outer shelf areas was relatively thin. It follows, that the sedimentary load was unevenly distributed over the margins, with the highest loads concentrated on the inner shelfs. Cloetingh et al. (1985) have shown that compressive

intraplate stresses may induce relative subsidence of the basin centers (i.e. inner shelfs) in such cases, and uplift of the basin margins (i.e. outer shelfs). This suggests that the relative uplift of the outer shelfs was a direct consequence of the change, in the Piemonte-Ligurian ocean, to a compressional regime .

Cenomanian - Early Paleocene: ongoing subduction

The initiation of a subduction zone during the Early Cretaceous led to the development of an intraoceanic accretionary complex. The near-surface deformation was characterized by the development of km-scale westerly vergent isoclinal folds, i.e. F1 in the Bracco Subunit and Lavagna Nappe (Hoogerduijn Strating & Van Wamel 1989; Chapter 2). At depth, high-pressure low-temperature conditions prevailed (blueschist- to eclogite facies), and the deformation was strongly localized in westerly directed ductile thrust zones, i.e. D1/M1 - D3/M3 in the units of the Voltri Group and Sestri-Voltaggio Zone (Chapters 3 and 4). Throughout the Cretaceous the size of the tectonic wedge gradually increased due to progressive underplating of oceanic (Voltri-Rossiglione and Beigua Units) and "continental" units (Erro-Tobbio Unit; Fig. 4.6). Stratigraphic and radiometric data indicate that Late Cretaceous deformation in the Sestri-Voltaggio Zone (D1/2-D3) and western Lavagna Nappe (D1/2; Chapter 3) occurred simultaneous with sedimentation of the arenaceous Ramaceto sandstones in the eastern Lavagna Nappe (Chapter 2). These turbiditic sequences were not deformed until the Early Paleocene. This suggests that a deformation front marking the eastern boundary of the subduction complex moved eastward through time, thereby successively incorporating the Cravasco-Voltaggio and "continental" Gazzo Isoverde Unit of the Sestri-Voltaggio Zone (Late Cretaceous?), the western Lavagna Nappe (Senonian), eastern Lavagna Nappe and Bracco Subunit of the Mélange Nappe (Early Paleocene; Fig. 6.4).

Van den Beukel (1990) has shown that 100-km scale sheets may be detached from a subducting plate and incorporated in the overlying accretionary wedge. The mechanical feasibility for detachment and underplating critically depends on the age, hence tensile strength, of the subducting lithosphere, shear stress along the plate contact, externally applied compressional forces, and the trench-parallel length of the subducting slab. Given these variables he concludes that detachment is most likely in case of interaction of an intermediate- to fast-spreading ridge segment with a subduction zone. It is obvious that the dynamics of subduction in the Piemonte-Ligurian ocean cannot completely be described by this model, as all geological evidence argues against such an active spreading ridge during subduction. However, it is envisaged that [1] a weak rheology of the subducting lithosphere due to serpentinization, transformation- and reaction-enhanced ductility, and transiently very high fluid pressures (Chapter 4), [2] high shear stresses along the upper 40 km of the subducting plate contact (Chapter 4), and [3] inferred high intraplate compressional forces due to strong plate coupling and buoyancy (see above), may have resulted in the detachment of smaller (i.e. 10 to 100 km-scale) sheets (i.e. Erro-Tobbio and Beigua Units; Fig. 6.4). It should be noted, that the subduction of small but buoyant continental crustal units with completely

different rheological and thermal characteristics (e.g. Dora Maira) may have had a drastic but presently unknown effect on the underplating and detachment mechanisms (see e.g. Molnar & Gray 1979, Van den Beukel 1991).

During the Late Cretaceous, the European outer shelf remained elevated, while the previously uplifted Adriatic outer shelf subsided (Fig. 6.4). This asymmetry may be explained by the development of a forebulge or outer rise, in response to large-wavelength bending of the lithosphere seaward (i.e. west) of the subduction complex (e.g. McAdoo et al. 1978; Stockmal et al. 1986). Given the limited width of the Piemonte-Ligurian ocean and the generally 100-km scale wavelength associated with lithospheric bending, the forebulge may well have affected the European continental margin during the Late Cretaceous, thereby inducing transient uplift of the outer shelf and slope. With progressive subduction, the forebulge is expected to have migrated westward, thereby affecting larger areas of the shelf. Meanwhile, deposition of calcareous and arenaceous turbidites prevailed in the trench and in the Internal and External Ligurian basins. In contrast to the European shelf, the Apulian shelf was only affected by thermal contraction during this stage, which resulted in subsidence of the inner shelf as well as of the previously uplifted outer shelf (Fig. 6.4).

Paleocene - Middle Eocene: decreasing convergence velocities, wedge collapse

The Paleocene is marked by the onset of a reorganisation of plate movements in the Tethys and a dramatic decrease of the rate of convergence between Africa and Europe (e.g. Dercourt et al. 1986; Dewey et al. 1989). It has been argued in Chapter 2, how decreasing rates of subduction may have led to uplift, gravitational instability and extension of the intraoceanic accretionary wedge in the Piemonte-Ligurian ocean. Along the eastern margin of the subduction complex, gravitational collapse was marked by a reversal of tectonic transport directions, and the development of low-angle normal faults, NE-facing recumbent folds and thrusts (Fig. 6.4). One such extensional detachment of major importance has been identified between the Erro-Tobbio unit and the Sestri-Voltaggio Zone (D4/5-D6 in the Sestri-Voltaggio Zone Chapter 3.3). Minor detachments mark the contact between the Sestri-Voltaggio Zone and the western Lavagna Nappe (D5/6 in the western Lavagna Nappe; Chapter 3.4), and occur within the eastern Lavagna Nappe and in the Bracco Subunit of the Mélange Nappe (F2; Chapter 2). It is inferred here that westerly directed folding and nappe emplacement continued along the front of the accretionary complex, while underplated and stacked (D4-M5) eclogite facies units (i.e. Voltri Group; Chapter 3.2) were subject to nearly isothermal uplift (see Fig. 3.26) concomitant with extension in the upper levels of the accretionary complex. Calcareous flysch sedimentation in front of the westerly advancing subduction complex ceased progressively from Paleocene-Early Eocene in the east, to Middle-Late Eocene in the west. This suggests progressive accretion of these sediments and subduction of the marginal parts of the oceanic lithosphere in the Alpine realm (Marini 1988; Fig. 6.4).

Simultaneous with gravitational collapse of the accretionary wedge and the eastward migration of the Internal Ligurian Units, loading and flexural downbending resulted in an eastward shift of the depocenter in the External Ligurian basin (cf Van Wamel

1987). In this basin, deposition of calcareous turbidites in a hemipelagic environment prevailed until the Middle Eocene. By that time, the advancing Internal Ligurian units (i.e. Antola nappe, Lavagna nappe, and the Bracco, Isciola-Biscia and Cassanova-Scabiazza subunits of the Mélange nappe) had overthrust the western parts of the External Ligurian basin.

During the Paleocene, uplift of the European shelf led to a regional regression (Fig. 6.4; Trümpy 1980; Jean et al. 1985). Such a tectono-stratigraphic event is consistent with model studies of Quinlan and Beaumont (1984), which suggest that a decreasing subduction rate may lead to relaxation of the forebulge. As a consequence, the bulge is expected to migrate towards the subduction zone (i.e. eastward in the case of the Piemonte-Ligurian ocean), leading to uplift and erosion of large parts of the inner shelf, and causing the basin in front of the accretionary complex to become narrower and deeper. In addition, decreasing intraplate stresses may have accentuated this process by inducing relative uplift of the inner shelf and subsidence of the outer shelf (cf. Cloetingh et al. 1985).

On the Adriatic shelf subsidence and sedimentation continued, resulting in deposition of limestones and marls on the inner shelf and calcarenitic turbidites and hemipelagic shales on the outer shelf (Fig. 4.6).

Late Eocene - Middle Oligocene: continental collision

After the Early Eocene, north-directed convergence between Africa and Europe accelerated again (Dercourt et al. 1986; Dewey et al. 1989). In the Piemonte-Ligurian domain, the European/Corsican margin entered the subduction zone (latest Eocene - earliest Oligocene) which marks the transition to continental collision.

The sediments and continental basement (including the basement complexes of the Savona Unit, see Fig. 3.2) of the European outer shelf were subducted to about 20 km depth and metamorphosed under high pressure greenschist facies conditions (400-600 MPa, 300-400°C; Goffé 1984; Messiga 1987). Underplating of buoyant continental lithosphere is inferred here to have accelerated uplift and extension of the accretionary complex and denudation of the underplated eclogitic units. The PT-time evolution of the thrust units in the Voltri Group (Chapter 3) shows, that eclogite facies rocks were uplifted to about 6 km (200 MPa) depth at the end of the Eocene and were eroded during the earliest Oligocene. Erosion resulted in the development of scarp breccias and continental to submarine alluvial fans. The basal sequences of these fans were subsequently involved in westerly-directed imbricate thrusting, indicating that they developed on a tectonically active basement.

The greenschist facies overprint observed in the subducted units (e.g. Chiesa et al. 1975; see also Platt 1986; Chapter 3) is consistent with an increase of the thermal gradient, expected in case of slowing and cessation of subduction (England, 1978; Oxburgh & England, 1980; see Chapter 3). This metamorphic event reached its peak during the Late Eocene (38-40 Ma) and is recognized throughout the Alps and on Corsica (e.g. Frey et al. 1974; Maluski, 1977). The changing thermal regime in the subducted continental crust and the increase of lithostatic pressure will have facilitated the development of mid- and lower crustal detachments (Ranalli & Murphy 1984;

Murphy 1989; Ord & Hobbs 1989; Van den Beukel 1991) and inversion of Triassic and Jurassic extensional faults (e.g. Gillcrist et al. 1987). Therefore, much of the shortening in the underplated continental lithosphere was accommodated by thick-skinned (i.e. involving basement and sedimentary cover) rather than thin-skinned tectonics (involving sediments exclusively; see e.g. Butler et al. 1986; Buness et al. 1990).

The subduction of the European outer shelf led to the development of a pronounced foreland basin. Loading and flexural downbending resulted in subsidence of the former inner shelf, westward migration of the forebulge and widening of the basin (cf. Quinlan & Beaumont 1984). In the western Alps, this stage is reflected by deposition of a westward transgressive sequence of marine nummulite limestones (Jean et al. 1985), covered by fluvial and alluvial fan deposits ("Molasse") containing detrital blue amphibole and lawsonite derived from the uplifted and advancing subduction complex (Mange-Rajetzky & Oberhänsli 1982).

In contrast to the complete subduction, in the Alpine domain, of oceanic crust and parts of the continental margin, there was still oceanic crust preserved in the Apennine realm (Reutter et al. 1978). In this region, NE directed thrusting of the Internal Ligurian nappes continued during the Late Eocene and Oligocene. Deposition of hemipelagic shales on the Adriatic shelf and distal terrigenous clastic turbidites on the slope of the Adriatic margin and the basin plane (i.e. the Canetolo complex) was continuously interrupted by the influx of precursor olistostromes from the advancing nappes to the west (Hoogerduijn Strating & Van Wamel 1989). This process essentially continued till the Middle Miocene, when this part of the Piemonte-Ligurian ocean closed as well and the Ligurian units became emplaced onto the Adriatic margin (Van Wamel 1987).

6.6 CONCLUSIONS

The structural and metamorphic data presented in this thesis, complemented with stratigraphic and plate movement constraints documented in the litterature, have been used here to infer a possible geodynamic scenario for the evolution of the Piemonte-Ligurian ocean. It is envisaged that several aspects of this scenario may also apply to the evolution of small, Alpine-type oceanic basins in general. These aspects, discussed in detail in the previous chapters, concern the mechanical behaviour of the oceanic crust as well as the tectonic style during extension, subduction, and uplift of HP rocks.

(1) Bulk extension of the Piemonte-Ligurian lithospheric mantle was accommodated by localized deformation in km- to 100 m-scale extensional shear zones. These shear zones penetrated into the upper mantle, and most probably controlled [a] the non-adiabatic, subsolidus uplift of virtually undepleted spinel lherzolites from the upper mantle towards the ocean floor, and [b] the asymmetric tectono-sedimentary evolution during the development of the European and Adriatic margins. In addition, [c] the microstructures in the shear zones strongly suggest progressive weakening of the shear zone rocks, which may have induced a drastic strength reduction of the extending upper mantle.

(2) The complete lack of evidence for an early-stage thermal anomaly suggests that opening of the Piemonte-Ligurian ocean may have involved passive rifting of the continental lithospere.

(3) Structural analysis in the oceanic basement units of the Voltri massif indicates that the HP-deformation during subduction was localized in serpentinite mylonite zones, developed in an oceanic crust dominated by serpentinite and serpentinized lherzolite. This indicates that the shear stresses along the subducting plate contact in the Piemonte-Ligurian ocean were controlled by the rheology of serpentinite rather than by the much stronger rheology of basaltic rocks.

A drastic decrease of the shear stresses is expected at depths between 40 to 60 km where eclogite-facies conditions prevail. This decrease, allied to the breakdown of antigorite to produce olivine, is inferred from [a] the development of ultrafine-grained olivine-bearing shear bands in serpentinite mylonites, in which deformation was most probably controlled by diffusion-accommodated grain boundary sliding, and [b] dehydration-induced hydraulic fracturing of the peridotite.

(4) The structural analysis presented in this study suggests that low-angle extensional faults acccomodated [a] the nearly isothermal uplift of underplated eclogite-facies units during the Late Cretaceous and Paleocene, and [b] the onset of the Paleocene polarity change, from Alpine to Apennine-directed nappe transport. It is shown that initiation of these processes predate Eo-Oligocene continental collision. It is therefore suggested, that uplift and gravitational instability of the accretionary wedge were primarily induced by underplating of oceanic units as well as by the Paleocene decrease of subduction velocity inferred in plate tectonic reconstructions of the Mediterranean Tethys.

REFERENCES

Abbate E. 1969. Geologia delle Cinque Terre e dell'entroterra di Lèvanto. Mem. Soc. Geol. It, 8, 923-1014.

——, Bortolotti V., Conti M., Marcucci M., Principi G., Passerini P. & Treves B. 1986. Apennines and Alps ophiolites and the evolution of the western Tethys. Mem. Soc. Geol. It., 31, 23-44.

——, ——, Passerini P. & Principi G. 1985. The rhythm of phanerozoic ophiolites. Ofioliti, 10, 109-138.

——, —— & Principi P. 1980. Apennine ophiolites: a peculiar oceanic crust. Rocci G. (edt.): Tethyan ophiolites - 1: Western area. Ofioliti, Spec. Issue, 59-96.

——, —— & —— 1984. Pre-orogenic tectonics and metamorphism in Western Tethys ophiolites. Ofioliti, 9, 245-278.

Allmendinger R.W., Hauge T.A., Hauser E.C., Potter C.J., Klemperer S.L., Nelson K.D., Knuepfer P. & Oliver J. 1987. Overview of the COCORP 40°N Transect,Western United States: The fabric of an orogenic belt. Geol. Soc. Am. Bull., 98, 308-319.

Amendolia M. & Capponi G. 1985. Fasi deformative ed interpretazione strutturale del Gruppo di Voltri: primo contributo. Boll. Soc. Geol. It., 104, 297-309.

Anderson O.L. & Grew P.C. 1977. Stress corrosion theory of crack propagation with applications to geophysics. Rev. Geophys. Space Phys., 15, 77-104.

Andri E. & Fannucci F. 1975. La risedimentazione dei Calcari a Calpionelle Liguri. Boll. Soc. Geol. It., 9, 915-925.

Argenti P., Luchetti G. & Penco A.M. 1986. Zeolite-bearing assemblages at the contact Voltri Group and Sestri-Voltaggio Zone (Liguria, Italy). N. Jb. Miner. Mh., 229-239.

Atkinson B.K. & Meredith P.G. 1987. Experimental fracture mechanics data for rocks and minerals. In: Atkinson B.K. (edt.) Fracture mechanics of rocks, Academic Press Geology Series, 477-525.

Avé Lallement H.G. 1985 Subgrain rotation and dynamic recrystallization of olivine, upper mantle diapirism and extension of the Basin and Range Province. Tectonophysics, 119, 89-118

—— & Carter N.L. 1970 Syntectonic recrystallization of olivine and modes of flow in the upper mantle. Geol. Soc. Am. Bull., 81, 2203-2220.

Bassi G. & Bonnin J. 1988. Rheological modelling and deformation instability of lithosphere under extension- II. Depth-dependent rheology. Geophys. J., 94, 559-565.

Barnicoat A.C. & Fry N. 1986. High-pressure metamorphism of the Zermatt-Saas ophiolite zone, Switzerland. J. Geol. Soc. Lond., 143, 607-618.

Barrett J.J. & Spooner E.F.C., 1977. Ophiolitic breccias associated with allochtonous oceanic crustal rocks in the East Ligurian Apennines, Italy - a comparison with observations from rifted oceanic ridges. Earth Planet. Sci. Lett., 35, 79-91.

Baumgartner P.O., 1987. Age and genesis of Tethyan Jurassic radiolarites. Eclogea Geol. Helv., 80, 831-879.

Bearth P. 1967. Die Ofiolite der Zone von Zermatt-Saas Fee. Beitr. zur Geol. Karte der Schweiz, N.F. 132.

Beccaluva L., Chiesa S. & Delaloye M. 1981. K/Ar age determinations on some Tethyan ophiolites. Rend. Soc. It. Min. Petrol., 37, 869-880.

——, Dal Piaz G.V. & Macciotta G. 1984. Transitional to normal MORB affinities in ophiolitic meta basalts from the Zermatt-Saas, Combin and Antrona Units, Western Alps: Implications for the paleogeographic evolution of the Western Tethyan Basin. Geol. Mijnbouw, 63, 165-177.

——, Macciotta G., Piccardo G.B. & Zeda O. 1989. Clinopyroxene composition of ophiolitic basalts as petrogentic indicator. Chem. Geol., 77, 165-182.

Bertotti G., Elter P., Marroni M., Meccheri M. & Santi R. 1986. Le Argilliti a blocchi di M. Veri: considerazione sull'evoluzione tettonica del Bacino ligure et Creataceo Superiore. Ofioliti, 11, 193-220.

Bertrand J. & Delaloye M. 1976. Datation par la méthode K-Ar de diverses ophiolites et granites du Flysch des Gêts (Haute-Savoie, France). Eclogea Geol. Helv., 69, 335-341.

Bezzi A. & Piccardo G.B. 1971. Structural features of the Ligurian ophiolites: petrologic evidence for the "oceanic" floor of the Northern Apennines geosyncline; a contribution to the alpine-type gabbro-peridotite associations. Mem. Soc. Geol. It., 10, 55-63.

Bigazzi G., Bonadonna F.P., Ferrara G. & Innocentio F. 1973. Fission track ages of zircons and apatites from Northern Apennine ophiolites. Fortschr. Mineral., 50, 51-53.

Biju Duval B., Dercourt J. & Le Pichon X. 1977. From the Tethys to the Mediterranean seas: a plate tectonic model of the evolution of the Western Alpine system. In: Biju-Duval B. & Montadert L. (eds) International symposium on the structural history of the Mediterranean basins, Editions Technip, Paris, 281-286.

Boccaletti M., Colli M., Decandia F.A., Gianelli E. & Lazzarotto A. 1980. Evoluzione dell'Appennino Settentrionale secondo un nuovo modello strutturale. Mem. Soc. Geol. It., 21, 359-373.

——, Elter P. & Guazzone G. 1971. Plate tectonics model for the development of the Western Alps and Northern Apennines. Nature, 234, 108-111.

Boillot G., Recq M., Winterer E.L., et al., 1987. Tectonic denudation of the upper mantle along passive margins: A model based on drilling results (ODP leg 103, western Galicia margin, Spain). Tectonophysics, 132, 335-342.

Bonatti E. (edt) 1988. Zabargad Island and the Red Sea Rift. Tectonophysics, 150, 1-251.

——1990. Subcontinental mantle exposed in the Atlantic ocean on St. Peter-Paul islets. Nature, 345, 800-802.

——, Ottonello G. & Hamlyn P.R. 1981. Peridotites from the island of Zabargad (St. John's), Red Sea: Petrology and geochemistry. J. Geophys. Res., 21, 599-631.

—— & Michael P.J. 1989. Mantle peridotites from continental rifts to oceanic basins to subduction zones. Earth Planet. Sci. Lett., 91, 297-311.

Bonazzi A., Cortesogno L., Galbiati B., Reinhardt M., Salvioli Mariani E. & Vernai L. 1987. Nuovi dati sul metamorphismo di basso grado nelle unità Liguride interne e loro possibile significato nell'evoluzione strutturale dell'Appennino settentrionale. Acta Nat. Ateneo Parmense, 23, 17-47.

Bortolotti V., Cortesogno L., Gianelli G., Piccardo G.B. & Serri G. 1976. I filioni basaltici delle ofioliti dell'Appennino settentrionale e il loro significato nella formazione del bacino oceanico Ligure. Ofioliti, 1, 331-64.

—— & Gianelli G. 1976. Le rocce gabbriche dell'Appennino settentrionale: I. Dati recenti su rapporti primari, posizione stratigrafica ed evoluzione tettonica. Ofioliti, 1, 332-364.

Boudier F. & Nicolas A. 1985. Harzburgite and lherzolite subtypes in ophiolitic and oceanic environments. Earth Planet. Sci. Lett., 76, 84-92.

Boullier A.-M. 1980. A preliminary study on the behaviour of brittle minerals in a ductile matrix: example of zircons and feldspars. J. Struct. Geol., 2, 211-217.

—— & Gueguen Y. 1975. SP-mylonites: Origin of some mylonites by superplastic flow. Contrib. Mineral. Petrol., 50, 93-104.

Brace W.F. & Kohlstedt D.L. 1980. Limits on lithospheric stress imposed by laboratory experiments. J. Geophys. Res., 85, 6248-6252.

Braun J. & Beaumont C. 1989. A physical explanation of the relation between flank uplifts and the breakup unconformity at rifted continental margins. Geology, 17, 760-764.

Brodie K.H. 1980. Variations in mineral chemistry across a phlogopite shear zone. J. Struct. Geol., 2, 137-150.

—— & Rutter E.H. 1987. The role of transiently fine-grained reaction products in syntectonic metamorphism: natural and experimental examples. Can. Jour. Earth Sci., 24, 556-564.

Brown E.H. 1977. The crossite content of Ca-amphibole as a guide to pressure of metamorphism. J. Petrol., 18, 53-72.

Buck W.R., Martinez F., Steckler M.S. & Cochran J.R. 1988. Thermal consequences of lithospheric extension: pure and simple. Tectonics, 7, 213-234.

Buness H., Giese P., Hirn A., Maistrello M., Nadir S., Nicolich R., Pedone R. & Scarascia S. 1991. The fragmented lithosphere of the Northwestern Adriatic plate as revealed by deep seismic sounding investigations. Tectonophysics, submitted.

Buttler R.W.H., Matthews S.J. & Parish M. 1986. The NW external Alpine thrust belt and its implications for the geometry of the western Alpine orogen. In: Coward M.P. & Ries A.C. (eds) Collision tectonics. Geol. Soc. Spec. Publ., 19, 245-260.

Byerlee J.D. 1968. Brittle-ductile transition in rocks. J. Geophys. Res., 73, 4741-4750.

—— 1978. Friction of rocks. Pure Appl. Geophys., 116, 615-626.

Capponi F., Scambelluri M. & Tallone S. 1986. Distinzione di fasi tettoniche al contatto tra le unità Ponzema, Voltri-Rossiglione ed Erro-Tobbio, Gruppo di Voltri, Alpi Liguri. Ofioliti, 11, 221-234.

——, Pacciani G., Rebora A. & Amendolia M. 1987. Analis e cartografia strutturale del settore centro meridionale del Massiccio di Voltri. Boll. Soc. Geol. It., 106, 99-111.

Carpena J. 1983. Ophiolite fission track ages in the French occidental Alps. Terra Cognita, 3, 183.
—— & Caby R. 1984. Fission track evidence for Late Triassic oceanic crust in the French Occidental Alps. Geology, 12, 108-111.
Carter N.L. & Kirby S.H. 1978. Transient creep and semi-brittle behaviour of crystalline rocks. Pure Appl. Geophys., 116, 807-839.
—— & Tsenn M.C. 1987. Flow properties of continental lithosphere. Tectonophysics, 136, 27-63.
Casey J.F. & Dewey J.F. 1984. Initiation of subduction zones along transform and accreting plate boundaries, triple juction evolution and forearc spraeding centres - Implications for ophiolite geology and obduction. In: Gass I.G., Lippard S.J. & Shelton A.W. (eds) Ophiolites and oceanic lithosphere. Geol. Soc. Lond. Spec. Publ., 13, 269-289.
Casnedi R. 1982. Sedimentazione e tettonica delle Unita Liguridi nell'Appennino Nord-Occidentali (Valli Lavagna - Sturla - Trebbia e Aveto). Atti. dell'Inst. Geol. Univ. Pavia, 30, 42-66.
—— 1987, Le Unità Liguridi nella Val Trebbia e zone limitrofe. Atti. Tic. Sc. Terra., 31, 91-107.
Cerrina Ferroni A., Martinelli P., Plesi G., Giammattei L., Franceschelli M. & Leoni L. 1985. La cristalinità dell' illite nelle argille e calcare (unità di Canetolo) tra La Spezia e l'Alta Val Parma (Appennino Settentrionale). Boll. Soc. Geol. It., 104, 421-427.
Channell J.E.T., D'Argenio B. & Horvath F. 1979. Adria, the African promontory, in the Mesozoic Mediterranean paleogeography. Earth Sci. Rev., 15, 213-292.
Chapple M.W. 1978. Mechanics of thin-skinned fold-and-thrust belts. Geol. Soc. Am. Bull., 89, 1189-1198.
Chiesa S., Cortesogno L., Forcella F., Galli M., Messiga B., Pasquarè G., Pedemonte G.M., Piccardo G.B. & Rossi P.M. 1975. Assetto strutturale ed interpretazione geodinamica del Gruppo di Voltri. Boll. Soc. Geol. It., 94, 555-581.
Chopra P.N. & Paterson M.S. 1981. The experimental deformation of dunites. Tectonophysics, 78, 453-473.
—— & —— 1984. The role of water in the deformation of dunite. J. Geophys. Res., 89, 7861-7876.
Cimmino F. & Messiga B. 1979. I calceschisti del Gruppo di Voltri (Liguria Occidentale): le variazioni compositionali delle miche bianche in rapporto alla evoluzione tettonico-metamorfica Alpina. Ofioliti, 4, 269-294.
——, Messiga B., Piccardo G.B. & Zeda O. 1979. Titanian clinohumite-bearing assemblages within antigorite serpentinites of the Gruppo di Voltri (Western Liguria): inferences on the geodynamic evolution of the Piemontese ultramafic section. Ofioliti, 4, 97-120.
Cloetingh S., McQueen S.H. & Lambeck K. 1985. On a tectonic mechanism for regional sealevel variations. Earth Planet. Sci. Lett., 75, 157-66.
—— & Wortel R. & Vlaar N.J. 1982. Evolution of passive continental margins and initiation of subduction zones. Nature, 297, 139-42.
——, —— & —— 1984. Passive margin evolution, initiation of subduction and the Wilson cycle. Tectonophysics, 109, 147-163.
Cohen C.R., Schweickert R.A. & Odom A.L. 1981. Age of emplacement of the Schistes Lustrés nappe, Alpine Corsica. Tectonophysics, 73, 276-284.
Cortesogno L., Di Battisini G., Luchetti G. & Venturelli G. 1979a. Metamorphic assemblages of two high pressure-low temperature ophiolitic units of central-western Liguria: mineralogical and chemical features and tectonic significance. Ofioliti, 4., 121-155.
——, —— & —— 1987. Nota alla "Carta geologica delle ofiolite del Bracco" e ricostruzione paleogeografia Giurassico-Cretacica. Ofioliti, 12, 261-342.
——, ——, —— & Venturelli G. 1978. Le brecce ofiolitiche della Liguria Orientale, nuove dati e discussione sui modelli paleogeografici. Ofioliti, 3, 99-160.
——, Gianelli G. & Piccardo G. 1975. Preorogenic metamorphic and tectonic evolution of the ophiolite mafic rocks (Northern Apennine and Tuscany). Boll. Soc. Geol. It., 94, 291-321.
——, Grandjacquet C. & Haccard D. 1979b. Contribution a l'etude de la liason Alpes-Apennis; evolution tectono-metamorphique des principeaux ensembles ophiolitiques de Ligurie (Apennins du nord). Ofioliti, 4, 157-172.
—— & Haccard D. 1984. Note illustrative alla Carta geologica della zona Sestri-Voltaggio. Mem. Soc. Geol. It., 28, 115-150.
—— & Venturelli G. 1978. Metamorphic evolution of the ophiolitic sequences and associated sediments in the Northern Apennines - Voltri group, Italy. In: Closs H., Roeder D. & Schmidt K. (eds) Alps, Apennines and Hellenides, 253-260.
Coward M.P. 1986. Heterogenous stretching, simple shear and basin development. Earth Planet. Sci.

Lett., 80, 325-236.
—— & Dietrich D. 1989. Alpine tectonics-an overview. In: Coward M.P., Dietrich D. & Park R.G. (eds) Alpine tectonics. Geol. Soc. Spec. Publ., 45, 1-29.
Cundari A. Dal Negro A., Piccirillo E.M., Della Giusta A. & Secco L. 1986. Intracrystalline relationships in olivine, orthopyroxene, clinopyroxene and spinel from a suite of spinel lherzolite xenoliths from Mt. Noorat, Victoria, Australia. Contrib. Mineral. Petrol., 94, 523-532.

Dahlen F.A. 1984. Noncohesive critical Coulomb wedges: an exact solution. J. Geophys. Res., 89, 10125-10133.
D'Antonio D., Gosso G., Messiga B., Scambelluri M. & Tallone S. 1984. Analisi strutturale e ricostruzione lithostratigraphia al margine sud-orientale del Massiccio di Voltri, zona piemontese-ligure, Alpi Liguri. Mem. Soc. Geol. It., 28, 447-460.
Davis D., Suppe J. & Dahlen F.A. 1983. Mechanics of fold and thrust belts and accretionary wedges. J. Geophys. Res., 88, 1153-1172.
Decandia F.A. & Elter P. 1972. La "zona" ofiolitifere del Bracco, nel settore compreso fra Le`vanto e la Val Graveglia. Mem. Soc. Geol. It., 11, 503-530.
Den Tex E. 1969. Origin of ultramafic rocks, their tectonic setting and history: a contribution to the discussion of the paper "The origin of ultramafic and ultrabasic rocks" by P.J. Wyllie. Tectonophysics, 7, 457-488.
Dercourt J., Zonenshain L.P. et al. 1986. Geological evolution of the Tethys Belt from the Atlantic to the Pamirs since the Lias. Tectonophysics, 123, 241-315.
Dewey J.F., 1976. Ophiolite obduction. Tectonophysics, 31, 93-120.
——, Helman M.L., Turco E., Hutton D.H.W. & Knott S.D. 1889. Kinematics of the western Mediterranean. In: Coward M.P., Dietrich D & Park R.G. (eds.) Alpine tectonics, Geol. Soc. Spec. Publ., 45, 265-283.
——, Pitman III W.C., Ryan W.B.F. & Bonnin J. 1973. Plate tectonics and the evolution of the Alpine system. Geol. Soc. Am. Bull., 84, 3137-3180.
Downes H. 1990. Shear zones in the upper mantle - Relation between geochemical enrichment and deformation in mantle peridotites. Geology, 18, 374-377.
Drury M.R., Hoogerduijn Strating E.H. & Vissers R.L.M. 1990. Shear zone structures and microsctructures in mantle peridotites from the Voltri Massif, Ligurian Alps, N.W. Italy. Geol. Mijnbouw, 69, 3-17.
Dunbar J.A. & Sawyer D.S. 1989. How preexisting weaknesses control the style of continental breakup. J. Geophys. Res., 94, 7278-7292.

Ellis D.J.& Green D.H. 1979. An experimental study of the effect of Ca upon garnet-clinopyroxene Fe-Mg exchange equilibria. Contrib. Mineral. Petrol., 71, 13-22.
Elter P. 1972. La zona ofiolitifera del Bracco nel quadro del Appennino settentrionale. 66° Congres Soc. Geol. It., Pisa-Sestri Levante.
—— & Pertusati P. 1973. Considerazione sul limite Alpi-Appennino e sulle sue relazioni con l'arco delle Alpi occidentali. Mem. Soc. Geol. It., 12, 359-375.
—— & Raggi G. 1965. Contributo alla conoscenza dell'Appennino Ligure 3. Tentativo di interpretazione delle brecce ofiolitiche cretacee in relazione con movimenti orogenetici dell' Appennino Ligure. Boll. Soc. Geol. It., 84, 1-14.
Engelder J.T., Logan J.M. & Handin J. 1975. The sliding characteristics of sandstone on quartz fault gouge. Pure Appl. Geophys., 113, 69-86.
Engi M. & Lindsley D.H. 1980. Stability of Titanian-clinohumite: experiments and thermodynamic analysis. Contrib. Mineral. Petrol., 72, 414-424.
England P.C. 1978. Some thermal considerations of the Alpine metamorphism - Past, present and future. Tectonophysics, 46, 21-40.
—— & Wortel R. 1980. Some concequences of the subduction of young slabs. Earth. Planet. Sci. Lett., 47, 403-415.
Ernst, W.G. 1975. Systematics of large-scale tectonics and age progression in Alpine and circum-Pasific blueschist belts. Tectonophysics, 26, 229-246.
—— 1976. Mineral chemistry of eclogites and related rocks from the Voltri Group, Western Liguria, Italy. Schwiez. Mineral. Petrogr. Mitt., 56, 293-343.
—— 1978. Petrochemical study of some lherzolitic rocks from the Western Alps. J. Petrol., 19, 341-392.
—— 1979. Coexisting sodic and calcic amphiboles from high pressure metamorphic belts and the stability

of barroisitic amphibole. Min. Mag., 43, 269-278.
—— 1988. Tectonic history of subduction zones inferred from retrograde blueschist P-T paths. Geology, 16, 1081-1084.
—— & Piccardo G.B. 1979. Petrogenesis of some Ligurian peridotites - I. Mineral and bulk-rock chemistry. Geochim. Cosmochim. Acta, 43, 219-37.
Evans B.W., Johannes J., Oterdoom W.H. & Trommsdorff V. 1976. Stability of chrysotile and antigorite in the serpentinite multisystem. Schweiz. Mineral. Petrogr. Mitt., 56, 79-93.
—— & Trommsdorff V. 1983. Fluorine hydroxyl titanian clinohumite in alpine recrystallized garnet peridotite: compositional controls and petrologic significance. Am. J. Sci., 283A, 355-369.

Fazzuoli M. & Sguazzoni G. 1986. Jurassic and Cretaceous isopic zones in the Tuscan domain. Mem. Soc. Geol. It., 31, 59-84.
Féraud G., Girardeau J., Beslier M.-O. & Boillot G. 1988. Datation 39Ar-40Ar de la mise en place des péridotites bordant la marge de la Galice (Espagne). C. R. Acad. Sci. Paris, 307, 49-55.
Ferrara G., Innocenti F., Ricci C.A. & Serri G. 1977. Ocean-floor affinity of basalts from Apennine ophiolites: geochemical evidence. Chem. Geol., 17, 101-111.
Fontignie D., Delaloye M. & Bertrand J. 1982. Ages radiométriques K/Ar des éléments ophiolitiques de la Nappe des Gêts (Haute-Savoie, France). Eclogea Geol. Helv., 75, 117-126.
Franz G. & Althaus E. 1977. The stability relations of the paragenesis paragonite-zoisite-quartz. N. Jb. Miner. Abh., 130, 159-167.
Frey M., Hunziker J.C., Frank W., Bocquet J., Dal Piaz D.V., Jäger E. & Niggli E. 1974. Alpine metamorphism of the Alps: A review. Schwiez. Min. Petr. Mitt., 54, 247-89.
Forsyth D.W. 1977. The evolution of the upper mantle beneath mid-ocean ridges. Tectonophysics, 38, 89-118.
Fyfe W.S., Price N.J. & Thompson A.B. 1978. Fluids in the earth's crust. Elsevier, Amsterdam, 383 pp.

Galbiati B. 1978. Su alcune significative strutture tettoniche dell'entroterra de Bonassola (Liguria). Atti. Inst. Geol. Univ. Pavia, 27, 69-77.
—— 1985. L'unità del Bracco e il suo ruolo nella paleogeografia liguride cretacica. Atti Inst. Geol. Univ. Pavia, 30, 316-336.
Garfunkel Z. 1988. Relation between continental rifting and uplifting: evidence from the Suez rift and northern Red Sea. Tectonophysics, 150, 33-49.
—— & Derin B. 1984. Permian-early Mesozoic tectonism and continental margin formation in Israel and its implications for the history of the Eastern Mediterranean. In: Dixon J.E. & Robertson A.H.F. (eds) The geological evolution of the eastern Mediterranean. Geol. Soc. Lond. Spec. Publ., 17, 187-201.
Gasanov T.A. 1986. Evolution of the Sevan Akera ophiolite zone, Lesser Caucasus. Geotectonics, 20, 147-156.
Gasparik T. 1984. Two-pyroxene thermobarometry with new experimental data in the system CaO-MgO-Al2O3-SiO2. Contrib. Mineral. Petrol., 87, 87-97.
Gealey W.K. 1988. Plate tectonic evolution of the Mediterranean-Middle East region. Tectonophysics, 155, 285-306.
Gianelli G. & Principi G. 1977. Northern Apennine ophiolite - an ancient transcurrent fault zone. Boll. Soc. Geol. It., 96, 53-8.
Gibbons W. Waters C. & Warburton J. 1986. The blueschist facies schistes lustrés of Alpine Corsica: A review. In: Evans B.W. & Brown E.H. (eds) Blueschists and eclogites, Geol. Soc. Am. Mem., 164, 301-311.
Giese P., Reutter K.J., Jakobshagen V. & Nicolich R. 1982. Explosion seismic crustal studies in the Alpine-Mediterranean region and their implications to tectonic processes. In: Breckhemer H. & Hsü K. (eds) Alpine-Mediterranean geodynamics, AGU, The geodynamics series, 7, 39-73.
Gillcrist R., Coward M. & Mugnier J-L. 1987. Structural inversion and its controls: examples from the Alpine foreland and the French Alps. Geodyn. Acta., 1, 5-34.
Goetze C. & Evans B. 1979. Stress and temperature in the bending lithosphere as constrained by experimental rock mechanics. Geophys. J.R. Astron. Soc., 59, 463-487.
Goffé B. 1984. Le facies a carpholite-chloritoide dans la couverture Briançonnaise des Alpes Ligures: un temoin de l'histoire tectono-metamorphique regionale. Mem. Soc. Geol. It., 28, 461-479.
Görler K. & Ibbeken H. 1963. Die Bedeutung der Zone Sestri-Voltaggio als Grenze zwischen Alpen und Apennin. Geol. Rundsch., 53, 73-84.

Grandjacquet C. & Haccard D. 1977. Position strutturale e role paléogéographique de l'unitá du Bracco au sien de contexte ophiolitique Liguro-Piemontais (Apennin-Italie). Bull. Soc. Géol. France, 19, 901-908.

Green H.W. & Brunley P.C. 1988. Pyroxene-spinel symplectites: Origin by decomposition of garnet confirmed [abstract]. EOS Trans. Am. Geophys. Soc., 69, 1514.

—— & Radcliffe S.V. 1972. Deformation processes in the upper mantle. Geophys. Mon., 16, 139-156.

Gueguen Y. 1977. Dislocations in mantle peridotite nodules. Tectonophysics, 39, 231-254.

Guiraud M., Holland T. & Powell R. 1990. Calculated mineral equilibria in the greenschist-blueschist-eclogite facies in the Na_2O-FeO-SiO_2-H_2O: Methods, results and geological applications. Contrib. Minral. Petrol., 104, 85-98.

Haccard D. & Lorenz C. 1979. Les déformations de l'Eocène supérieure au Stampanien de la terminasion septentrionale de la zone de Sestri-Voltaggio. Bull. Soc. Géol. France, 21, 401-413.

Halbach H. & Chatterjee N.D. 1982. An empirical Redlich-Kwong-type equetion of state for water to 1000°C and 200 kbar. Contrib. Mineral. Petrol., 79, 337-345.

Hamelin B. & Allègre C.J. 1988 Lead isotope study of orogenic lherzolite massifs. Earth Planet. Sci. Lett., 91, 117-131.

Handy M.R. 1989. Deformation regimes and the rheological evolution of fault zones in the lithosphere: the effects of pressure, temperature, grain size and time. Tectonophysics, 163, 119-152.

Harland W.B., Llewellyn P.G., Pickton C.A.G., Smith A.G. & Waters R. 1982. A Geological Timescale. Cambridge Univ. Press, 131 pp.

Harper G.D. 1988. Episodic magma chambers and amagmatic extension in the Josephin ophiolite. Geology, 16, 831-834.

Harris B.L. 1985. Direction changes in thrusting the Schistes Lustrés in Alpine Corsica. Tectonophysics 120, 37-56.

Hébert R., Serri G. & Hékinian R. 1989. Mineral chemistry of ultramafic tectonites and ultramafic to gabbroic cumulates from major oceanic basins and the Northern Apennine ophiolites (Italy) - A comparison. Chem. Geol., 77, 183-207.

Helgeson H.C., Delany J.M., Nesbitt H.W. & Bird D.K. 1978. Summary and critique of the thermodynamic properties of rock-forming minerals. Am. J. Sci., 278A, 229 pp.

Hill K.C. & Hayward A.B. 1988. Structural constraints on the tertiary plate tectonic evolution of Italy. Mar. Petrol. Geol., 5, 2-16.

Holland T.J.B. 1980. The reaction albite = jadite + quartz determined experimentally in the range 600-1200°C. Am. Mineral., 65, 129-134.

—— 1983. The experimental determination of activeties in disordered and short-range ordered jadeitic pyroxenes. Contrib. Mineral. Petrol., 82, 214-220.

Hoogerduijn Strating E.H. 1988. High temperature shear zones in the gabbroic Bracco Massif (northern Apennines, Italy) - Implications for models of ocean floor generation. Ofioliti, 13, 111-126.

—— 1989. Development of tectonostratigraphic terrains along extensional margins in the Alps-Apennine system (Abstract). Terra Abstracts, 1, 58.

—— 1990. Folding of oceanic lithosphere in the Piemonte-Ligurian ocean. Geol. Mijnbouw, 69, 31-41.

——, Drury M.R., Vissers R.L.M. & Van der Wal D. 1989. The uplift history of mantle peridotites during whole-lithosphere extension, Voltri Massif, North Italy (Abstract). Terra Abstracts, 1, 258.

—— & Vissers R.L.M. 1990. Dehydration-induced fracturing of eclogite-facies peridotites a possible mechanism for small, shallow-focus earthquakes insubduction zones. Tectonophysics, submitted.

——, Piccardo G.B., Rampone E., Scambelluri M. & Vissers R.L.M., 1990. The structure and petrology of the Erro-Tobbio peridotite (Voltri Massif, Ligurian Alps): a two days excursion with emphasis on processes in the upper mantle. Ofioliti, 15, 119-184.

—— & Van Wamel W.A. 1989. The structure of the Bracco ophiolite complex (Ligurian Apennines, Italy) - A change from Alpine to Apennine polarity. J.Geol.Soc. Lond., 146, 933-944.

Hoscheck G. 1969. The stability of staurolite and chloritoid and their significance in metamorphism of pelitic rocks. Contrib. Mineral. Petrol., 22, 208-232.

Hunziker J.C. 1974. Rb-Sr and K-Ar age determination and the Alpine tectonic history of the western Alps. Mem. Inst. Geol. Min. Univ. Padova, 31, 1-54.

——, Desmons J. & Martinotti G. 1989. Alpine thermal evolution in the central and western Alps. In: Coward M., Dietrich D. & Park R.G. (eds) Alpine tectonics. Geol. Soc. Spec. Publ., 45, 353-367.

—— & Martinotti G. 1984. Geochronology and evolution of the western Alps: a review. Mem. Soc. Geol. It., 29, 43-56.

Hynes A. 1990. Two-stage rifting of Pangea by two different mechanisms. Geology, 18, 323-326.

Ibbeken H., Marini M., Schleyer R. & Tongiorgi M. 1984. Nuovi dati su elementi ad affinità brianzonese ligure interna nella zona Sestri-Voltaggio. Mem. Soc. Geol. It., 28, 481-486.
Ishiwatari A. 1985. Alpine ophiolites: product of low-degree mantle melting in a Mesozoic transcurrent rift zone. Earth Planet. Sci. Lett., 76, 93-108.
Issler D., McQueen H. & Beaumont C. 1989. Thermal and isostatic consequences of simple shear extension of the continental lithosphere. Earth Planet. Sci. Lett., 91, 341-358.

Jean S., Kerckhove C., Perriaux J. & Ravenne C. 1985. Un modele paleogene de bassin a turbidites: Les Gres d'Annot du NW du Massif de l'Argentera-Mercantour. Géologie Alpine, 61, 115-143.
Jenkins D.M. 1983. Stability and composition relations of calcic amphiboles in ultramafic rocks. Contrib. Mineral. Petrol., 83, 375-384.
Johannes W. & Puhan D. 1971. The calcite-aragonite transition reinvestigated. Contrib. Mineral. Petrol., 31, 28-38.
Jolivet L., Huchon P. & Rangin C. 1989. Tectonic setting of Western Pacific marginal basins. Tectonophysics, 160, 23-47.
Jordan P.G. 1987. The deformational behaviour of bimineralic limestone-halite aggregates. Tectonophysics, 135, 185-197.
—— 1988. The rheology of polymineralic rocks - an approach. Geol. Rundsch., 77, 285-294.

Kanamori H. 1986. Rupture process of subduction-zone earthquakes. Ann. Rev. Earth Planet. Sci., 14, 293-322.
Karato S.I., Paterson M.S. & Fitzgerald J.D. 1986. Rheology of synthetic olivine aggregates: Influence of grainsize and water. J. Geophys. Res., 91, 8151-8176.
——, Toriumi M. & Fujii T. 1980. Dynamic recrystallisation of olivine single crystals during high temperature creep. Geophys. Res. Lett., 7, 649-652.
Kastens K., Mascle J. et al. 1988. ODP Leg 107 in the Tyrrhenian Sea: insights into passive margin and back arc evolution. Geol. Soc. Am. Bull., 100, 1140-1156.
Kelts K. 1981. A comparison of some aspects of sedimentation and translational tectonics from the Gulf of California and the Mesozoic Tethys, Northern Penninic Margin. Eclogea Geol. Helv. 74, 317-338.
Kerrich R., La Tour T.E. & Willmore L. 1984. Fluid participation in deep fault zones: Evidence from geological, geochemical and $^{18}O/^{16}O$ relations. J. Geophys. Res., 89, 4331-4343.
Kienast J.R. & Pognante U. 1988. Chloritoid-bearing assemblages in eclogitized metagabbros of the Lanzo peridotite body (western-Italian Alps). Lithos, 21, 1-11.
Kirby S.H. 1985. Rock mechanics observations pertinent to the rheology of the continental lithosphere and the localisation of strain along shear zones. Tectonophysics, 119, 1-27.
Klemperer S.L. 1988. Crustal thinning and nature of extension in the northern North Sea from deep seismic reflection profiling. Tectonics, 7, 803-822.
Knipper A., Ricou L.-E. & Dercourt J. 1986. Ophiolites as indicators of the geodynamic evolution of the Tethyan ocean. Tectonophysics, 123, 213-240.
Koons P.O. 1986. Relative geobarometry for high pressure rocks of quartzo feldspatic composition from the Sezia Zone, Western Alps, Italy. Contrib. Mineral. Petrol., 93, 322-334.
Kusznir N.J. & Park R.G. 1987. The extensional strength of the continental lithosphere: its dependence on geothermal gradient, and crustal composition and thickness. In: Coward M.P., Dewey J.F. & Hancock, P.L. (eds), Continental extensional tectonics. Geol. Soc. Spec. Publ., 28, 35-52.

Lacassin R. 1989. Plate-scale kinematics and the compatibility of crustal shear zones in the Alps. In: Coward M.P. & Dietrich D. (eds) Alpine tectonics, Geol. Soc. Spec. Publ., 45, 339-352.
Lagabrielle Y. & Cannat M. 1990. Alpine Jurassic ophiolites resemble the modern central atlantic basemnet. Geology, 18, 319-322.
Latin D. & White N. 1990. Generating melt during lithospheric extension: Pure shear vs. simple shear. Geology, 18, 327-331.
Laubscher H.P. 1971. The large-scale kinematics of the western Alps and northern Apennines and its palinspastic implications. Am. J. Sci. 271, 193-226.
—— 1988. The arcs of the western Alps and northern Apennines: an updated review. Tectonophysics 146, 67-78.

—— & Bernoulli D. 1977. Mediterranean and Tethys. In: Nairn A.E.M., Kanes W.H. & Stehli F.G. (eds) The ocean basin and margins, 4A, The Eastern Mediterranean. Plenum Press, New York, 1-28.
Lawn B.R. & Wilshaw T.R. 1975. Fracture of brittle solids. Cambridge University Press, 204 pp.
Lemoine M. 1983. Rifting and early drifting: Mesozoic central Atlantic and Ligurian Tethys. Init. Repts. DSDP, 76, 885-895.
——, Bas T., Arnaud-Vanneau A., Arnaud H., Dumont T., Gidon M., Bourbon M., de Graciansky P.C., Rudkiewicz J.L. & Tricart P. 1986. The continental margin of the Mesozoic Tethys in the Western Alps. Marine Petrol. Geol., 3, 178-199.
——, Tricart P. & Boillot G. 1987. Ultramafic and gabbroic ocean floor of the Ligurian Tethys (Alps, Corsica, Apennines): in search of a genetic model. Geology, 15, 622-625.
—— & Trümpy R. 1987. Pre-oceanic rifting in the Alps. Tectonophysics, 133, 305-20.
LePichon X. & Barbier F 1987. Passive margin formation by low-angle faulting within the upper crust: the northern Bay of Biscay margin. Tectonics, 6, 133-150.
Le Pichon X., Sibuet J.C. & Francheteau J. 1977. The fit of the continents around the North Atlantic ocean. Tectonophysics, 38, 169-209.
Liou J.G. 1971. Analcime equilibria. Lithos, 4, 389-402.
——, Kim H.S. & Maruyama S. 1983. Prehnite-epidote equilibria and their petrologic application. J. Petrol., 24, 321-342.
Lister G.S., Etheridge M.A. & Symonds P. 1986. Detachment faulting and the evolution of passive continental margins. Geology,14, 246-50.
—— & Snoke A.W. 1984. S-C mylonites. J. Struct. Geol., 6, 617-38.
Lombardo B. & Pognante U. 1982. Tectonic implications in the evolution of the western Alps ophiolite metagabbros. Ofioliti, 7, 371-394.
Lorenz C.R. 1969. Contribution à l'étude stratigraphique de l'Oligocène et du Miocène inférieur des confins liguro-piemontais (Italie) Atti Inst. Geol. Univ. Genova, 6, 235-888.
Loubet M. & Allègre C.J. 1982. Trace elements in oropgenic lherzolites reveal the complex history of the upper mantle. Nature, 298, 809-814.
Lowrie W. 1986. Paleomagnetism and the Adriatic promontory: a reappraisal. Tectonics, 5, 797-807.
Lynch H.D. & Morgan P. 1987. The tensile strength of the lithosphere and the localization of extension. In: Coward, M.P., Dewey, J.F. & Hancock, P.L. (eds) Continental extensional tectonics. Geol. Soc. Spec. Publ, 28, 53-65.

Maluski H. 1977. Aplication de la méthode 40Ar-39Ar aux minéraux des roches cristallines pertubées par des événements thermiques et tectoniques en Corse. PhD thesis, University of Montpellier, 113 pp.
Mange-Rajetzky M. & Oberhänsli R. 1982. Detrial lawsonite and blue sodic amphibole in the Molasse of Savoy, France and their significance in assessing Alpine evolution. Schweiz. Mineral. Petrogr. Mitt., 62, 415-436.
Maresch W.V. 1977. Experimental studies on glaucophane: an analysis of present knowledge. Tectonophysics, 43, 109-125.
Marini M. 1982. Distinzione di tre diverse serie-tipo nell'unita carbonatica della Zona Sestri-Voltaggio (Appennino settentrionale). Boll. Soc. Geol. It., 101, 17-26.
—— 1984. Il quadro deformativo del setore ligure della zone Sestri-Voltaggio con particolare riguardo alle strutture a granda scala. Mem. Soc. Geol. It., 28, 519-536.
—— 1988. Evoluzione tettonico-sedimentaria e geodynamica dei Flysch Cretacico-Eocenici della Liguria occidentale. Boll. Soc. Geol. It., 107, 193-218.
—— 1989. Lithostratigrafia e assetto strutturale delle Valpolcevera (Appennino ligure): revisione, nuovi dati e nuovi prospettive. Gior. Geol., 51, 1-14.
Marroni M., Della Croce G. & Meccheri M. 1988. Structural evolution of the Mt. Gottero Unit in the Mt. Zatta - Mt. Ghiffi sector (Ligurian-Emilian Apennines). Ofioliti, 13, 269-242.
Martini IP, Rau A. & Tongiorgi M. 1986. Syntectonic sedimentation in a middle Triassic rift, Northern Apennines, Italy. Sedim. Geol., 47, 191-219.
Massonne H.-J. & Schreyer W. 1987. Phengite geobarometry based on the limiting assemblage with K-feldspar, phlogopite and quartz. Contrib. Mineral. Petrol., 96, 212-224.
Matter A., Homewood P., Caron C., Rigassi D., van Stuijvenbergen J., Weidmann M. & Winkler M. 1980. Flysch and molasse of western and central Switzerland - Excursion 5. In: Schweiz. Geol. Komm. (edt). Geology of Switzerland, a guide book, part B: Geologic excursions, 216-269.
McAdoo D.C. & Sandwell D.T. 1985. Folding of oceanic lithosphere. J. Geophys. Res., 90, 8563-69.

——, —— & Turcotte D.L. 1978. On the elastic-perfectly plastic bending of the lithosphere under generalized loading with application to the Kuril trench. Geophys. J. R. astr. Soc., 54, 11-26.
McKenzie D. 1978. Some remarks on the development of sedimentary basins. Earth Planet. Sci. Lett., 40, 25-32.
—— 1984. The generation and compaction of partially molten rock. J. Petrol., 25, 713-765.
Meccheri M., Marroni M., Casella A., della Croce G. & Sergiampietri L. 1986. L'unità de Colli/Tavarone nel quadro dell evoluzione stratigrafica e strutturale del domino ligure (alta Val di Vara, Appennino settentrionale). Ofioliti, 11, 275-292.
Mercier J.-C.C. 1980 Single pyroxene thermobarometry. Tectonophysics, 70, 1-37.
——, Benoit V. & Girardeau J. 1984. Equilibrium state of diopside-bearing harzburgites from ophiolites: geobarometric and geodynamic implications. Contrib, Mineral. Petrol., 85, 391-403.
Messiga B. 1987. Alpine metamorphic evolution of Ligurian Alps (North-West Italy): chemography and petrological constraints inferred from metamorphic climax assemblages. Contrib. Mineral. Petrol., 95, 269-277.
—— & Piccardo G.B. 1974. Rilevamento geo-petrografico e strutturale del Gruppo di Voltri. Il settore nord-orientale: la zona fra M. Tacco e M. Orditano. Mem. Soc. Geol. It., 13, 301-15.
——, —— & Ernst W.G. 1983. High-pressure eo-alpine parageneses developed in magnesian metagabbros, Gruppo di Voltri, Western Liguria, Italy. Contrib. Mineral. Petrol., 83, 1-15.
——, ——, Rampone E. & Scambelluri M. 1989. Primary characters and high-pressure metamorphic evolution of the subducted oceanic lithosphere of the Voltri Massif (Ligurian Alps - Northern Italy). Ofioliti, 14, 157-175.
Mitchell A.H.G. 1986. Ophiolite detachment related to syn-collision thrusting. J. Geodynamics, 5, 257-274.
Mitrovica J.X., Beaumont C. & Javis G.T. 1989. Tilting of continental interiors by the dynamic effects of subduction. Tectonics, 8, 1079-1094.
Molnar P. & Gray D. 1979. Subduction of continental lithosphere: Some constraints and uncertainties. Geology, 7, 58-62.
Monechi S.& Treves B. 1984. Osservazioni sulle età delle arenarie del Gottero: Dati del nanoplancton calcareo. Ofioliti, 9, 93-96.
Montanari S.L. & Rossi M. 1982. Evoluzione dell' unità stratigrafico-strutturale terziarie del Nord Appennino: 1. l'unità di Canetolo. Boll. Soc. Geol. It., 101, 275-289.
Moody J.B., Meyer D. & Jenkins J.E. 1983. Experimental characterization of the greenschist-amphibolite boundary in mafic systems. Am. J. Sci., 283, 48-92.
Moores E.M. 1982. Origin and emplacement of ophiolites. Rev. Geophys. Space Phys., 20, 735-60.
Morelli G., Giese P., Hirn A., Colombi B., Eva C., Guerra I., Letz H., Nicolich R., Reichert C., Scarascia S. & Wigger P. 1977. Seismic investigations of crustal and upper mantle structure of the Northern Apennines and Corsica. In: Biju-Duval B. & Montadert L. (eds) International symposium on the structural history of the Mediterranean basins, Editions Technip, Paris, 281-286.
Morgan W.J. 1981. Hotspot tracks and the opening of the Atlantic and Indian ocean. In. Emiliani C. (edt) The Sea, 7, John Wiley, New York, 443-487.
Murphy D.C. 1989. Crustal paleorheology of the southeastern Canadian Cordillera and its influence on the kinematics of Jurassic convergence. J. Geophys. Res., 94, 15723-15739.
Murrell S.A.F. & Ismail I.A.H. 1976. The effect of decomposition of hydrous minerals on the mechanical properties of rock. Tectonophysics, 31, 207-258.
Mutter J.C., Larson R.L. & Northwest Australia Study Group 1989. Extension of the Exmouth Plateau, offshore northwestern Australia: Deep seismic reflection/refraction evidence for simple and pure shear mechanisms. Geology, 17, 15-18.

Nicolas A. 1986a. Structure and petrology of peridotites: Clues to their geodynamic environment. Rev. Geophys., 24, 875-895.
—— 1986b. A melt extraction model based on structural studies in mantle peridotites. J. Petrol., 27, 999-1022.
—— 1989. Structures of ophiolites and dynamics of oceanic lithosphere. Petrology and Structural Geology, 4, Kluwer Academic Publishers, 367 pp.
——, Bouchez J.L., Boudier F. & Mercier J.C. 1971 Textures, structures and fabrics due to solid state flow in some European lherzolites. Tectonophysics, 12, 65-68.
Nitsch K.H. 1971. Stabilitätsbeziehungen von Prehnit- und Pumpellyit-haltige Paragenesen. Contrib. Mineral. Petrol., 30, 240-260.

Norrell G.T. & Harper G.D. 1988. Detachment faulting and amagmatic extension at mid oceanic ridges: the Josephine ophiolite as an example. Geology, 16, 827-830.
——, Teixell A. & Harper G.D. 1989. Microstructure of serpentinite mylonites from the Josephine ophiolite and serpentinization in retrogressive shear zones, California. Geol. Soc. Am. Bull., 101, 673-682.

Oba T. 1980. Phase relations in the Tremolite-Pargasite join. Contrib. Mineral. Petrol., 71, 247-256.
Obata M. 1980. The Ronda peridotite: Garnet-, spinel- and plagioclase-lherzolite facies and the P-T trajectory of a high temperature mantle intrusion. J. Petrol., 21, 533-572.
Oberhänsli R., Hunziker J.C., Martinotti G. & Stern W.B. 1985. Geochemistry, geochronology and petrology of Monte Mucrone: An example of Eo-Alpine eclogitization of Permian granitoids in the Sesia-Lanzo Zone, Western Alps, Italy. Chem. Geol., 52, 165-184.
Ohnaka M. 1973. The quantintative effect of hydrostatic confining pressure on the compressive strength of crystalline rocks. J. Phys. Earth., 21, 125-140.
Ohnenstetter M. 1979. La série ophiolitifère de Rospigliani (Corse) est-elle un témoin des phénomènes tectoniques, sédimentaires et magmatiques liés au fonctionnement des zones transformante? C. R. Acad. Sc. Paris, 289, D, 1199-1202.
Ord A. & Hobbs B.E. 1989. The strength of the continental crust, detachment zones and the development of plastic instabilities. Tectonophysics, 158, 269-289.
Oterdoom W.H. 1978. Tremolite and diopside bearing serpentinite assemblages in the CaO-MgO-SiO_2-H_2O multisystem. Schweiz. Mineral. Petrogr. Mitt., 58, 127-138.
Ottonello G., Joron J.L. & Piccardo G.B. 1984. Rare earth and 3d transition element geochemistry of peridotitic rocks: II. Ligurian peridotites and associated basalts. J. Petrol., 25, 373-393.
——, Piccardo G.B. & Ernst W.G. 1979. Petrogenesis of some Ligurian peridotites - II. Rare earth element chemistry. Geochim. Cosmochim. Acta, 43, 1273-1284.
Oxburgh E.R. & England P.C. 1980. Heat flow and metamorphic evolution of the eastern Alps. Eclog. Geol. Helv., 73, 379-398.

Page R.A., Stephens C.D. & Lahr J.C. 1989. Seismicity of the Wrangell and Aleutian Wadati-Benioff zones and the North American plate along the Trans-Alaska Crustal Transect, Chugach Mountains and Copper River Basin , Southern Alaska. J. Geophys. Res., 94, 16059-16082.
Passchier C.W. & Simpson C. 1986. Porphyroclast systems as kinematic indicators. J. Struct. Geol., 8, 831-43.
Passeri L. 1984. Le successioni Triassico-Giurassische dell'Appennino Settentrionale e delle Alpi Liguri nel quadro dell'evoluzione preoceanica della Tetide Occidentale. Mem. Soc. Geol. It., 28, 353-369.
Perchuk L.L. & Aranovich M.A. 1980. The thermodynamic regime of metamorphism in the ancient subduction zone. Contrib. Mineral. Petrol., 75, 407-414.
Pertusati P.C. & Horrenberger J.C. 1976. Studio strutturale degli scisti di Val Lavagna (Unità del Monte Gottero, Appennino ligure). Boll. Soc. Geol. It., 94, 1375-1436.
Philippot P. 1987. "Crack-seal" vein geometry in eclogitic rocks. Geodyn. Acta, 1, 171-181.
Piccardo G.B. 1976. Petrologia del massiccio di Suvero (La Spezia). Ofioliti, 1, 279-318.
——, Cortesogno L., Messiga B., Galli M. & Pedemonte G.M. 1977. Excursion to the metamorphic ophiolites of the Gruppo di Voltri - guide book. Rend. Soc. Ital. Min. Petr., 33, 295-314.
——, Messiga B. & Cimmino F. 1980. Antigoritic serpentinites and rodingites of the Voltri Massif: some petrological evidence for their evolution. Ofioliti, 5, 11-114.
——, —— & Mazzucotelli A. 1979. Chemical petrology and geodynamic evolution of the ophiolitic metavolcanites (prasinites) from the Voltri Massif Piemontese ophiolite nappe (western Liguria, Italy). Ofioliti, 4, 373-402.
——, —— & Vannucci, R. 1988 The Zabargad peridotite-pyroxenite association: petrological constraints on its evolution, Tectonophysics, 150, 135-162.
——, Rampone E. and Scambelluri M. 1988. The Alpine evolution of the Erro-Tobbio peridotites (Voltri Massif - Ligurian Alps): some field and petrographic constraints. Ofioliti, 13, 169-174.
——, —— & Vanucci R. 1990. Upper mantle evolution during continental rifting and oceanization: evidence from the Alpine-Apennine system and modern oceans. Proceedings of the meeting "Deep structure of the Alps", Paris 12-13 December 1988, Mem. Soc. Géol. France, 156, in press.
Pitman W.C. & Talwani M. 1972. Sea floor spreading in the North Atlantic. Geol. Soc. Am. Bull., 83, 619-649.

Platt J.P. 1986. Dynamics of orogenic wedges and the uplift of high-pressure metamorphic rocks. Geol. Soc. Am. Bull., 97. 1037-1053.
——, Behrmann J.H., Cunningham P.C., Dewey J.F., Helman M., Parish M., Shepley M.G., Wallis S. & Weston P.J., 1989. Kinematics of the Alpine arc and the motion history of Adria. Nature, 337, 158-161.
—— & Vissers R.L.M. 1980. Extensional structures in anisotropic rocks. J. Struct. Geol., 2, 397-410.
Pognante U. 1981. Magmatic and metamorphic evolution of two Fe-Ti gabbroic series from the Piemonte Ophiolite Nappe in the Susa Valley area, Italian Western Alps. Mem. Sci. Geol. Pavia, 35, 21-34.
—— 1985. Coronitic reactions and ductile shear zones in eclogitic ophiolitie metagabbros, Western Alps, Italy. Chem. Geol., 50, 99-109.
——, Perotto A., Salino C. & Toscani L. 1986. The ophiolite peridotites of the western Alps: record of the evolutiuon of a small oceanic-type basin in the Mesozoic Tethys. TMPM Tschermaks Min. Petr. Mitt., 35, 47-65.
Polvé M. & Allègre C.J. 1980. Orogenic lherzolite complexes studied by 87Rb-87Sr: a clue to understand the mantle convection processes. Earth Planet. Sci. Lett., 51, 71-93.
Price R.A. 1973. Large-scale gravitational flow of supracrustal rocks, Southern Canadian Rockies. In: De Jong K.A. & Scholten R. (eds) Gravity and tectonics. New York, Wiliey, 491-502.
Principi G. & Treves B. 1984. Il sistema Corso-Appenninico come prisma d'accrezione - Riflessi sul problema generale del limite Alpi-Appennini. Mem. Soc. Geol. It., 28, 549-576.

Quick, J.A., 1981. The origin and significance of large tabular dunite bodies in the Trinity peridotite, Northern California. Contrib. Mineral. Petrol., 78, 413-422.
Quinlan G.M. & Beaumont G. 1984. Appalachian thrusting, lithospheric flexure and the Paleozoic stratigraphy of the Eastern Interior of North America. Can. J. Earth Sci., 21, 973-996.

Raleigh C.B. & Paterson M.S. 1965. Experimental deformation of serpentinite and its tectonic implications. J. Geophys. Res., 70, 3965-3985.
Ramsay J.G. 1967. Folding and fracturing of rocks. McGraw-Hill, New York, 568 pp.
—— 1980. The crack-seal mechanism of rock deformation. Nature, 284, 135-139.
Ranalli G. & Murphy D.C. 1987. Rheological stratification of the lithosphere. Tectonophysics, 132, 281-295.
Reston T.J. 1990 Mantle shear zones and the evolution of the North Sea basin. Geology, 18, 272-275.
Reutter K.J., Günther K. & Groscurth J. 1978. An approach to the geodynamics of the Corsica-Northern Apennines double orogene. In: Closs H., Roeder D. & Schmidt K. (eds) Alps, Apennines and Hellenides, 299-311.
Roux M., Bourseau J.-P., Bas T., Dumont T., de Graciansky P.-C., Lemoine M. & Rudkiewicz J.-L. 1988. Bathymetric evolution of the Tethyan margin in the Western Alps (data from stalked crinoids): a reappraisal of eustatism problems during the Jurassic. Bull. Soc. Geol. France, 8 (IV), 633-41.
Rowley D.B. & Sahagian D. 1986. Depth-dependent stretching: A different approach. Geology, 14, 32-35.
Rubie D.C. 1983. Reaction-enhanced ductillity: the role of solid-solid univariant reactions in deformation of the crust and mantle. Tectonophycs, 96, 331-352.
Rudkiewicz J.-L. 1988. Quantitative subsidence and thermal structure of the European margin of the Tethys during early and middle Jurassic times in the Western Alps (Grenoble-Briançon transect). Bull. Soc. Géol. France, 8, 623-632.
Ruppel C., Royden L. & Hodges K.V. 1988. Thermal modelling of extensional tectonics: application to pressure-temperature-time histories of metamorphic rocks. Tectonics, 7, 947-957.
Rutter E.H. & Brodie K.H. 1988a. Experimental "syntectonic" dehydration of serpentinite under conditions of controlled pore water pressure. J. Geophys. Res., 93, 4907-4932.
—— & —— 1988b. The role of tectonic grain size reduction in the rheological stratification of the lithosphere. Geol. Rundsch., 77, 295-308.

Sachtleben Th. & Seck H.A. 1981. Chemical control of Al-solubility in orthopyroxenes and its implications on pyroxene geothermometry. Contrib. Mineral. Petrol., 78, 157-165.
Sagri M. & Marri C. 1980. Paleobatimetria e ambiente di deposizione delle unità torbiditiche Cretaceo-Superiori dell'Appennino Settentrionale. Mem. Soc. Geol. It., 21, 231-240.
Savostin L.A., Sibuet J.-C., Zonenshain L.P., LePichon X. & Roulet M.J. 1986. Kinematic evolution of the Tethys belt from the Atlantic Ocean to the Pamirs since the Triassic. Tectonophysics, 123, 1-35.

Sawyer D.S. 1985. Brittle failure in the upper mantle during extension of continental lithosphere. J. Geophys. Res., 90, 3021-3025.
Scambelluri M. 1987. New microstructural and mineral chemistry data on retrograde post-eclogitic assemblages from the Voltri Massif, Ligurian Alps. Ofioliti 12, 415-418.
——, Hoogerduijn Strating E.H., Piccardo G.B., Vissers R.L.M. & Rampone E. 1990. Alpine olivine- and titanian clinohumite-bearing assemblages in the Erro-Tobbio peridotite. J. Metam. Geol., 8, in press.
Schamel S. 1974. Eocene subduction in central Liguria, Italy. PhD Thesis, Yale University, 167 pp.
Schmidt S.M. 1982. Laboratory experiments on rheology and deformation mechanisms in calcite rocks and their application to studies in the field. Mitt. Geol. Inst. ETH Zurich, 241, 106 pp.
Schneider J. 1934. Das Grenzgebiet von Alpen und Apennin. Abh. Ges. Wiss. Göttingen, Math.-Phys. Kl., III, 14.
Sengör A.M.C. & Burke K. 1978. Relative timing of rifting and volcanism on earth and its tectonic implications. Geophys. Res. Lett., 5, 419-421.
Serri G. 1981. The petrochemistry of ophiolite gabbro complexes: A key for the classification of ophiolites into low-Ti and high-Ti types. Earth Planet. Sci. Lett., 52, 203-212.
Shelton G. & Tullis J.A. 1981. Experimental flow laws for crustal rocks. EOS Trans. Amer. Geophys. Union, 62, 396.
Sheridan R.E. 1988. Recent drilling results document pulsating tectonics as the control of breakup and paleoceanography between Africa and North America. J. African Earth Sci., 7, 325-343.
Smith A.G. 1982. Tectonic syntheses of the Alpine-Mediterranean region: a review. In: Berckhemer H. & Hsü K. (eds.) Alpine-Mediterranean geodynamics. Geodyn. Ser. Am. Geophys. Union, 7, 15-38.
Smith D. 1977. The origin and interpretation of spinel-pyroxene clusters in peridotite. J. Geol., 85, 476-482.
Srivastava S.P., Schouten H., Roest W.R., Klitgord K.D., Kovacs L.C., Verhoef J. & Macnab R. 1990. Iberian plate kinematics: a jumping plate boundary between Eurasia and Africa. Nature, 344, 756-759.
Stockmal G.S., Beaumont C. & Boutilier R. 1986. Geodynamic models of convergent margin tectonics: transition from rifted margin to overthrust belt and concequences for foreland basin development. Am. Assoc.Petrol. Geol., 70, 181-190.

Takahashi E. & Kushiro I. 1983. Melting of a dry peridotite at high pressures and basalt magma genesis. Am. Mineral., 68, 859-879.
Tatsumi Y., Otofuji Y.-I., Matsuda T. & Nohda S. 1989. Opening of the Sea of Japan back-arc basin by asthenospheric injection. Tectonophysics, 166, 317-329.
Thompson A.B. & England P.C. 1984. Pressure-temperature-time paths of regional metamorphism II. Their inference and interpretation using mineral assemblages in metamorphic rocks. J. Petrol., 25, 929-955.
Treves B. 1984. Orogenic belts as accretionary prisms: The example of the Northern Apennines. Ofioliti, 9, 577-618.
Trommsdorff V. & Evans B.W. 1980. Titanian hydroxyl-clinohumite: formation and breakdown in antigorite rocks (Malenco, Italy). Contrib. Mineral. Petrol., 72, 229-242.
Trümpy R. 1980. An outline of the geology of Switzerland, Part A.105 pp.
—— 1982. Alpine paleogeography: a reappraisal. In: Hsü K.J. (edt.) Mountain building processes,149-156.
—— 1988. A possible Jurassic-Cretaceous transform system in the Alps and the Carpathians. Geol. Soc. Am. Spec. Paper, 218, 93-109.

Van den Berg J. 1983. Reappraisal of paleomagnetic data from Gargano (Southern Italy. Tectonophysics, 98, 29-41.
Van den Beukel J. 1990. Breakup of young oceanic lithosphere in the upper part of subduction zone: Implications for the emplacement of ophiolites. Tectonics, 9, 825-844.
—— 1991. Some thermo-mechanical aspects of the subduction of continental lithosphere. Tectonics, submitted.
—— & Wortel R. 1988. Thermo-mechanical modelling of arc-trench regions. Tectonophysics, 154, 177-193.

Van der Wal, D., Drury M.R. & Vissers, R.L.M., 1991. Oblique fabrics in Alpine-type peridotite tectonites: a shear sense indicator for upper mantle flow. J. Struct. Geol. submitted.
Vanossi M., Cortesogno L., Galbiati B., Messiga B., Piccardo G. & Vannucci R. 1984. Geologia delle Alpi Liguri: dati, problemi, ipotesi. Mem. Soc. Geol. It., 28, 5-57.
Van Wamel W.A. 1987. On the tectonics of the Ligurian Apennines (northern Italy). Tectonophysics, 142, 87-98.
——, Bons A.J., Franssen R.C.M.W., Van Lingen W., Postuma W. & Van Zutphen A.C.A. 1985. A structural geologic traverse through the Northern Apennines from Rapallo to Betola (N. Italy). Geol. Mijnbouw, 64, 181-197.
Van Zutphen A.C.A., Van Wamel W.A. & Bons A.J. 1985. The structure of the Lavagna Nappe in the region of the Monte Ramaceto and Val Graveglia (Ligurian Apennines, Italy). Geol. Mijnbouw, 64, 373-384.
Vlaar N.J. 1983. Thermal anomalies and magmatism due to lithospheric doubling and shifting. Earth Planet. Sci. Lett., 65, 322-330.
—— & Cloetingh S.A.P.L. 1984. Orogeny and ophiolites: Plate tectonics revisited with reference to the Alps. Geol. Mijnb., 63, 159-164.
Voggenreiter W., Hötzl H. & Mechie J. 1988. Low-angle detachment origin for the Red Sea rift system? Tectonophysics, 150, 51-75.

Warner M. & McGeary S. 1987. Seismic reflection coefficients from mantle fault zones. Geophys. J. R. Astr. Soc., 89, 223-30.
Watts A.B., Weissel J.K. & Larson R.L. 1977, Sea-floor spreading in marginal basins of the western Pacific. Tectonophysics, 37, 167-181.
Weissert H.J. & Bernoulli D. 1985. A transform margin in the Mesozoic Tethys: evidence from the Swiss Alps. Geol. Rundsch., 74, 665-679.
Wells P.R.A. 1977. Pyroxene thermometry in simple and complex systems. Contrib. Mineral. Petrol., 62, 129-140.
Wernicke B. 1985. Uniform sense normal simple shear of the continental lithosphere. Can. J. Earth Sci., 22, 108-125.
White S.H. & Knipe R. 1978. Transformation- and reaction-enhanced ductility in rocks. J. Geol. Soc. Lond., 135, 513-516.
Winterer E.L. & Boselini A. 1981. Subsidence and sedimentation on the Jurassic passive continental margin, Southern Alps, Italy. Am. Assoc. Petr. Geol. Bull., 65, 394-421.
Wood B.J. & Banno S. 1973. Garnet-orthopyroxene and orthopyroxene-clinopyroxene relations in simle and complex systems. Contrib. Mineral. Petrol., 42, 109-124.
Wortel M.J.R. 1980. Age-dependent subduction of oceanic lithosphere. PhD diss. University of Utrecht, 147 pp.
Wyllie P.J. 1979. Magmas and volatile components. Am. Mineral., 64, 469-500.

Zuber M.T. 1987. Compression of oceanic lithosphere: An analysis of intraplate deformation in the

APPENDIX: MINERAL CHEMISTRY

In this appendix representative microprobe analysis are presented. Major element analyses were performed by combined wavelength- (WDS) and electron-dispersive spectrometry (EDS) using a Jeol Superprobe, operating at 15 kV and a beam current of 10 nA. The analyses were performed at the Institute of Earth Sciences, Utrecht. The electron microprobe facility is financially supported by The Netherlands Organisation for the Advancement of Pure Reasearch (NWO). All samples are from E.H. Hoogerduijn Strating unless mentioned otherwise.

A. 1. Mineral chemistry Alpine assemblages in the Erro-Tobbio peridotite.

Representative analyses of coexisting olivine (Ol), titanian clinohumite (Ti-Chu), antigorite (Atg) and diopside (Di) from Alpine veins in the Erro-Tobbio peridotite (microstructure of analyzed sample shown in Fig. 4.5B), and from olivine-bearing extensional crenulation cleavages (ecc's) developed in serpentinite mylonites in the Erro-Tobbio peridotite (microstructure of analyzed sample shown in Fig. 4.4A). The jadeite (Jd) analyses is from a sheared gabbroic dyke in the Erro-Tobbio peridotites and is representative for synkinematic Na-pyroxenes developed at the expense of plagioclase in such dykes. This Na-pyroxene is analyzed by M. Scambelluri (Scambelluri et al. 1990).

	Ecc (E-89-10)				Vein (E-89-31)				Dyke (E-89-26)
	Ol	Ti-Chu	Atg	Di	Ol	Ti-Chu	Atg	Di	Jd
SiO_2	39.54	33.52	41.33	54.72	40.37	35.62	44.71	55.30	59.20
TiO_2	—	5.47	—	—	—	5.54	—	—	—
Al_2O_3	—	—	2.10	—	—	—	—	—	24.54
Cr_2O_3	—	—	—	—	—	—	—	—	—
FeO	14.01	14.37	4.01	1.16	13.12	12.48	3.28	0.77	0.83
MnO	0.36	0.37	0.09	—	0.39	0.37	—	—	n.d.
MgO	46.06	42.40	39.45	18.55	46.87	44.54	40.74	17.73	0.41
CaO	—	—	—	25.65	—	—	—	25.96	1.81
K_2O	—	—	—	—	—	—	—	—	n.d.
Na_2O	—	—	0.07	0.06	—	—	—	0.11	12.92
F	—	—	—	—	—	—	—	—	n.d.
Total	100.07	96.13	86.96	100.05	100.72	98.55	88.73	99.87	99.71
Oxygen	4	17	7	6	4	17	7	6	6
Si	1.00	3.78	1.95	1.99	1.00	3.86	2.05	2.01	2.00
Ti	—	0.46	—	—	—	0.45	—	—	—
Al	—	—	0.12	—	—	—	—	—	0.98
Cr	—	—	—	—	—	—	—	—	—
Fe	0.29	1.35	0.16	0.04	0.27	1.13	0.13	0.03	0.02
Mn	0.01	0.03	—	—	0.01	0.03	—	—	n.d.
Mg	1.71	7.12	2.77	1.00	1.73	7.20	2.78	0.96	0.02
Ca	—	—	—	1.00	—	—	—	0.99	0.07
K	—	—	—	—	—	—	—	—	n.d.
Na	—	—	0.01	—	—	—	—	0.01	0.85
F^-	—	—	—	—	—	—	—	—	n.d.

A 2. Mineral chemistry Alpine assemblages in metagabbros and metabasalts in the Beigua Unit

Representative analyses of coexisting garnet (Grt), omphacite (Omp), phengite (Ph) and glaucophane (Gln) from eclogite metamorphic metabasalt (sample E-88-7) and, of coexisting Grt, Omp, Gln, apatite (Ap) and sphene (Spn) from a blueschist facies shear zone developed in Mg metagabbro. See Ernst (1976) and Messiga et al. (1983) for representative analyses of eclogitic Fe- and Mg metagabbros, respectively.

	Eclogitic metabasalt (E-88-7)				Blueschist shear zone in metagabbro (E-89-43)				
	Grt	Omp	Ph	Gln	Grt	Omp	Gln	Ap	Spn
SiO_2	36.68	54.57	52.71	56.57	37.59	53.63	56.63	—	29.52
TiO_2	0.16	—	0.18	0.20	0.10	0.06	—	—	38.95
Al_2O_3	20.92	7.70	20.57	10.92	20.90	6.65	11.28	—	0.60
Cr_2O_3	—	—	—	—	—	0.20	—	—	0.26
FeO	34.47	12.87	5.08	15.39	24.16	11.81	13.74	—	0.20
MnO	0.11	—	0.05	—	5.09	0.09	—	0.08	0.01
MgO	0.80	5.16	4.33	7.04	0.41	6.38	7.79	———	0.01
CaO	6.80	11.33	0.17	0.32	11.36	13.26	0.52	55.87	28.63
K_2O	—	—	10.49	—	—	—	—	0.20	0.11
Na_2O	—	8.21	0.08	7.40	—	6.89	7.18	—	0.04
P_2O_5	n.d.	n.d.	n.d.	n.d.	—	—	—	41.63	—
F	n.d.	n.d.	n.d.	n.d.	0.39	—	—	1.60	—
Total	99.94	99.84	93.66	97.84	100.00	98.88	97.14	99.38	98.16
Oxygen	12	6	11	23	12	6	23	26	5
Si	2.99	2.01	3.63	7.95	3.02	2.02	7.95	—	0.99
Ti	0.01	—	0.01	0.02	0.01	—	—	—	0.98
Al	1.99	0.34	1.67	1.81	1.98	0.30	1.87	—	0.02
Cr	—	—	—	—	—	0.01	—	—	—
Fe	2.32	0.40	0.29	1.81	1.62	0.37	1.82	—	—
Mn	0.01	—	—	—	0.35	—	—	0.01	—
Mg	0.10	0.29	0.44	1.47	0.05	0.36	1.61	—	—
Ca	0.59	0.45	0.01	0.05	1.00	0.53	0.07	10.68	1.03
K	—	—	0.92	—	—	—	—	0.04	—
Na	—	0.59	0.01	2.00	—	0.50	1.96	—	—
p	n.d.	n.d.	n.d.	n.d.	—	—	—	6.29	—
F^-	n.d.	n..d	n.d.	n.d.	0.10	—	—	0.90	—

A 3. Mineral chemistry mantle assemblages in the Erro-Tobbio peridotite

Representative analyses of stable mineral assemblages developed in different extension-related mantle shear zones in the Erro-Tobbio lherzolites. In the granular spinel lherzolite core compositions are listed of coexisting olivine (Ol), slightly exolved clinopyroxene (Cpx), unexolved orthopyroxene (Opx), and spinel (Spl). Mineral compositions of Ol, Cpx and Opx in the other samples pertain to rim compositions of synkinematically recrystallized grains. The Ol, Cpx, Opx and pargasitic hornblende (Prg) from a spinel-bearing peridotite mylonite (SG 18177) are from a very fine grained, amphibole-rich band adjacent to an Opx porphyroclast (see Fig. 5.10 for microstructure sample). The edenitic hornblende (Ed) analysis is from a fibrous amphibole aggregate developed on a pulled apart Opx porphyroclast (microstructure shown in Fig. 5. 13). Sample SG 18177 provided by D. van der Wal.

	Granular Spl-lherzolite (E-89-55)				Spl-bearing tectonite (E-88-13)				(E-89-8A)
	Ol	Cpx	Opx	Spl	Ol	Cpx	Opx	Spl	Ol
SiO_2	40.58	51.39	55.75	0.20	40.80	52.11	55.82	—	41.05
TiO_2	—	0.32	0.10	—	—	0.28	0.12	—	—
Al_2O_3	—	5.99	3.40	54.57	—	4.63	3.46	51.04	—
Cr_2O_3	—	1.29	—	12.16	—	0.70	0.35	17.52	—
FeO	9.29	2.66	6.81	13.78	9.53	2.77	6.07	12.95	9.98
MnO	—	—	—	—	—	—	0.09	—	—
MgO	49.53	16.83	33.74	18.57	50.01	16.71	33.58	18.34	49.88
CaO	—	21.02	1.13	0.21	—	23.09	0.74	—	—
K_2O	—	—	—	—	—	—	—	—	—
Na_2O	—	0.66	—	—	0.04	0.68	—	0.08	—
Total	99.40	100.16	100.93	99.49	100.34	100.77	100.24	99.93	100.91
Oxygen	4	6	6	4	4	6	6	4	4
Si	1.00	1.86	1.91	0.01	1.00	1.89	1.92	—	1.00
Ti	—	0.01	—	—	—	0.01	—	—	—
Al	—	0.26	0.14	1.71	—	0.20	0.14	1.61	—
Cr	—	0.04	0.01	0.26	—	0.02	0.01	0.37	—
Fe	0.19	0.08	0.18	0.31	0.20	0.09	0.17	0.29	0.20
Mn	—	—	—	—	—	—	—	—	—
Mg	1.81	0.91	1.72	0.74	1.81	0.90	1.72	0.73	1.80
Ca	—	0.82	0.04	0.01	—	0.90	0.03	—	—
K	—	—	—	—	—	—	—	—	—
Na	—	0.05	—	—	—	0.03	—	—	—

Table continued from previous page

	Pl-bearing mylonite (E-89-8A)			Spl-bearing mylonite (SG 18177)					
	Cpx	Opx	Spl	Ol	Cpx	Opx	Spl	Ed	Prg
SiO_2	51.21	55.49	—	40.58	53.63	55.60	—	47.70	44.43
TiO_2	0.57	0.13	0.14	—	0.08	0.03	—	0.34	1.42
Al_2O_3	3.87	1.47	43.86	—	1.38	0.93	49.49	9.65	11.92
Cr_2O_3	1.13	0.45	22.29	—	0.47	0.34	16.65	n.d.	1.13
FeO	3.16	7.08	17.55	10.59	2.12	7.54	16.72	4.09	4.01
MnO	0.06	—	0.18	0.07	—	—	—	—	—
MgO	16.02	33.88	15.09	49.38	17.19	35.28	15.73	19.93	18.95
CaO	22.74	0.62	—	—	24.11	0.39	0.07	12.58	12.20
K_2O	—	—	—	—	—	—	—	—	0.07
Na_2O	0.50	—	—	—	0.20	—	0.06	2.54	3.06
Total	99.20	99.12	99.11	100.62	99.18	100.11	98.65	97.00	97.12
Oxygen	6	6	4	4	6	6	4	23	23
Si	1.87	1.94	—	1.00	1.96	1.94	—	6.77	6.35
Ti	0.02	—	—	—	—	—	—	0.07	0.16
Al	0.17	0.06	1.46	—	0.06	0.04	1.61	1.61	2.01
Cr	0.03	0.01	0.50	—	0.01	0.01	0.36	n.d.	0.13
Fe	0.10	0.21	0.41	0.22	0.07	0.22	0.39	0.48	0.48
Mn	—	—	—	—	—	—	—	—	—
Mg	0.89	1.77	0.64	1.81	0.94	1.83	0.65	4.21	4.04
Ca	0.91	0.02	—	—	0.95	0.02	—	1.91	1.87
K	—	—	—	—	—	—	—	—	0.02
Na	0.04	—	—	—	0.01	—	—	0.70	0.84

Curiculum Vitae

23-08-1962 Geboren in Winschoten.

1974-1980 Atheneum B, Scholengemeenschap te Winschoten.

06-03-1983 Kandidaats examen G3, Rijksuniversiteit Utrecht.

24-11-1986 Doctoraal examen Structurele en toegepaste Geologie, met bijvakken Exploratie Geofysica en Exploratie Geochemie, Rijksuniversiteit Utrecht.

1987-present Assistent in Opleiding bij de vakgroep Geologie, Rijksuniversiteit Utrecht.

ENCLOSURES

Enclosure 1
Structural sections through the Bracco ophiolite complex (see Fig. 2.1). Location of sections indicated on the tectonic map (inset). Small-scale F1 and F2 folds are not shown, except for the F1 folds in the duplex NE of the Bracco Massif (sections 6 and 8 to 10), where the dashed lines indicate the S1 cleavage.

Enclosure 2
Tectonic map of the Northeastern Votri Massif (Liguria, Italy)

Enclosure 3
Tectonic map of the Erro-Tobbio unit, Northeastern Voltri Massi (Liguria, Italy).

STRUCTURAL CROSS-SECTIONS THROUGH THE BRACCO OPHIOLITE COMPLEX (LIGURIAN APENNINES, ITALY) Hoogerduijn Strating & van Wamel

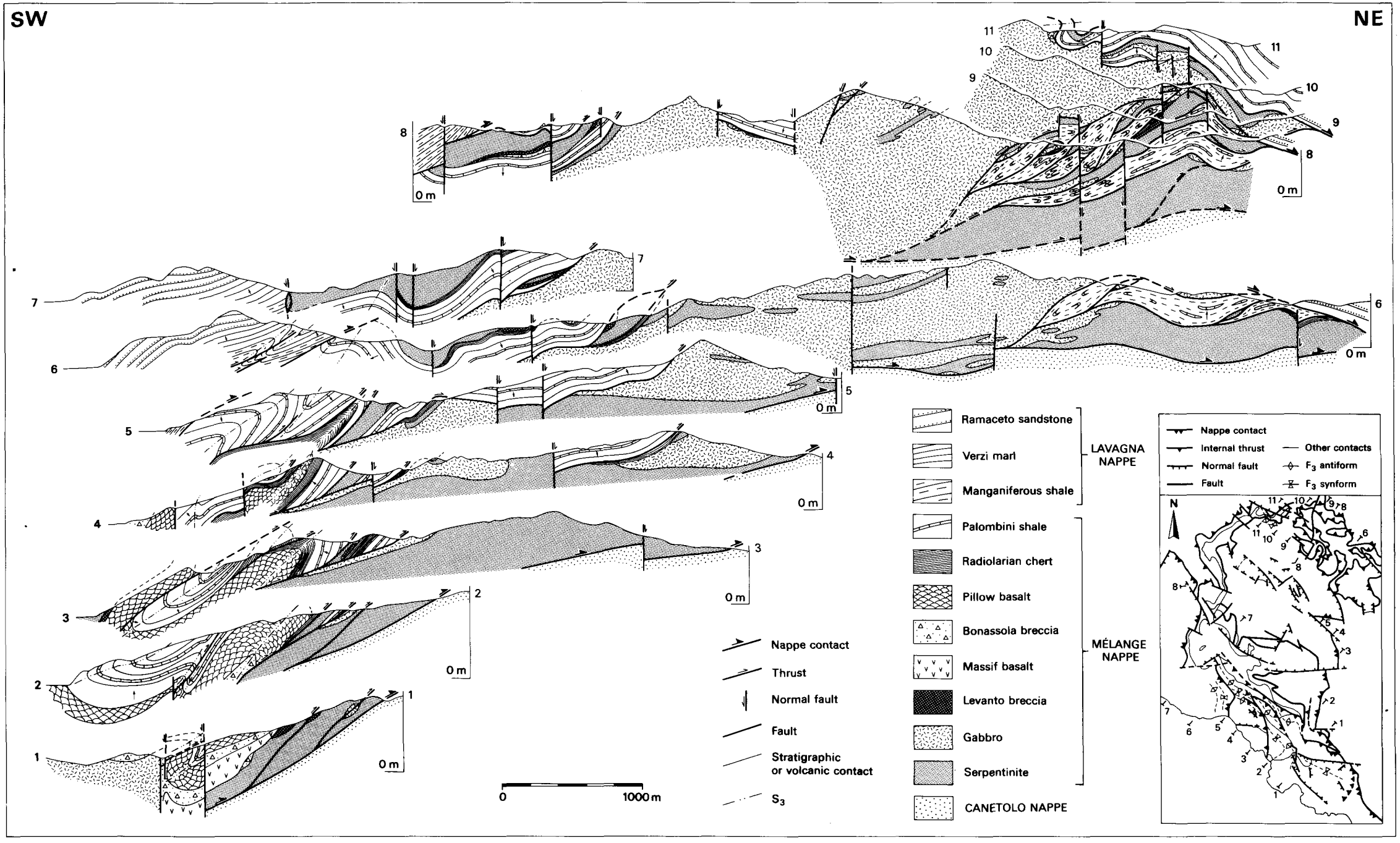

TECTONIC MAP OF THE NORTH-EASTERN VOLTRI MASSIF (LIGURIA, ITALY)

COMPILED BY E.H. HOOGERDUYN STRATING

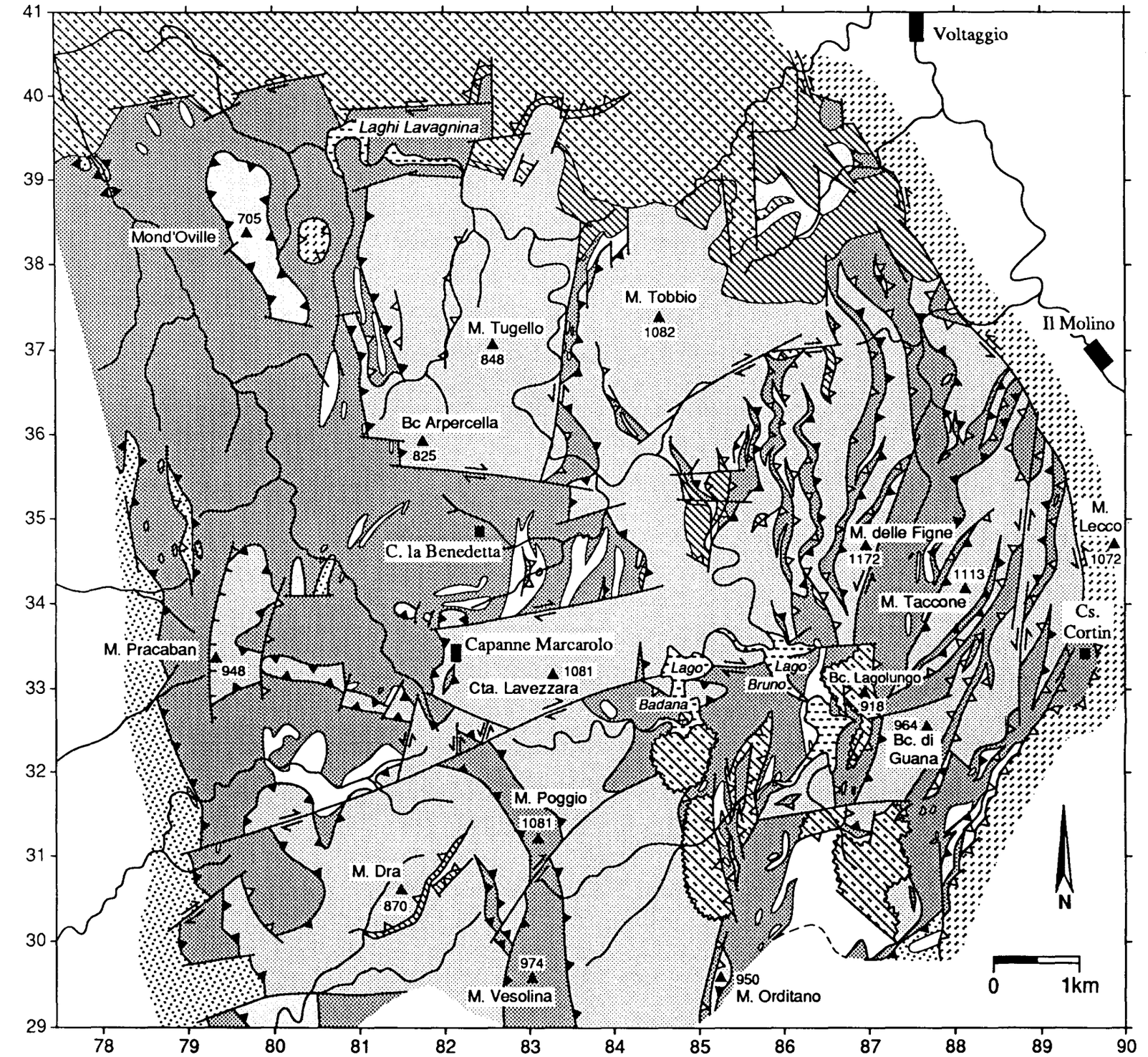

- Limestone breccia, Piotta conglomerate
- Tobbio breccia
- TERTIARY OF PIEMONTE BASIN
- SESTRI-VOLTAGIO ZONE
- Peridotite — ERRO-TOBBIO UNIT
- Antigorite serpentinite
- Eclogitic metagabbro albite amphibolite
- BEIGUA UNIT
- Calc-schist — VOLTRI-ROSSIGLIONE UNIT

- Ductile nappe contact (barbs in upper block)
- Brittle thrust (barbs in upper block)
- Brittle normal fault (barbs in down-thrown block)
- Brittle strike slip fault
- Brittle contacts
- Other contacts
- Unconformity

TECTONIC MAP OF THE ERRO-TOBBIO UNIT
NORTH-EASTERN VOLTRI MASSIF (LIGURIA, ITALY)

E.H. HOOGERDUIJN STRATING, D. VAN DER WAL & M.R. DRURY

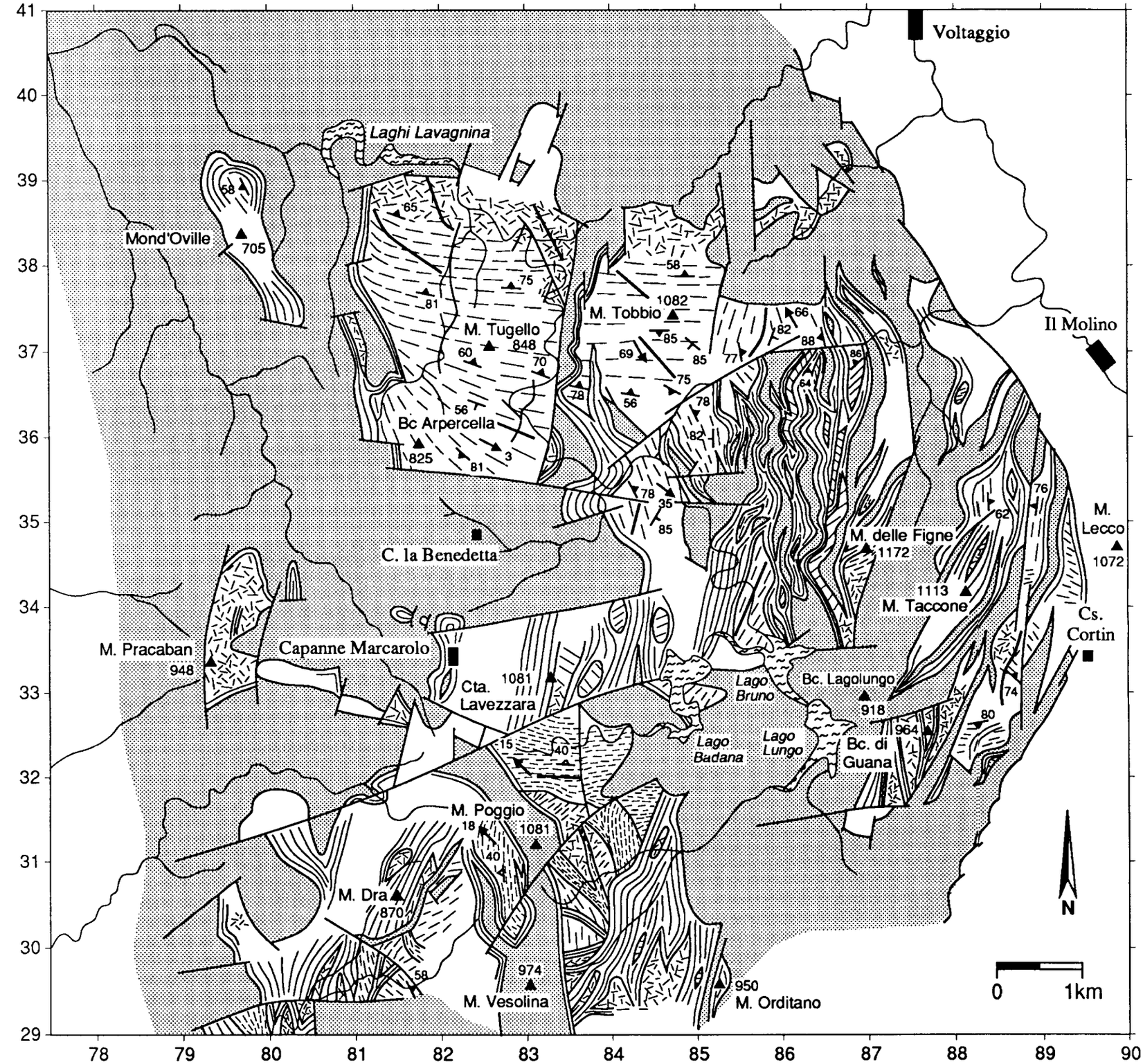

GRANULAR PERIDOTITE

PERIDOTITE TECTONITE

PERIDOTITE MYLONITE

OTHER UNITS

PYROXENITE BAND

SERPENTINITE MYLONITE

UNDIFFERENTIATED PERIDOTITE

Pyroxenite band

Tectonite foliation

Mylonite foliation

Stretching lineation